PHASE IV NCAT PAVEMENT TEST TRACK FINDINGS

Final Report

By

Randy West
David Timm
Richard Willis
Buzz Powell
Nam Tran
Don Watson
Maryam Sakhaeifar
Ray Brown
Mary Robbins
Adriana Vargas-Nordcbeck
Fabricio Leiva Villacorta
Xiaolong Guo
Jason Nelson

National Center for
Asphalt Technology

NCAT

at AUBURN UNIVERSITY

277 Technology Parkway ■ Auburn, AL 36830

PHASE IV NCAT PAVEMENT TEST TRACK FINDINGS

Draft Report

By

Randy West
David Timm
James R. Willis
R. Buzz Powell
Nam Tran
Don Watson
Maryam Sakhaeifar
Mary Robbins
Ray Brown
Adriana Vargas-Nordcbeck
Fabricio Leiva Villacorta
Xiaolong Guo
Jason Nelson

October 2012

i

DISCLAIMER

The contents of this report reflect the views of the authors who are responsible for the facts and accuracy of the data presented herein. The contents do not necessarily reflect the official views or policies of Alabama DOT, Florida DOT, Georgia DOT, Mississippi DOT, Missouri DOT, North Carolina DOT, Oklahoma DOT, South Carolina DOT, Tennessee DOT, Federal Highway Administration, Kraton Polymers, Polycon Manufacturing, Oldcastle Materials Group, Trinidad Lake Asphalt, Shell Oil Products, the National Center for Asphalt Technology, or Auburn University. This report does not constitute a standard, specification, or regulation. Comments contained in this paper related to specific testing equipment and materials should not be considered an endorsement of any commercial product or service; no such endorsement is intended or implied.

TABLE OF CONTENTS

CHAPTER 1 INTRODUCTION

1.1 Background on the Track

The NCAT Pavement Test Track, operated by the National Center for Asphalt Technology (NCAT), has been a successful pavement research program for many reasons. First, the 1.7-mile oval test track is a unique accelerated pavement testing facility that brings together real-world pavement construction with live heavy trafficking for rapid testing and analysis of asphalt pavements. Since the test track is funded and managed as a cooperative project, highway agencies and industry sponsors have specific research objectives for their section(s) and shared objectives for the track as a whole. The results of the experiments typically are not abstract or ambiguous; they are easy to interpret, so findings are quickly put into practice by sponsors. Highway agencies have used test track findings to improve their asphalt mix specifications, construction practices, and pavement design methods. Industry sponsors have used the test track as a proving ground to publicly demonstrate their technologies to the pavement engineering community.

The track has 46 different 200-ft. test sections. Twenty-six sections are located on the two straight segments of the track, and ten sections are located in each of the two curves. Sections are sponsored on three-year cycles. The first part of each cycle begins with building or replacing test sections, which normally takes about six months. Trafficking is applied over a two-year period using a fleet of heavily loaded tractor-trailer rigs to provide the equivalent of 10 million 18,000 pound single-axle loads (ESALs). During the trafficking phase, performance of the test sections is closely monitored using surface measurements and non-destructive structural response methods. Also during the trafficking phase, samples of the mixtures obtained during construction are tested and analyzed in NCAT's state-of-the-art laboratory. The final part of the cycle involves forensic analyses of damaged sections to determine factors that may have contributed to the distresses.

Figure 1.1 Aerial Photograph of the NCAT Test Track in November 2009

This report documents the experiments, analyses, and findings from the fourth cycle of the test track that was conducted from 2009 to 2011.

The first test track cycle began in 2000. The track was originally constructed to evaluate only surface mix performance for all 46 test sections. The pavement structure under the test sections was built extremely thick (20 inches of HMA over a granular base and a stiff subgrade) so that damage would be limited to the surface layers in the test sections. The second cycle, started in 2003, included replacing 24 test sections. Eight of those sections were the first "structural sections" designed and built to analyze the entire pavement structure, not just the surface layers. Construction of the structural sections required removal of the original thick pavement structure down to the subgrade material, then rebuilding the subgrade, aggregate base, and asphalt layers to result in test sections with asphalt pavement thicknesses of five, seven, and nine inches. Strain gauges were built into the bottom of the asphalt layers of the structural sections to monitor how the sections responded to the traffic and environmental changes throughout the two-year trafficking phase. This analysis was important to validate and calibrate elements of the new Mechanistic-Empirical Pavement Design Guide (MEPDG). The 2003 cycle also included the evaluation of 14 new surface layers. The remaining original 26 test sections were left in place with no changes to further evaluate their performance through the second cycle.

The third cycle of the test track started in 2006. Twenty-two new sections were built in 2006, including 15 new surface mix performance sections, five new structural study sections, and two reconstructed structural sections. Sixteen sections from the second cycle remained in place and had accumulated 20 million ESALs at the end of the third cycle. Eight original sections built in 2000 remained in place and accumulated 30 million ESALs by the end of the third cycle in 2008.

1.2 Key Findings from Previous Cycles

Many highway agencies have used findings from the test track to improve their materials specifications, construction practices, and pavement design policies for asphalt pavements. This section provides a summary of major test track research findings that have resulted in better specifications, as well as more economical mixes and pavement designs for the sponsoring agencies. Some of the findings have already influenced multiple states or have the potential for broader implementation. These key findings are organized into six areas: (1) mix design, (2) aggregate characteristics, (3) binder characteristics, (4) structural design and analysis, (5) relationships between laboratory results and field performance, and (6) tire-pavement interaction.

Mix Design

High RAP Content Mixtures. Six test sections in the third cycle were devoted to evaluating the performance of pavements with both moderate (20%) and high (45%) reclaimed asphalt pavement (RAP) contents. Results through the third cycle indicate that high RAP content mixes can provide excellent rutting performance and none of the sections exhibited any cracking. Field performance through two years indicated that using a standard grade of virgin binder grade in high RAP content mixes provided performance equal to using a softer binder. These sections were left in place for the fourth cycle to further evaluate their durability (see Section 3.2).

Warm-Mix Asphalt. An early version of MeadWestvaco's Evotherm WMA technology was used in the repair of two test sections that had extensive damage near the end of the 2003 research cycle. The two WMA test sections were opened to heavy loading from the track fleet immediately after construction.

Both sections remained in service throughout the 2006 track, with no cracking and rutting performance comparable to HMA for 10.5 million ESALs. One section endured more than 16 million ESALs on the 2009 track before the test section was used for a different project. The performance of those test sections was early evidence that WMA can hold up to extremely heavy traffic.

Stone-Matrix Asphalt (SMA) Mixtures. Through the first three cycles of the test track, 19 SMA sections (eight on the 2000 track, eight on the 2003 track, and three on the 2006 track) were put to the test. Excellent performance of the SMA test sections in the first cycle prompted several states to adopt this premium mix type for heavy traffic highways. Mississippi and Missouri then used the test track to evaluate lower-cost aggregates in SMA, which have helped make the mix type more economical.

Fine-Graded vs. Coarse-Graded Mixtures. In the early years of Superpave implementation there was an emphasis on coarse-graded mixtures to improve rutting resistance. However, that notion was called into question when the results of Westrack showed that a coarse-graded gravel mix was less resistant to rutting and fatigue cracking than a fine-graded mix with the same aggregate. In the first cycle of the test track, the issue was examined more completely. Twenty-seven sections were built with a wide range of aggregate types to compare coarse-, intermediate- and fine-graded mixtures. Results showed that fine-graded Superpave mixes perform as well as coarse-graded and intermediate-graded mixes under heavy traffic and tend to be easier to compact, less prone to segregation, and less permeable. Based on these findings, many state highway agencies revised their specifications to allow the use of more fine-graded mix designs.

Design Gyrations. Test track research has shown that higher asphalt contents improve mix durability, leading to longer pavement life. Higher asphalt contents can be achieved by reducing the laboratory compactive effort and increasing the VMA required during mix design. Numerous mixes on the test track designed with 50 to 70 gyrations in the Superpave gyratory compactor (SGC) have held up to the heavy loading on the track with great performance.

4.75 mm Nominal Maximum Aggregate Size (NMAS) Mix. Thin HMA overlays (less than 1¼-inch thick) are a common treatment for pavement preservation. Currently, about half of U.S. states utilize 4.75 mm NMAS mixtures in thin overlay applications. An advantage of the 4.75 mm mixtures is that they can be placed as thin as ½ inch, allowing the mix to cover a much larger area than thicker overlays. In the second test track cycle, the Mississippi DOT sponsored a test section of 4.75 mm surface mix containing limestone screenings, fine crushed gravel, and a native sand. The section has been in place for over seven years and carried more than 30 million ESALs with only seven millimeters of rutting and no cracking. This section is proof that well-designed 4.75 mm mixes are a durable option for pavement preservation.

Aggregate Characteristics

Polishing and Friction. The South Carolina DOT used the test track to assess the polishing behavior of a new aggregate source in 2003. A surface mix containing the aggregate was designed, produced, and placed on the track. Friction tests conducted at regular intervals showed a sharp decline in friction, indicating that the aggregate was not suitable for use in surface mixes. The test track enabled South Carolina to make this assessment in less than two years without putting the driving public at risk. Mississippi and Tennessee DOTs constructed sections to assess blends of limestone and gravel on mix performance and friction. Both states concluded that mixes containing crushed gravels provide satisfactory performance and revised their specifications to allow more gravel in their surface mixes.

Test sections sponsored by the Florida DOT used a limestone aggregate source that was known to polish. When the sections became unsafe for the NCAT track fleet, a special surface treatment containing an epoxy binder and calcined bauxite aggregate was evaluated to restore good friction performance. That surface treatment has provided excellent friction results and has endured over 30 million load applications.

Elimination of the Restricted Zone. Part of the original Superpave mix design procedure included a restricted zone within the gradation band for each nominal aggregate size. Test track sections with a variety of aggregate types proved that mixtures with gradations through the restricted zone could have excellent rutting resistance. The restricted zone was subsequently removed from the Superpave specifications.

Flat and Elongated. The Georgia DOT has led the way in using SMA since the early 1990s and soon after began to modify their open-graded friction course (OGFC) mixes toward a coarser, thicker porous European mix. Based on European experience, Georgia established strict aggregate shape limits for these premium mixes. However, few aggregate producers invested in the extra processing needed to make the special coarse aggregate for these mixes. As prices for the special aggregates rose to more than four times the price of conventional coarse aggregates, the Georgia DOT used the track to evaluate the effect using aggregates with a relaxed flat and elongated requirement for their OGFC mix. Test track performance showed the lower cost aggregates actually improved drainage characteristics.

Toughness. The South Carolina DOT also used the test track to evaluate an aggregate that had a LA abrasion loss that exceeded their specification limit. Aggregate degradation was assessed through plant production, construction, and under traffic. Although the aggregate did break down more than other aggregates through the plant, the test section performed very well. Rutting performance on the track was similar to that of other sections, and there were no signs of raveling, as indicated by texture changes. Based on these results, the agency revised its specifications to allow the aggregate source.

Binder Characteristics

Effect of Binder Grade on Rutting. Superpave guidelines have recommended using a higher PG grade for high-traffic volume roadways to minimize rutting. Results from the first cycle of testing showed that permanent deformation was reduced by 50% , on average, when the high-temperature grade was increased from PG 64 to PG 76. This two-grade bump is typical for heavy traffic projects. These results validated one of the key benefits of modified asphalt binders. The Alabama DOT also sponsored test sections to evaluate surface mixes designed with ½ percent more asphalt binder. Results of those sections showed that increasing the asphalt content of mixes containing modified binders did not affect rutting resistance; however, mixes produced with neat binders were more sensitive to changes in asphalt content.

Comparison of Different Types of Binder Modification. Experiments with paired test sections in the first cycle compared mixes containing PG 76-22 polymer-modified asphalt binders using styrene butadiene styrene (SBS) and styrene butadiene rubber (SBR). Test sections included dense-graded Superpave mixes, SMA mixes, and porous friction course mixes. Excellent performance was observed in all mixes produced with modified binders, regardless of the type of modifier used. A similar experiment sponsored by the Missouri DOT in the 2009 cycle compared the performance of a surface mix containing an SBS-modified binder and a ground tire rubber-modified binder.

Structural Design and Analysis

Asphalt Layer Coefficient for Pavement Design*.* Although many highway agencies are preparing for implementation of a mechanistic-based pavement design method, thousands of projects are still designed using the pavement design method based on the AASHO Road Test in the 1950s. In simplified terms, the current AASHTO pavement design method relates the pavement serviceability to the expected traffic and the structural capacity of the pavement structure. The pavement's structural capacity is calculated by summing the products of the thickness and the layer coefficient of each layer. The asphalt layer coefficient used by most states is 0.44, which was established during the AASHO Road Test, long before modern mix design methods, polymer modification, modern construction equipment and methods, and quality assurance specifications. A study funded by the Alabama DOT re-examined the asphalt layer coefficient based on the performance and loading history of all structural sections from the second and third cycles. These test sections represented a broad range in asphalt thicknesses, mix types, bases, and subgrades. The analysis indicated that the asphalt layer coefficient should be increased from 0.44 to 0.54. This 18% increase in the layer coefficient translates directly to an 18% reduction in the design thickness for new pavements and overlays. ALDOT implemented the new layer coefficient in its pavement design practice in 2010 and estimates this change will save $25 to $50 million per year in construction costs.

Strain Threshold for Perpetual Pavements. Analysis of data from in-situ pavement instrumentation from three cycles of the test track indicates that these pavements can withstand higher levels of strain than suggested by lab tests without accumulating fatigue damage. This may allow pavement engineers to design perpetual pavements with thinner cross-sections and, thus, make HMA pavements more economical and more competitive in life-cycle cost comparisons.

Relationships between Laboratory Results and Field Performance

Air Voids. Air voids of laboratory-compacted specimens is one of the most common pay-factors for asphalt pavements. The Indiana DOT sponsored test track research to identify an appropriate lower limit for this acceptance parameter. Surface mixes were intentionally produced with QC air voids between 1.0 and 3.5% by adjusting the aggregate gradation and increasing the asphalt content. Results showed that rutting increased significantly when the air voids were less than 2.75%. When test results are below that value and the roadway is to be subject to heavy traffic, removal and replacement of the surface layer is appropriate. It is important to note that the experiment used only mixes with neat asphalt binder. Other sections on the track with surface mixes containing modified binders with air voids less than 2.5% have held up very well under the extreme traffic on the track.

Top-Down Cracking. Florida DOT's pavement management system has shown that top-down cracking is the state's most prevalent form of pavement distress. Previous research has indicated that the energy ratio determined from properties of the surface mixture and stress conditions in the pavement structure can be used to predict top-down cracking. Florida DOT-sponsored sections in the 2006 cycle validated the energy ratio concept and showed that using a polymer-modified binder in dense-graded surface layers increases a pavement's resistance to top-down cracking.

Asphalt Pavement Analyzer (APA). The APA is a popular test for assessing rutting potential of asphalt mixes and has consistently provided reasonable correlations with test track performance. Based on a correlation between APA results and rutting on the track in the third cycle, an APA criteria of 5.5 mm

was established for heavy traffic pavements. As a result of this testing at the track, the Oklahoma DOT implemented a specification requiring the use of the APA on new mix designs.

Flow Number*. In the last few years, the Flow Number (FN) test has gained popularity among researchers as a lab test to evaluate the rutting resistance of asphalt mixes. Recently, NCHRP Report 673, *A Manual for Design of Hot Mix Asphalt with Commentary*, and NCHRP Report 691, *Mix Design Practices for Warm Mix Asphalt*, both recommended the FN test for assessing the rutting resistance of mix designs. Although a consensus has not been reached regarding which variation of the test method is best, NCAT has used a confined test with 10 psi and a repeated axial stress of 70 psi. A strong correlation was found between the results of the FN test using these conditions and rutting on the track. A minimum FN criterion of 800 cycles was recommended for heavy traffic pavements.

Dynamic Modulus Prediction. In mechanistic-based pavement design methods, dynamic modulus (E*) is a primary input for asphalt pavement layers since this property characterizes the rate of loading and temperature dependency of asphalt concrete. Three predictive dynamic modulus models and laboratory-measured E* values were compared to determine which model most accurately reflected E* values determined in laboratory testing. The Hirsch model proved to be the most reliable E* model for predicting the dynamic modulus of an HMA mixture.

Lab Testing of Friction and Texture Changes. NCAT used test track data to validate a method for determining texture and friction changes of any asphalt surface layer subjected to traffic. The procedure involves making slabs of the pavement layer in the laboratory and subjecting the slabs to simulated trafficking in the 3-wheel polishing device developed at NCAT. The slabs are periodically tested for friction and texture using the ASTM standards for the Dynamic Friction Tester and the Circular Track Meter, respectively. Excellent correlations were established between the friction results in the lab and the field.

Tire-Pavement Interaction

Tire-Pavement Noise and Pavement Surface Characteristics. Noise generated from tire-pavement interaction is substantially influenced by the macrotexture and porosity of the surface layer. Tire-pavement noise testing on the track indicates that the degree to which these factors influence noise levels is related to the weight of the vehicle and tire pressures. For lighter passenger vehicles, the porosity of the surface, which relates to the degree of noise attenuation, is the dominant factor. For heavier vehicles (with higher tire pressures), the macrotexture of the surface and the positive texture presented at the tire-pavement interface has a greater influence.

New Generation Open-Graded Friction Course Mixes. Each of the three previous cycles of the test track have included new-generation open-graded friction course (OGFC) mixtures featuring a variety of aggregate types. Testing has shown that OGFC surfaces, also known as porous friction courses (PFC), eliminate water spray, provide excellent skid resistance, and significantly reduce tire-pavement noise.

High-Precision Diamond Grinding. Smoothness is the most important pavement characteristic from the perspective of users. Occasionally, pavement maintenance results in a bump in the roadway surface that needs to be removed. Precision diamond grinding has been used on the test track to smooth out transitions between some test sections in each cycle. None of the areas leveled with the grinding equipment have exhibited any performance issues. Some of the leveled areas have been in service for up to 10 years with no performance problems. No sealing was applied to these treated surfaces.

1.3 Overview of the 2009 Test Track (Fourth Cycle)

As with the previous two cycles, the 2009 test track included new sections and continued evaluation of existing sections. Of the 46 total sections, 25 new experimental pavements were built, nine were left in place from the 2006 cycle, nine were left in place from the 2003 cycle, and three sections remained from the original construction.

The research objectives for the 2009 test track are described below in alphabetical order by sponsor. Six agencies worked together to establish a group of experimental test sections with a common cross-section to assess the performance and structural response of pavements constructed with warm-mix asphalt (WMA) technologies, high RAP contents, the combination of high RAP content and WMA, and a porous friction course containing 15% RAP. This collection of six test sections has been referred to as the "Group Experiment," which includes:
1. A control section built with three dense-graded layers of hot-mix asphalt using all virgin materials
2. A section built with an open-graded friction course as the surface layer in place of the dense-graded surface course in the control section
3. A section using the same layers and mix designs as the control section except the mixes were produced as WMA using a water-injection foaming process
4. A section using the same layers and mix designs as the control section except the mixes were produced as WMA using a chemical additive
5. A section with mix designs containing 50% RAP in each of the three layers
6. A section with the same 50% RAP mix designs except the mixtures were produced as warm-mix asphalt using a water-injection foaming process

All of the Group Experiment sections were constructed on the same stiff subgrade and graded aggregate base. A designed asphalt pavement thickness of seven inches was selected for all the Group Experiment test sections because previous test sections built with that thickness had exhibited moderate fatigue cracking within one cycle. Therefore, the Group Experiment test sections were expected to have a range of fatigue cracking due to different mix properties used in the sections. Specific objectives of the Group Experiment were to
- compare dense-graded HMA to PFC surface layer with regard to structural response to determine how PFC mixes should be treated in structural pavement design;
- compare HMA, foamed asphalt WMA, and Evotherm WMA with regard to rutting, fatigue cracking, and other possible forms of distress;
- compare virgin HMA, 50% RAP HMA, and 50% RAP WMA with regard to rutting, fatigue cracking, and other possible forms of distress; and
- compare performance data for all Group Experiment sections to MEPDG predictions for model validations.

Alabama Department of Transportation (ALDOT) - ALDOT is one of the sponsoring agencies for the Group Experiment described above. The department also sponsored continued trafficking and evaluation of two 9-inch structural sections built in 2003, which are still exhibiting excellent performance. Performance and stain data from these two sections are vital to establishing a fatigue threshold for asphalt pavements.

Florida Department of Transportation (FDOT) - In addition to being a Group Experiment sponsor, FDOT is evaluating the potential benefits of OGFC and tack coats to mitigate top-down cracking. The OGFC experiment involves using a pavement structure and Superpave mix that was proven to be susceptible to top-down cracking in the previous cycle. The tack coat between the Superpave mix and the OGFC was applied with two methods in adjoining test sections. The first section used a spray-paver to apply a heavy tack coat, and the second section used a tack coat application applied with a conventional tack distributor. The OGFC mix included 15% RAP as an experimental feature.

Federal Highway Administration (FHWA) - FHWA provided funding to support continued monitoring of the dual-layer OGFC section placed in 2006 and the high RAP content surface layers built in 2006. The dual-layer OGFC section is the smoothest, quietest, and safest pavement on the track. FHWA has also continued to provide three of the heavy triple-trailers used for loading of the test track sections.

Georgia Department of Transportation (GDOT) - Georgia sponsored a test section to evaluate the possibility of reducing their stringent flat and elongated requirement for coarse aggregates used in SMA. This experiment follows a previous evaluation of the same requirement for OGFC aggregates that demonstrated the economic and performance benefit of aggregates that were much easier to produce.

Kraton Polymers - The largest supplier of polymers for the asphalt paving industry, Kraton, sponsored a structural section with a complete array of stress and strain instrumentation to demonstrate the economic and structural benefit of using highly modified asphalt binders in all layers of a reduced thickness pavement structure.

Lake Asphalt of Trinidad and Tobago Ltd.- Lake Asphalt of Trinidad and Tobago sponsored a structural section using a conventional asphalt binder modified with 25% pelletized Trinidad Lake Asphalt (TLA) in the surface, intermediate, and base layer. The fully instrumented TLA section was built with the same cross-section as the control section in the Group Experiment to provide a head-to-head comparison of performance and pavement responses to heavy loading and environmental conditions.

Mississippi Department of Transportation (MSDOT) - Mississippi sponsored the continuation of traffic and monitoring of its gravel OGFC layer over a gravel SMA built in 2006. They have also sponsored a new surface mix test section containing 45% RAP and aggregates from Mississippi.

Missouri Department of Transportation (MODOT) - Missouri sponsored two test sections to directly compare an asphalt binder modifier, styrene butadiene styrene (SBS) polymer, to a binder modified with ground tire rubber (GTR). Both binders were used in the same Superpave mix design using aggregates from Missouri. The objective of the MODOT experiment is to determine if GTR can be used as an alternative to SBS modification for heavy traffic surface layers.

North Carolina Department of Transportation (NCDOT) - North Carolina is one of the sponsors of the Group Experiment.

Oklahoma Department of Transportation (OKDOT) - Oklahoma is a sponsor of the Group Experiment and also funded the continuation of traffic and performance monitoring of its perpetual pavement test section built as part of the previous cycle. A thinner companion section designed using OKDOT's traditional pavement thickness design approach had extensive fatigue cracking and had to be repaired. OKDOT sponsored the evaluation of an experimental rehabilitation of the failed section that included

milling the top five inches, placing a leveling course, two paving fabrics in two subsections, followed by the same asphalt mix designs that were removed.

Oldcastle Materials Group - Oldcastle sponsored the continued evaluation of the moderate and high RAP content surface layers built in the previous cycle. Its funding was also used to provide a more complete laboratory characterization of all test track mixes.

Polycon Manufacturing - Polycon sponsored an evaluation of their polymer-composite micro surface treatment product E-Krete. The product was applied to an older test section that had extensive block cracking to assess durability, friction, and light reflectivity through the two year trafficking cycle.

Shell Oil Products USA - Shell sponsored two fully instrumented structural sections to evaluate the pelletized sulfur WMA technology marketed as Thiopave®. The Thiopave® binder replaced 22 to 39 percent of the asphalt binder in the base and intermediate layers for both test sections. One of the Thiopave® sections was built with a total thickness of seven inches to match the Group Experiment control section. The other section was built two inches thicker to evaluate the material in a perpetual pavement design.

South Carolina Department of Transportation (SCDOT) - South Carolina is one of the sponsors of the Group Experiment.

Tennessee Department of Transportation (TNDOT) - Tennessee is also one of the sponsors of the Group Experiment.

Table 1 lists all of the test sections on the track starting at Section E2 and moving around the track in a clockwise direction. New test sections are identified with bold text.

Numerous companies provide generous donations of equipment, materials, and human resources to help build test sections, operate the trucking fleet, and conduct the extensive research monitoring each cycle. This support helps minimize test track costs and ensure that the highest quality research is achieved. As before, Astec Industries provided personnel and equipment to assist production of the experimental mixes and construction test sections. Compaction and placement equipment has been provided by Bomag Americas, Dynapac, and Ingersoll Rand. Construction materials were provided by Boral Material Technologies, the Blaine Companies, Dravo Lime, Martin Marietta Aggregates, MeadWestvaco, Oldcastle Materials Group, and Vulcan Materials Company. Many other material supply companies donated materials directly to state DOT sponsors. Equipment for mix and pavement quality testing has been provided by CPN International, the Gilson Company, HMA Lab Supply, Instrotek, Transtech Systems, and Troxler Electronic Laboratories.

Table 1.1 Complete Listing of Test Sections on the 2009 NCAT Test Track

Test Sec	Study HMA (in)	Surface Mix Stockpile Materials	Year of Completion	Design Methodology	Specified Binder	Total HMA (in)	Base Material	Sub-Grade	Research Objective(s)
E2	4	Calcined Bauxite	2005	Proprietary	Epoxy	24	Granite	Stiff	HVS PG67 Validation w/ High Friction Epoxy Surface
E3	4	Calcined Bauxite	2005	Proprietary	Epoxy	24	Granite	Stiff	HVS PG76 Validation w/ High Friction Epoxy Surface
E4	4	Granite	2000	Superpave	PG76-22	24	Granite	Stiff	Performance of Coarse Gradation
E5	**2**	**Grn/Lms/Snd (45% RAP)**	**2006**	**Superpave**	**PG67-22**	**24**	**Granite**	**Stiff**	**RAP Mix Design/Construction/Performance**
E6	**2**	**Grn/Lms/Snd (45% RAP)**	**2006**	**Superpave**	**PG76-22**	**24**	**Granite**	**Stiff**	**RAP Mix Design/Construction/Performance**
E7	2	Grn/Lms/Snd (45% RAP)	2006	Superpave	PG76-22s	24	Granite	Stiff	RAP Mix Construction/Performance w/ Sasobit
E8	**1.5**	**Granite**	**2010**	**Superpave**	**PG67-22**	**24**	**Granite**	**Stiff**	**Hot Control for WMA Certification Program 5/11/10**
E9	**1.5**	**Granite**	**2010**	**Superpave**	**PG67-22**	**24**	**Granite**	**Stiff**	**Shell Thiopave WMA Certification Program 5/11/10**
E10	2	Granite/Limestone/Sand	2005	Superpave	PG76-22	24	Granite	Stiff	Evotherm Warm Mix w/ Latex
N1	**0.75**	**Granite (15% RAP)**	**2009**	**PFC**	**PG76-22**	**7.75**	**Limerock**	**Stiff**	**Surface Cracks in PFC via Spray Paver & M-E Design**
N2	**0.75**	**Granite (15% RAP)**	**2009**	**PFC**	**PG76-22**	**7.75**	**Limerock**	**Stiff**	**Surface Cracks in PFC via Tack Paving & M-E Design**
N3	**9**	**Granite/Limestone/Sand**	**2003**	**Superpave**	**PG67-22**	**9**	**Granite**	**Stiff**	**M-E Design Validation/Calibration**
N4	**9**	**Granite/Limestone/Sand**	**2003**	**Superpave**	**PG76-22**	**9**	**Granite**	**Stiff**	**M-E Design Validation/Calibration**
N5	**9**	**Granite/Sand/Limestone**	**2009**	**Superpave**	**PG76-22**	**9**	**Granite**	**Stiff**	**GE+ Thick Shell Thiopave Perpetual & M-E Design**
N6	**7**	**Granite/Sand/Limestone**	**2009**	**Superpave**	**PG76-22**	**7**	**Granite**	**Stiff**	**GE+ Standard Shell Thiopave & M-E Design**
N7	**5.75**	**Granite/Sand/Limestone**	**2009**	**Superpave**	**PG88-22**	**5.75**	**Granite**	**Stiff**	**GE+ Thin Kraton High Polymer & M-E Design**
N8	**5.75**	**Granite/Sand/Limestone**	**2009**	**Superpave**	**PG88-22**	**10**	**Stiff Sub**	**Soft**	**Kraton High Polymer for Extreme Rehabilitation**
N9	**14**	**Oklahoma Granite**	**2006**	**SMA**	**PG76-28**	**14**	**Stiff Sub**	**Soft**	**Perpetual Pavement & M-E Design**
N10	**7**	**Sand/Granite (50% RAP)**	**2009**	**Superpave**	**PG67-22**	**7**	**Granite**	**Stiff**	**GE 50% RAP Hot Mix Asphalt & M-E Design**
N11	**7**	**Sand/Granite (50% RAP)**	**2009**	**Superpave**	**PG67-22**	**7**	**Granite**	**Stiff**	**GE 50% RAP Warm Mix Asphalt & M-E Design**
N12	**2**	**Granite (28% 3:1 F&E)**	**2009**	**SMA**	**PG76-22**	**24**	**Granite**	**Stiff**	**Performance of SMA with High F&E Aggregates**
N13	4	Georgia Granite	2006	PFC	PG76-22	24	Granite	Stiff	Twin Layer Drainable Mix w/ F&E Aggs
W1	4	Georgia Granite	2000	SMA	PG76-22	24	Granite	Stiff	Columbus Granite SMA
W2	**1.5**	**Granite**	**2010**	**Superpave**	**PG67-22**	**24**	**Granite**	**Stiff**	**Shell Thiopave Demo with Latex 5/11/10**
W3	2	Grn/Lms/Snd (20% RAP)	2006	Superpave	PG76-22	24	Granite	Stiff	RAP Mix Design/Construction/Performance
W4	2	Grn/Lms/Snd (20% RAP)	2006	Superpave	PG67-22	24	Granite	Stiff	RAP Mix Design/Construction/Performance
W5	**2**	**Grn/Lms/Snd (45% RAP)**	**2006**	**Superpave**	**PG52-28**	**24**	**Granite**	**Stiff**	**RAP Mix Design/Construction/Performance**
W6	1	Limestone/Gravel/Sand	2003	Superpave	PG76-22	24	Granite	Stiff	Low Volume Road Preservation
W7	**1.5**	**Granite**	**2010**	**Superpave**	**PG67-22**	**24**	**Granite**	**Stiff**	**Shell Thiopave Demo with Latex 5/11/10**
W8	**0**	**Research Blends**	**2011**	**Research**	**Epoxy**	**24**	**Granite**	**Stiff**	**Two Different Epoxy Surface Treatments**
W9	**0**	**Research Blends**	**2011**	**Research**	**Epoxy**	**24**	**Granite**	**Stiff**	**Six Different Epoxy Surface Treatments**
W10	4	Gravel/Limestone	2000	Superpave	PG76-22	24	Granite	Stiff	Durability of Coarse Gravel Mix
S1	4	South Carolina Granite	2003	SMA	PG76-22	24	Granite	Stiff	High LA Abrasion Loss SMA Aggregates
S2	**4**	**Gravel/Sand (45% RAP)**	**2009**	**Superpave**	**PG67-22**	**24**	**Granite**	**Stiff**	**High RAP Content Gravel Superpave**
S3	**2.5**	**Gravel**	**2006**	**OGFC**	**PG76-22**	**24**	**Granite**	**Stiff**	**100% Gravel OGFC Performance**
S4	4	Limestone	2003	OGFC	PG76-22	24	Granite	Stiff	100% Limestone OGFC Performance
S5A	**0**	**Proprietary Blend**	**2009**	**Proprietary**	**Epoxy**	**24**	**Granite**	**Stiff**	**Proprietary Epoxy Surface Treatment**
S5B	**0**	**Proprietary Blend**	**2009**	**Proprietary**	**Epoxy**	**24**	**Granite**	**Stiff**	**Proprietary Epoxy Surface Treatment**
S6	**1.75**	**Limestone/Porphyry**	**2009**	**Superpave**	**PG76-22**	**24**	**Granite**	**Stiff**	**SBS-Modified Superpave Mix**
S7	**1.75**	**Limestone/Porphyry**	**2009**	**Superpave**	**PG76-22**	**24**	**Granite**	**Stiff**	**GTR-Modified Superpave Mix**
S8	**7**	**Granite (15% RAP)**	**2009**	**PFC**	**PG76-22**	**7**	**Granite**	**Stiff**	**GE Buildup with PFC Surface & M-E Design**
S9	**7**	**Granite/Sand/Limestone**	**2009**	**Superpave**	**PG76-22**	**7**	**Granite**	**Stiff**	**GE Control Section Conventional Mix & M-E Design**
S10	**7**	**Granite/Sand/Limestone**	**2009**	**Superpave**	**PG76-22**	**7**	**Granite**	**Stiff**	**GE Foamed Warm Mix & M-E Design**
S11	**7**	**Granite/Sand/Limestone**	**2009**	**Superpave**	**PG76-22**	**7**	**Granite**	**Stiff**	**GE Additized Warm Mix & M-E Design**
S12	**7**	**Granite/Sand/Limestone**	**2009**	**Superpave**	**PG67-28**	**7**	**Granite**	**Stiff**	**GE+ Trinidad Lake Asphalt Pellets & M-E Design**
S13	**0**	**Proprietary Blend**	**2010**	**Proprietary**	**Polycon**	**24**	**Granite**	**Stiff**	**Polycon Surface Treatment on Distressed Pavement**
E1	4	Tennessee Limestone	2003	SMA	PG76-22	24	Granite	Stiff	100% Limestone SMA Performance

Note: Sections shown in bold were funded as part of Phase 4. Non-bolded sections remained in place as unfunded sections.

Construction

New test sections were prepared by milling to the appropriate depth for each section. Roadtec Inc. generously provided milling machines and highly skilled operators at no cost to the test track budget. Milling locations and depths were coordinated by the test track manager. NCAT personnel operated dump trucks to collect and haul millings.

Instrumentation for Structural Test Sections

The instrumentation system developed and improved through previous cycles of the NCAT test track was again used to measure pavement responses in all structural test sections. The instrumentation plan and analysis routines have proven to be robust and effective in gathering data for mechanistic pavement analysis. This system and methodology is thoroughly detailed in NCAT Report 09-01(*1*).

Figure 1.2 Installation of Strain Gauges and a Pressure Plate Before Placing the Asphalt Base Course

East Alabama Paving Company was awarded the contracts to produce the asphalt mixtures and construct the test sections through a competitive bidding process through Auburn University. Due to space limitations on the contractor's yard, it was necessary to stage some materials at paved storage locations on the track property before they were needed for mix production.

A special production sequence was used to produce each mix. The plant's cold feed bins were calibrated for each unique stockpile. Production of each mix began with running the aggregate through the drier and mixer without the addition of asphalt binder to ensure a uniform gradation. This uncoated material was discharged at the by-pass chute on the slat conveyor. Liquid asphalt was then turned on, and the mix was discharged at the bypass chute until the aggregates were well coated. The bypass chute was then closed and the mixture was conveyed into the storage silo until the plant controls indicated that approximately one truckload had accumulated. This material was discharged into a truck and hauled to a future recycled materials pile on the contractor's yard. At this point, it was assumed that the plant had reached steady state conditions and that subsequent mix run into the silo would be uniform in terms of aggregate gradation, asphalt content, and temperature. After the desired quantity of mix had been produced, the aggregate and asphalt flows were stopped, the remaining materials in the drier and mixer were discharged at the bypass chute, and the plant was shut down. The cold feed bins were unloaded, and the plant was readied for the next test mix.

Prior to placement of mixes on each test section, a trial mix was produced to evaluate the mix quality control requirements of the sponsor. The trial mixes were hauled to the track and sampled by NCAT personnel for laboratory testing and evaluation. Test results of the trial mix were presented to the sponsor to determine appropriate adjustments in plant settings for the subsequent production of mix for placement in test sections.

Mix produced for placement on the test sections followed the same production sequence described above. Mix production continued until a sufficient quantity of material was available to lay the required mat. The contractor was responsible for hauling mixes to the track, and the paving equipment and crew were staged at the track.

Figure 1.3 Paving the Surface Layer of a Test Section on the 2009 NCAT Test Track

Before placing mixtures on the test sections, the contractor tacked the underlying asphalt pavement with either a PG 67-22 binder or NTSS-1HM emulsion, depending on the sponsor's preference. The target application rates were generally between 0.04 to 0.07 gallons per square yard (residual for emulsion), unless otherwise directed.

Mixtures were dumped from end-dump haul trucks into a Roadtec SB2500 material-transfer machine, which was operated from the track inside lane so that only the paving machine operated on the actual test sections. Compaction was accomplished by at least three passes of a steel-wheeled roller. The roller was capable of vibrating during compaction; however, this technique was not used on every test section. After the steel-wheeled roller was removed from the pavement mat, the contractor continued compacting the mat with a rubber tire roller until the desired density was achieved.

Traffic

Trafficking for the 2009 test track was applied in the same manner as with previous cycles. Two shifts of professional drivers operated four trucks pulling triple flat-bed trailers (Figure 1.4) and one truck pulling a triple box trailer from 5 a.m. until approximately 10:40 p.m. Tuesday through Saturday. At the request of sponsors, trafficking on this cycle was initiated earlier in the year to evaluate how the newly constructed sections would perform under hotter weather. Trafficking began on August 28, 2009, and ended September 30, 2011. The total traffic applied to the sections during this cycle was 10,142,140 ESALs.

Figure 1.4 One of the Heavily Loaded Triple-Trailers used for Accelerated Loading on the Test Track

Axle weights for each of the five trucks are shown in Table 1.2. On some occasions, either due to a specialized study or mechanical malfunction, trailers were removed from the operation. This left the truck pulling either a single flat-bed trailer or a combination of double flat-beds.

Table 1.2 Axle Weights (lbs.) for the 2009 Truck Fleet

Truck	Steer	Tandem		Single				
ID	Axle 1	Axle 2	Axle 3	Axle 4	Axle 5	Axle 6	Axle 7	Axle 8
1	10,150	19,200	18,550	21,650	20,300	21,850	21,100	19,966
2	11,000	20,950	20,400	20,950	21,200	21,000	20,900	20,900
3	10,550	20,550	21,050	21,000	21,150	21,150	21,350	20,850
4	10,550	21,050	20,700	21,100	21,050	21,050	20,900	21,050
5	11,200	19,850	20,750	20,350	20,100	21,500	19,500	20300
Avg.	10,680	20,320	20,290	20,760	20,760	21,310	20,550	20,613
COV, %	3.9	3.9	4.9	2.2	2.5	1.7	3.6	2.2

Performance Monitoring

Performances of the test sections are evaluated with a comprehensive range of surface measurements. Additionally, the structural health and response of the structural sections are routinely evaluated using embedded stress and strain gauges and falling-weight deflectometer (FWD) testing. Table 1.3 summarizes the performance-monitoring plan. Rut depths, IRI, mean texture depth, and cracking results were reported on the test track's website: www.pavetrack.com.

Table 1.3 NCAT Test Track Performance-Monitoring Plan

Activity	Sections	Frequency	Method
Rut depth	all	weekly	ARAN van
Mean Texture Depth	all	weekly	ARAN van, ASTM E1845
Mean Texture Depth	select	quarterly	CTM, ASTM E2157-09
International Roughness Index	all	weekly	ASTM E950, AASHTO R43
Crack mapping	sponsored	2 times/mo.	Buzz 2000
FWD	structural	3 times/mo.	AASHTO T 256-01
Stress/Strain response to live traffic	structural	weekly	NCAT method
Pavement temperature @ 4 depths	all	hourly	Campbell Sci. 108 thermisters
Pavement reflectivity/albedo	new	quarterly	ASTM E 1918-06
Field permeability	OGFC/PFCs	quarterly	NCAT method
Core density	sponsored	quarterly	ASTM D979, AASHTO T 166
Friction	all	monthly	ASTM E274, AASHTO T242
Friction	select	quarterly	DFT, ASTM E1911
Tire-pavement noise	all	quarterly	OBSI, AASHTO TP 76-11 CPX, ISO 11819-2 Absorption, ASTM E1050-10

Laboratory Testing

Mixture samples for quality assurance testing were obtained from the beds of the haul trucks using a sampling stand located at the test track. Typical quality assurance tests were conducted immediately on the hot samples. Table 1.4 lists the test methods used for the quality assurance testing. The results of these tests were reviewed by the respective test section sponsor for acceptance. In cases where the QA results did not meet the sponsor's criteria, the mixture placed on the section was removed, adjustments were made at the plant, and another production run was made until the mix properties were satisfactory. Results of the quality assurance tests and the mix designs for each layer for all test sections were reported on www.pavetrack.com.

Table 1.4 Tests Used for Quality Assurance of Mixes

Test Description	Test Method	Replicates
Splitting samples	AASHTO T 328-05	as needed
Asphalt Content	AASHTO T 308-05	2
Gradation of Recovered Aggregate	AASHTO T 30-07	2
Laboratory Compaction of Samples	AASHTO T 312-04	2
Maximum Theoretical Specific Gravity	AASHTO T 209-05	2
Bulk Specific Gravity of Compacted Specimens	AASHTO T 166-07	2

NCAT staff also obtained large representative samples of each unique mixture placed on the test track for additional testing. These samples were obtained by diverting mix from the conveyor of the material transfer machine going into the paver into the bucket of a front-end loader. The front-end loader then brought the mix to the rear of the track laboratory where the mix was then shoveled in to 5-gallon buckets and labeled. In total, over 900 buckets of mix were sampled for additional testing.

A testing plan for advanced characterization of the 27 unique mixtures was established to meet section specific and general test track research objectives.   Samples of the asphalt binders were also obtained at the plant for characterization. Table 1.5 summarizes the tests and which materials or layers were typically evaluated. Results of these tests are maintained in a database at NCAT.

Table 1.5 Summary of Testing for Advanced Materials Characterization

Test Description	Test method	Material or Layer
PG Grade	AASHTO R 29	tank binders and recovered binders from mixes containing RAP &/or WMA
Multiple Stress Creep Recovery	AASHTO TP 70-09	all binders
Moisture Susceptibility	AASHTO T 283	all mixes
Hamburg Wheel Tracking	AASHTO T 324	surface mixes and certain other mixes
Asphalt Pavement Analyzer	AASHTO TP 63	surface mixes and certain other mixes
Dynamic Modulus	AASHTO TP 62	all mixes
Flow Number - unconfined	AASHTO TP 62	surface mixes
Bending Beam Fatigue	AASHTO T 321	base mixes
AMPT Fatigue (S-VECD)	NC State	surface and base mixes
IDT Creep Compliance & Strength	AASHTO T 322	surface mixes
Energy Ratio	Univ. of Florida	surface and base mixes

CHAPTER 2   SURFACE LAYER PERFORMANCE EXPERIMENTS

2.1 Georgia DOT Evaluation of Effect of Flat and Elongated Aggregates on SMA Performance

Introduction and Problem Statement

Aggregate Properties. Since the introduction of stone-matrix asphalt (SMA) from Europe in 1990, there have been questions about aggregate requirements needed for these high-performance mixtures. European SMA specifications were reported to require aggregates with no more than 30% Los Angeles (LA) abrasion loss (AASHTO T96) and no more than 20 percent flat and elongated particles when measured at a 3:1 ratio of length to maximum thickness (ASTM D 4791). These values were adopted as guidelines by a Technical Working Group (TWG) in 1991 (*2*). The TWG guidelines set standards for early implementation in order to help ensure the success of SMA performance. However, Ruth et. al. concluded that good SMA mixtures could be produced with aggregates that were outside the TWG guidelines and that pavement performance is the best indicator of which aggregates and aggregate blends could be used successfully *(3).*

Generally, it is believed that flat and elongated aggregates will result in inferior performance due to break-down of aggregate particles or realignment of those particles under the kneading action of traffic. Fracturing of aggregate particles will expose two uncoated faces and may lead to premature stripping and fatigue cracking. Reorientation of aggregate particles may also result in pavement deformation under loading conditions.

A limited study of the effect of flat and elongated (F&E) aggregate particles on hot-mix asphalt performance conducted by the NCAT found that the aggregate abrasion value is influenced to some degree by particle shape (*4*). Fatigue tests of Superpave mixtures using two aggregate sources showed that fatigue resistance actually improved as the percent 3:1 F&E particles increased. There was also no significant difference in test results for moisture susceptibility or in aggregate breakdown for the 75 µm sieve size. The study did show significant differences in rutting resistance and breakdown on the 4.75 mm sieve size when the percent F&E varied from 2 to 57% F&E at the 3:1 ratio. The study concluded that there may be an upper limiting value for F&E at the 3:1 ratio somewhere between 30 to 50%. The study further recommended that the F&E criteria be based on LA abrasion rather than just using one requirement for all aggregate and mix types.

Barksdale also related F&E values to abrasion loss in a Georgia DOT study *(5)*. Figure 2.1 summarizes the data from that study and was used by GDOT as the basis for increasing the maximum LA abrasion loss to 45% if the maximum 3:1 F&E value was held to 20%. However, the rutting criteria of 0.25 in., rut-testing equipment, and load and test temperature values used in Barksdale's study were different than that currently used by GDOT.

Test Procedure for F&E. The way GDOT determines F&E particles is also different than that specified in ASTM D 4791 so that more cubical aggregate is generally produced. The ASTM procedure uses the longest dimension (measured at the maximum elongation point) to thinnest dimension (measured at the maximum thickness point, not the average thickness), as shown in Figure 2.2a and Figure 2.2b to classify flat and elongated particles. The GDOT procedure, GDT 129, uses the

maximum length to average thickness to define flat and elongated particles. While the procedure has been used by GDOT for many years, it is somewhat subjective in that technicians have to estimate where the point of average thickness is.
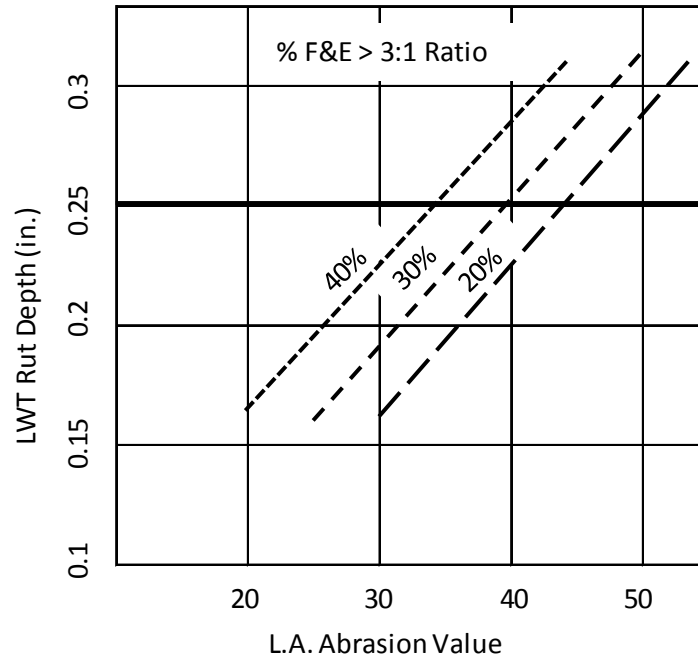
Figure 2.1 LWT Rut Depth as a Function of LA Value
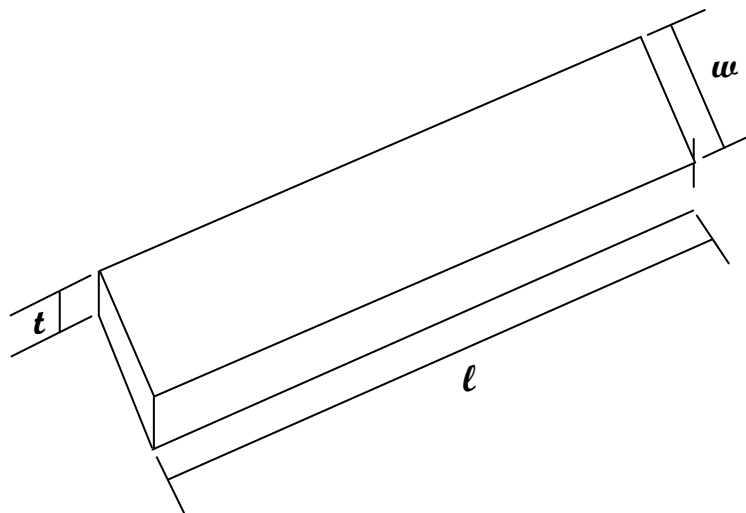
Figure 2.2 Dimensions for Calculating F&E (l:t)

17

An in-house study conducted by GDOT about ten years ago revealed that the 5:1 ratio for F&E by test method GDT 129 was almost equivalent to the 3:1 ratio determined by ASTM D 4791. The comparison was done in an effort to see if the nationally recognized ASTM procedure could be used instead of the state-specific GDT 129 procedure. It was found that most quarries in Georgia could meet the 3:1 ratio of F&E when the ASTM procedure was used.

Project Objectives

The objective of this study was to evaluate the performance of GDOT's SMA mixes designed with a high percentage of flat and elongated aggregate. The experimental hypothesis was that aggregates that meet GDOT's quality standards for conventional asphalt mixtures would also perform well in SMA mixtures.

Analysis

In order to evaluate the performance of high levels of F&E aggregate in SMA mixtures, a 12.5 mm nominal maximum-aggregate size (NMAS) SMA mixture with aggregate from a granite source approved for conventional dense-graded mixtures was constructed on Section N12.

The Columbus, Georgia, granite had 28% F&E particles when tested at the 3:1 ratio, according to the GDT test procedure. Otherwise, typical GDOT procedures and materials were used; the SMA mixture used SBS polymer-modified PG 76-22 binder and 1.0% hydrated lime and was designed using the 50-blow Marshall procedure. The design resulted in an optimum asphalt content of 6.5% with an average VMA of 19.1%. The mix was produced at a production temperature of 340˚F and was compacted to 94.7% of theoretical density on the roadway.
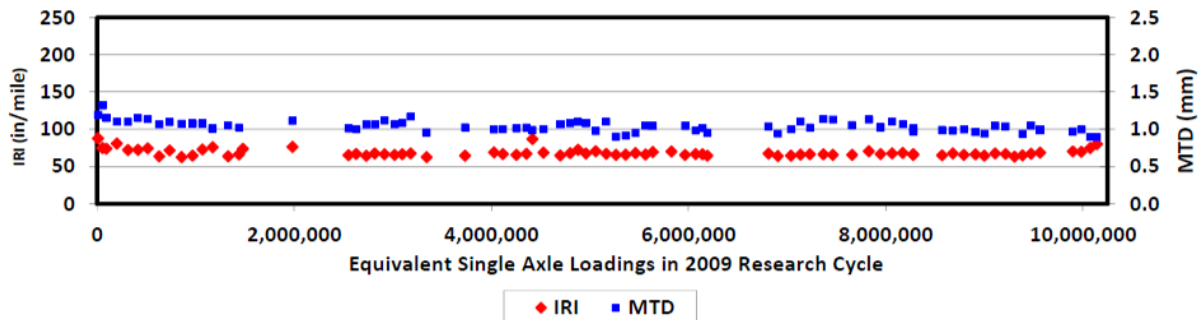
After more than 10 million ESALs, the mix performed very well with respect to rutting resistance with less than 5 mm of total rutting being measured, as shown in Figure 2.3. In fact, the figure shows that the only apparent rutting resulted from the initial consolidation under traffic at the onset of trafficking.
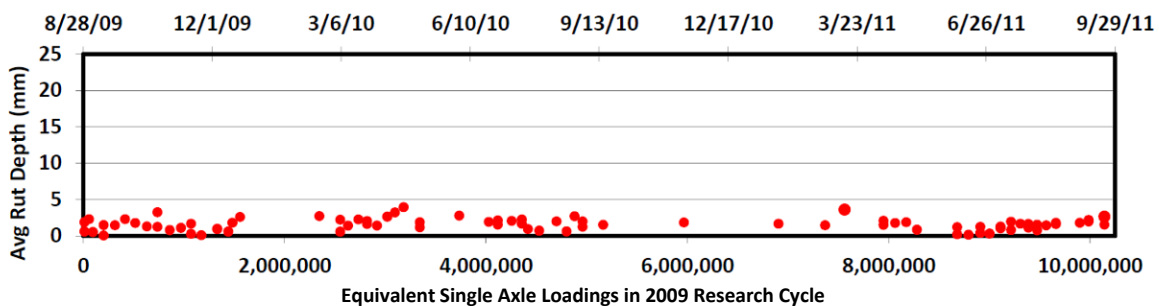
Figure 2.3 SMA Rutting Performance

Another concern was that fractured aggregate from the F&E coarse aggregate material would increase the potential for stripping. This distress often results in increased roughness and increased mean texture depth as the fractured particles ravel out under traffic. Smoothness and mean texture depth of the track

sections measured using NCAT's Automatic Road Analyzer (ARAN) van show that these surface characteristics for Section N12 (Figure 2.4) were unchanged throughout the two-year testing cycle.

Figure 2.4 Mean Texture Depth and IRI Performance of Section N12

The F&E particles did not appear to have a detrimental effect on the fatigue life of the SMA. After more than 10 million ESALs, there was no cracking evident within the test section.

Conclusions/Recommendations

1. The use of aggregate with up to 28% F&E particles as measured by GDT 129 at the 3:1 ratio performed well with respect to rutting resistance, resistance to raveling, and cracking resistance. Based on these results, GDOT could increase the maximum allowable F & E value from 20% to 29% at a 3:1 ratio as determined by GDT Procedure 129 without adversely affecting performance of SMA mixtures.
2. Specifications for SMA aggregate properties that were based on early guidelines may be too restrictive and may eliminate materials that will perform well under heavy loading conditions. Agencies are encouraged to use mixture performance testing as a practical manner for setting specification limits.

2.2 Mississippi DOT Evaluation of Open-Graded Friction Course Mixture Durability and 45% RAP Mix Performance

Background

The Mississippi DOT (MSDOT) has sponsored research at the NCAT Pavement Test Track since the first cycle. Most of its experiments have focused on using gravel aggregate native to the state in different mix types. In the first cycle of the test track, Superpave and SMA mixes using Mississippi gravel were put to the test and performed extremely well. Both test sections were left in place for the second cycle. The Superpave mix began to show extensive block cracking during the second cycle. Cores showed that the cracks were limited to the upper two layers of the pavement. No cracking was observed in the SMA test section.

Mississippi also sponsored a test section in 2003 to evaluate a 4.75 mm nominal maximum aggregate size (NMAS) mix. The mix contained limestone screenings, crushed gravel, natural sand, and an SBS-modified PG 76-22 binder. The mix, placed approximately 0.8 inches thick, has remained in place through three cycles and now has endured 8 years of extreme traffic with no signs of distress.

In the third cycle, the original Mississippi Superpave mix was replaced with a new Superpave surface layer designed with fewer gyrations to be consistent with the MSDOT specifications at the time. The original mix design used 100 gyrations in accordance with the AASHTO standards at the time; the 2006 mix design used 85 gyrations.   However, the plant-produced mixes had almost the same volume of effective binder. The performance of the 2006 mix was similar to that of the original MSDOT Superpave mix on the test track, with very little rutting but extensive block cracking. MSDOT also constructed a 1.3-inch OGFC surface layer using 100% gravel on top of a gravel SMA mix in the third cycle. The 12.5-mm NMAS OGFC and SMA combination performed so well through the cycle that MSDOT began using OGFC over SMA on several interstate jobs in 2009.

Objectives

For the fourth cycle, MSDOT elected to continue trafficking on the OGFC test section (S3) to better assess its durability. MSDOT also designed and sponsored a new Superpave mix test section, but this time the mix contained 45% RAP. Since the current maximum amount of RAP allowed in surface mixes by MSDOT is 15%, this was a bold experiment.

Design and As-Built Properties of the Mississippi Gravel OGFC

Tables 2.1 and 2.2 show the mix details for the OGFC mixture.

Table 2.1 MSDOT OGFC Mix Design Information

Design Gyrations	50	
Asphalt Binder	PG 76-22 (SBS modified)	6.4%
Aggregates		
	-3/8" +8 Monticello gravel	63.4%
	-1/2" Georgetown gravel	35.6%
	Hydrated Lime	1.0%
Fibers	Cellulose	0.3%

Table 2.2 Properties of the MSDOT OGFC Mix

Sieve	Mix Design	Quality Control
½" (12.5 mm)	100	100
3/8" (9.5 mm)	93	92
No. 4 (4.75 mm)	23	31
No. 8 (2.36 mm)	11	12
No. 16 (1.18 mm)	10	9
No. 30 (0.60 mm)	9	8
No. 50 (0.30 mm)	7	6
No. 100 (0.15 mm)	5	5
No. 200 (0.075 mm)	4.2	3.8
Asphalt Content (%)	6.4	6.7
Lab Air Voids (%)	20.0	21.8
In-Place Density (% of Gmm)		75.7

Test Track Performance of the Mississippi OGFC

The Mississippi OGFC section continues to perform well but began a steady progression of raveling during its second cycle. Photographs of the test section taken after the second cycle are shown in Figures 2.5 and 2.6. The foreground of Figure 2.5 shows extensive raveling (close-up shown in inset) in the right wheelpath of the beginning of the section. This is a common construction defect with OGFC layers due to the initial portion of the mix cooling too much as it comes in contact with unheated parts of the transfer device and the paver. As noted in Chapter 1, the first and last 25 feet of each test section are excluded from performance analysis due to transition effects such as this.

Figure 2.5 Photograph of the Initial Part of the Gravel OGFC Test Section after Two Cycles

**Figure 2.6 Photograph of the Mississippi Gravel OGFC Section Beyond the Transition Area**

No cracking has been observed in the test section. Permanent deformation in the wheelpaths is only 6.3 mm after more than 20 million ESALs. Surface macrotexture, measured using a high-speed laser in the wheel path via NCAT's ARAN van, is shown in Figure 2.7. For comparison, the surface texture data for

two previously constructed OGFC test sections are also shown. These data show that the texture of the MS gravel OGFC section began to increase after about 10 million ESALs, which is indicative of the raveling.
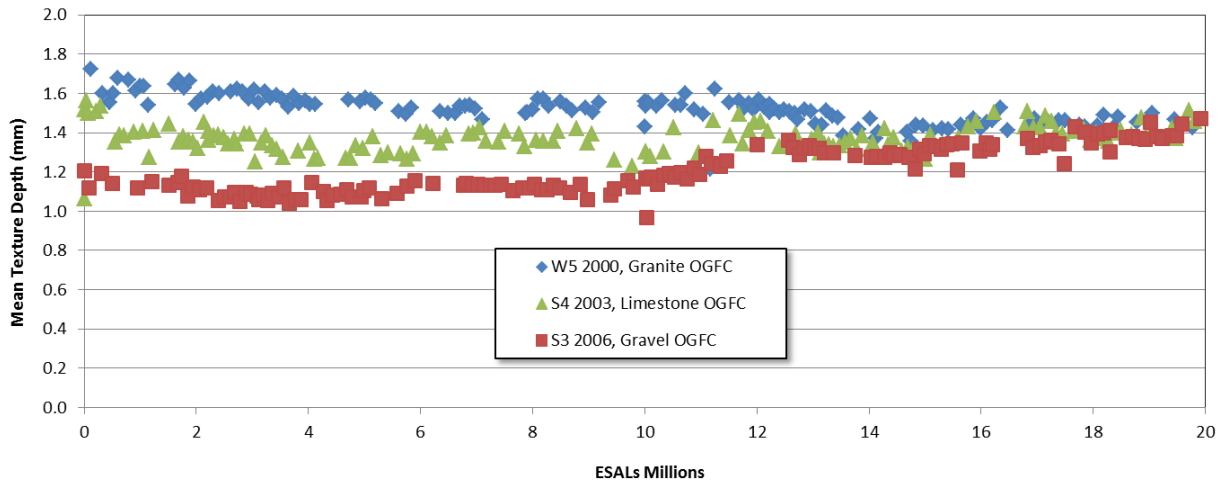
Figure 2.7 Plot of Mean Texture Depth for OGFC Sections Through Two Cycles

Pavements roughness, quantified using IRI, for these same OGFC sections are shown in Figure 2.8. These data show that all the OGFC sections maintained excellent smoothness through two cycles. Although the IRI results for the MS gravel section are slightly higher than for the other OGFC sections, it is still a very smooth section, and there does not appear to be any change through two cycles.
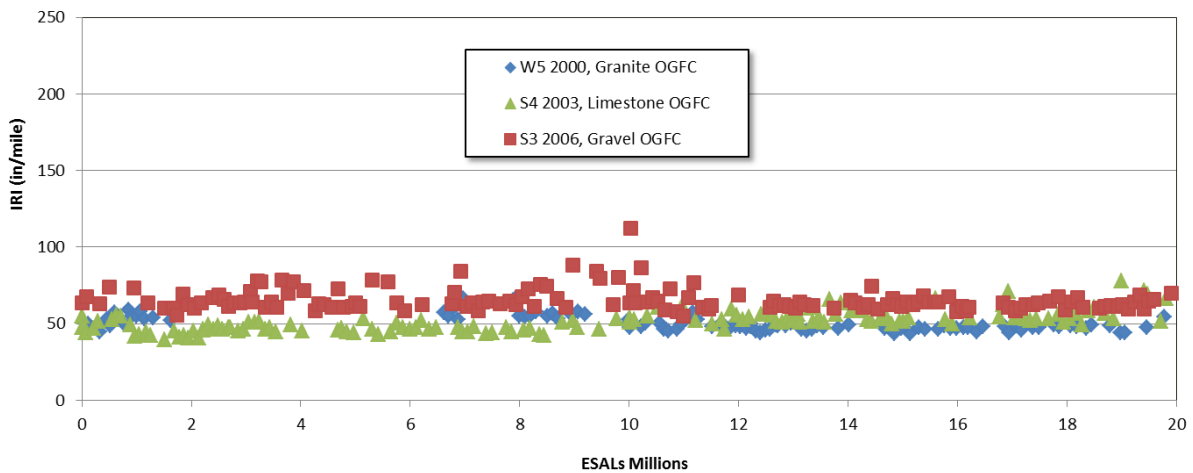

Figure 2.8 IRI for OGFC Test Sections Through Two Cycles

Permeability of OGFC sections on the test track were measured using two methods. The first method was measured on the track surface using the falling-head field permeameter. Results for this method, shown in Figure 2.9, indicate that permeability of the gravel OGFC layer remains very high and appears to be increasing slightly with time. It is important to note that no treatments have been applied to the

23

test sections for snow or ice. Use of treatments for snow and ice containing fine aggregate are believed to clog OGFC layers and significantly diminish their effectiveness.
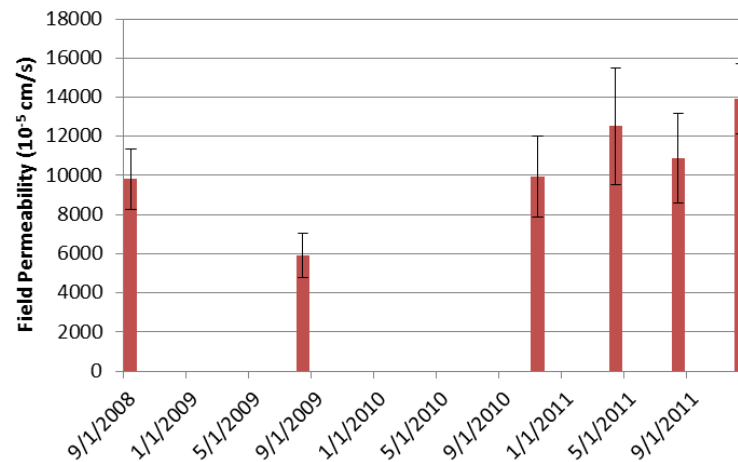
Figure 2.9 Field Permeability Results for the MS Gravel OGFC

Design and As-Built Properties of the Mississippi DOT High RAP Section

The MSDOT high RAP content test section was constructed by milling four inches from the existing test section (S2), followed by two lifts of the new 9.5-mm NMAS, 45% RAP mix. A summary of the 45% RAP mix design prepared by MSDOT is shown in Table 2.3. For comparison, the mix design for the 15% RAP mix used in the previous cycle is also included. For the 2009 45% RAP mix, the binder contributed by the two RAP stockpiles was 2.28%, or 41% of the total binder content. NCAT's quality control data for the mixes sampled during production are shown in Table 2.4.

Table 2.3 Mix Design Information for MSDOT 2006 15% RAP and 2009 45% RAP Mixes

Mix/Year Const.	15% RAP, 2006		45% RAP, 2009	
Design Gyrations	85		85	
Asphalt Binder	PG 7-22	6.1%	PG 67-22 (unmodified)	5.6%
Aggregates				
Agg. 1	-3/8 Monticello	61%	Crystal Springs ½" gravel	20%
Agg. 2	-3/8 +#8 Monticello	13%	Crystal Springs 3/8" gravel	26%
Agg. 3	Mount Olive sand	10%	Crystal Springs coarse sand	8%
RAP 1	S2 Millings	15%	S2 Millings	15%
RAP 2			Newton RAP	30%
	Hydrated Lime	1%	Hydrated Lime	1%

Table 2.4 Properties of the MSDOT 45% RAP Mix

Sieve	Mix Design	Quality Control	
		Binder	Surface
¾" (19.0 mm)	100	100	100
½" (12.5 mm)	97	98	98
3/8" (9.5 mm)	93	93	95
No. 4 (4.75 mm)	61	62	62
No. 8 (2.36 mm)	39	40	40
No. 16 (1.18 mm)	28	29	29
No. 30 (0.60 mm)	21	21	22
No. 50 (0.30 mm)	13	13	14
No. 100 (0.15 mm)	7	8	9
No. 200 (0.075 mm)	5.6	6.6	7.2
Asphalt Content (%)	5.6	5.3	5.2
Lab Air Voids (%)	4.0	4.0	5.0
VMA (%)	15.1	14.9	15.6
VFA (%)	74	73	68
In-Place Density (% of Gmm)		93.8	92.1

Test Track Performance of the Mississippi High RAP Content Mix

The 45% RAP mix with Mississippi gravel has performed very well. Only 3.0 mm of deformation was measured in the wheelpaths at the end of the cycle. Figure 2.10 shows a map of the cracking in the section at the end of the cycle. All of these cracks are low severity (< 6mm wide) and are primarily between the wheelpaths. Since they are in different locations than the previous cycle, reflection cracking can be ruled out as a cause. Although the cracking may be related to environmental aging and/or paver induced segregation, since the same virgin binder and equipment were used in other test sections that have not had any cracking, there are likely other contributing factors. Since block cracking has been evident with all of the Mississippi Superpave mix test sections since the first cycle, it seems logical that there is an interaction effect involving aggregate characteristics. The total length of cracking for the section was 61 feet. This compares to 80 feet of cracking for the Superpave mix with 15% RAP previously used in this test section after one cycle. Therefore, the 45% RAP mixture appears to perform equal or better than the mixture with 15% RAP.
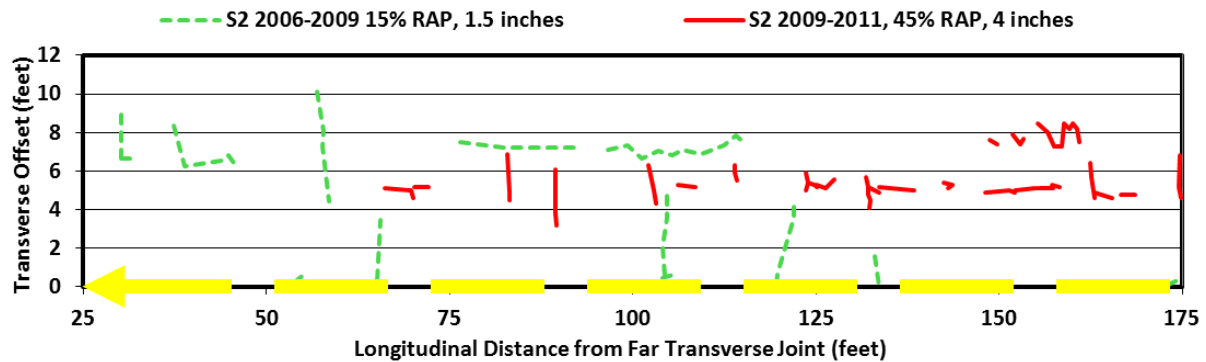
Figure 2.10 Crack Map for Section S2 at the End of Respective Cycles for the 15% and 45% RAP Mixes

Figure 2.11 shows photographs of the test section taken after trafficking was completed for the cycle. A close-up photograph of one of the cracks is shown in the inset. The other cracks in the test section had a similar appearance.


Figure 2.11 Photograph of the MSDOT 45% RAP Test Section after Once Cycle

Figure 2.12 shows the texture change of the Mississippi 45% RAP mix through the cycle. The same data for the Mississippi Superpave 15% RAP mix from the previous cycle is shown for comparison. The mix with 45% RAP has a slightly higher increase in macrotexture through one cycle.

26
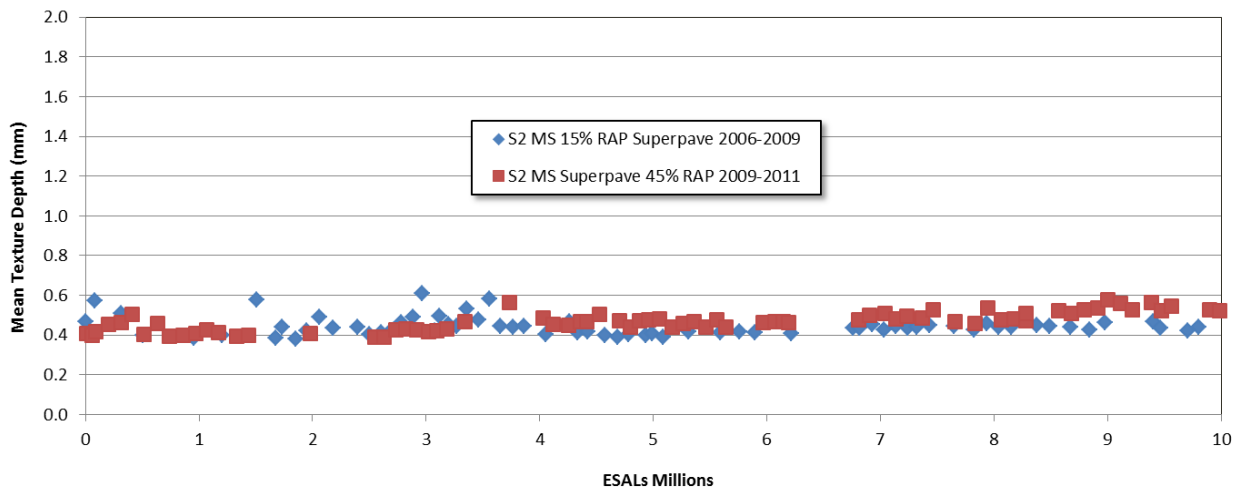
Figure 2.12 Mean Texture Depth for Mississippi 15% and 45% RAP Test Sections after One Cycle

Pavement smoothness results for the MSDOT test sections are shown in Figure 2.13. The IRI data for the 45% RAP mix test section are slightly higher than for the 15% RAP mix previously used in this section. However, since the data for both sections are very consistent throughout the respective cycles, the slight difference in smoothness is probably due to construction effects rather than an effect of the mix or RAP content.
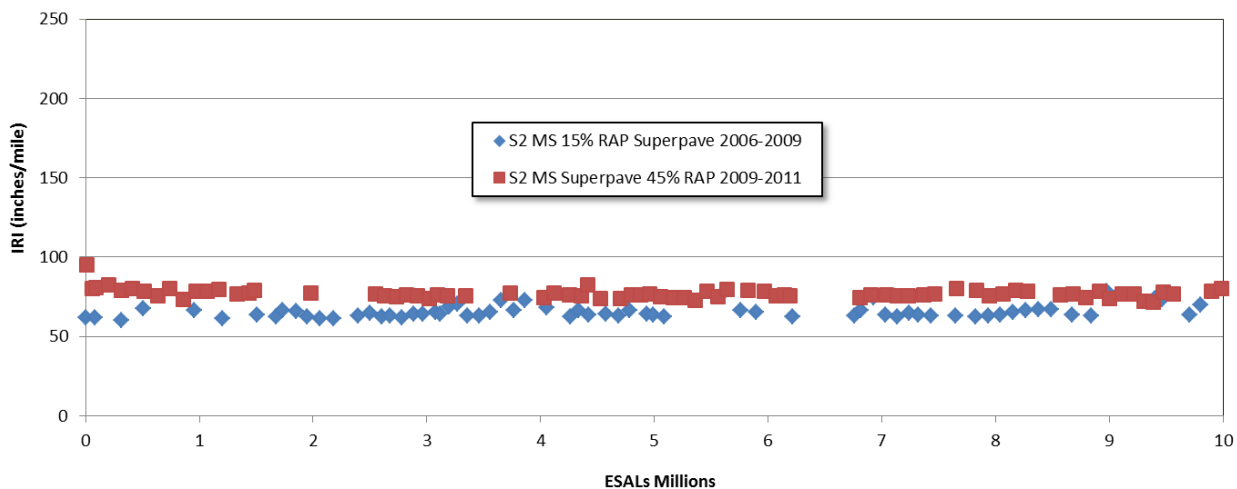
Figure 2.13 Comparison of IRI for the 15% and 45% RAP Mixes from Mississippi

Mix Design Economics

Since the primary motivation to use higher RAP contents is to reduce the cost of pavements, a simple examination of the potential savings is provided in Table 2.5. Assumed materials costs were used with the mix designs used in the past two cycles to estimate the total mix costs, not including production or placement and compaction costs. The 45% RAP mix cost is 47% lower than the mix with 15% RAP due largely to the reduced virgin binder content and the lower cost of the unmodified binder. These savings and the performance of the 45% RAP test section are compelling evidence for higher RAP contents.

27

Table 2.5 Comparison of Example Mix Design Costs for a 15% and 45% RAP Mix

15% RAP Mix (2006 Mix)				45% RAP Mix (2009 Mix)			
Components	*% of Mix*	*Cost/Ton*		*Components*	*% of Mix*	*Cost/Ton*	
PG 76-22	6.1%	$750	$45.75	PG 67-22	3.3%	$600	$19.80
Aggregates	77.1%	$15	$11.56	Aggregates	50.7%	$15	$7.61
Hydrated Lime	1%	$150	$1.50	Hydrated Lime	1%	$150	$1.50
RAP	15%	$6	$0.90	RAP	45%	$6	$2.70
Total	100		$59.71	Total	100		$31.61

Conclusions

- When constructing OGFC mixtures, a common defect occurs at the start of paving due to the placement of mix that may be cooled by contact with cooler paving equipment and due to handwork of the mix at the construction joint. Training for paving crews that place OGFC mixes should discuss best practices for minimizing this issue.
- Using Mississippi gravel in OGFC mixes can provide good performance for a few years. Performance measurements on the test track show that the OGFC is rut resistant, provides very good smoothness, and maintains excellent permeability provided that winter maintenance activities do not apply materials that clog the porous layer. However, raveling of the gravel OGFC does appear to increase after a few years.
- The Mississippi 45% RAP test section performed very well, with only 3 mm of rutting through 10 million ESAL applications. The cracking that has occurred in the test section is low severity and is mostly between the wheelpaths. This type of cracking has occurred with previous test sections using Mississippi gravel in Superpave mixes.
- An estimated 47% materials savings can be achieved by using 45% RAP compared to the current limit of 15% RAP. This estimated savings is largely due to the reduced virgin binder content and the

2.3 Missouri DOT Evaluation of a Crumb Rubber-Modified Asphalt Mixture

The utilization of scrap tire rubber in asphalt started in the mid-1960s when ground rubber was placed in asphalt surface treatments, such as chip seal applications. Later, in the 1970s, crumb rubber-modified (CRM) asphalt chip seals were used as a stress-absorbing membranes interlayer (SAMI). Its use extended to hot mix asphalt (HMA) and has continued to evolve due to the rubber's enhancement of mixture performance, including improved rutting resistance, and cracking resistance. Other reported benefits include reduction in maintenance, improved smoothness, enhanced skid resistance, and noise reduction *(6, 7, 8).*

While the environmental benefits of using CRM asphalt mixtures are important, some state agencies and contractors are investigating CRM asphalt mixtures as a substitute for using polymers in asphalt mixtures such as styrene-butadiene-styrene (SBS). If CRM mixtures can perform equivalently to polymer-modified mixtures, state agencies and contractors will have an alternative modifier if another polymer shortage occurs.

Objective

The objective of this research was to determine if CRM asphalt could adequately replace SBS in dense-graded Superpave mixtures without sacrificing mixture performance. To accomplish this objective, an asphalt mixture containing 11% #40 mesh ambient ground mesh rubber and an SBS-modified asphalt mixture were placed on the NCAT Test Track. The field performance of these two mixtures were monitored for 10 million equivalent single axle loads (ESALs) to determine if there was any overall difference in mixture rutting, cracking, texture, and smoothness. Additionally, mix was sampled during construction and taken to the NCAT laboratories, where standard asphalt mixture performance tests were used to characterize the mixtures for resistance to rutting, cracking, and moisture damage.

Methodology

In 2009, the Missouri Department of Transportation built two test sections at the Test Track to determine if CR would be an adequate substitute for SBS in asphalt mixtures. These two test sections were constructed on a thick pavement foundation to ensure the distresses (whether cracking or rutting) were indicative of the surface mixture's performance and not the subgrade or base material.   The underlying pavement structure for the test sections includes 23 inches of asphalt mix, a dense-graded aggregate base and a firm subgrade soil. Descriptions of this cross-section have been documented elsewhere (*9*).

One test section used a 12.5 mm nominal maximum aggregate size (NMAS), 100 gyration, SBS-modified dense-graded Superpave surface mixture. The second test section used a similar aggregate skeleton and compactive effort; however, instead of modifying the asphalt with polymer, a PG 67-22 asphalt binder was terminally blended with 11% rubber and 4.5% transpolyoctenamer (TOR) by weight of the rubber to act as a co-linking agent between the rubber and the asphalt binder. Both mixtures were constructed 1.75 inches thick at approximately 93% density. Quality control gradations and volumetrics for both mixtures are given in Table 2.6. The primary difference between the two mixtures is the asphalt content. The CR-modified asphalt mixture had a 0.6% higher binder content. This reduced the mixture's air voids to 3.5%.

Table 2.6 Mixture Quality Control Results

Percent Passing – QC Gradation		
Sieve Size	**CRM**	**SBS**
3/4"	100	100
1/2"	97	96
3/8"	89	86
#4	59	55
#8	37	34
#16	22	21
#30	13	13
#50	9	9
#100	7	7
#200	5.6	5.4
Mix Information		
Quantity	**CRM**	**SBS**
Design Gyrations	100	100
Virgin Binder Grade	PG 67-22	PG 76-22
Binder Additive	GTR	SBS
QC Binder Content	6.0	5.4
Effective Binder Content	5.1	4.5
QC VMA	15.0	14.8
QC Air Void Percentage	3.3	4.5
Dust-to-Binder Ratio	1.1	1.2

Laboratory Evaluation

Each mixture was evaluated in the laboratory to evaluate the mixtures' resistances to various distresses. A list of laboratory tests conducted with the associated method are provided in Table 2.7. The laboratory tests were conducted to assess the susceptibility of the mixture to moisture damage, rutting, and cracking. Additional test results for these two mixtures have been documented elsewhere (*10*).

Table 2.7 Testing Plan

Test	Method	Assessment
Performance Grade of Asphalt Binder	AASHTO M320-10	Binder Properties
Tensile Strength Ratio	AASHTO T283-07	Moisture Susceptibility
Asphalt Pavement Analyzer	AASHTO TP63-09	Rutting
Flow Number	AASHTO TP 79-09	Rutting
Energy Ratio	University of Florida	Surface Cracking

Results

The following subsection documents the results of the laboratory tests conducted on the CRM and SBS binders and mixtures.

Binder Grade. The binders in the asphalt mixtures were sampled from the tank at the plant and tested at the NCAT binder laboratory to determine the performance grade (PG) in accordance with AASHTO M 320-10. Table 2.8 summarizes the true grade and performance grade of each binder. The results confirmed that all binders used in the construction of the two sections were PG 76-22 binders, as requested by the Missouri Department of Transportation. While both binders were classified using the PG system as PG 76-22 binders, the CRM binder has a high-temperature true grade 5.1°C higher than the SBS-modified binder. Thus, the CRM binder is expected to be stiffer at hotter temperatures and, thus, more resistant to rutting. The higher critical temperature for the CRM asphalt binder reflected the binder being engineered to meet Missouri's elastic recovery specification.

Table 2.8 Binder Test Results for Missouri Mixtures

Mixture	True Grade	Performance Grade
CRM	81.7 – 25.0	76 – 22
SBS	76.6 – 26.3	76 – 22

Moisture Susceptibility. Table 2.9 provides the average conditioned tensile strength, average unconditioned tensile strength, and tensile-strength ratio for each mixture. AASHTO M323-07 recommends a tensile strength ratio (TSR) (the ratio of conditioned indirect tensile strength to unconditioned indirect tensile strength) of 0.8 and above for moisture-resistant mixes. While the CRM mixture has a higher TSR value, the TSR values for both mixtures exceed the criterion of 0.80, suggesting the mixtures are resistant to moisture damage.

Two-sample *t*-tests ($\alpha = 0.05$) were conducted to compare the tensile strengths of the two mixtures in both the conditioned and unconditioned states. The CRM mixture was statistically stronger in indirect tension at room temperature than the SBS mixture in both the conditioned ($p = 0.001$) and unconditioned ($p = 0.006$) states.

Table 2.9 TSR Results for Missouri Mixtures

Mixture	Average Conditioned Tensile Strength, psi	Average Unconditioned Tensile Strength, psi	TSR
SBS	148.1	171.4	0.86
CRM	203.3	220.0	0.92

Rutting Susceptibility. Both the CRM and SBS mixtures were assessed for rutting using the Asphalt Pavement Analyzer (APA) and Flow Number (FN) tests. The average APA rut depths and flow numbers for both mixtures are given in Table 2.10. Detailed test results are provided in Appendix A.

Table 2.10 Rutting Laboratory Test Results

Mixture	APA Results		Flow Number Results	
	Rut Depth, mm	COV, %	Flow Number, cycles	COV, %
CRM	1.37	17.5	659	24.8
SBS	1.41	24.4	321	19.3

A statistical two-sample *t*-test of the rut depths from the six samples (α = 0.05) was not able to distinguish any difference between the APA rut depths measured in the CRM and SBS mixtures. However, the APA is typically used as a "go/no go" test to prevent production of rutting-susceptible mixtures. A maximum rut depth of 5.5 mm in the APA was previously established as for mixtures having less than 12.5 mm of rutting at the test track under 10 million ESALs of trafficking. Both mixtures had fewer than 5.5 mm of rutting; therefore, they were expected to resist rutting in the field.

When comparing the results of the flow number test, numerically, the CRM mixture withstood over twice as many repeated loads as the SBS mixture before reaching tertiary flow. A two-sample *t*-test (α = 0.05) confirmed statistically the CRM mixture has superior resistance to permanent deformation (p = 0.028) using the flow number test. Overall, both mixtures were proven rut-resistant, but the flow number test suggests the CRM mixture could be more resistant to rutting. This is possibly the result of the critical high-temperature grade of the CRM binder being more than 5°C higher than the SBS binder.

Cracking. As both mixtures were placed on a very thick pavement structure in a southern climate, the primary cracking distress assessed for this mixture was surface cracking, also referred to as top-down cracking. The energy ratio was developed to assess the resistance of a mixture to surface cracking. The larger the energy ratio, the more crack-resistant a mixture should be. Based on recommendations from the developer of this method, if a mixture has an energy ratio greater than 1.95, it should be able to withstand 1,000,000 ESALs of trafficking per year (*11).*

After testing each mixture for resilient modulus, creep compliance, and indirect tensile strength at 10°C using the protocol described elsewhere in the report the CRM had an energy ratio of 4.96 while the SBS mixture had an energy ratio of 4.43. Both mixtures exceeded the current criterion of 1 million ESALs of trafficking per year, with the CRM mixture being slightly more resistant to cracking.

Field Performance. After 10 million ESALs, neither mixture has shown signs of cracking. Both test sections have smoothness values of approximately 50 in/mile and rut depths less than 5 mm. The primary difference between these two test sections is texture. When constructed, the SBS mixture had almost 0.5 mm more texture than the CRM mixture; however, neither mixture has gained texture over the course of trafficking. Therefore, neither mix has proven to be susceptible to raveling in the field.

Summary

The primary objective of this study was to determine if a CRM asphalt mixture could perform as well as or better than a polymer-modified asphalt mixture. The Missouri DOT sponsored the experiment to

compare two surface mixtures on the NCAT Pavement Test Track. Additionally, laboratory experiments were performed to compare the moisture susceptibility, rutting susceptibility, and cracking performance of the two mixtures. Both laboratory tests and field measurements show CRM mixtures can perform as well or better than polymer-modified mixtures.

CHAPTER 3   STRUCTURAL EXPERIMENTS

3.1 Perpetual Pavements and High-Polymer Mix (HPM) Rehabilitation

Background

Although the concept of perpetual pavements was introduced about 10 years ago, few pavement designs have utilized the ideas to actually engineer such long-life, low life-cycle-cost pavement structures. According to the Asphalt Pavement Alliance, perpetual pavements are designed to avoid damage to lower pavement layers so that the pavement structure will last more than 50 years without major structural rehabilitation or reconstruction. Only periodic surface renewal (e.g., preservation treatments) is needed to maintain a high standard for smoothness and safety. In 2006, the Oklahoma Department of Transportation (OKDOT) sponsored two test sections to compare a perpetual pavement design to a conventional pavement design based on current AASHTO standards.

Objective

The first objective of this investigation was to compare the performance of an intentionally designed perpetual pavement against a section designed to have a terminal life expectancy. The second objective was to evaluate the effectiveness of several rehabilitation treatments of the non-perpetual pavement.

Test Sections and Performance

The sections used in this investigation were originally placed on the NCAT Pavement Test Track in 2006. Figure 3.1 illustrates the cross-sectional history of Section N8 (non-perpetual) and N9 (perpetual). As shown in the figure, the non-perpetual section received two rehabilitation treatments after original construction, while the perpetual section survived both the 2006 and 2009 traffic applications (approximately 20 million equivalent single axle loads (ESALs)).   The performance history was divided into three main parts, coinciding with the three cross-sections shown in Figure 3.1 for N8. Each of the subsections below provides further details of each phase in terms of performance and rehabilitation.
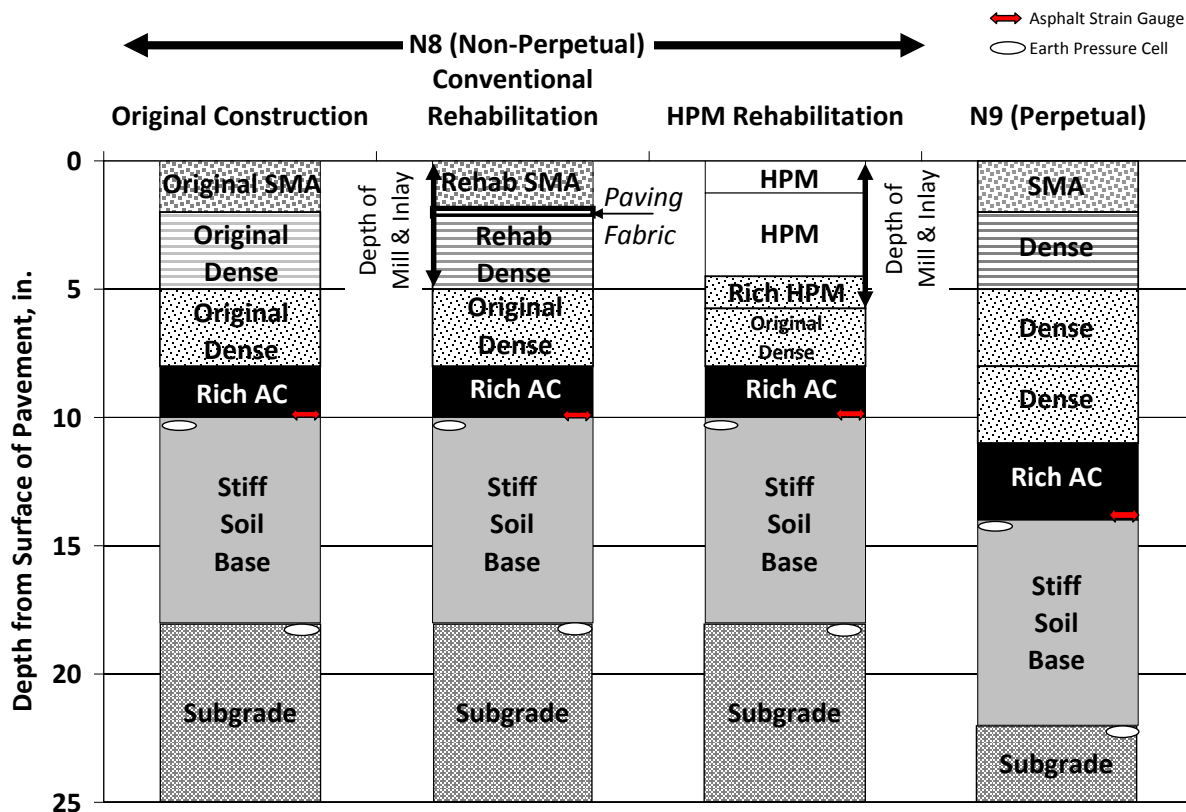
Figure 3.1 Cross-Sectional History of N8 and N9

Phase I – Original Construction. Section N8 was the thinner of two test sections sponsored by OKDOT in the 2006 NCAT Pavement Test Track research cycle to study the perpetual pavement thickness design concept. The pavement thickness for this section was based on the 1993 AASHTO pavement design guide. The original stiff test track subgrade under these two sections was excavated to a depth of 4 feet and replaced with a soft subgrade that was more representative of soils in Oklahoma. The top 8 inches of the imported soft subgrade was replaced with the same stiff material that had been removed to simulate lime stabilization. As seen in Figure 3.1, Section N8 had a total asphalt thickness of 10 inches, consisting of a 2-inch rich bottom layer, 6 inches of dense Superpave mix, and a 2-inch stone matrix asphalt (SMA) surface. The rich-bottom layer was a mixture designed to 2% air voids rather than 4% in the other Superpave layers (thus, a higher binder content). All of the asphalt layers used aggregates hauled from Oklahoma and asphalt binder grades consistent with OKDOT specification. Information on the design, production, and placement of all the layers in both sections has been previously documented (*1, 12, 13*). Roughness began to increase in Section N8 near the end of the 2006 research cycle after approximately 7 million ESALs. Cracking first reached the surface after 8.3 million ESALs, and the section was in need of rehabilitation by the end of the 2006 cycle (i.e., 10 million ESALs). Conversely, the perpetual section (N9) had performed well during the same trafficking cycle with minimal rutting and no cracking.

Phase II – Mill-and-Inlay with Paving Fabric. As seen in Figure 3.1, the initial rehabilitation of the failed section consisted of a conventional 5-inch mill-and-inlay, which is OKDOT's standard practice for the type of structural failure observed. The 5-inch inlay consisted of 3 inches of dense Superpave mix under

2 inches of SMA. The mill and inlay was conducted prior to reopening the test track to traffic for the 2009 research cycle. The mixes used for this inlay were identical to the original mixes placed in the structure. At the request of OKDOT researchers and the approval of the particular geotextile suppliers, fabric interlayers were used in two different areas of the inlay to determine if they would improve resistance to reflection cracking.

Although cracks took longer to appear in the areas where the fabric interlayers were placed, the pavement condition deteriorated more rapidly in the areas where fabric interlayers were installed relative to those areas without fabric interlayers. Figure 3.2 illustrates the failed pavement surface in the most severely distressed area, which was in close proximity to the installed paving fabric. The cracks in this picture are primarily surface shearing cracks, though cracking did extend down into the pavement structure, as confirmed forensically. The rehabilitated structure was completely failed after approximately 3.5 million ESALs, at which point other rehabilitation options were considered. Section N9 (perpetual) continued to perform very well with minimal rutting and no cracking, as shown in Figure 3.2.

Figure 3.2 N8 Pavement Failure after Conventional Mill and Inlay

Phase III – Mill-and-Inlay with High-Polymer content Mix (HPM). A nearby, newly constructed and unrelated highly polymer modified (HPM) section exhibited excellent performance (N7). The section had three lifts of HPM with 7.5% low viscosity styrene-butadiene-styrene (SBS) polymer modification. The 2.25-inch base lift and 2.25-inch intermediate lift were both ¾" NMAS with 7.5% SBS polymer in the binder, while the 1.25-inch thick wearing course was designed with a 3/8-inch NMAS aggregate blend. The PG grade of the binder containing the 7.5% polymer content was PG 88-22. OKDOT officials

endorsed using the HPM design but elected to change the bottom lift of the inlay to a rich 3/8 inch NMAS mix, duplicating the wearing course composition and thickness. The thickness of the intermediate layer was increased to 3.25 inches to accommodate the change in the lower layer.

Fabric interlayers were not used in the second rehabilitation of N8. No unusual problems were encountered in the production or placement of the HPM mix. This rehabilitation strategy performed very well for the remaining part of the cycle. After more than 5.5 million ESALs on the HPM rehabilitation (2 million more ESALs than the conventional rehabilitation), no changes in pavement condition have been noted. No cracking has been observed and measured rutting was less than 1/8 inch.

Structural Characterization

The sections were subjected to both falling weight deflectometer (FWD) and dynamic pavement response testing over the two-year research cycle to measure structural integrity. Figure 3.3 illustrates the backcalculated asphalt concrete modulus, normalized to 68˚F, for the perpetual section (N9) and the non-perpetual section (N8). N8 is further subdivided into before and after the HPM mill and inlay was applied. The differences before and after the HPM are clearly visible. Both the magnitude and variability of the modulus appeared to change dramatically after the HPM. The average modulus before the HPM inlay was 500,000 psi, while it increased to an average of 721,000 psi after the inlay (44% increase). Furthermore, the coefficient of variation (standard deviation/mean) in the "before HPM" condition was 36%, while it was reduced to 25% in the "after HPM" condition. Highly variable and relatively low moduli would be expected for a deteriorating pavement. The HPM appears to not only increase the modulus of the section, but also make it more homogeneous throughout with less overall variability on any given date of testing. N9, in contrast, maintained relatively constant and high moduli throughout the entire two-year trafficking cycle, indicative of a non-deteriorating pavement.

Figure 3.1 indicated the placement of earth pressure cells and asphalt strain gauges for the direct measurement of pavement response. Weekly measurements were made during the two-year cycle in each section. Figure 3.4 summarizes the average temperature-normalized pavement response and standard deviation for N8 (before and after HPM) and N9 (perpetual). As expected, given the significant differences in asphalt modulus before and after the HPM placement, there was a significant reduction in tensile strain, base and subgrade pressure after the HPM was placed. Asphalt strain was reduced by approximately 20%, base pressure by nearly 48%, and subgrade pressure by 20%. Statistical *t*-testing (α = 0.05) indicated all these differences were significant. The perpetual section, with its overall greater AC thickness, maintained very low pavement responses throughout the research cycle with an average strain less than 70 $\mu\varepsilon$ at 68˚F, which likely contributed to its superior performance.
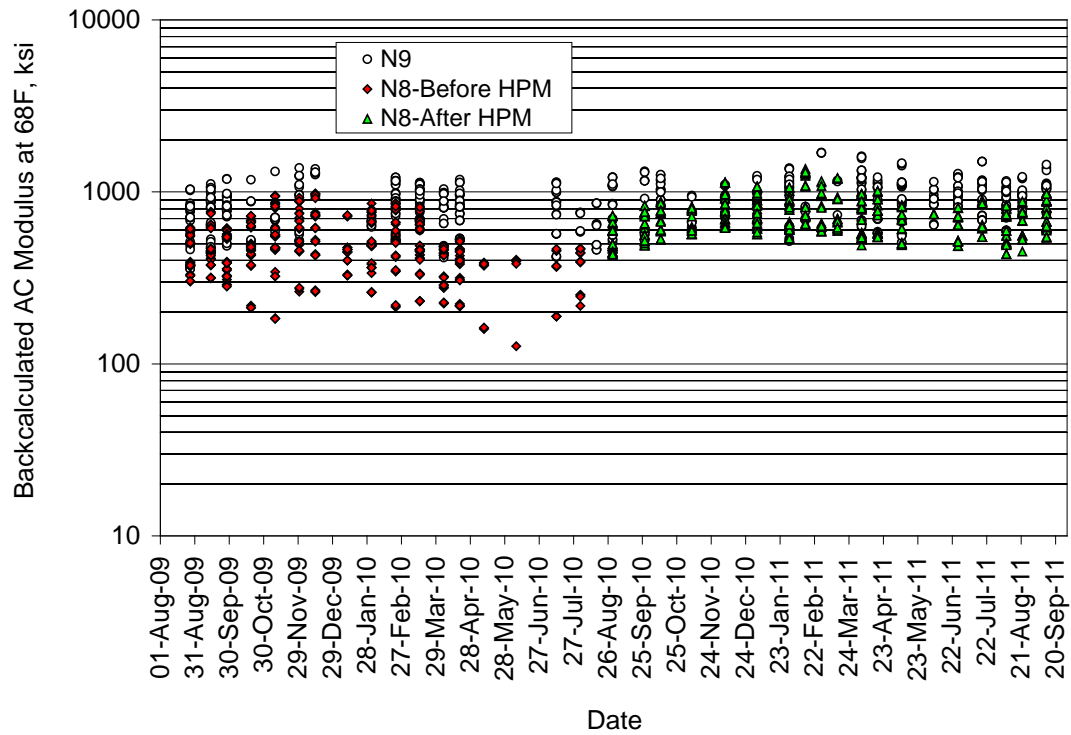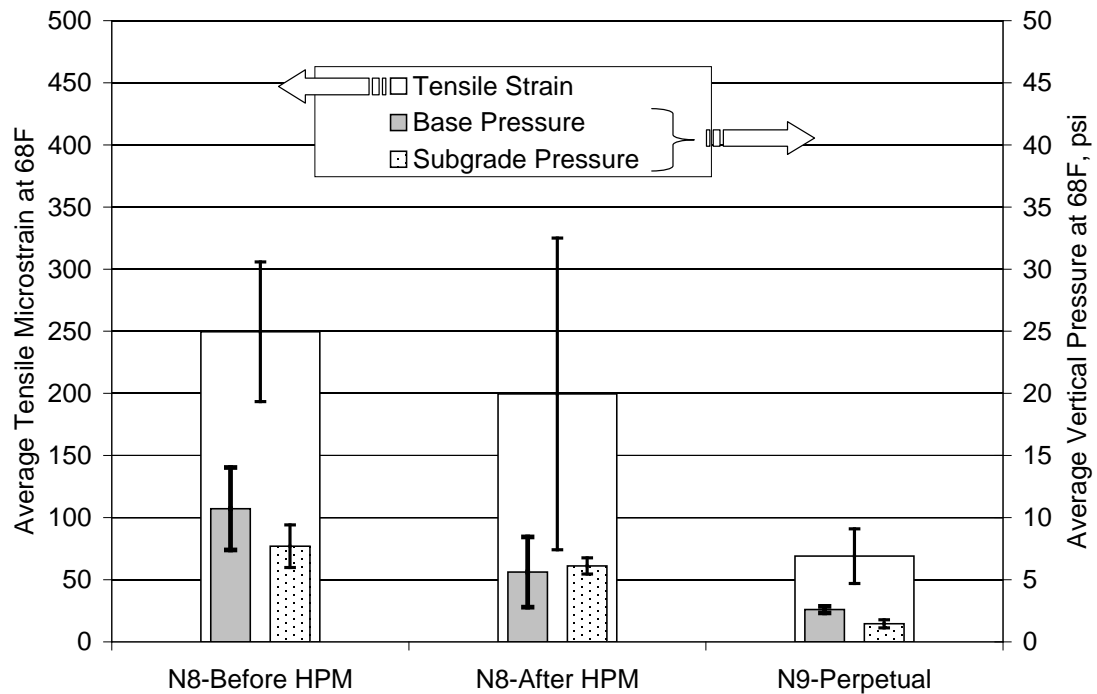
Figure 3.3 Backcalculated AC Modulus

Figure 3.4 Average Pavement Responses

Conclusions

1. There are no indications that the HPM rehabilitation has incurred any damage to date. Traffic applied to the HPM rehabilitation has now surpassed that which completely failed the original conventional rehabilitation. Measured rut depths are less than 1/8 inch, roughness has not changed since the HPM was placed, and no cracking has been observed.
2. The HPM had an immediate and statistically significant impact on the AC modulus of the pavement. An approximate 44% modulus increase was noted with reduced section-wide variability in AC modulus. The coefficient of variation went from 36% in the "before HPM" condition to 25% after the HPM was placed.
3. The HPM had statistically significant impacts on measured AC strain, base pressure, and subgrade pressure. Strains normalized to 68˚F were reduced by 20%, aggregate base pressure was reduced 48%, and subgrade pressure was reduced 20%. In the context of mechanistic-empirical pavement analysis, these reductions are key to good performance of the section.
4. HPM mixes may be an effective rehabilitation option on roads where high strains are expected and increasing pavement thickness is not an option. They may also be useful for preventing the reflection of severe distresses as well as for preventing rutting in heavy, slow-traffic applications.
5. The perpetual pavement section had relatively constant moduli throughout the two-year cycle, an indicator of its excellent structural health.
6. The perpetual pavement section had significantly lower strain and pressure measurements resulting from the increased initial investment in AC thickness, which resulted in its superior performance.
7. Cracking was evidently too severe for the paving fabrics to mitigate reflection cracking. Furthermore, the fabrics appeared to contribute to an interfacial bond problem that manifested as surface shearing cracks.

3.2 High RAP Content Mixtures

Background

More than half of the highway agencies in the U.S. have modified their specifications in the past few years to allow higher reclaimed asphalt pavement (RAP) contents. Contractors are using the opportunity to use higher RAP contents to be more competitive. Recent NAPA surveys indicate that the national average RAP content has increased from about 12% to about 17% in the past four years (*14*). Research at the NCAT Pavement Test Track has helped demonstrate the technical viability of high RAP content mixes.

Performance of 2006 RAP Experiment Test Sections

On the test track, four overlays with 45% RAP built in 2006 are still performing very well. One of the research goals of the 2006 RAP test sections was to determine if it was necessary to use a softer grade of virgin binder with the high RAP content mixes. Current AASHTO guidelines recommend using a softer binder when the RAP binder content is between 15 and 25% of the total binder content, and when the RAP binder content is over 25%, a more detailed analysis is needed to select the grade of the virgin binder. The detailed analysis involves performing extraction and recovery of the RAP binder and grading it in the PG system. Either blending charts or equations are then used to determine what virgin binder should be used. For the 45% RAP mixes, about 42% of the total binder was contributed by the RAP. Based on the blending chart approach, the virgin binder should be a PG 52-28. That was the lowest grade of binder used in the four test sections. The other sections used a PG 67-22, a PG 76-22, and a PG 76-22 with Sasobit. Sasobit, a well-known WMA additive, was used as a compaction aid in one of the sections because prior to construction it was not known how difficult it would be to meet the same density specification with the high RAP mixes that applied to virgin mixes. During construction of the test section overlays, a slight improvement in compactability was observed for the mixes with softer virgin binders. However, target densities were obtained even with the mixes containing the stiffer binders. Further details of the mixtures and construction for this experiment are provided in previous reports (*15, 16*).

After more than 20 million ESALs and some of the hottest summers on record in east Alabama, all four 45% RAP test sections have less than 5 mm of rutting, and International Roughness Index (IRI) results have actually improved slightly (sections have gotten smoother) over the five year period. A very minor amount of cracking began to appear in the test sections after four years. Table 3.1 shows the date that cracking first appeared and the total length of cracking for each of the sections at the end of the second cycle. Although the cracks are low-severity cracks that would not even be detected with automated pavement evaluation systems, the amount of cracking in the sections is related to the virgin binder grades, with stiffer grades exhibiting cracking before softer grades.

Table 3.1 Observed Cracking for the 2006 High RAP Content Experiment

Test Section	RAP Content[1]	RAP Binder Percentage[2]	Virgin Binder Grade	Date of First Crack	ESALs at First Crack	Total Length of Cracking after 2 Cycles
W4	20%	17.6%	PG 67-22	no cracking		
W3	20%	18.2%	PG 76-22	4/7/2008	6,522,440	34.0
W5	45%	42.7%	PG 58-28	8/22/2011	19,677,699	3.5
E5	45%	41.0%	PG 67-22	5/17/2010	13,360,016	13.9
E6	45%	41.9%	PG 76-22	2/15/2010	12,182,331	53.9
E7	45%	42.7%	PG 76-22+S[3]	1/28/2008	5,587,906	145.5

[1] RAP content as a percentage of the total aggregate

[2] The percentage of RAP binder relative to the total binder content
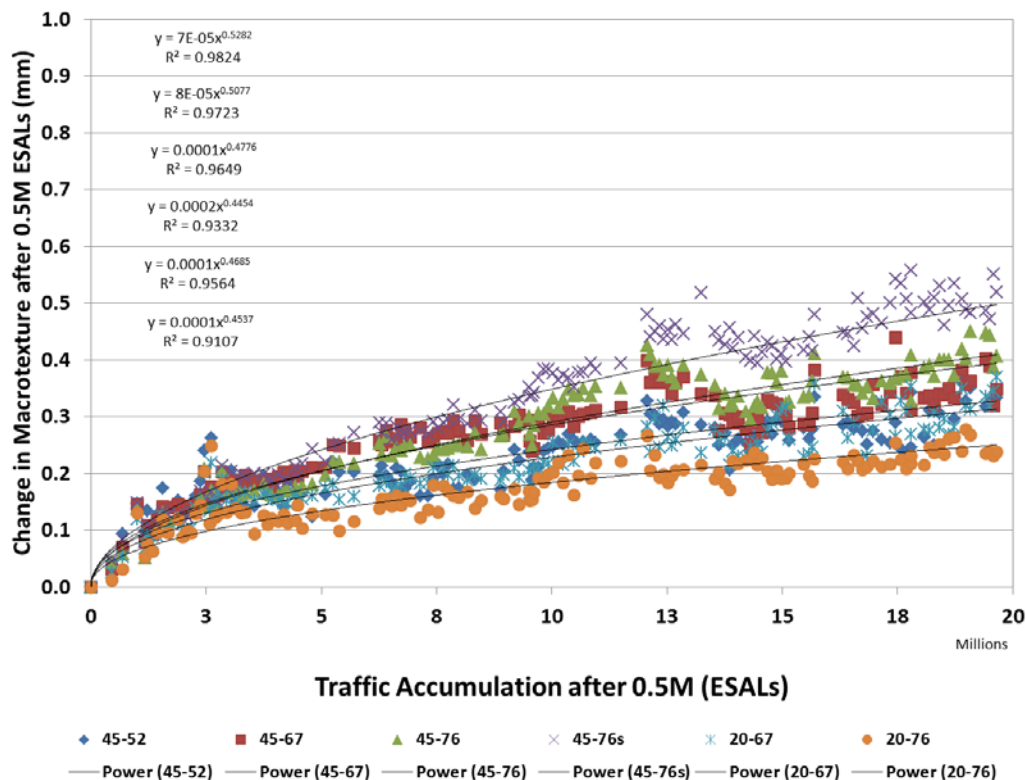
[3] This virgin binder contained 1.5% Sasobit.

Figure 3.5 Close-up Photograph of Section W5 Showing Texture and Hairline Crack Just Below the Scale

Figure 3.6 Close-up Photograph of Section E5 Showing Texture and Crack

Surface texture measurements are made weekly on all test sections. An increase in texture over time can be an indicator of raveling. As shown in Figure 3.7, the changes in surface texture for the RAP sections are also related to the virgin binder grade and RAP content of the mixtures. Of the 45% RAP test sections, the section produced using the PG 52-28 virgin binder has exhibited the least change in texture, while the section with PG 76-22 plus Sasobit, which stiffens the mix at ambient temperatures, has exhibited the most change.

Figure with regression equations:
$y = 7\text{E-}05x^{0.5282}$, $R^2 = 0.9824$
$y = 8\text{E-}05x^{0.5077}$, $R^2 = 0.9723$
$y = 0.0001x^{0.4776}$, $R^2 = 0.9649$
$y = 0.0002x^{0.4454}$, $R^2 = 0.9332$
$y = 0.0001x^{0.4685}$, $R^2 = 0.9564$
$y = 0.0001x^{0.4537}$, $R^2 = 0.9107$

Y-axis: Change in Macrotexture after 0.5M ESALs (mm)
X-axis: Traffic Accumulation after 0.5M (ESALs), Millions

Legend: 45-52, 45-67, 45-76, 45-76s, 20-67, 20-76, Power (45-52), Power (45-67), Power (45-76), Power (45-76s), Power (20-67), Power (20-76)

Figure 3.7 Texture Change for the 2006 RAP Test Sections

2009 High RAP Content Experiment

In 2009, three more high RAP content test sections were built on the test track. The Mississippi DOT sponsored Section S2 with a "mill and fill" of their gravel Superpave section from the previous track research cycle. The performance of that section is discussed in Chapter 2. Two 7-inch structural sections were built as part of the "Group Experiment" with 50% RAP in the each of the three layers of the asphalt cross-section. Both sections used a PG 67-22 as the virgin binder, but one of the sections was produced using the Astec Double Barrel Green WMA asphalt foaming system.

Objective

The objective of the 2009 high RAP content experiment was to compare the structural pavement responses and short-term performance of 50% RAP HMA, 50% RAP WMA, and a virgin mix control test section under full-scale accelerated pavement testing. The mixtures used in these test sections were also evaluated based on several performance-related laboratory tests.

Test Sections and As-Built Properties

Mix design information for the 50% RAP mixtures and the control section (S9) mixtures are shown in Table 3.2. All mix designs were prepared by NCAT in accordance with AASHTO R35 and M323 using 80 gyrations in a Superpave Gyratory Compactor. The 50% RAP mixtures produced as WMA used the same mix designs as the 50% RAP HMA mixtures. The surface mixtures were fine-graded 9.5 mm nominal maximum-aggregate size (NMAS) gradations; the intermediate and base mixtures were all fine-graded 19.0 mm NMAS gradations.

Table 3.2 Mix Design Information

Layer	Surface		Intermediate		Base	
	Control	50% RAP	Control	50% RAP	Control	50% RAP
Virgin Binder	PG76-22	PG67-22	PG76-22	PG67-22	PG67-22	PG67-22
Total Binder %	5.8%	6.2%	4.7%	4.8%	4.6%	4.8%
RAP Binder %		37%		50%		50%
No.78 Opelika limestone	30%		30%	15%	30%	15%
No.57 Opelika limestone	18%		18%	15%	18%	15%
M10 Columbus granite	25%		25%		25%	
No.89 Columbus granite		24%	27%		27%	
Shorter Sand	27%	20%		20%		20%
Fine RAP		15%		20%		20%
Coarse RAP		35%		30%		30%

Quality control test results for the mixtures are shown in Table 3.3. These results show that the mixtures met tight control standards to assure valid comparisons among the mixtures. In order to have valid comparisons of performance among the high RAP content test sections and the control section, the research team established a tolerance of ±0.2% on the effective asphalt contents between the 50% RAP mixtures and the control mix for each respective layer. Volumetric properties were also maintained within normal production tolerances. Average in-place density results for the test sections were similar and above the acceptable limit of 92.0%.

Table 3.3 Quality Control Results for the 50% RAP and Control Mixes

Sieve	Surface			Intermediate			Base		
	Control	50% RAP HMA	50% RAP WMA	Control	50% RAP HMA	50% RAP WMA	Control	50% RAP HMA	50% RAP WMA
1" (25.0mm)	100	100	100	99	98	99	99	99	97
¾" (19.0 mm)	100	100	100	92	93	93	95	95	89
½" (12.5 mm)	100	100	99	84	86	86	87	89	83
3/8" (9.5 mm)	100	95	95	76	79	79	77	82	75
No. 4 (4.75 mm)	81	67	69	57	56	58	56	58	54
No. 8 (2.36 mm)	59	48	51	47	46	47	46	47	44
No. 16 (1.18 mm)	46	39	41	38	37	39	37	39	37
No. 30 (0.60 mm)	31	27	27	26	26	27	26	27	25
No. 50 (0.30 mm)	16	12	12	15	13	14	15	14	13
No. 100 (0.15 mm)	9	7	7	9	8	8	9	9	8
No. 200 (0.075 mm)	6.0	4.7	4.8	5.3	5.6	5.7	5.1	5.8	5.3
Asphalt Content (%)	6.1	6.0	6.1	4.4	4.4	4.7	4.7	4.7	4.6

Effective Asphalt (%)	5.4	5.2	5.3	3.9	3.8	4.1	4.2	4.1	4.0
Lab Air Voids (%)	4.0	3.8	3.2	4.4	4.5	3.7	4.0	4.2	4.1
VMA (%)	16.5	15.8	15.5	13.5	13.6	13.6	13.9	13.8	13.7
VFA (%)	76	76	79	68	67	72	71	70	70
Dust to Binder Ratio	1.1	0.9	0.9	1.4	1.5	1.4	1.2	1.4	1.3
Plant Discharge Temp. (°F)	335	325	275	335	325	275	325	325	275
In-Place Density (% of Gmm)	93.1	92.6	92.1	92.8	92.9	93.1	92.6	95.0	94.2

Test Track Performance Results

Through 10 million ESALs, the 50% RAP HMA, 50% RAP WMA, and the control section performed extremely well: less than 5 mm of rutting, no cracking, steady IRI, and very small changes in texture. Final average rut depths and changes in mean texture depths for the test sections are shown in Table 3.4. These sections will remain in place and traffic will continue in the next research cycle until they reach a predetermined threshold level of distress, at which time a pavement preservation treatment will be applied.

Table 3.4 Final Rut Depths and Texture Changes

Test Section	Description	Final Wire-line Rut Depth (mm)	Mean Texture Depth Change (mm)[1]
S9	Control	7.1 mm	0.227 mm
N10	50% RAP HMA	1.8 mm	0.178 mm
N11	50% RAP WMA	3.7 mm	0.189 mm

[1] Texture changes were normalized to Mean Texture Depth at 500,000 ESALs.

Results of Laboratory Tests

Rutting. The surface mixtures from the 50% RAP and control test sections were tested for rutting potential using the Asphalt Pavement Analyzer (APA) and Flow Number (FN) tests. APA tests were conducted on laboratory-molded cylinders and tested at 64°C in accordance with AASHTO TP 63-09. Flow number tests were conducted on unconfined specimens at 59.5°C in accordance with AASHTO TP 79-09. The APA rut depths and flow numbers for the surface mixtures are given in Table 3.5.   The APA results for the 50% RAP HMA and control mix are below the maximum 5.5 mm criterion for heavy duty pavements, which was established in previous test track research (*16*); however, the APA rut depth for the 50% RAP WMA is just above that criterion. The average flow number for the control section surface mix was 164, and the 50% RAP HMA surface mix was 73, which exceeded the minimum value of 53 recommended for mix design to be subjected to between 3 and 10 million ESALs according to NCHRP Report 673 (*17*). The recommended flow number criteria for WMA mix designs, according to NCHRP Report 691, are considerably lower. For WMA to be subjected to between 3 to 10 million ESALs, the minimum flow number criterion is 30. The flow number for the 50% RAP WMA met that criterion. Note that both of the laboratory tests indicate that the control mix is the most resistant to permanent deformation. However, the field results do not match the lab results. On the track, the control section had the most rutting.

Table 3.5 Rutting Laboratory Test Results for Surface Mixtures

Test Section	APA Results		Flow Number Results	
	Rut Depth (mm)	COV, %	Flow Number (cycles)	COV, %
Control	3.1	19.0	164	9.7
50% RAP HMA	4.6	19.1	73	5.5
50% RAP WMA	5.7	24.5	47	8.5

Cracking. Resistance to cracking was assessed with two laboratory test methods. Resistance to surface, or top-down, cracking was evaluated using the Energy Ratio method discussed more thoroughly in Chapter 4. As the name implies, this test was used to evaluate only the surface layers in the high RAP experiment. Results of the Energy Ratio and Fracture Energy methods are summarized in Table 3.6. In general, a higher fracture energy and energy ratio is expected to indicate better resistance to cracking.

Table 3.6 Summary of Cracking Resistance Results from the Energy Ratio Analyses

Test Section	Fracture Energy (kJ/m^3)	Energy Ratio
Control	8.1	11.1
50% RAP HMA	1.6	5.5
50% RAP WMA	3.4	3.8

Structural Analysis Methodology. Horizontal strains were measured at the bottom of the AC layer in the longitudinal and transverse directions, while vertical pressures were measured at the top of the granular base and at the top of the subgrade. This analysis focused only on longitudinal tensile strain and vertical subgrade pressure. Longitudinal strain was selected since previous studies at the test track had shown that longitudinal strains were about 36% higher than transverse strain measurements ([18, 19]). Vertical subgrade pressure was used since classic pavement design procedures are based on limiting the vertical response at the top of the subgrade to prevent rutting [20]. Data were subdivided by axle type (i.e., steer, single and tandem). Only the single-axle data are presented in this study because they represent the majority of axle passes on each section. Additionally, the values shown correspond to the "best hit" on each section for each test date, which was defined as the 95th percentile of the readings obtained on a given test date.

Falling weight deflectometer (FWD) testing was performed to quantify the seasonal behavior of the pavement layer moduli. The data presented in this report correspond to the measurements taken in the outside wheelpath with the 9 kip load. The pavement layer moduli were backcalculated from deflection data using EVERCALC 5.0 for a three-layer cross-section (asphalt concrete, aggregate base, and subgrade soil). Since the same aggregate base and subgrade were used throughout the test track, this study focuses only on the asphalt concrete layer moduli. Data were filtered to eliminate results with root-mean-square error (RMSE) exceeding 3%.

Strain and Pressure. The mid-depth pavement temperature was used to correlate the measured responses (strain and pressure) to temperature. Previous studies at the test track have shown the effectiveness of using mid-depth temperature for these correlations ([18, 21]). The relationship between these parameters follows an exponential function, as shown in Equation 1:

$$response = k_1 e^{k_2 T} \tag{1}$$

Where:
response = pavement response (microstrain or subgrade pressure(psi))
T = mid-depth AC temperature(°F)
k_1, k_2 = section-specific regression coefficients

Figures 3.8 and 3.9 show the longitudinal strain and vertical subgrade pressure versus mid-depth temperature for each section. To determine if the response-temperature relationships were statistically similar among the sections, hypothesis tests were performed on the intercepts (k_1) and slopes (k_2). In most cases, at a 95% confidence level there was no evidence that the regression coefficients of the high RAP sections were statistically different from the control. In the WMA-RAP and HMA-RAP sections, strain and pressure were less influenced by temperature, respectively. The lower slopes are presumably due to the increased stiffness due to the high RAP contents.
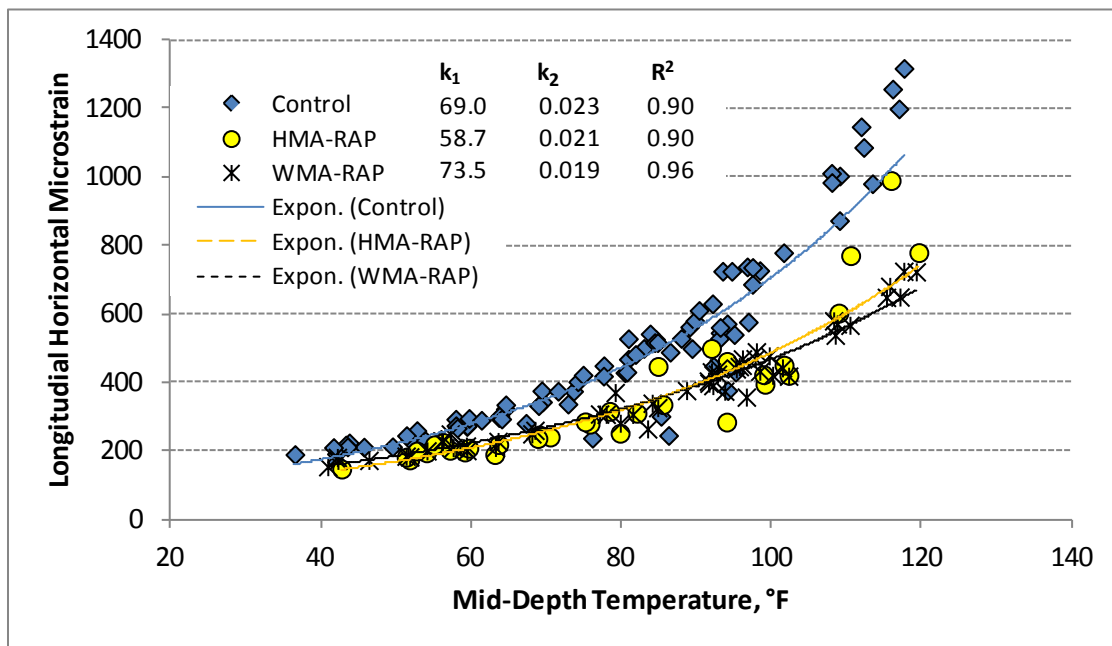
Figure 3.8 Longitudinal Strain versus Temperature
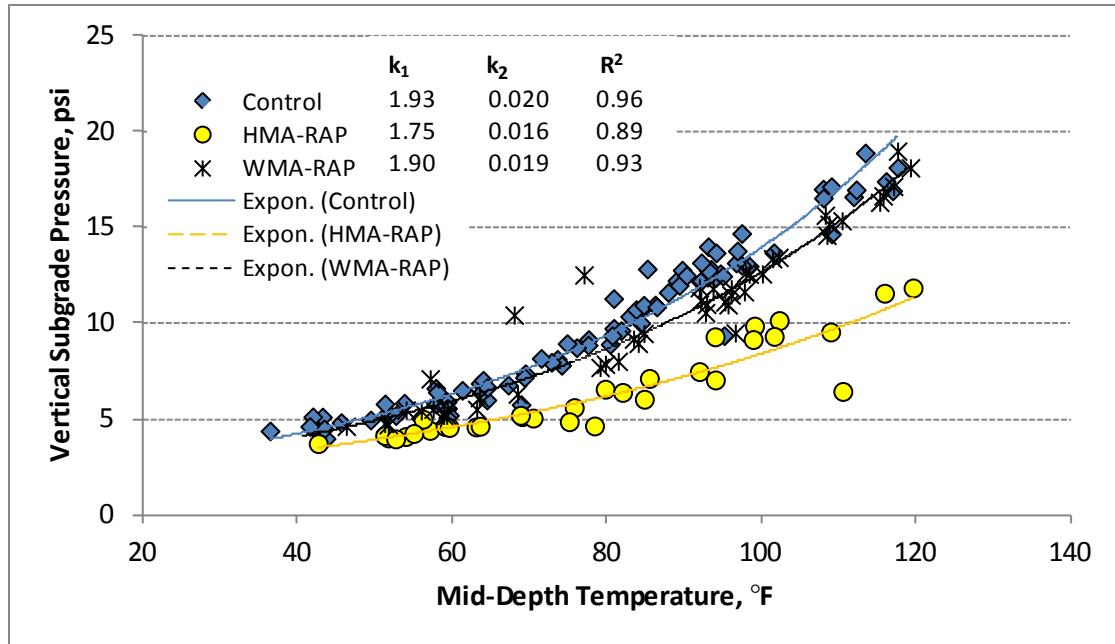
Figure 3.9 Subgrade Pressure versus Temperature

To fairly compare the different test sections, it was necessary to normalize the responses to a reference temperature. Three temperatures (50, 68 and 110°F) were used to include the range of temperatures at which testing was conducted. This was accomplished by dividing Equation 1 with reference temperature (T_{ref}) by the same equation with measured temperature (T_{meas}) and solving for temperature-normalized response (response$_{Tref}$), as shown in Equation 2.

$$response_{Tref} = [response_{Tmeas}][e^{k_2(T_{ref}-T_{meas})}]$$ (2)

Where:
response$_{Tref}$ = normalized response (microstrain or subgrade pressure(psi)) at reference temperature T_{ref}
response$_{Tmeas}$ = measured response (microstrain or subgrade pressure(psi))at temperature T_{meas}
T_{ref} = mid-depth reference temperature (°F)
T_{meas} = measured mid-depth temperature at time of test (°F)
k_2 = section-specific regression coefficient from Figures 3.8 and 3.9.

Because measured responses are also dependent on the thickness of the pavement layers, it was necessary to apply a correction to account for slight differences in as-built pavement thickness. The correction factors were obtained based on theoretical relationships between layer thickness and longitudinal strain or vertical pressure from layered elastic analysis. Although differences during construction were subtle, this correction allowed for a fairer comparison of the test sections. Figures 3.10 and 3.11 illustrate the average temperature-normalized and thickness-corrected longitudinal strain and subgrade pressure, respectively. A Tukey's post-ANOVA test was performed to compare the different sections. At a 95% confidence level, the measured strain and pressure responses of the high RAP sections were significantly lower than those of the control. Strains ranged from 7 to 31% lower, while pressures were between 14 and 55% lower than the control, with the largest differences observed at the highest reference temperature.
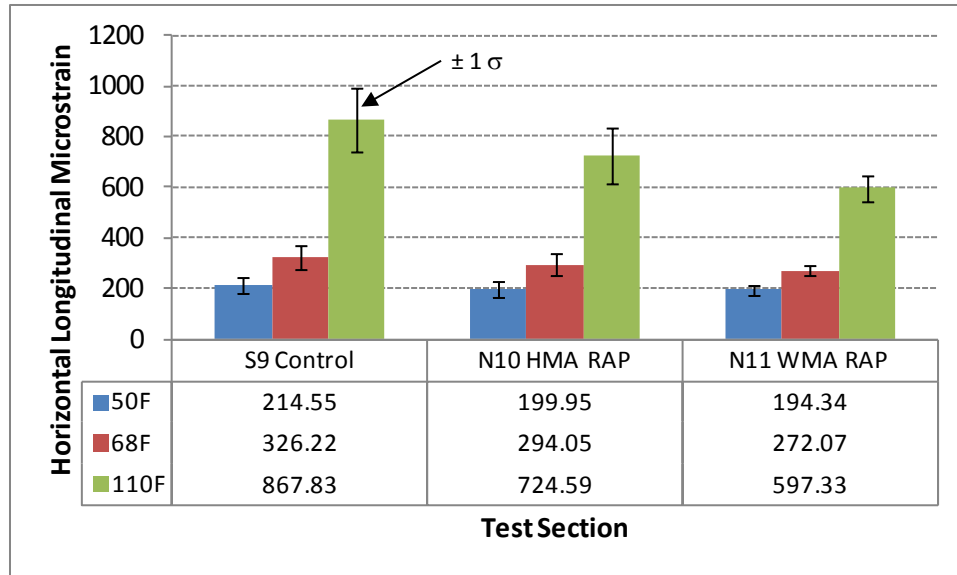
Figure 3.10 Average Longitudinal Strain at Reference Temperature

	S9 Control	N10 HMA RAP	N11 WMA RAP
50F	214.55	199.95	194.34
68F	326.22	294.05	272.07
110F	867.83	724.59	597.33
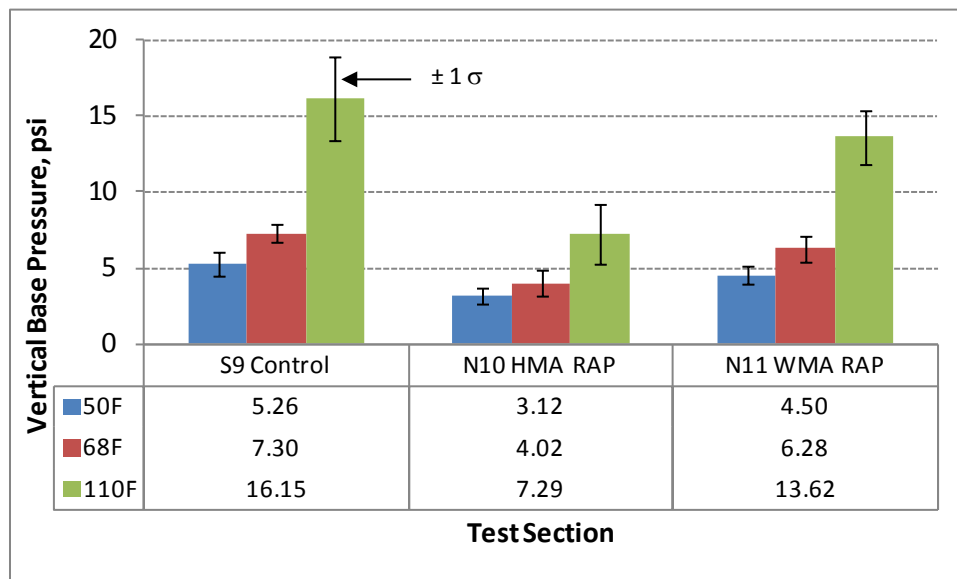
Figure 3.11 Average Vertical Pressure at Reference Temperature

	S9 Control	N10 HMA RAP	N11 WMA RAP
50F	5.26	3.12	4.50
68F	7.30	4.02	6.28
110F	16.15	7.29	13.62

Backcalculated AC Modulus. The backcalculated AC modulus obtained from FWD testing was also dependent on pavement mid-depth temperature and followed a function similar to the one shown in Equation 1. The moduli of each section and the regression coefficients are shown in Figure 3.12. Hypothesis tests performed on the intercepts (k_1) and slopes (k_2) indicated that the high RAP sections had similar intercepts and lower slopes than the control. This means that the high RAP sections had higher moduli at all temperatures due to the presence of stiffer aged binder and that the moduli of these sections were less susceptible to changes in temperature than the control, a trend also observed for strain and pressure measurements.
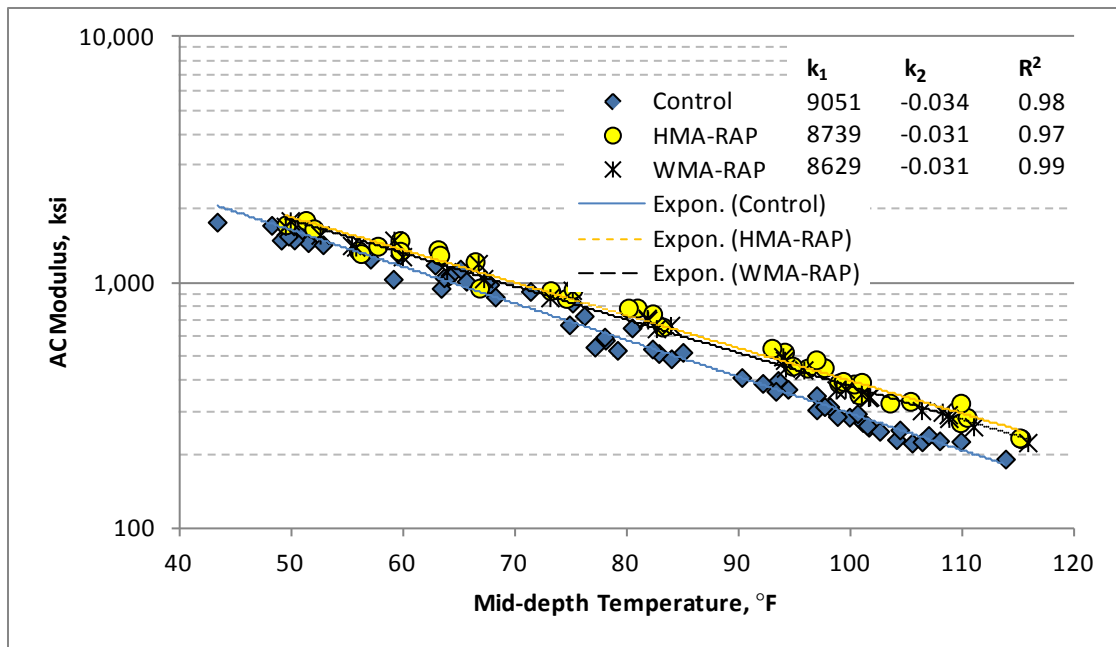
Figure 3.12 Backcalculated AC Modulus versus Temperature

Figure 3.13 shows the average temperature-normalized moduli. Results were normalized to three reference temperatures using the same procedure applied for strain and pressure. Statistical testing indicated that there were significant differences among all sections. Overall, the high RAP sections had higher moduli than the control (between 16 and 43% higher), with the largest differences observed at the higher reference temperatures.

	S9 Control	N10 HMA RAP	N11 WMA RAP
50F	1645.9	1880.4	1813.9
68F	887.6	1079.2	1033.5
110F	206.4	295.5	278.1
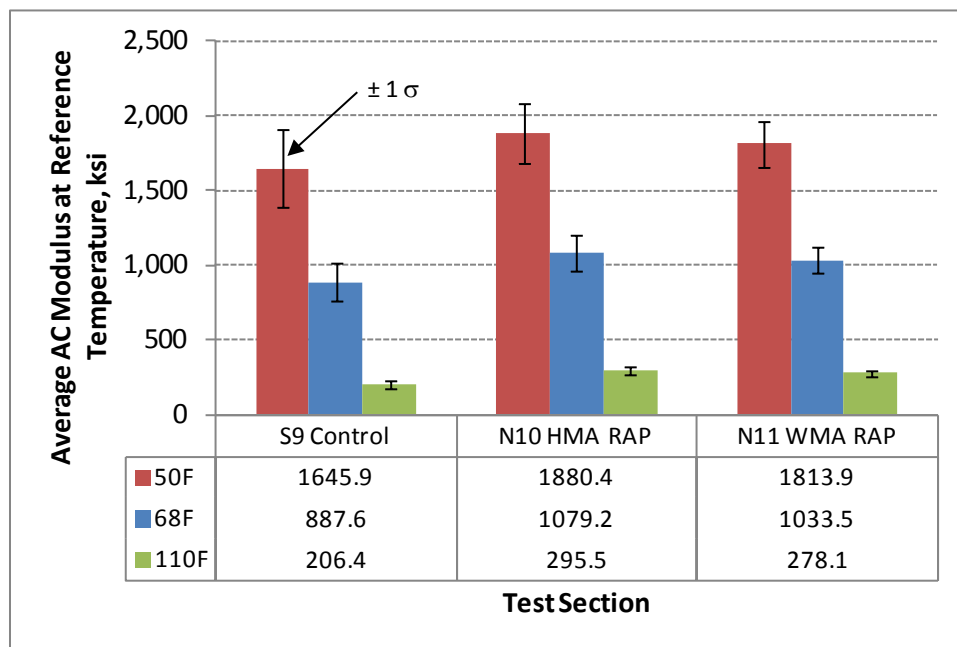
Figure 3.13 Average AC modulus at Reference Temperature

No cracking was observed in the control section or high RAP sections during the test cycle. However, laboratory testing performed on plant-produced mix samples was conducted in accordance with AASHTO T 321-07 to evaluate the fatigue resistance of the mixtures in the bottom layer of asphalt for each of these sections. The results of the beam fatigue test are shown in Figure 3.14. The relationships developed between cycles to failure and beam fatigue strain magnitude for each of the sections were used to estimate the number of cycles until failure at the 68°F field strain using Equation 3.

$$N_f = \alpha_1 \left[\frac{1}{\varepsilon_{68}}\right]^{\alpha_2}$$ (3)

Where:
N_f = cycles until failure
ε_{68} = estimated field strain at 68°F from Figure 3
α_1, α_2 = section-specific regression constant from Figure 8
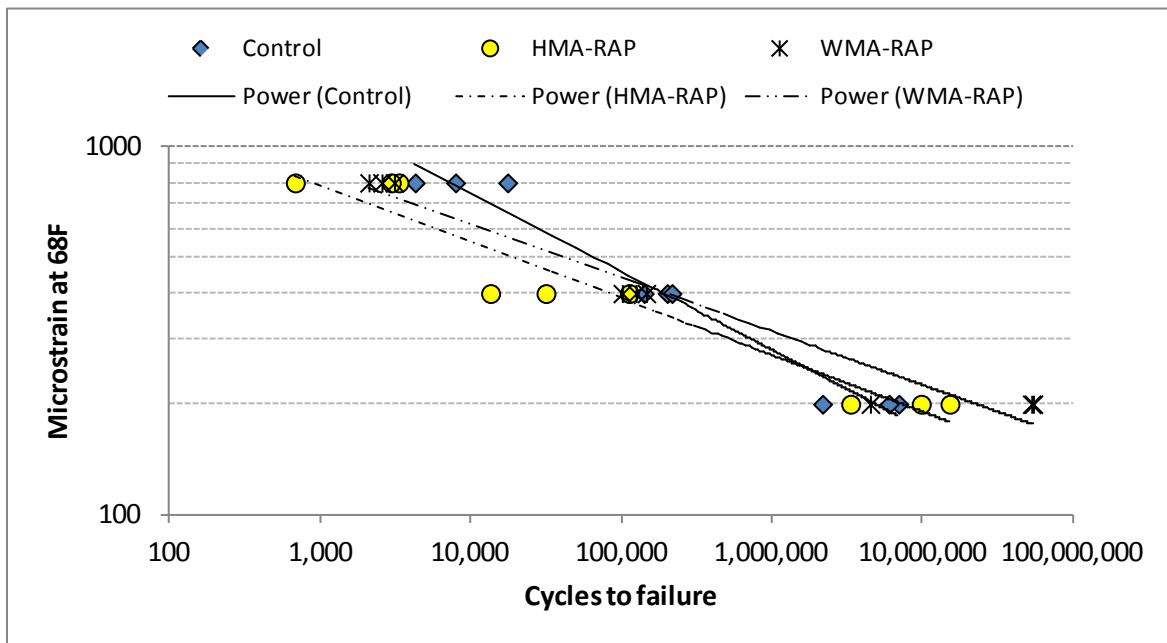
Figure 3.14 Bending Beam Fatigue Results

Table 3.7 provides the variables for each fatigue transfer function, the field strain at 68°F (from Figure 3.13), and the estimated cycles until failure at the field strain. It also contains the number of cycles until failure as a percentage of the control section. The results indicate that the high RAP sections are expected to have better fatigue performance than the control at 68°F due to their lower strain level and corresponding fatigue transfer functions. However, further monitoring of field performance is needed to support these findings.

Table 3.7 Fatigue Transfer Functions and Predicted Cycles to Failure at 68°F

Mixture	α_1	α_2	R^2	ε_{68} (from Figure 3)	N_f @ ε_{68}	N_f % of control
S9 – Control	1.00E+17	4.5321	0.97	326	405,982	100
N10 – HMA RAP	4.00E+20	6.0192	0.93	294	554,782	137
N11 – WMA RAP	3.00E+22	6.5846	0.96	272	2,790,868	687

Conclusions

Continued monitoring of the high RAP content overlays built in the 2006 RAP experiment has indicated that using a softer virgin binder grade appears to improve resistance to cracking and raveling.

Analyses of the structural responses of 2009 high RAP pavement sections under traffic loads and their short-term performances lead to the following conclusions:

- The use of mixtures containing high RAP contents affected pavement responses to loads and environmental changes, resulting in critical tensile strains and subgrade pressures lower than the control, with differences of 7 to 31% lower for strain and 14 to 55% lower for pressure.
- Statistical differences existed among the AC moduli of the sections, with the high RAP sections having moduli 16 and 43% higher than the control. The modulus-versus-time relationship of each section was consistent with the trends observed for strain and pressure versus time. The increased stiffness of high RAP content mixes can be used as an advantage as high modulus structural layers for perpetual pavement designs.
- The use of high RAP contents improved the rutting resistance of the mixtures. Results of APA and flow number tests on the surface mixes from this experiment indicated the mixes would have adequate resistance to rutting based on criteria established in NCHRP studies. However, both of the lab tests incorrectly ranked the rutting resistance of the mixtures based on test track performance.
- No cracking has been observed in any of the sections involved in this experiment. Based on relationships developed between laboratory test results and field-measured strains at 68°F, the high RAP sections in the structural experiment are expected to have better fatigue performance than the control. However, further monitoring of field performance is needed to support this finding.

3.3 Warm-Mix Asphalt

Background

Use of warm-mix asphalt (WMA) continues to increase dramatically in the U.S. due to its environmental benefits, energy savings, and construction advantages. New WMA technologies continue to be developed, and research studies have provided recommendations on how to design WMA mixes and predict how WMA will affect long-term pavement performance. As WMA moves into mainstream use, one of the challenges with implementation is understanding how WMA will interact with other new technologies, such as higher RAP content mixtures, and implementation of mechanistic-based pavement design methods.

Objective

The objective of this investigation was to evaluate the pavement responses and short-term performance of warm-mix asphalt (WMA) pavement sections under full-scale accelerated pavement testing.

Test Sections and As-Built Properties

The test sections in this experiment were part of the NCAT Pavement Test Track Group Experiment. Two WMA technologies were used: Astec's Double Barrel Green water injection asphalt-foaming process and MeadWestvaco's Evotherm DAT chemical additive, identified in this section as WMA-F and WMA-A, respectively. These two WMA technologies were selected by the sponsors of the Group Experiment. At that time, these were the most popular WMA technologies in the U.S. The Group Experiment control test section using conventional hot-mix asphalt provides the basis of comparisons. The test sections were built on a stiff subgrade (about 30 ksi) and a graded aggregate base commonly used at the test track. The asphalt cross sections for each of the test sections consisted of a 3-inch base course, a 2.75-inch intermediate layer, and a 1.25-inch surface layer. WMA was used in all three layers. The mix designs for each layer, shown in Table 3.8 were the same for the control and both WMA sections. The mixtures were designed in accordance with Superpave mix specifications using 80 gyrations. As-built properties of the test sections are shown in Table 3.9. Gradations, asphalt contents, and volumetric properties were reasonably consistent among the three test sections.

Table 3.8 Summary of Mix Designs for WMA Experiment

Layer	Surface	Intermediate	Base
Virgin Binder Grade	PG76-22	PG76-22	PG67-22
NMAS	9.5 mm	19.0 mm	19.0 mm
Asphalt Content %	5.8%	4.7%	4.6%
No.78 Opelika limestone	30%	30%	30%
No.57 Opelika limestone	18%	18%	18%
M10 Columbus granite	25%	25%	25%
No.89 Columbus granite		27%	27%
Shorter Sand	27%		

Table 3.9 As-Built Data for WMA and Control Mixes

Sieve	Surface			Intermediate			Base		
	Control	WMA-F	WMA-A	Control	WMA-F	WMA-A	Control	WMA-F	WMA-A
1" (25.0mm)	100	100	100	99	99	98	99	99	99
¾" (19.0 mm)	100	100	100	92	96	94	95	94	95
½" (12.5 mm)	100	100	100	84	89	87	87	85	87
3/8" (9.5 mm)	100	100	100	76	80	80	77	76	80
No. 4 (4.75 mm)	81	81	83	57	60	60	56	57	61
No. 8 (2.36 mm)	59	60	61	47	48	48	46	47	50
No. 16 (1.18 mm)	46	47	47	38	39	38	37	38	40
No. 30 (0.60 mm)	31	32	31	26	27	25	26	21	28
No. 50 (0.30 mm)	16	17	16	15	14	13	15	12	16
No. 100 (0.15 mm)	9	10	9	9	9	8	9	9	9
No. 200 (0.075 mm)	6.0	6.7	6.1	5.3	5.3	4.9	5.1	5.7	5.3
Asphalt Content (%)	6.1	6.1	6.4	4.4	4.7	4.6	4.7	4.7	5.0
Effective Asphalt (%)	5.4	5.5	5.7	3.9	4.1	4.0	4.2	4.1	4.5
Lab Air Voids (%)	4.0	3.3	3.4	4.4	4.3	4.9	4.0	4.1	3.0
VMA (%)	16.5	16.0	16.7	13.5	14.3	14.5	13.9	14.0	13.7
VFA (%)	76	80	80	68	68	66	71	71	78
Dust to Binder Ratio	1.1	1.2	1.1	1.4	1.3	1.2	1.2	1.2	1.2
Plant Discharge Temp. (°F)	335	275	250	335	275	250	325	275	250
In-Place Density (% of Gmm)	93.1	92.3	93.7	92.8	92.9	92.9	92.6	92.3	93.9

The asphalt binders from the plant-produced mixtures were extracted, recovered, and graded following AASHTO T 164, ASTM D5404, and AASHTO R39, respectively. The solvent used in this testing was reagent-grade trichloroethylene. Results are shown in Table 3.10. It can be seen that critical high temperatures for the binders recovered from WMA-A mixtures are a few degrees lower than for WMA-F. This is likely due to less aging of the binder, resulting from the lower plant mixing temperatures used for WMA-A.

Table 3.10 PG Grade of Binders Recovered from WMA and Control Mixes

Layer	Section	True Grade	PG
Surface	Control	81.7 – 24.7	76-22
	WMA-F	82.0-25.7	82-22
	WMA-A	80.3-25.7	76-22
Intermediate	Control	85.1-25.1	82-22
	WMA-F	86.6-23.9	82-22
	WMA-A	82.5-25.1	82-22
Base	Control	77.1-24.1	76-22
	WMA-F	75.6-25.1	70-22
	WMA-A	73.7-25.4	70-22

Test Track Performance Results

The control and WMA sections performed very well through the cycle. No cracking was evident, IRI data were steady, texture changes were very small, and rut depths were satisfactory. Final average rut depths and changes in mean texture depths for the test sections are shown in Table 3.11. Although the rut depths for the WMA sections were slightly higher than those for the control section, likely as a result of the softer binders in the WMA sections, the differences are considered acceptable. The higher rut depth for the WMA-A section may be due to the softer binders and slightly higher effective asphalt content of its surface layer. These sections will remain in place and traffic will continue in the next test track cycle until the sections reach a predetermined threshold level of distress, at which time a pavement preservation treatment will be applied.

Table 3.11 Final Rut Depths and Texture Changes

Test Section	Description	Final Wire-line Rut Depth (mm)	Mean Texture Depth Change (mm)[1]
S9	Control	7.1 mm	0.227 mm
S10	WMA-F (foam)	9.0 mm	0.270 mm
S11	WMA-A (additive)	11.0 mm	0.262 mm

[1] Texture changes were normalized to Mean Texture Depth at 500,000 ESALs

Results of Laboratory Tests

Rutting. The surface mixtures from the WMA and control test sections were tested for rutting potential using the Asphalt Pavement Analyzer (APA) and Flow Number (FN) tests. APA tests were conducted on laboratory-molded cylinders and tested at 64°C in accordance with AASHTO TP 63-09. Flow number tests were conducted on unconfined specimens at 59.5°C in accordance with AASHTO TP 79-09. The APA rut depths and flow numbers for the surface mixtures are given in Table 3.12.   The APA results for the WMA and control mixes are below the maximum 5.5 mm criterion for heavy duty pavements established in previous test track research (*16*). This indicates good rutting resistance for the mixtures. The ranking of the flow number results for these three mixtures is also consistent with the actual rutting measured on the test sections. The flow number results in Table 3.12 were compared to criteria for HMA and WMA recommended in NCHRP reports 673 and 691, respectively. For HMA mix designs, NCHRP 673 recommends (Table 13) a minimum flow number of 53 for 3 to 10 million ESALs. For WMA mix designs, NCHRP 691 recommends (Table 3) a minimum flow number of 30 for 3 to 10 million ESALs. As can be seen, the results in Table 3.12 meet the respective recommended flow number criteria. However the WMA-A section results were marginal.

Table 3.12 Laboratory Rutting Test Results for Surface Mixtures

Test Section	APA Results Rut Depth (mm)		Flow Number Results Flow Number (cycles)	
	Average	*Std. Dev.*	*Average*	*Std. Dev.*
Control	3.1	0.6	164	16
WMA-F	4.3	0.9	51	19
WMA-A	3.7	0.7	36	6

Cracking. Cracking potential was evaluated using with three laboratory tests. Top-down cracking of the surface mixtures was evaluated using the Energy Ratio method discussed more thoroughly in Chapter 4. IDT Fracture Energy is a component of Energy Ratio. Previous research has also indicated a strong correlation between Fracture Energy at 20°C and fatigue cracking at WesTrack (*86*). Results of the Energy Ratio and Fracture Energy of the surface mixtures in this experiment are summarized in Table 3.13. In general, a higher fracture energy and energy ratio is expected to indicate better resistance to cracking. Based on criteria established by Roque et al. (*11*), the Energy Ratio results for all three mixtures are excellent. The Energy Ratio for the control mix is more than double that of the WMA surface mixes. Since no cracking has occurred in these test sections, it is not possible at this time to verify that Fracture Energy or Energy Ratio can be used to predict cracking.

Table 3.13 Summary of Cracking Resistance Results from Energy Ratio Analyses

Test Section	Fracture Energy (kJ/m^3)	Energy Ratio
Control	8.1	11.1
WMA-F	12.5	5.8
WMA-A	9.9	5.1

Fatigue-cracking potential of the base asphalt layers was evaluated using the bending beam fatigue test. Analyses of the beam fatigue results, starting on page 57, utilized pavement response data from the structural analysis, as described in the following section.

Structural Analysis Methodology

Horizontal strains were measured at the bottom of each asphalt layer in the longitudinal and transverse directions, while vertical pressures were measured at the top of the granular base and at the top of the subgrade. This study focused only on longitudinal tensile strain and vertical subgrade pressure. Longitudinal strain was selected since previous studies at the test track showed that longitudinal strains were about 36% higher than transverse strain measurements (*18, 19*). Vertical subgrade pressure was used since classic pavement design procedures are based on limiting the vertical response at the top of the subgrade to prevent rutting (*20*). Data were subdivided by axle type (e.g., steer, single, and tandem). Only the single-axle data are presented in this study because they represent the majority of axle passes on each section. Additionally, the values shown correspond to the "best hit" on each section for each test date, which was defined as the 95th percentile of the readings obtained on a given test date.

Falling-weight deflectometer (FWD) testing was performed to quantify the seasonal behavior of the pavement layer moduli. The data presented in this report correspond to the measurements taken in the outside wheelpath with the 9 kip load. The pavement layer moduli were backcalculated from deflection data using EVERCALC 5.0 for a three-layer cross-section (asphalt-concrete, aggregate base, and subgrade soil). Since the same aggregate base and subgrade were used throughout the test track, this study focuses only on the asphalt-concrete layer moduli. Data were filtered to eliminate results with root-mean-square error (RMSE) exceeding 3%.

Strain and Pressure. The mid-depth pavement temperature was used to correlate the measured responses (strain and pressure) to temperature. Previous studies at the test track have shown the effectiveness of using mid-depth temperature for these correlations (*18, 21*). The relationship between these parameters follows an exponential function, as shown in Equation 1:

$$response = k_1 e^{k_2 T} \tag{1}$$

Where:
response = pavement response (microstrain or subgrade pressure(psi))
T = mid-depth AC temperature (°F)
k_1, k_2 = section-specific regression coefficients

Figures 3.15 and 3.16 show the longitudinal strain and vertical subgrade pressure versus mid-depth temperature for each section. To determine if the response-temperature relationships were statistically similar among the sections, hypothesis tests were performed on the intercepts (k_1) and slopes (k_2). At 95% confidence level, there was no evidence that the regression coefficients of the WMA sections were statistically different from the control. In other words, neither WMA technology appeared to affect pavement response versus temperature relative to the control section.
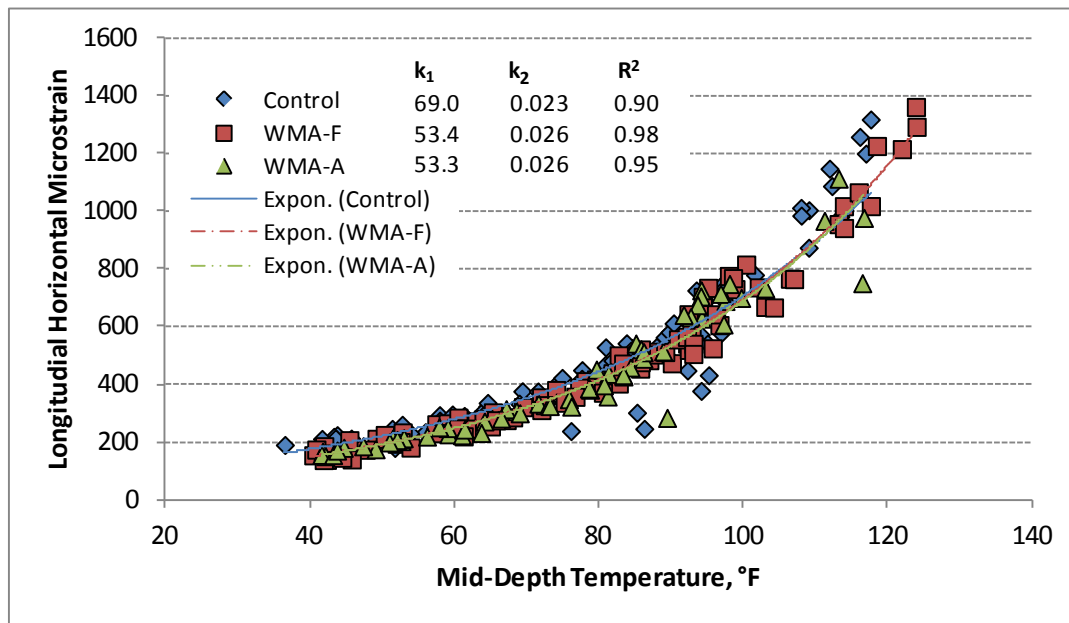
Figure 3.15 Longitudinal Strain versus Temperature
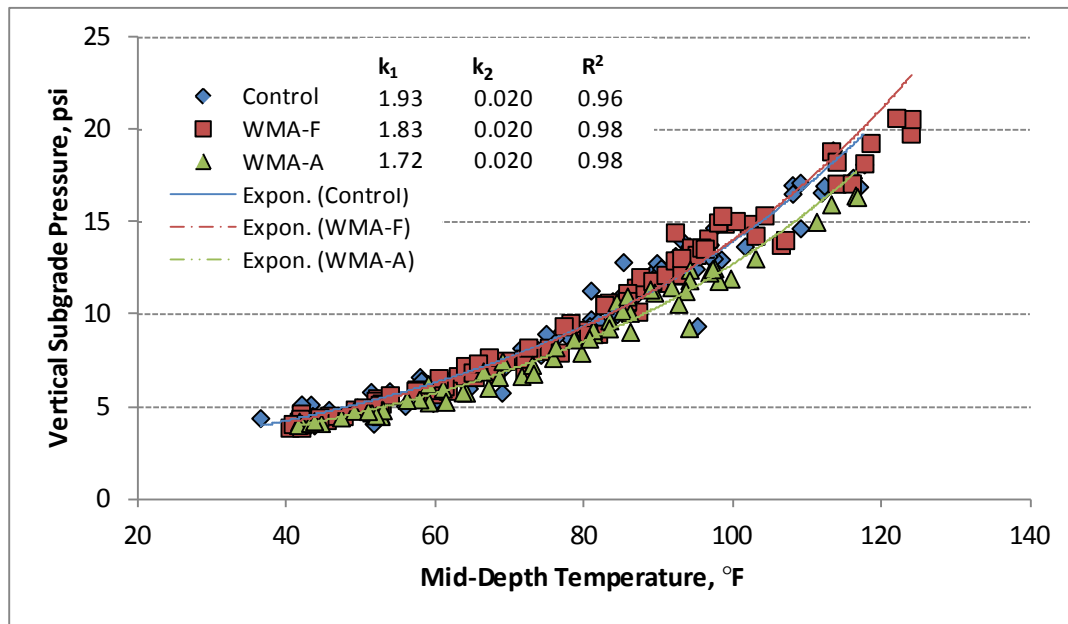
Figure 3.16 Subgrade Pressure versus Temperature

Backcalculated AC Modulus. The backcalculated AC modulus obtained from FWD testing was also dependent on pavement mid-depth temperature and followed a function similar to the one shown in Equation 1. The moduli of each section and the regression coefficients are shown in Figure 3.17. Hypothesis tests performed on the intercepts (k_1) and slopes (k_2) indicated that in general the WMA sections had lower intercepts than the control and similar slopes. This means that the WMA sections had lower moduli at all temperatures, likely due to the reduced binder-aging within these sections.
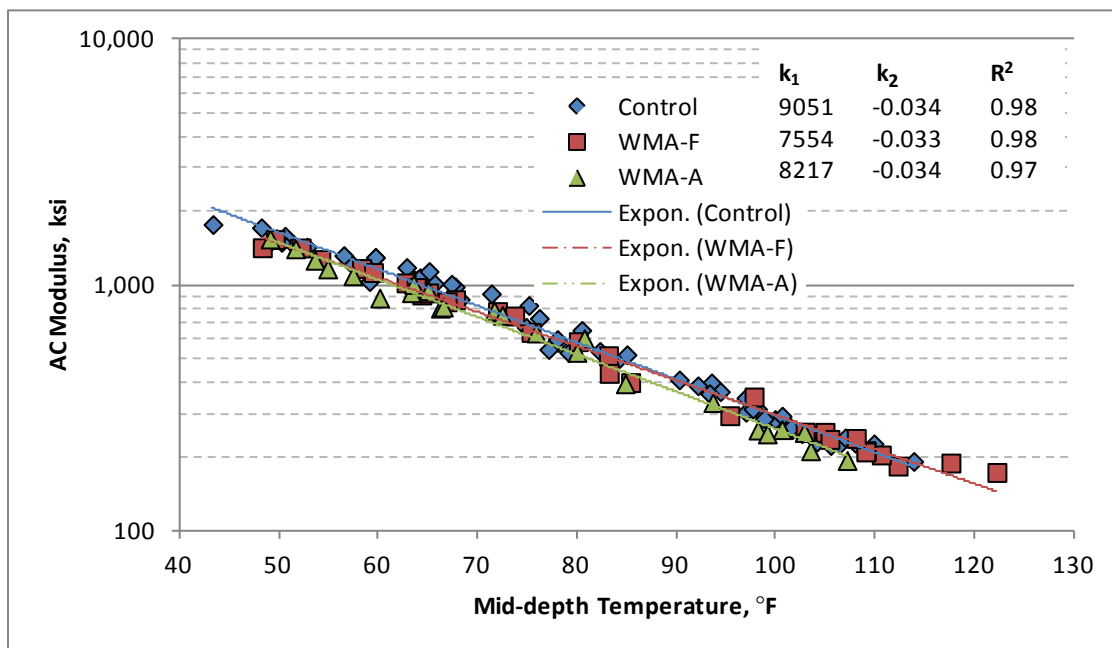
Figure 3.17 Backcalculated AC Modulus versus Temperature

To fairly compare the different test sections, it was necessary to normalize the AC moduli to a reference temperature. Three values (50, 68, and 110°F) were used to include the range of temperatures to which pavement sections were subjected during the test cycle. This normalization was accomplished by dividing the exponential equation for AC modulus obtained from the regression analysis with reference temperature (T_{ref}) by the same equation with measured temperature (T_{meas}) and solving for temperature-normalized modulus (E_{Tref}), as shown in Equation 2.

$$E_{Tref} = E_{Tmeas}e^{k_2(T_{ref}-T_{meas})} \hspace{4cm} (2)$$

Where:
E_{Tref} = normalized AC modulus at reference temperature T_{ref} (ksi)
E_{Tmeas} = measured AC modulus at temperature T_{meas} (ksi)
T_{ref} = mid-depth reference temperature (°F)
T_{meas} = measured mid-depth temperature at time of test (°F)
k_2 = section-specific regression coefficient from Figure 3.17

Figure 18 shows the average temperature-normalized moduli. A Tukey's post-ANOVA test was performed to compare the different sections. At 95% confidence level, the results indicated that there were statistical differences among all sections. Overall, WMA sections had lower moduli than the control; however, these differences were only 7 to 10% lower and may not have practical significance.

	S9 Control	S10 WMA-F	S11 WMA-A
50F	1645.9	1489.5	1480.6
68F	887.6	828.7	797.6
110F	206.4	211.0	188.3
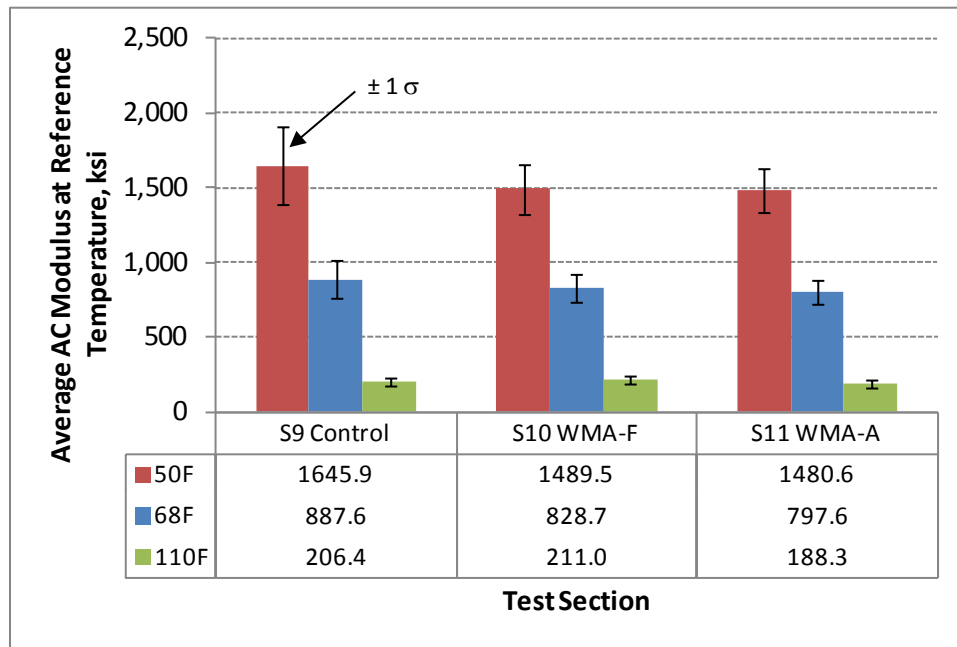
Test Section

Figure 3.18 Average AC Modulus at Reference Temperature

Fatigue Cracking. Although no cracking was observed in the control section or WMA sections during the test cycle, laboratory beam fatigue tests were conducted to evaluate the fatigue resistance of the plant-produced mixtures. The results of the beam fatigue test are shown in Figure 3.19. The relationships developed between cycles to failure and beam fatigue strain magnitude for each of the sections were used to estimate the number of cycles until failure at the 68°F field strain using Equation 3.
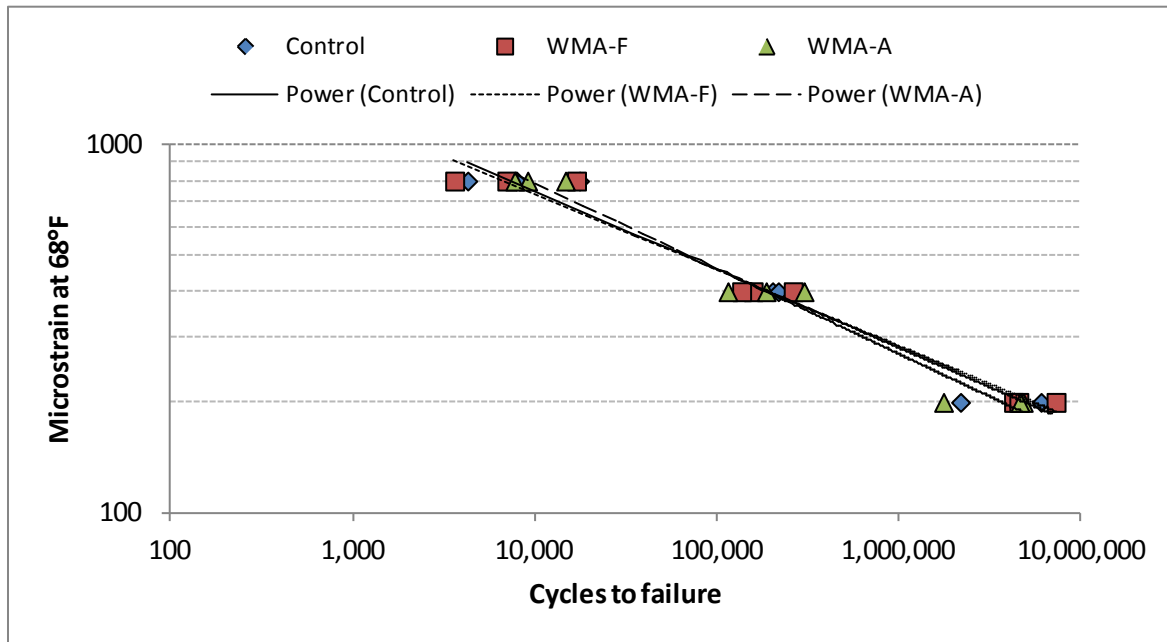
$$N_f = \alpha_1 \left[\frac{1}{\varepsilon_{68}}\right]^{\alpha_2} \tag{3}$$

Where:

N_f = cycles until failure

ε_{68} = estimated field strain at 68°F from Figure 3.15

α_1, α_2 = section-specific regression constant from Figure 3.19

Figure 3.19 Bending Beam Fatigue Results

Table 3.14 provides the variables for each fatigue transfer function, the field strain at 68°F (from Figure 3.18), and the estimated cycles until failure at the field strain. It also contains the number of cycles until failure as a percentage of the control section. The results indicate that the WMA sections are expected to have better fatigue performance than the control at 68°F due to their strain levels and corresponding fatigue transfer functions. However, further monitoring of field performance is needed to support these findings.

Table 3.14 Fatigue Transfer Functions and Predicted Cycles to Failure at 68°F

Mixture	α_1	α_2	R^2	ε_{68} (from Figure 3)	N_f @ ε_{68}	N_f % of control
S9 – Control	1.00E+17	4.5321	0.97	326	405,982	100
S10 – WMA-F	4.00E+17	4.7140	0.98	289	1,002,169	247
S11 – WMA-A	1.00E+16	4.1923	0.97	295	439,539	108

Conclusions

This experiment compared the test track performance, laboratory test results, and structural responses of WMA pavement sections to a control test section. The following conclusions were reached:

- Performance of the control and WMA sections on the test track was very good. No cracking was evident, IRI data were steady, texture changes were very small, and rut depths were satisfactory. The rut depths for the WMA sections were slightly greater than those for the control section, likely due to reduced binder aging associated with WMA production.
- The APA results indicated good rutting resistance. The flow number results were consistent with the recommended criteria for HMA and WMA. The flow number results correctly ranked the mixtures with regard to rutting measurements on the track and indicated that the WMA-A surface mix was marginal for the traffic on the track.
- Neither WMA technology (Astec's Double Barrel Green water injection asphalt-foaming process or MeadWestvaco's Evotherm DAT chemical additive) appeared to affect pavement response (strain and stress) versus temperature relative to the control section.
- Statistical differences existed among the AC moduli of the sections, with the WMA sections having moduli 7 and 10% lower than the control. From a practical perspective, these differences may not be considered significant.
- Laboratory beam fatigue test results normalized to actual field-measured strains at 68°F indicate that the WMA-F base mix has a much higher resistance to fatigue damage compared to the control mix. However, further monitoring of field performance is needed to support these findings.

3.4 Structural Characterization of Open-Graded Friction Course (OGFC)

Objective

The main objective of this investigation was to compute a structural coefficient for OGFC using data from full-scale pavement sections on the NCAT Pavement Test Track.

Test Sections

The sections used in this investigation were constructed in adjacent locations on the south tangent of the test track in August 2009. The locations were selected to minimize differences between sections by paving continuously between the two sections for the underlying pavement lifts, with only the surface materials differing between them. Figure 3.20 illustrates the two cross sections where S8 contains the OGFC surface while S9 served as the control section. Both sections were designed for a total asphalt concrete (AC) depth of 7 inches. Individual lifts are indicated with accompanying nominal maximum aggregate size (NMAS) and binder grade. The depths shown in Figure 3.20 represent average as-built depths determined from survey records. Slight differences on the order of tenths of inches between sections were deemed acceptable and unavoidable in the context of real pavement construction. Finally, though there were slight differences in as-built properties, both sections met the test track specifications for asphalt content and compacted density and were within the expected range of variation for these parameters.
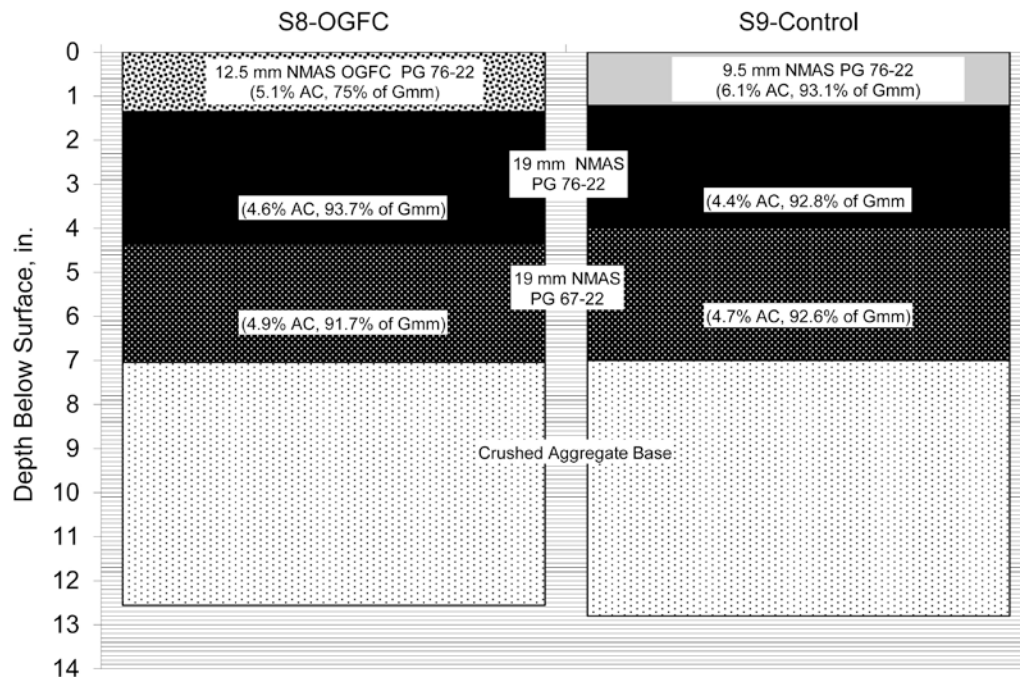
Figure 3.20 OGFC and Control Test Sections

FWD Testing and Analysis

Beginning on August 28, 2009, the control section was subjected to falling weight deflectometer (FWD) testing three Mondays per month. The OGFC section was tested every other Monday. This schedule was necessary because of time constraints and the need to test other sections on a regular basis. The off Monday within each month was used to perform relative calibration of the FWD equipment. The deflection data ranged from August 28, 2009 through April 11, 2011.

Two key adjustments to the raw deflection data were needed to properly use the AASHTO (1993) approach to find the structural number. First, the deflection data were normalized to the standard loading of 9,000 lb. For each set of deflection data at a given location on a given date, a best fit linear regression equation was determined for the center (D1) and outer (D9) deflection measurements. The best-fit equation was then used to compute deflection at exactly 9,000 lb. The second deflection data adjustment was to account for varying temperatures across the numerous test dates included in this investigation. The AASHTO method (*22*) requires deflections corrected to 68˚F. The previous correction provided deflections at 9,000 lb but varied as a function of temperature. The AASHTO Guide (1993) provides generic correction factors for temperature, but it was decided to develop section- and location-specific corrections using measured deflection versus temperature. Further details regarding load and temperature normalization have been documented elsewhere (*23*).

After all the data was normalized for load (9,000 lb) and temperature (68˚F), the AASHTO equations (1993) were utilized to determine SN_{eff}. The equations first used the outermost deflection to determine soil modulus (M_r). The soil modulus is then used to determine composite pavement modulus (E_p) from which effective the structural (SN_{eff}) number is calculated. A total of 358 effective structural numbers were computed for S8 while 619 were computed for S9. The difference in number of observations stems from more frequent testing on S9 as noted above. The average and standard deviations of SN_{eff} are summarized in Figure 3.21. S9 was more variable than S8, though both were deemed within acceptable limits of natural construction and performance variation, with coefficients of variation less than 20%. Two-tailed statistical *t*-tests ($\alpha = 0.05$) assuming unequal variance indicated statistical differences in mean values between S8 and S9 (*p*-value < 0.0000). Therefore, the average difference of 0.45 between sections can be viewed as statistically significant.

Figure 3.21 also shows the computation of the OGFC structural coefficient (a_{OGFC}). The computation assumed that everything beneath the surface lifts was the same so that the structural contributions canceled out between the two sections. Therefore, attributing the entire difference ($\Delta SN=0.45$) in SN_{eff} to the OGFC using the current structural coefficient ($a_{control}=0.54$) for dense-graded mixtures in Alabama (*24)* and surveyed average depths of each surface layer (D_{OGFC} and $D_{control\ surface}$) produces a computed a_{OGFC} equal to 0.15. This value is comparable to that often used for aggregate base materials.

Using 0.15 to represent the OGFC and 0.54 to represent the other asphalt materials, an equivalent thickness was determined to achieve the same total structural number. Assuming a 7-inch control section, a section with OGFC would require 6.6 inches of control material topped with 1.25 inches of OGFC to have an equivalent structural number. This assumes the pavement designer would select 1.25 inches for the depth of OGFC, which was used at the test track. Increases or decreases in selected OGFC thickness would alter the final cross section. In the context of this example, however, an OGFC section would require 7.85 inches total AC depth to equal a 7-inch cross section consisting of dense-graded mixes. This is a 12% increase in thickness, which was in the 10-20% range found through mechanistic analysis (*25*). Note that this total thickness is 0.4 inches thinner than what would be recommended in a

state where no structural value is currently attributed to OGFC. In such a state, if the structural design called for 7 inches, there would be 7 inches of dense-graded material topped with the OGFC surface.


$$a_{OGFC} = \frac{a_{control} D_{control\ surface} - \Delta SN}{D_{OGFC}}$$

$$a_{OGFC} = \frac{0.54 * 1.22 - 0.45}{1.35} = 0.15$$
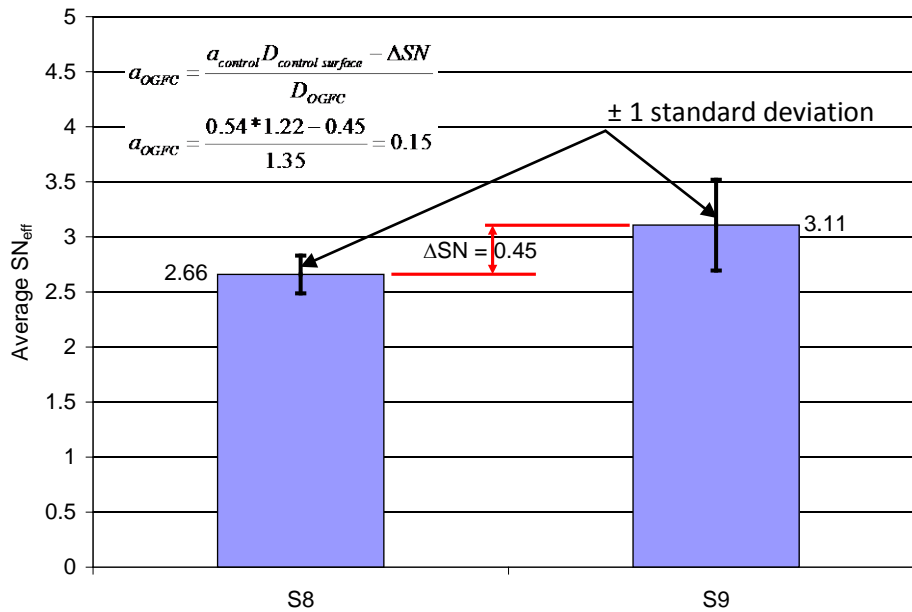
Figure 3.21 Computed SN$_{eff}$ and Computed OGFC Structural Coefficient

Strain Measurement and Analysis

The above computations were based purely on deflection testing and empirical correlation to SN$_{eff}$ using the AASHTO approach. To validate the resulting structural coefficient, it was warranted to utilize embedded strain gauges in the pavement to determine an equivalent thickness of the OGFC section relative to the control section that would produce an equivalent strain between sections. This was done using strain measurements under live traffic conditions.

Tensile microstrain under single axles versus temperature is plotted in Figure 3.22. These data represent weekly measurements obtained from the start of traffic through April 2011. Data from both sections follow an exponential trend with reasonably high R^2. It is interesting to note that the control section had lower strain up to about 95˚F, at which point it crossed over and was generally higher than the OGFC section. While the reason for this behavior was not immediately clear, it also appeared in backcalculated AC modulus from FWD testing. Figure 3.23 shows the backcalculated AC modulus for each section versus temperature. At cooler temperatures, S9 had higher modulus, but became softer at higher temps (above 105˚F). Though this doesn't correspond directly with the temperature from the strain data, it is in a similar range. In both the strain and backcalculated data sets, the regression coefficients of the exponent were higher for the control section. This indicates a greater sensitivity to the temperature of this section. Further investigation of this behavior in the context of mechanistic-empirical pavement design is warranted. For the purposes of this investigation related to the structural coefficient, however, the main interest is in the behavior at the AASHTO reference temperature of 68°F, marked by the vertical line in both Figures 3.22 and 3.23.
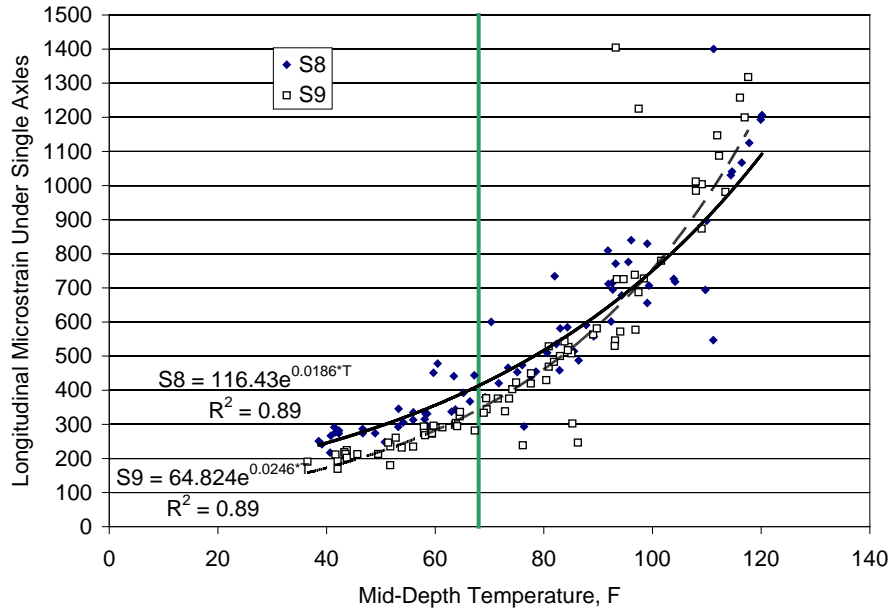
Figure 3.22 Strain Response of S8 (OGFC) and S9 (Control) Sections
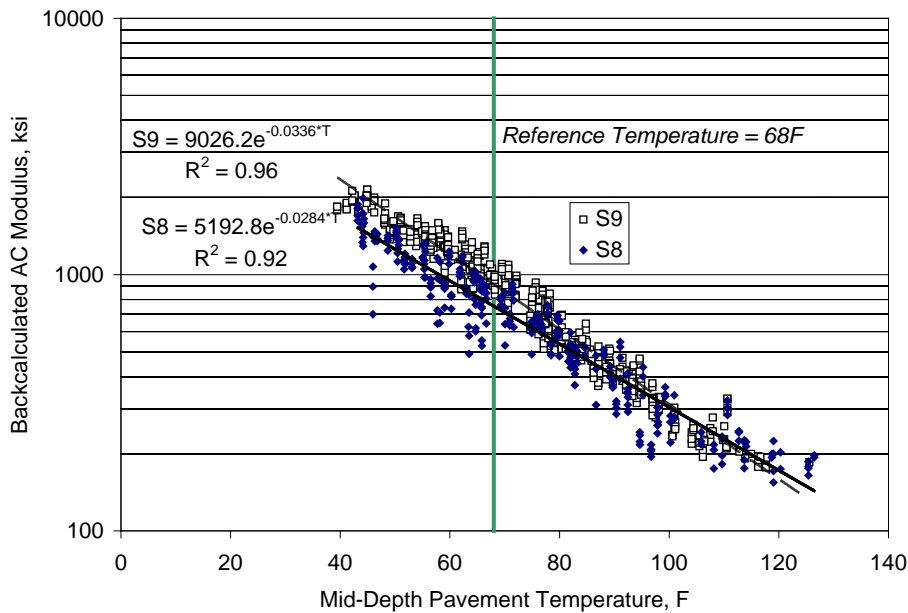

Figure 3.23 Backcalculated AC modulus of S8 (OGFC) and S9 (Control)

Following a similar procedure as described for normalizing deflections to 68˚F (*23*), the strain responses were also normalized to this temperature. Figure 3.24 summarizes the average strain and standard deviation for each section. The differences were found to be statistically significant using a two-tailed *t*-test (α=0.05). Given that the 80 microstrain difference was found to be statistically significant, the primary issue was determining the amount of additional thickness of OGFC required to obtain an equivalent strain. This was determined by using the approximate inverse squared relationship ($\varepsilon \approx 1/h^2$) between strain and thickness (*26*) for a given set of materials in a cross-section.

Figure 3.25 plots the strain-thickness relationship for the OGFC section. The plot has been normalized such that 7 inches yields the field-measured strain of 413 $\mu\varepsilon$. Reducing strain at $1/h^2$ yields a thickness of 7.8 inches to achieve 333 $\mu\varepsilon$, the field-measured strain level in the control section. Recall that using a_{OGFC} required a thickness of 7.85 inches to achieve an equivalent structural number. The strain-determined thickness was thus considered a validation of the AASHTO-derived structural coefficient.
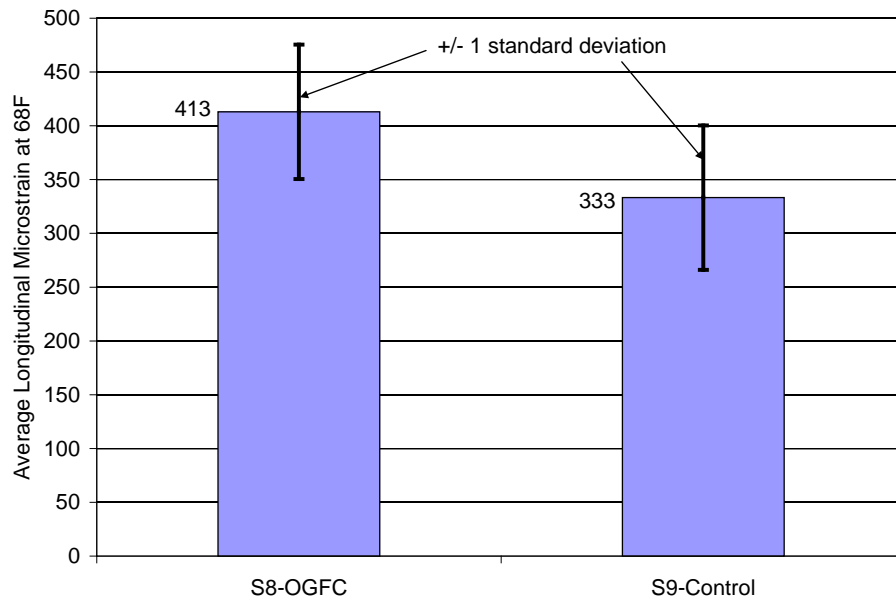
Figure 3.24 Strain Response Normalized to 68˚F
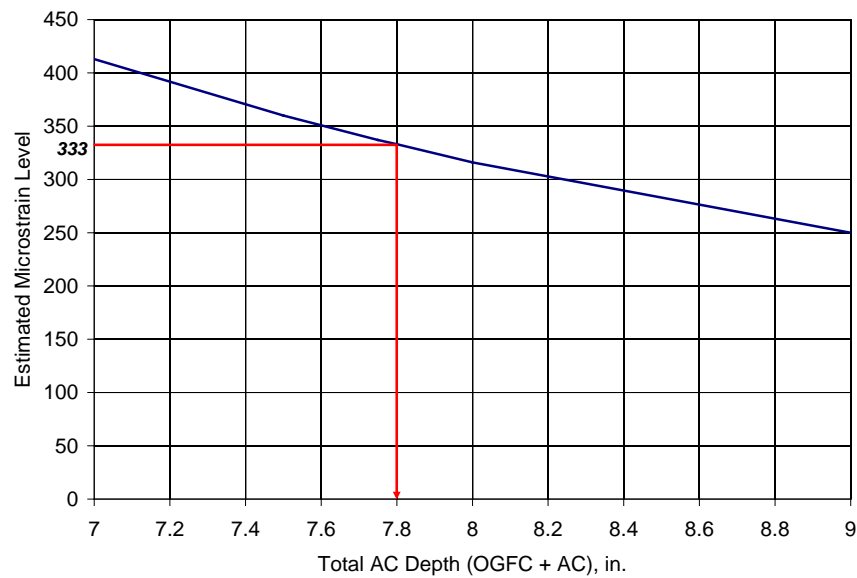
Figure 3.25 Approximate Relationship between Strain and Thickness

Performance

Sections were inspected weekly for signs of cracking and multiple measurements of rutting were made. There was no observed cracking in either section throughout the experiment. Both sections had similar rut depths (approximately 5 mm), as shown in Figure 3.26.
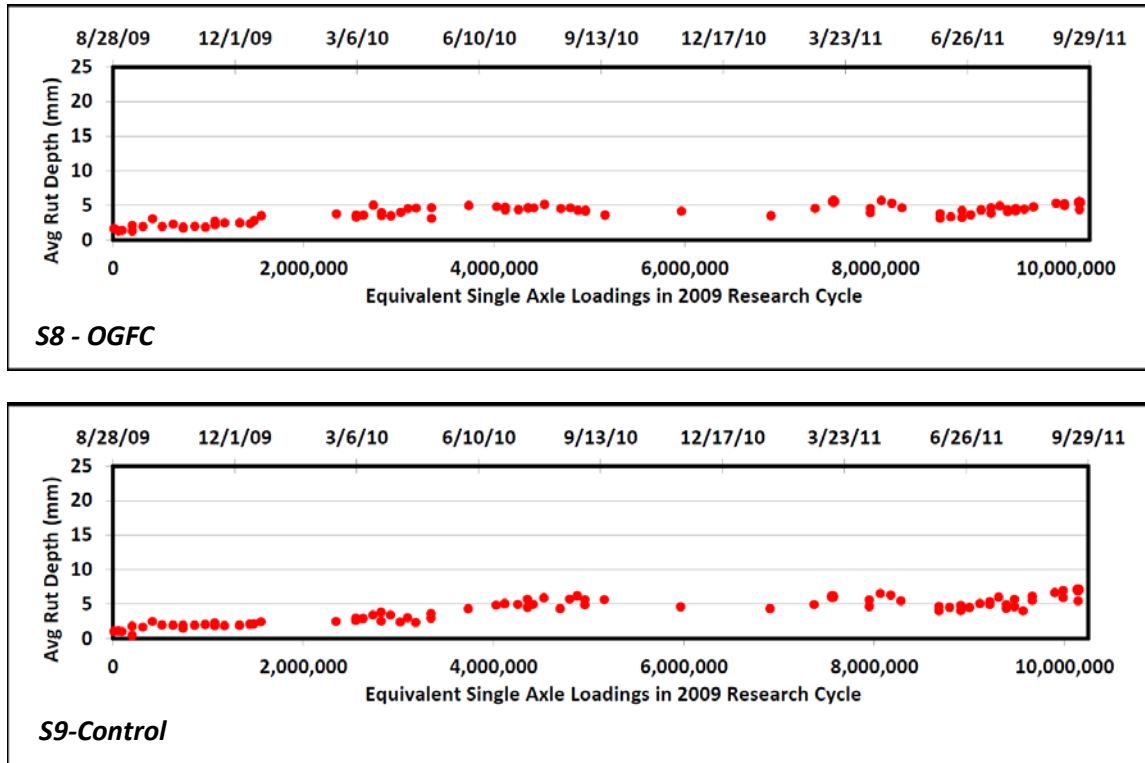
Figure 3.26 Rutting Performance of OGFC (S8) and Control (S9) Sections

Conclusions and Recommendations

The objective of this study was to determine a structural coefficient for OGFC material. Based on the data presented, the following conclusions and recommendations are made:

1. A statistical difference in effective structural number using measured pavement deflection was found between the OGFC and control cross-sections. The difference was directly attributed to the presence of the OGFC, from which a structural coefficient of 0.15 was determined.
2. The increase in required pavement thickness (12%) to achieve the same structural number as a dense-graded cross section, using 0.15 to represent the OGFC, was in the range of a previous independent study that found a 10-20% required thickness increase (*25*).
3. An examination of measured strain response in both sections was used to estimate the required increase in pavement thickness to achieve equivalent strain in the OGFC section relative to the control. The predicted increase was within 0.05 inches of that determined from using a_{OGFC}, equal to 0.15, which further validated this coefficient.
4. Both sections are performing well in terms of fatigue cracking and rutting. Further monitoring and evaluation through the 2012 research cycle are recommended.
5. Though the above findings are based on only two test sections, they have particular value in that the sections were subjected to identical traffic; identical climate; and were paved at the same time using

the same equipment, materials, and paving crew so that many confounding factors typical of a larger sample size were effectively eliminated.

6. Further study is warranted to fully validate the a_{OGFC}, with particular emphasis on field sections.

7. Further study is also warranted to investigate how to best incorporate OGFC materials in mechanistic-empirical pavement design.

8. The reason for less temperature sensitivity within the OGFC section should be further investigated.

3.5 Structural Characterization and Performance of Shell Thiopave® Test Sections

Background

Increasing asphalt prices have renewed interest in utilizing sulfur as a binder extender. Instead of adding sulfur in molten liquid form directly to the asphalt binder, as done in the 1970s, sulfur pellets combined with a warm-mix asphalt (WMA) additive, known as the Shell Thiopave[1] system (Figure 3.27), are introduced into the mixture during production. The Thiopave system developed by Shell Sulfur Solutions allows for mix production around 275°F (135°C), which can significantly reduce hydrogen sulfide emissions (Timm et al., 2011).

Figure 3.27 Thiopave Sulfur Pellets and Compaction Aid (*27*)

NCAT has conducted several laboratory and field studies *(27, 28, 29, 30, 31)* to evaluate the use of Thiopave in asphalt mixtures. Among these studies is the recently completed evaluation of Thiopave at the NCAT Pavement Test Track. This evaluation was conducted in two phases. In Phase I, extensive laboratory testing and structural pavement analysis were conducted to help select pavement cross sections for evaluation at the Test Track (*28, 29*). Based on the results of the Phase I study, two sections were constructed in 2009 for evaluation in Phase II. Section N6 was 7 inches thick to compare directly against the Group Experiment control section having the same thickness design. Section N5 was 9 inches thick to evaluate perpetual pavement concepts (*27*). The focus of this summary report is on the Phase II study.

Objective

The main objective of the Phase II study was to evaluate the structural behavior and performance of the two Thiopave® test sections relative to a control section.
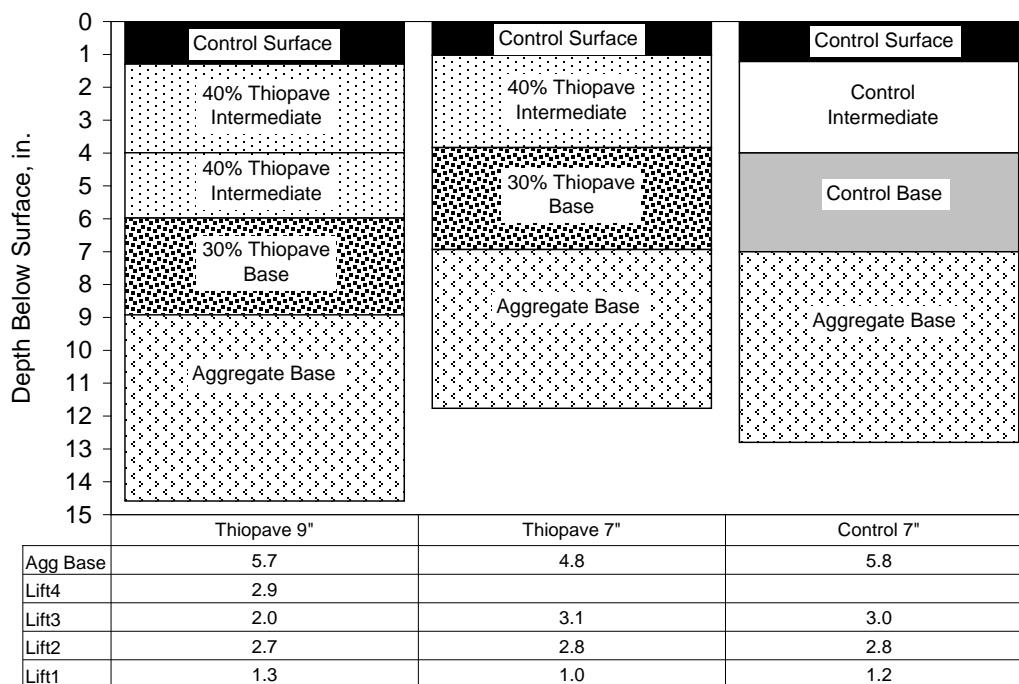
Test Sections and As-Built Properties

There were five mixtures in this study subdivided into "Thiopave-modified" and "control" mixtures. The control mixtures included surface, intermediate and base courses while the Thiopave mixtures were intermediate and base courses. The aggregate gradations were a blend of granite, limestone and sand using locally-available materials. Distinct gradations were developed for each control mixture (surface, intermediate and base) to achieve the necessary volumetric targets as the binder grade and nominal

---

[1] Shell Thiopave is a trade mark of the Shell Group of Companies

maximum aggregate size (NMAS) changed between layers. The Thiopave mixture gradations matched the control intermediate mixture gradation.

Figure 3.28 illustrates the as-built thicknesses of each test section while Table 3.15 contains other pertinent as-built properties. Lift 1 in each section was comprised of the control surface mixture with identical asphalt contents and similar in place densities. Lifts 2 and 3 in N5 and lift 2 in N6 were designed to have 40% Thiopave, but due to production issues at the asphalt plant, slightly lower-than-expected Thiopave contents (33 to 39%) were obtained. Similarly, the bottom lifts in N5 and N6 were intended to have 30% Thiopave but were produced at 22%. After discussions between the NCAT researchers and Shell Sulfur Solutions engineers, it was decided to proceed with the experiment with these as-built Thiopave contents. The higher total asphalt contents in the lower lifts of N5 and N6 relative to the control resulted from designing the Thiopave mixtures at 2% design air voids while the control mixtures were designed at 4%. The lower design air voids were meant to yield higher asphalt contents with the expectation of better fatigue performance. It should also be noted that a PG 67-22 binder served as the base asphalt for the Thiopave mixes. The PG 76-22 mixtures (lift 1 in all sections and lift 2 in the control section) were modified with SBS polymer. All sections and lifts met or exceeded 92.5% of maximum theoretical density (less than 7.5% air voids).

	Thiopave 9"	Thiopave 7"	Control 7"
Agg Base	5.7	4.8	5.8
Lift4	2.9		
Lift3	2.0	3.1	3.0
Lift2	2.7	2.8	2.8
Lift1	1.3	1.0	1.2

Figure 3.28 Thiopave and Control Cross Sections – As Built Thicknesses

Table 3.15 As-Built Properties of Asphalt Concrete

Section	N5 (Thiopave 9")				N6 (Thiopave 7")			S9 (Control 7")		
Lift	1	2	3	4	1	2	3	1	2	3
NMAS, mm[a]	9.5	19	19	19	9.5	19	19	9.5	19	19
PG Grade (Virgin Binder)[b]	76-22	67-22	67-22	67-22	76-22	67-22	67-22	76-22	76-22	67-22
Delivery Temperature, F[c]	288	243	229	225	282	238	249	275	316	254
% Total Binder[d]	6.1	5.7	5.6	6.2	6.1	5.7	6.1	6.1	4.4	4.7
% Thiopave[e]	0	39	33	22	0	35	22	0	0	0
%G_{mm}[f]	94.1	93.0	92.9	93.6	93.8	92.9	93.7	93.1	92.8	92.6

[a]NMAS: nominal maximum aggregate size
[b]PG Grade (Virgin Binder): asphalt grade without Thiopave modification
[c]Delivery Temperature: surface temperature of mix measured directly behind paver with infrared device
[d]% Total Binder: total gravimetric asphalt content (includes Thiopave material where indicated). Determined by ignition oven.
[e]%Thiopave: percent of total binder percentage that is Thiopave
[f]%G_{mm}: percent of maximum theoretical specific gravity

Laboratory Performance Testing

During production of the mixtures at the plant, samples of mix were obtained for laboratory testing and characterization. This section summarizes testing results for each mixture; detailed results were presented in a previous report (*27*).

For specimen fabrication, the mix was re-heated and then split into appropriately-sized samples for laboratory testing. The individual samples of mix were returned to an oven set at the target compaction temperature. Once the loose mix reached the target compaction temperature, the mix was compacted into the appropriately-sized testing specimen. No short-term mechanical aging (AASHTO R30) was conducted on the plant-produced mixes. The Thiopave-modified mixtures were treated a little differently from the control mixtures based on the advice of the Shell. The target compaction temperature for these mixtures was 250°F. However, to achieve full re-melting of the crystals formed by the sulfur-modifier, these mixes were reheated to 285°F and thoroughly stirred prior to being allowed to cool to the compaction temperature.

Figure 3.29 compares the unconfined E* testing results performed in accordance with AASHTO TP 79-09 for the mixtures used in the three test sections. The control surface mix was the softest mix across the full range of temperatures and frequencies in an unconfined state. This mix was used in both Thiopave sections and the control section. The stiffest mix was the Thiopave-modified intermediate course followed by the control intermediate course with a polymer-modified binder. The Thiopave-modified base course showed higher moduli at the high temperature, low-frequency end of the spectrum than the control base course with unmodified binder. However, these mixes showed similar stiffness behavior at the intermediate temperatures and frequencies.

Bending beam fatigue testing was performed in accordance with AASHTO T 321-07 to determine the fatigue limits of the 19 mm control and Thiopave-modified base mixtures. Nine beam specimens were tested for each mix. Within each set of nine, three beams each were tested at 200, 400, and 800 microstrain. Figure 3.30 compares the fatigue cracking results of the two mixtures. At the high strain level (800 microstrain), the Thiopave mixture exhibited 25% shorter fatigue life. However, for the lower

strain levels (200 and 400 microstrain), the Thiopave mixture exhibited longer fatigue life, and the average fatigue life of the Thiopave mixture was 38 and 436% greater than that of the control mixture, respectively. However, at 200 microstrain, the percent increase should be viewed with some caution since the two beams for the Thiopave-modified mixture had not reached the failure point when the tests were terminated at 12 million loading cycles. The number of cycles until failure was extrapolated using a three-stage Weibull function. Past research has shown this to be the most efficient methodology for estimating the number of cycles to failure without running the beam past 12 million cycles (*32*).
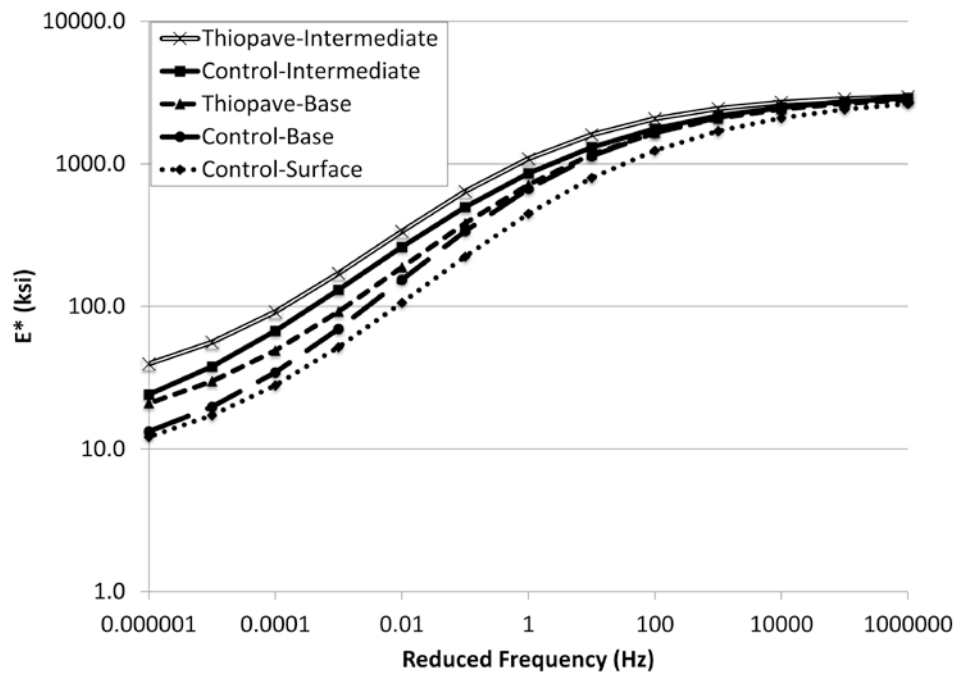
Figure 3.29 Comparison of Unconfined E* Testing Results
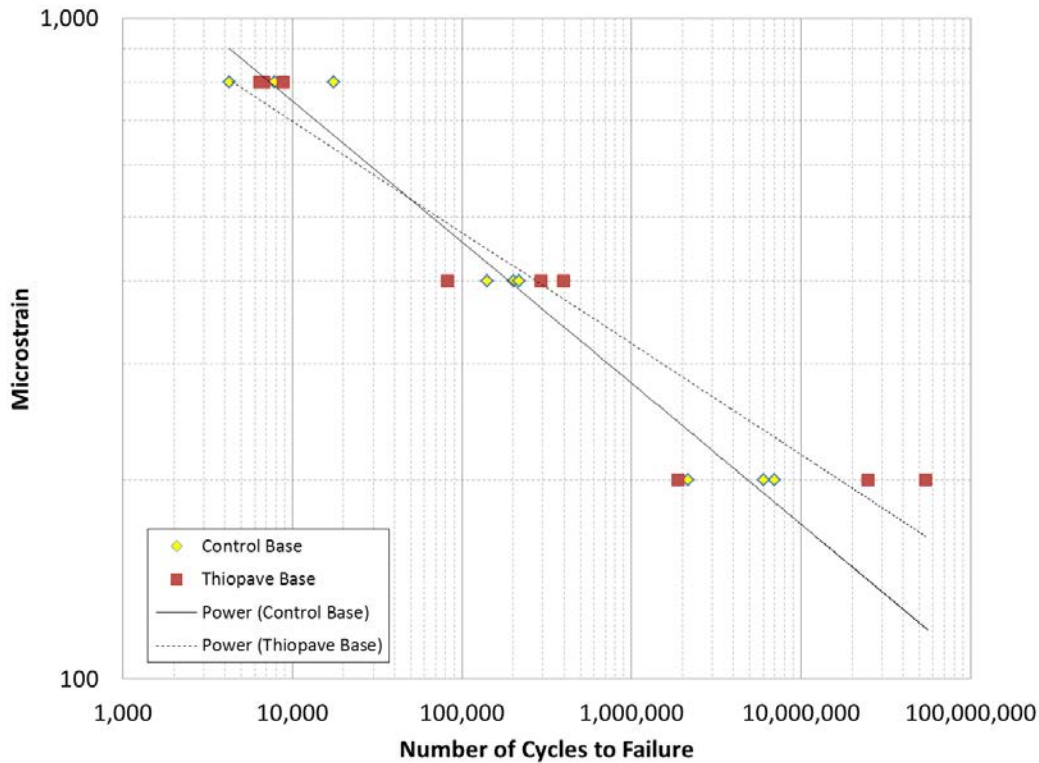
Figure 3.30 Comparison of Fatigue Resistance

Table 3.16 shows the 95% one-sided lower prediction of endurance limit for each of the two mixes based on the number of cycles to failure (Figure 3.30) determined in accordance with AASHTO T 321. The procedure for estimating the endurance limit was developed under NCHRP 9-38 (*32*). Based on the results shown in Table 3.16, the 30% Thiopave mixture had a fatigue endurance limit 19.8% higher than the control mixture. The asphalt binder contents are almost the same in the two mixtures; thus, the improvement may be attributed to the addition of Thiopave, resulting in a higher total binder content in the Thiopave mixture.

Table 3.16 Predicted Endurance Limits

Mixture	% Asphalt Binder	% Thiopave	% Total Binder	Endurance Limit (Microstrain)
Control Base	4.7	0.0	4.7	91
Thiopave Base	4.8	1.4	6.2	109

*Note that percentages are of total mixture.

The rutting susceptibility of the four mixtures—the Thiopave, base control, and surface control mixes—was evaluated using the APA test procedure in accordance with AASHTO TP 63-09. The samples were tested at a temperature of 64°C (the 98% reliability temperature for the high PG grade of the binder for the Test Track). Manual depth readings were taken at two locations on each sample after 25 loading cycles and at the conclusion of testing (8,000 cycles) to determine the sample rut depth.

The rate of secondary rutting was also determined for each mixture by fitting a power function to the rut depths measured automatically in the APA during testing. Rutting typically occurs in three stages: primary, secondary, and tertiary. The confined state provided by the molds prevents the mixture from

ever truly achieving tertiary flow. Therefore, once the mixture has overcome the stresses induced during primary consolidation, it is possible to determine the rate at which secondary rutting occurs.

Table 3.17 summarizes the APA test results. Past research at the Test Track has shown that if a mixture has an average APA rut depth less than 5.5 mm, it should be able to withstand 10 million equivalent single axle loads (ESALs) of traffic at the Test Track without accumulating more than 9.5 mm of field rutting. Thus, both Thiopave mixtures and the control mixtures are not suspected to fail in terms of rutting during the 2009 trafficking cycle.

Table 3.17 Summary of APA Test Results

Mixture	Average Rut Depth, mm	StDev, mm	COV,%	Rate of Secondary Rutting, mm/cycle
Control-Surface	3.07	0.58	19	0.000140
Control-Base	4.15	1.33	32	0.000116
Thiopave-Intermediate	2.00	0.68	34	0.000067
Thiopave-Base	4.07	1.36	34	0.000161

Of the four mixtures, the Thiopave intermediate mix had the best, or smallest, rate of rutting. This mixture also had the lowest amount of total rutting in the APA. While the Thiopave base mix had a lower total rut depth than the control base mix in the APA, it had a higher rate of secondary consolidation. This suggests the Thiopave-rich bottom base mix accrues rutting at a faster rate than the control base mix once initial consolidation occurs, which is expected. Overall, the relative rankings of the mixtures were as expected. The Thiopave intermediate mix with a higher design air voids (3.5%) and greater amount of Thiopave was more resistant to rutting than both the Thiopave base mix (2% design air voids) and control mixtures (4% design air voids).

FWD Testing and Analysis

During the two-year research cycle, the control section was subjected to FWD testing three Mondays per month. The Thiopave sections were tested on alternating Mondays. This schedule was necessary because of time constraints and the need to test sixteen sections within the structural experiment. Within each section, twelve locations were tested with three replicates at four drop heights. The data presented below only represent the results at the 9,000-lb. load level, using EVERCALC 5.0 to backcalculate composite layer properties with RMSE errors less than 3%.

Figure 3.31 illustrates the strong relationship between mid-depth asphalt concrete (AC) temperature and backcalculated AC modulus. Interestingly, the best-fit exponential regression lines cross at approximately 70˚F with the Thiopave sections exhibiting slightly higher composite moduli for all AC lifts at cooler temperatures and slightly lower moduli at higher temperatures. This observation was not consistent with the laboratory dynamic modulus mastercurves presented earlier for each individual lift, which showed the Thiopave mixtures were consistently stiffer than the corresponding control mixtures throughout the temperature-frequency range.

To statistically examine the differences between sections in backcalculated composite AC moduli over a range of temperatures, the moduli were normalized to three reference temperatures (50, 68 and 110˚F) that represented the range of FWD test temperatures. The results are summarized in Figure 3.32. Tukey-Kramer testing at each temperature found statistically-significant differences at 50 and 110˚F

between all sections. At 68˚F, only N6 (Thiopave 7") and S9 (control) were found to be different from each other. Though the differences were statistically significant, it is important to understand that at 50˚F, the composite Thiopave AC moduli were only 7-10% higher than the control while at 110˚F they were 12-18% lower. The difference detected between N6 and S9 at 68˚F was only 1.4% in average moduli. One could certainly argue whether these differences are practically significant.
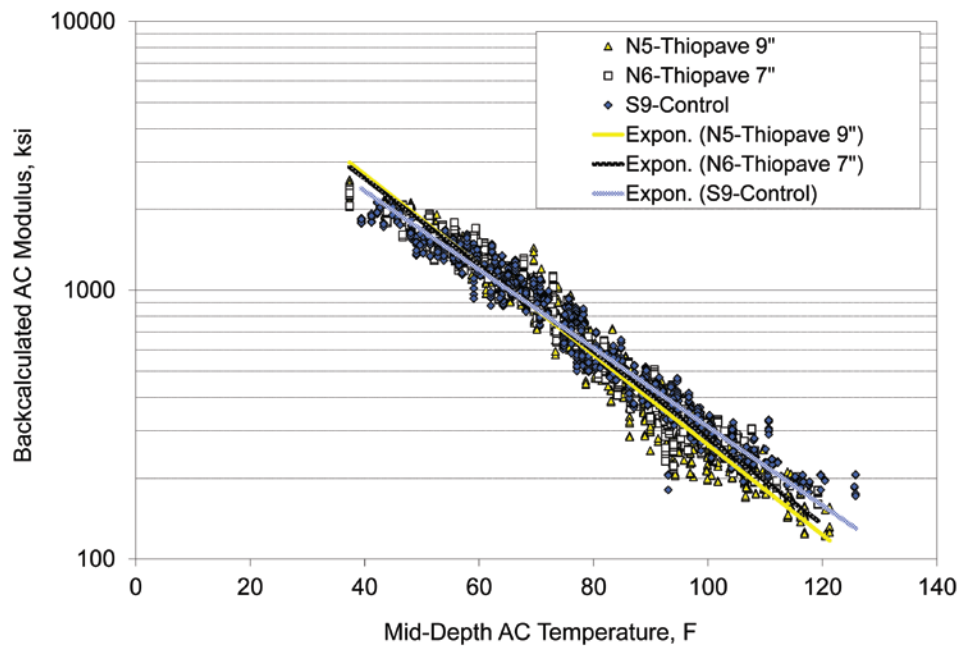
Figure 3.31 Backcalculated AC Modulus vs Temperature
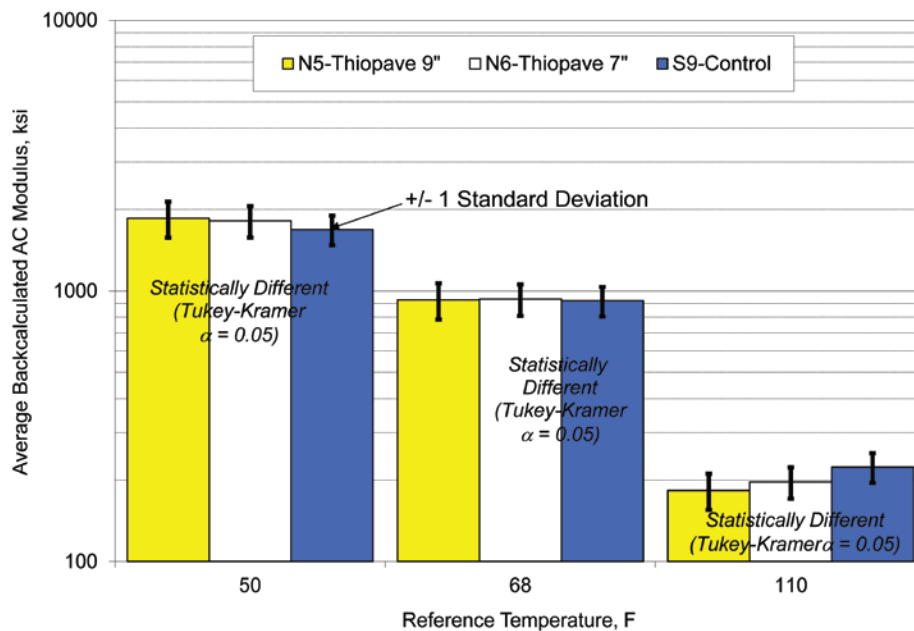
Figure 3.32 Temperature-normalized Backcalculated AC Modulus

Pavement Response Measurement and Analysis

On a weekly basis over the two-year research cycle, asphalt strain measurements from 15 truck passes were obtained in each section. Figure 3.33 summarizes the strain data from the bottom of the AC from single axles related to mid-depth pavement temperature. Each section's data were fit with an exponential regression equation from which temperature-normalized strains were determined and summarized in Figure 3.34.

As expected, the thicker Thiopave section (N5) exhibited the lowest strain throughout the entire temperature spectrum. Compared to the control, strain in N5 was approximately 22-37% lower. Since the moduli were only marginally different from the control, as discussed above, the strain reduction can be primarily attributed to increased thickness. At 50˚F, N6 and S9 were statistically similar, while at the two higher temperatures, N6 exhibited statistically higher strain than S9 (approximately 6-9%, respectively). This is consistent with the backcalculated composite moduli that indicate the Thiopave mixtures were slightly less stiff than the control at higher temperatures. However, it should be noted that the as-built aggregate base thickness of N6 is approximately 17% less than that of S9, which could also impact the measured strains.
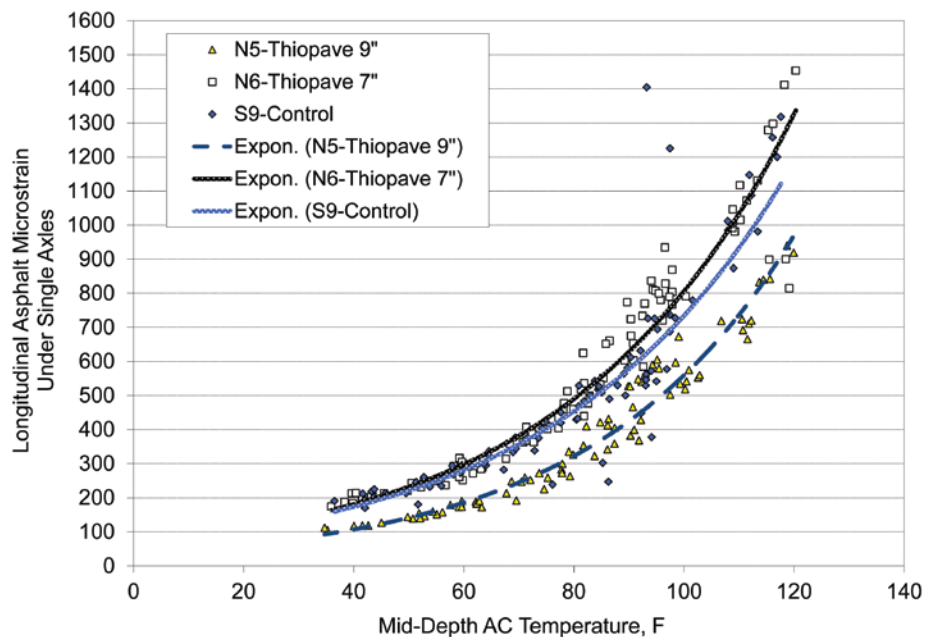
Figure 3.33 Measured Asphalt Strain versus Temperature
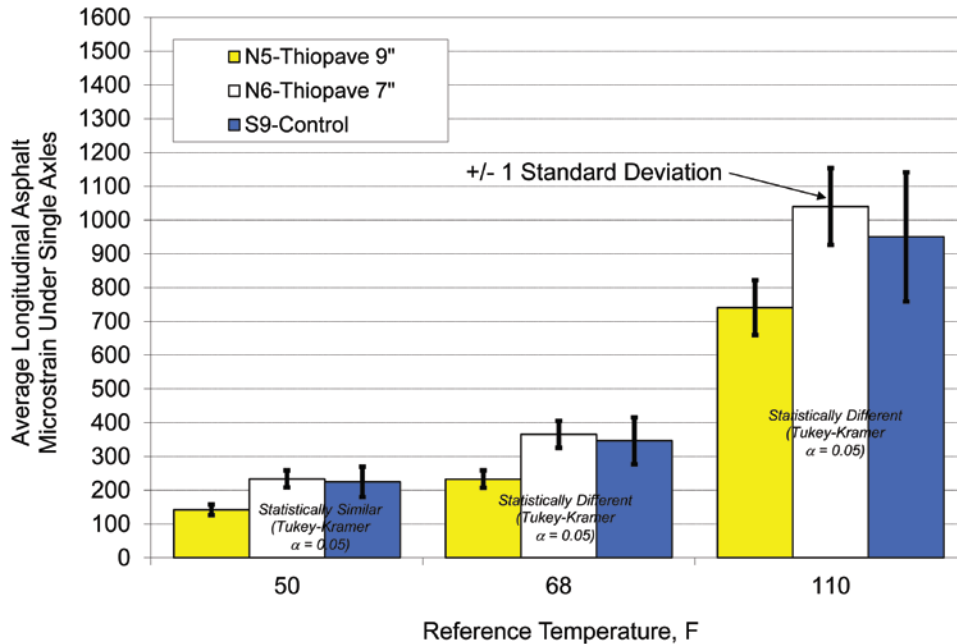
Figure 3.34 Temperature-normalized Asphalt Strain

Although the strain levels in N6 were statistically higher than that in the control section at 68°F, the expected fatigue cracking performance is expected to exceed the control. A previous report (*27*) documented the laboratory-derived fatigue transfer functions for the base mixtures in each section. Using these transfer functions to predict fatigue performance from measured strain, Table 3.18 shows the average measured strain at 68°F, expected repetitions until fatigue cracking failure, and corresponding life as a percentage of the control section. The greatly increased predicted life for N5 results primarily from lower strain levels, while the more moderate – yet significant – increase in N6 fatigue life over S9 results from better fatigue characteristics of the Thiopave base mixture.

Table 3.18   Expected Fatigue Life at 68˚F

Section	Average Strain at 68˚F	Expected Repetitions	% of Control
N5 – Thiopave 9"	233	5,206,041	1418%
N6 – Thiopave 7"	365	453,767	123%
S9 - Control	346	367,064	100%

Performance

Weekly monitoring of each section was conducted on Mondays. Sections were inspected for signs of cracking, and multiple measurements of rutting were made. Throughout the experiment, there was no observed cracking on any of the three sections. Figure 3.35 illustrates the progression of rutting. The Thiopave sections had slightly more rutting than the control with 8 mm versus 5 mm, respectively. This is not unexpected given the slightly lower moduli of the Thiopave sections at warmer temperatures. However, after 10 million standard load applications, all the sections have performed very well in terms of rutting.
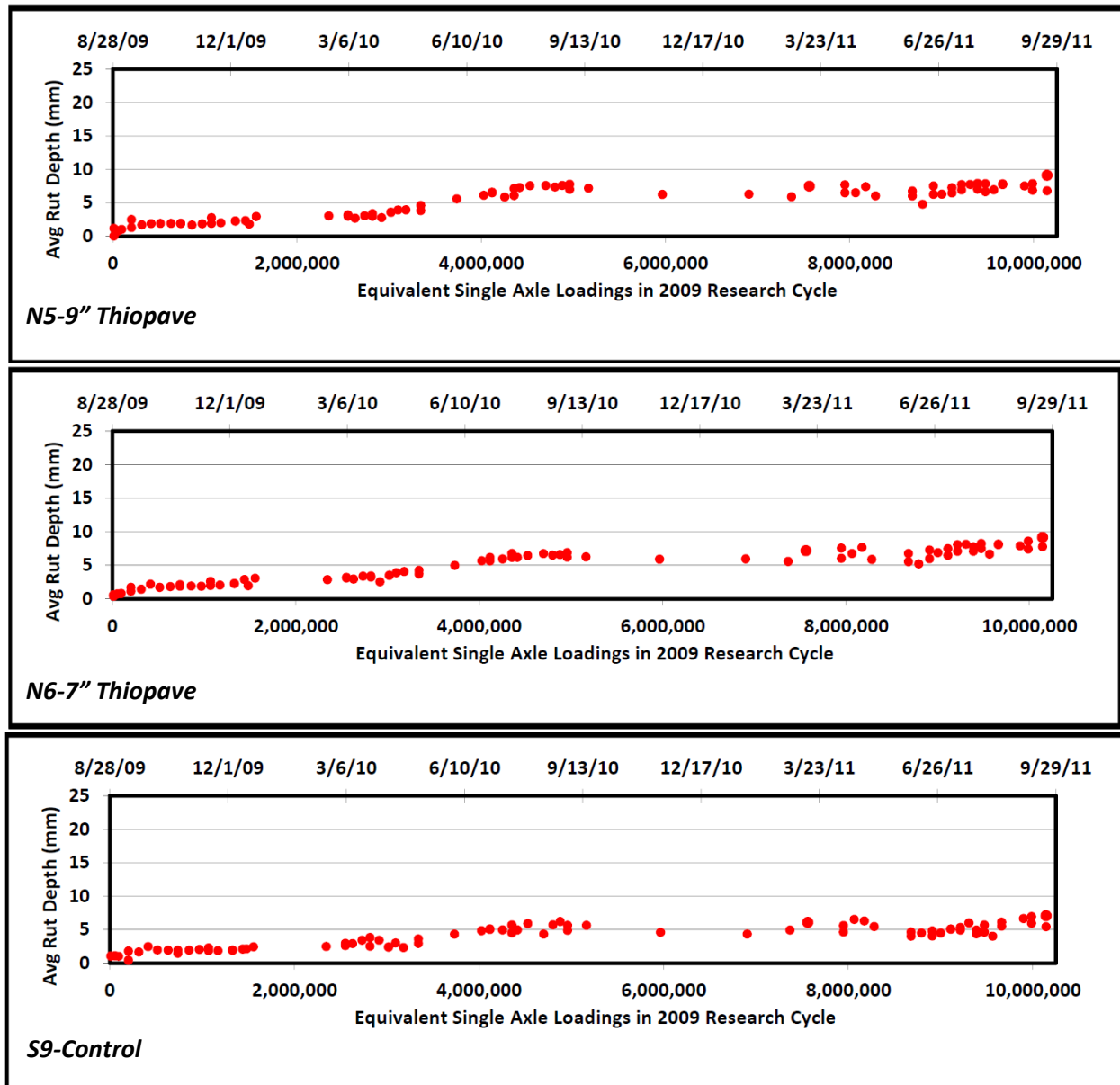
Figure 3.35 Rutting Performance of Thiopave (N5, N6) and Control (S9) Sections

Conclusions and Recommendations

Based on the results of Phase II study at the test track, the following conclusions and recommendations are offered:

1. Dynamic modulus testing of plant-produced laboratory-compacted specimens ranked the mixtures according to decreasing stiffness as follows: Thiopave-intermediate, control-intermediate, Thiopave-base, control-base, and control-surface. The Thiopave-base and control-base mixtures were the most similar mixtures among the five tested.

2. Beam fatigue testing of the base layers demonstrated significantly higher cycles to failure for the Thiopave-base mix relative to the control-base mix. This was especially apparent at the lowest strain level tested (200 microstrain), where the average number of cycles to failure was 436% greater for the Thiopave mixture. This increased performance prediction should be viewed with

caution, however, since the numbers of cycles to failure were extrapolated at 200 microstrain. The predicted endurance limit for the Thiopave-base mixture was 19.8% higher than the control-base mixture.

3. The results of APA testing on the control-surface, control-base, Thiopave-intermediate, and Thiopave-base mixtures were all less than 5.5 mm of rutting after 8,000 cycles. As shown in the measured field rut-depth data, all three sections were able to withstand the 10 million ESALs applied over the two-year traffic cycle without developing 9.5 mm of rutting.

4. At lower temperatures, the backcalculated composite moduli of the Thiopave pavements were slightly higher than that of the control. At higher temperatures, the reverse was true. These differences may be partially attributed to lower-than-designed Thiopave contents in the plant-produced materials; however, the laboratory dynamic modulus results of the same individual plant-produced mixture lifts did not show this trend.

5. The Thiopave section having the 2-inch thickness advantage had significantly lower measured strain levels, as expected.

6. The Thiopave section, with approximately the same thickness as the control, exhibited statistically higher strains compared to the control at moderate to hot temperatures. This trend was expected based on the observed trends in field backcalculated composite AC modulus results and the measured as-built aggregate base thicknesses.

7. Despite slightly higher strain levels in N6 (Thiopave 7"), its better laboratory fatigue behavior resulted in an expected 1.2 times increase in predicted fatigue performance compared to the 7" control section. The factor increased by approximately 14 times for the thicker 9" Thiopave section relative to the control.

8. All sections performed well with respect to rutting, with no measured depths exceeding 10 mm. The Thiopave sections had slightly greater rut depths, with approximately 8 mm of rutting compared to approximately 5 mm in the control section.

9. It is recommended that the sections be left in place for further trafficking to fully evaluate fatigue cracking behavior.

3.6 Structural Characterization and Performance of Kraton Test Section

Background

Ever-increasing traffic intensities and loadings accompanied by depleted agency budgets demand that pavement structures achieve better performance more efficiently to reduce the overall life-cycle cost by utilizing asphalt materials that can carry loads through a thinner cross-section. Polymer-modified asphalt (PMA), a well-established product for improving the effectiveness of asphalt pavements (*33, 34*), has the potential to meet this demand. Use of PMA in intermediate and base courses has been limited due partly to the perception that underlying courses, which are less affected by temperature and traffic conditions, do not need modification. However, the ability of PMA to resist fatigue cracking could, in theory, be used to reduce the overall cross-section of a flexible pavement. With high-polymer loadings (i.e., greater than 7%), PMA can even improve cracking resistance to a much higher level. However, there is a challenge in formulating binders with high-polymer loadings for paving applications due to compatibility and constructability issues.

Kraton Polymers, LLC, has developed a PMA formulation that has a much higher polymer content (7 – 8%) than a typical modification polymer loading of 2.5 – 3% yet has practical compatibility and viscosity for drum plant or pug mill production and for laydown and compaction. At this high content, the polymer forms a continuous network in the asphalt, turning it into an elastomer with substantially increased resistance to permanent deformation and fatigue cracking. Four-point bending beam fatigue testing on mixtures with highly polymer-modified (HPM) binders has shown well over an order of magnitude increase in fatigue life (*35, 36, 37*). In addition, 3D finite element modeling using the continuum damage Asphalt Concrete Response (ACRe) model developed by TU Delft (38, 39) predicts improved resistance to permanent deformation and fatigue damage even with a 40% reduction in thickness *(33, 34, 40*). More technical information about the PMA formulation is presented in another report (*41).*

While the laboratory and simulation work done on this HPM formulation was promising, field trials were necessary to fully understand the in-situ performance characteristics. A full-scale experimental HPM section sponsored by Kraton Polymers, LLC, was constructed at the National Center for Asphalt Technology (NCAT) Pavement Test Track in 2009. The field performance characteristics of this test section were compared to those of a control section. The HPM section was designed to be thinner than the control section to investigate whether equal or better performance could be achieved cost-effectively using HPM materials.

Objective

The main objective of this investigation was to evaluate the structural behavior and performance of the Kraton test section relative to a control section.

Test Sections

Two design gradations were used in this study. The surface layers utilized a 9.5 mm nominal maximum aggregate size (NMAS) while the intermediate and base mixtures used a 19 mm NMAS gradation. The aggregate gradations were a blend of granite, limestone, and sand using locally available materials. Distinct gradations were developed for each control mixture (surface, intermediate, and base) to

achieve the necessary volumetric targets as the binder grade and nominal maximum aggregate size (NMAS) changed between layers. The Kraton gradations were very similar to those of the control mixtures.

Table 3.19 contains pertinent as-built information for each lift in each section. As documented by Timm et al. (*42*), the primary differences between S9 and N7 were the amount of polymer and overall HMA thickness. Section N7 contained 7.5% SBS polymer in each lift while S9 utilized more typical levels of polymer in the upper two lifts with no polymer in the bottom lift. The nominal binder PG grade of the HPM mixtures in N7 was PG 88-22. However, the formulation was designed to meet mixture toughness criteria (or damage resistance) as determined by beam fatigue and finite element modeling (*37, 39*), rather than a specific Superpave PG binder grade. The total HMA thickness in N7 was approximately 1.4 inches thinner than S9 to evaluate its ability to carry larger strain levels more efficiently.

The actual mixing and compaction temperatures, listed in Table 3.19, were very close to the target temperatures, which were decided on through discussions with the polymer supplier, plant personnel, and the research team *(42)*. Test mix was generated at the plant, and test strips were paved to determine optimum compaction temperatures. As shown in Table 3.19, the HPM mixtures required higher mixing and generally higher compaction temperatures due to the increased polymer content.

	Kraton	Control
Agg Base	5.5	5.8
Lift3	2.5	3.0
Lift2	2.1	2.8
Lift1	1.0	1.2
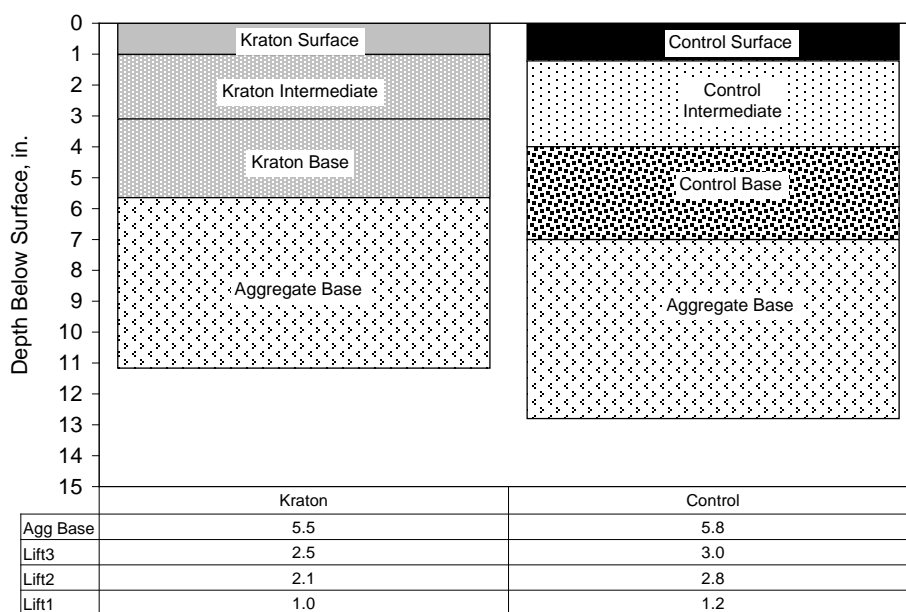
Figure 3.36 Kraton and Control Cross Sections – As Built Thicknesses

Table 3.19 Asphalt Concrete Layer Properties – As Built (Timm et al., 2011)

Lift	1-Surface		2-Intermediate		3-Base	
Section	N7-Kraton	S9-Control	N7-Kraton	S9-Control	N7-Kraton	S9-Control
Thickness, in.	1.0	1.2	2.1	2.8	2.5	3.0
NMAS[a], mm	9.5	9.5	19.0	19.0	19.0	19.0
%SBS	7.5	2.8	7.5	2.8	7.5	0.0
PG Grade[b]	88-22	76-22	88-22	76-22	88-22	67-22
Asphalt, %	6.3	6.1	4.6	4.4	4.6	4.7
Density, % of Gmm	93.7	93.1	92.7	92.8	92.8	92.6
Plant Temp, ^{o}F[c]	345	335	345	335	340	325
Paver Temp, ^{o}F[d]	307	275	286	316	255	254
Comp. Temp, ^{o}F[e]	297	264	247	273	240	243

[a]Nominal Maximum Aggregate Size
[b]Superpave Asphalt Performance Grade
[c]Asphalt plant mixing temperature
[d]Surface temperature directly behind paver
[e]Surface temperature at which compaction began

Laboratory Performance Testing

During mixture production at the plant, samples of binder and mix were obtained for laboratory testing and characterization. This section summarizes testing results for each mixture; detailed results were presented in a previous report (*41*).

For sample fabrication, the mix was re-heated in the 5-gallon buckets sampled during production at approximately 20°F above the documented lay-down temperature for the test track. When the mix was sufficiently workable, the mix was placed in a splitting pan. A quartering device was then used to split out appropriately sized samples for laboratory testing. The splitting was done in accordance with AASHTO R47-08. The individual samples of mix were then returned to an oven set to 10-20°F above the target compaction temperature. Once a thermometer in the loose mix reached the target compaction temperature, the mix was compacted into the appropriately sized performance testing sample. No short-term mechanical aging (AASHTO R30-02) was conducted on the plant-produced mixes from the test track since these mixes had already been short-term aged during production. A summary of the target laboratory compaction temperatures for this project is provided in Table 3.20.

Table 3.20 Summary of Laboratory Compaction Temperatures (Timm et al., 2011b)

Lift	1-Surface		2-Intermediate		3-Base	
Section	N7-Kraton	S9-Control	N7-Kraton	S9-Control	N7-Kraton	S9-Control
NMAS[a], mm	9.5	9.5	19.0	19.0	19.0	19.0
%SBS	7.5	2.8	7.5	2.8	7.5	0.0
PG Grade[b]	88-22	76-22	88-22	76-22	88-22	67-22
Lab Comp. Temp, ^{o}F	315	290	315	310	315	310

Table 3.21 summarizes the true grade and performance grade of each binder determined in accordance with AASHTO M 320-10. The results confirmed that all the binders used in the construction of the two sections were as specified in the mix designs. It should be noted that while the binder used in N7 had a

high-temperature performance grade of 88°C and rotational viscosity of 3.6 Pa·S, its workability and compactability were similar to those of a PG 76-22 binder both in the laboratory and in the field.

Table 3.21 Grading of Binders

Mixture	True Grade	Performance Grade
All Lifts of N7 (Kraton)	93.5 – 26.4	88 – 22
Base Lift of S9 (Control)[f]	69.5 – 26.0	64 – 22
Intermediate Lift of S9 (Control)	78.6 – 25.5	76 – 22
Surface Lift of S9 (Control)[g]	81.7 – 24.7	76 – 22

Note: [f]*The binder used in the base lift of Section S9 was graded as PG 67-22 in the Southeast.*
[g]*The original binder used in the mix was mistakenly sampled at the plant, so the binder extracted from the mix was tested.*

Dynamic modulus (E*) testing of five plant-produced mixes was performed both confined and unconfined in accordance with AASHTO TP 79-09. The base and intermediate courses for Section N7 were from the same 19 mm NMAS mix design; hence, the base-lift material was sampled and tested as representative of both materials. The confined testing was conducted at 20 psi confining pressure, and each compacted specimen was tested at all temperatures and frequencies in the confined mode before proceeding with unconfined testing. The addition of confinement did not have an impact on the relative stiffness ranking of the mixes but in the magnitude of the dynamic modulus values at the high-temperature end of the master curve. Hence, for this report, only unconfined E* testing results are presented; a comprehensive analysis of all E* test results is presented in a previous report (*41*).

Figures 3.37 and 3.38 compare the E* master curves for the surface mixes (9.5 mm NMAS) and the intermediate and base course mixes (19 mm NMAS), respectively, for the unconfined data. Visual inspection of the E* master curves for the surface mixes shows the Kraton mix to be stiffer than the control surface mix. For the 19-mm mixes, the intermediate control mix has higher stiffness than the Kraton 19-mm mix and control base mix at the high-temperature portion of the curve. Visually, the separation in moduli between the mixes increases from the low-temperature end (right side) to the high-temperature end of the curve (left side).
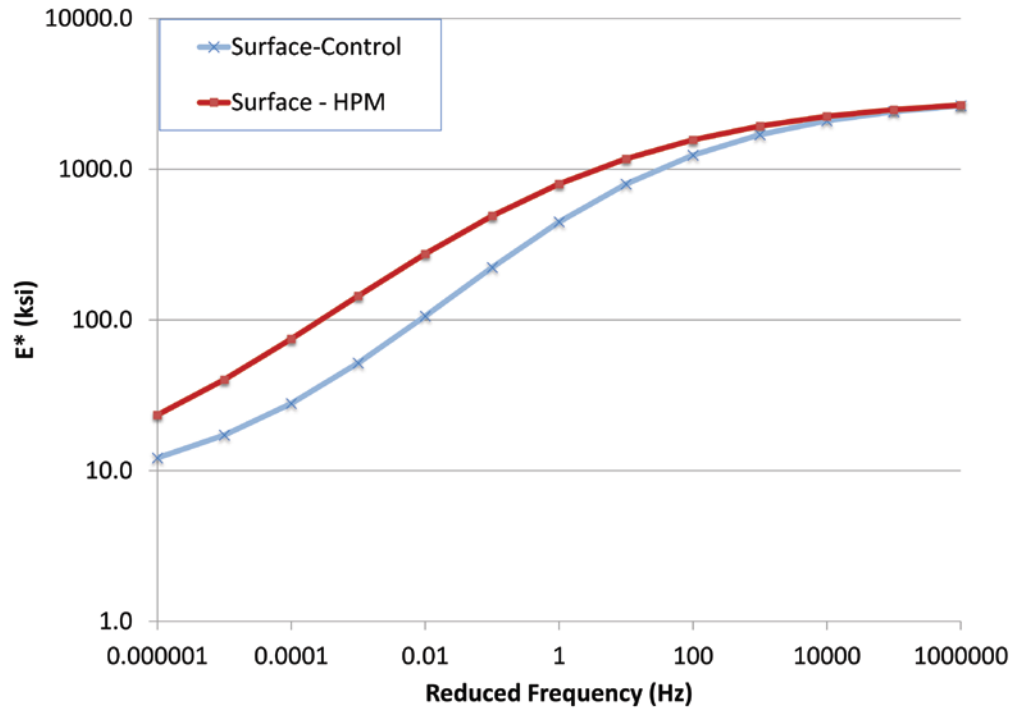
Figure 3.37 Unconfined Dynamic Modulus Testing Results – 9.5 mm NMAS Mixtures
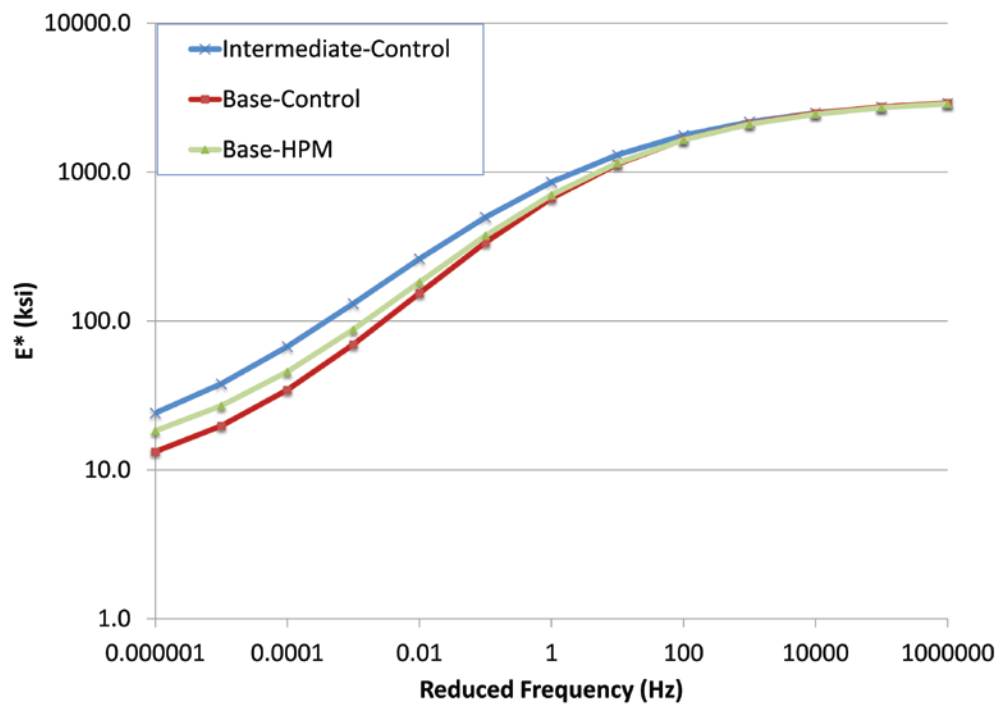

Figure 3.38 Unconfined Dynamic Modulus Testing Results – 19 mm NMAS Mixtures

The rutting susceptibility of the Kraton and control base and surface mixtures were evaluated using the Asphalt Pavement Analyzer (APA) in accordance with AASHTO TP 63-09. Often, only surface mixtures are evaluated for the susceptibility. For this experiment, however, it was directed by the sponsor to test all the Kraton mixtures. For comparison purposes, the control base mixture was also evaluated. The control intermediate mix was not sampled in sufficient quantities to allow for testing since it was not part of the original testing plan.

The samples were tested at a temperature of 64°C (the 98% reliability temperature for the high PG grade of the binder for the control base mix). Manual depth readings were taken at two locations on each sample after 25 loading cycles and at the conclusion of testing to determine the average rut depth.

The rate of secondary rutting was also determined for each mixture by fitting a power function to the rut depths measured automatically in the APA during testing. Rutting typically occurs in three stages: primary, secondary, and tertiary. The confined state provided by the molds prevents the mixture from truly ever achieving tertiary flow. Therefore, once the mixture has overcome the stresses induced during primary consolidation, it is possible to determine the rate at which secondary rutting occurs.

Table 3.22 summarizes the APA test results. Past research at the test track has shown that if a mixture has an average APA rut depth less than 5.5 mm, it should be able to withstand 10 million ESALS at the test track without accumulating more than 12.5 mm of field rutting. Thus, both Kraton mixtures and the control mixtures performed very well in terms of rutting during the 2009 trafficking cycle.

Table 3.22 APA Test Results

Mixture	Average Rut Depth, mm	StDev, mm	COV,%	Rate of Secondary Rutting, mm/cycle
Control-Surface	3.07	0.58	19	0.000140
Control-Base	4.15	1.33	32	0.000116
Kraton-Surface	0.62	0.32	52	0.0000267
Kraton-Base	0.86	0.20	23	0.0000280

Bending beam fatigue testing was performed in accordance with AASHTO T 321-07 to determine the fatigue limits of the base mixtures of the Kraton and control sections. Nine beam specimens compacted to a target air void level of 7 ± 1.0% were tested for each mix. Within each set of nine, three beams each were tested at 400 and 800 microstrain. The remaining three beams for the Kraton mixture were tested at 600 microstrain, while the three control mixture beams were tested at 200 microstrain.

Figure 3.39 compares the fatigue cracking results of the two mixtures. At the highest strain magnitude, the Kraton base mix was able to withstand almost 4 times more loading cycles than the control base mixture. At 400 microstrain, the average fatigue life of the Kraton mixture was much better than that of the control mixture. The average cycles until failure for the control mixture was 186,193 while the number of cycles to failure of the Kraton mixture averaged 6,043,907.
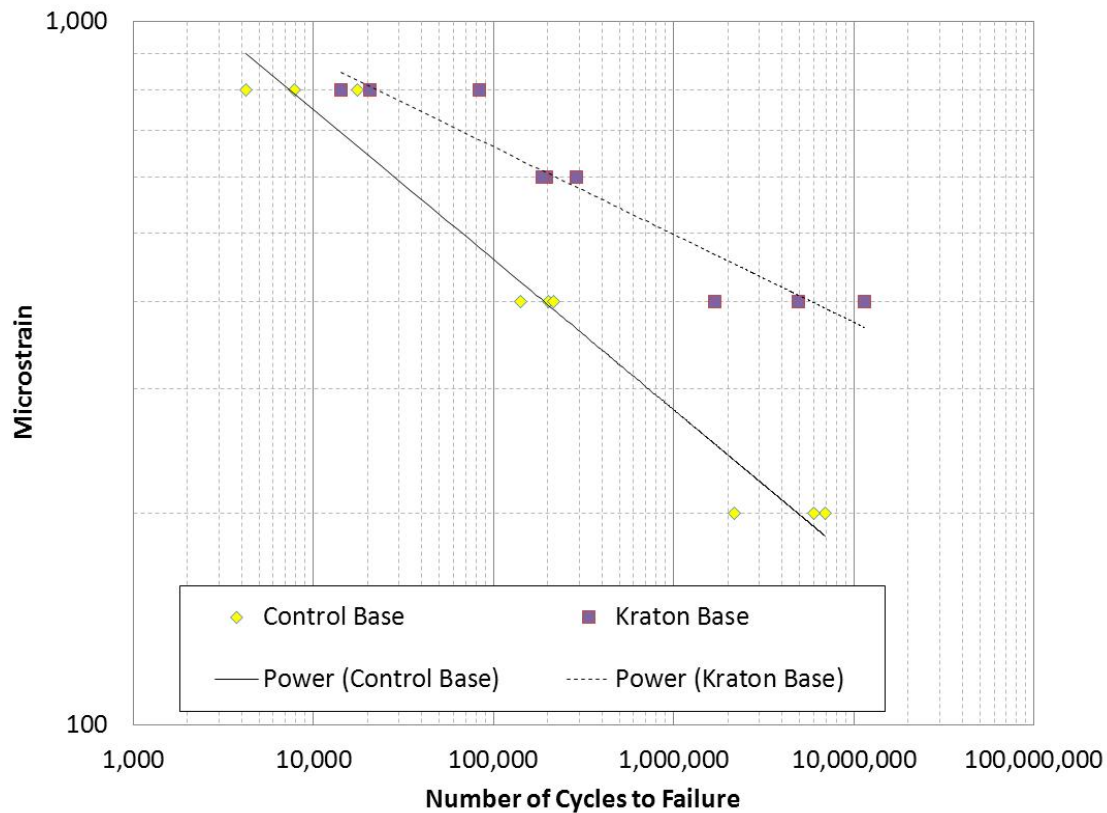
Figure 3.39 Comparison of Fatigue Resistance for Mixtures

Table 3.23 shows the 95% one-sided lower prediction of the endurance limit for each of the two mixes tested in this study based on the number of cycles to failure determined in accordance with AASHTO T 321-07. The procedure for estimating the endurance limit was developed under NCHRP 9-38 (*32*). Based on the results shown in Table 3.23, the Kraton base mixture had a fatigue endurance limit about 2.6 times larger than the control mixture.

Table 3.23   Predicted Endurance Limits

Mixture	Endurance Limit (Microstrain)
Control Base	92
Kraton Base	241

FWD Testing and Analysis

During the two-year research cycle, the control section was subjected to FWD testing three Mondays per month. The Kraton section was tested on alternating Mondays. This schedule was necessary because of time constraints and the need to test a total of 16 sections within the structural experiment. Within each section, 12 locations were tested with three replicates at four drop heights. The data presented below only represent the results at the 9,000-lb. load level using EVERCALC 5.0 to backcalculate layer properties with RMSE errors less than 3%.

Figure 3.40 illustrates the strong relationship between mid-depth asphalt concrete (AC) temperature and backcalculated AC modulus. Interestingly, the best-fit exponential regression lines cross at approximately 77˚F with the Kraton section exhibiting lower moduli at cooler temperatures and higher moduli at higher temperatures. Presumably, the polymer has a more significant impact at higher temperatures, which is consistent with traditional use of polymer modification to control rutting at warm temperatures by increasing the modulus.

To statistically examine the differences between sections in backcalculated AC moduli over a range of temperatures, the moduli were normalized to three reference temperatures (50, 68 and 110˚F) that represented the range of FWD test temperatures. The results are summarized in Figure 3.41. Two-tailed t-tests (α=0.05) at each temperature found statistically significant differences at all three temperatures, indicating the differences seen in Figure 3.41 are significant despite the scatter in data. At 50˚F, the Kraton section had 13% lower AC modulus, at 68˚F it was only 4% lower, while at 110˚F, it was 22% higher than the control.
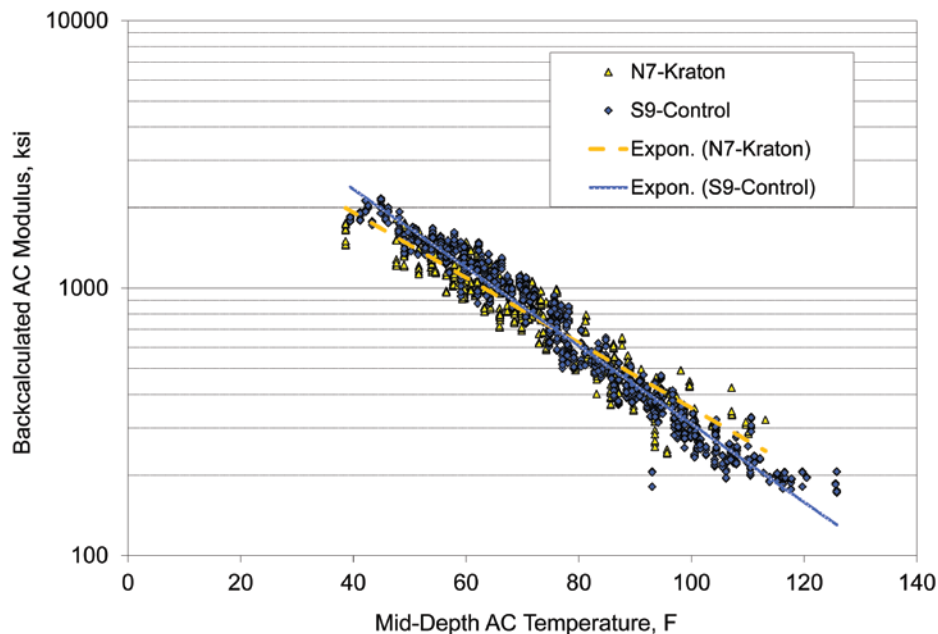
Figure 3.40 Backcalculated AC Modulus vs Temperature
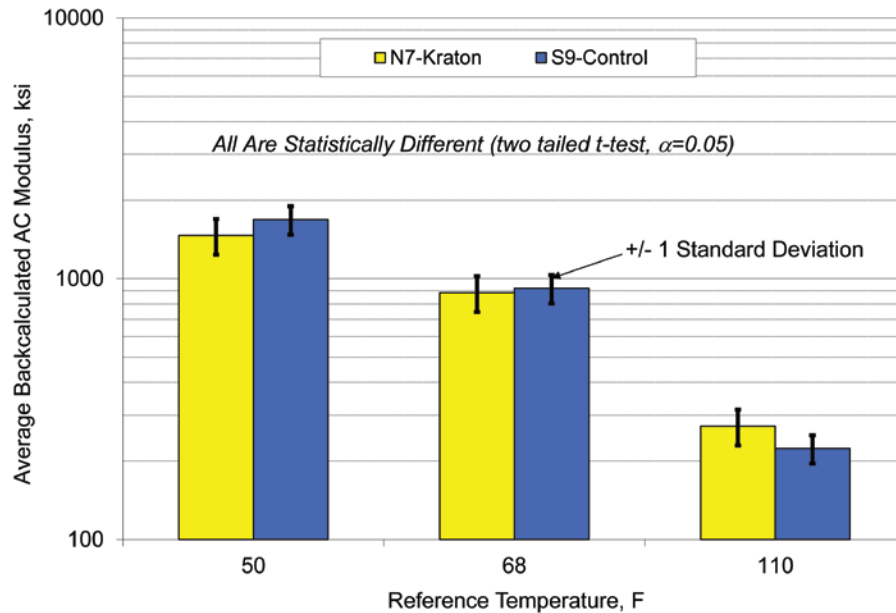
Figure 3.41 Temperature-normalized Backcalculated AC Modulus

Pavement Response Measurement and Analysis

On a weekly basis over the two-year research cycle, asphalt strain measurements from 15 truck passes were obtained in each section. Figure 3.42 summarizes the strain data from the bottom of the AC from single axles related to mid-depth pavement temperature. Each section's data were fit with an exponential regression equation from which temperature-normalized strains were determined and summarized in Figure 3.43.

Figure 3.42 illustrates considerable scatter in the strain data for N7 (Kraton). Previous investigations indicated that increased scatter began in February 2010 (*41*), but a definitive cause for the increased scatter will await further forensic investigation during the 2012 research cycle. The large degree of scatter resulted in no statistical differences between the sections at the lower two reference temperatures. Though this may seem a negative result, it is important to recognize that the Kraton section was 1.2 inches *thinner* than the control, so one would naturally expect higher strain levels. Furthermore, at the warmest temperature, the differences were large enough that the Kraton section's average strain was statistically lower than the control (11% lower). This was due to increased modulus of the Kraton section at the warmest temperature.

Since no cracking had been observed in either section at the conclusion of trafficking, estimates of fatigue cracking performance were made based on field-measured strain at 68˚F. A previous report (*41*) documented the laboratory-derived fatigue transfer functions for the base mixtures in each section. Using these transfer functions to predict fatigue performance from measured strain, Table 3.24 shows the average measured strain at 68˚F, expected repetitions until fatigue cracking failure, and corresponding life as a percentage of the control section. The greatly increased predicted life for N7 was expected since the material was intentionally designed by Kraton to exhibit enhanced fatigue resistance characteristics.

Table 3.24 Expected Fatigue Life at 68˚F

Section	Average Strain at 68˚F	Expected Repetitions	% of Control
N7 – Kraton	334	23,376,065	6363%
S9 - Control	346	367,368	100%
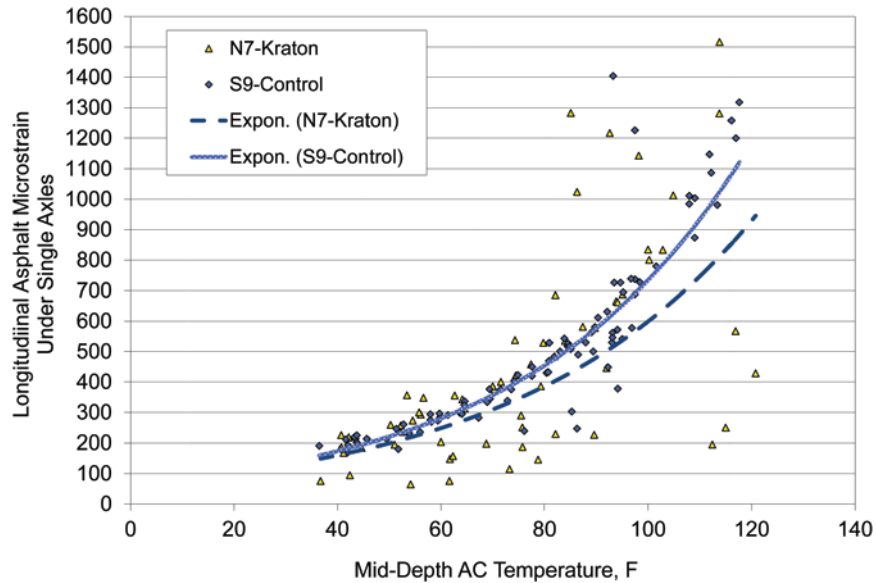
Figure 3.42 Measured Asphalt Strain versus Temperature
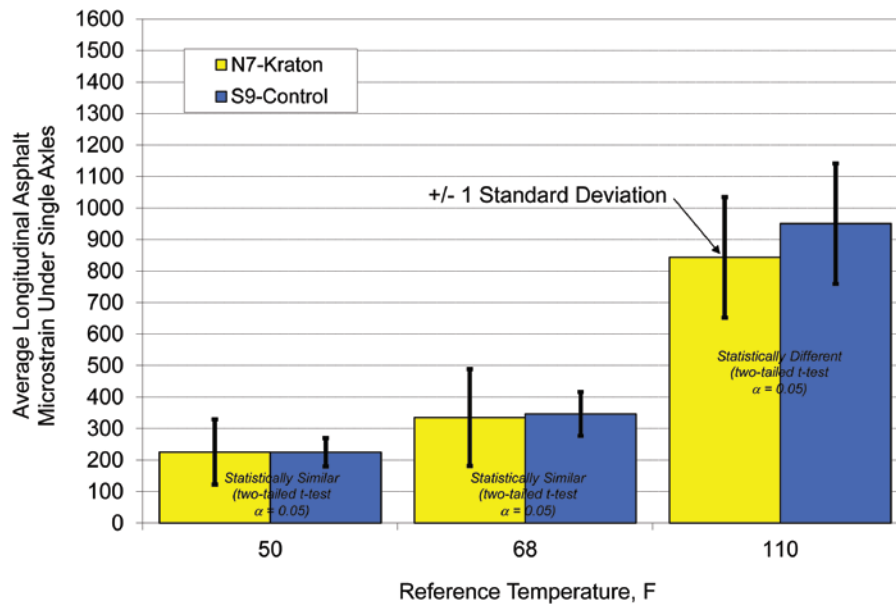
Figure 3.43 Temperature-normalized Asphalt Strain

Performance

Weekly monitoring of each section was conducted on Mondays. Sections were inspected for signs of cracking, and multiple measurements of rutting were made. Throughout the experiment, there was no observed cracking in either section. Figure 3.44 illustrates the rutting progression of each section. The Kraton section had approximately half the total rutting compared to the control, though both performed extremely well. As mentioned above, the improved rutting performance was likely due to higher moduli at warmer temperature controlling rut growth.
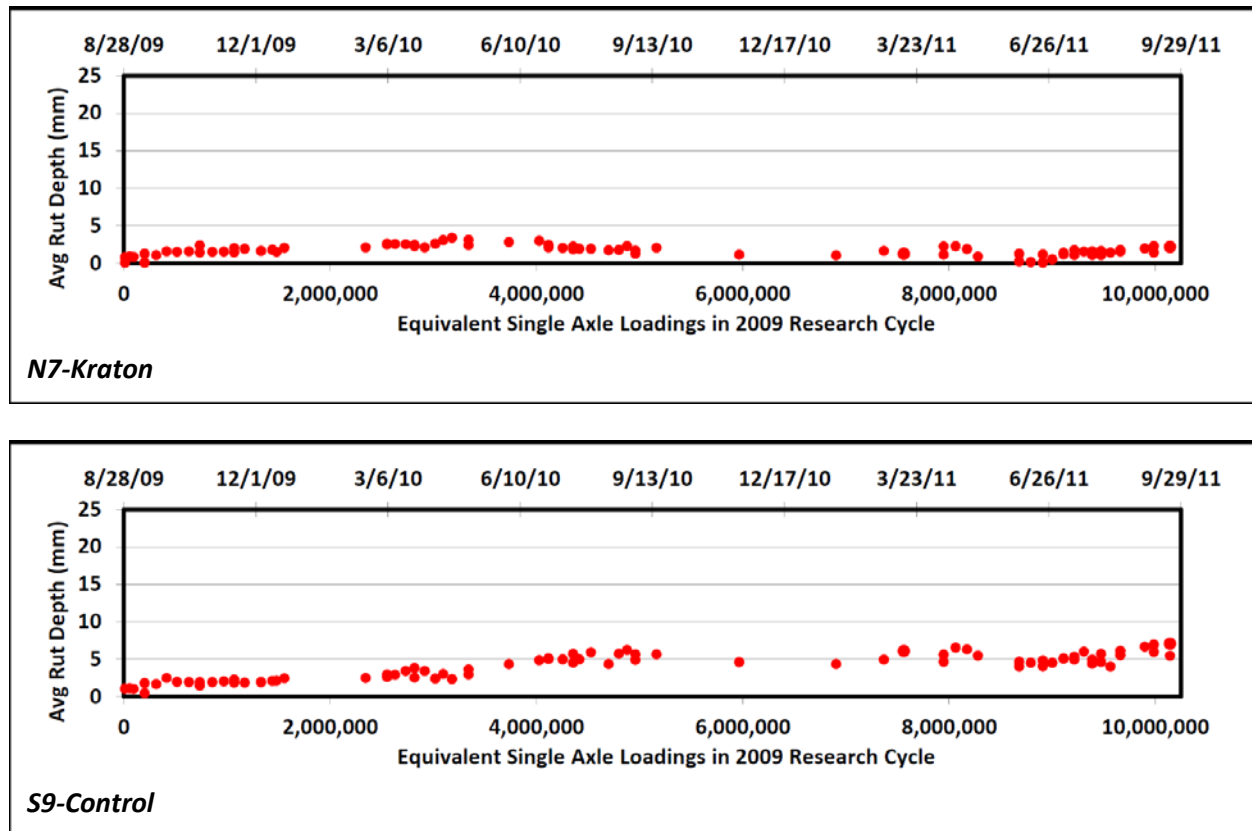

Figure 3.44 Rutting Performance of Kraton (N7) and Control (S9) Sections

Conclusions and Recommendations

1. The Kraton section has performed as well as, or better, than the control section despite having a 1.2-inch thinner cross-section.
2. Based on dynamic modulus testing, the Kraton 9.5-mm NMAS surface mix was significantly stiffer than the control surface mix. For the 19-mm NMAS mixes, the control intermediate layer was stiffer than the Kraton intermediate/base mixture and the control base mixture.
3. In bending beam fatigue testing, the Kraton mixture had a greater number of cycles until failure than the control mixture at both 400 and 800 microstrain. Additionally, the Kraton base mixture had a fatigue endurance limit 2.6 times greater than the control base mixture.

4. Based on the results of APA testing, the Kraton mixtures had statistically lower rut depths than the control mixtures; both sections withstood the 10 million ESALs applied over the two-year traffic cycle without developing 12.5 mm of rutting.
5. Backcalculated AC moduli indicated a lower modulus for the Kraton section at low temperatures while it was higher than that of the control at warm temperatures.
6. Significant scatter in the measured strain data was noted in the Kraton section. The reason for this is pending further investigation. Despite the scatter, statistical testing indicated no differences in measured strains at the lower two reference temperatures. At the warmest temperature (110˚F), the Kraton section exhibited statistically lower strain levels (11% lower). This was due to increased AC modulus at the warmest temperature.
7. It is expected that the Kraton section will exhibit better resistance to fatigue cracking upon further trafficking. Preliminary estimates, based on measured strain at 68˚F and laboratory-determined fatigue transfer functions, indicate the Kraton section has nearly 64 times the fatigue life of the control section.
8. It is recommended that the Kraton and control sections be left in place for the 2012 research cycle to further validate these findings.

3.7 Long-Term Performance Evaluation of Sections N3 and N4

Background

The sections in this investigation were originally built as part of the 2003 structural experiment (*43, 45, 46*) and are shown in Figure 3.45. The two sections were built to differ only in the asphalt binder grade. Section N3 was built with an unmodified PG 67-22 asphalt binder in all three layers, whereas N4 contained an SBS polymer modified binder in all lifts. The thickness of the test sections were designed using the 1993 AASHTO Design Guide with a structural coefficient of 0.44, the standard value used by the Alabama Department of Transportation at that time. The test sections were expected to reach terminal serviceability at 10 million equivalent single axle loads (ESALs), which corresponds to approximately 2 years of traffic at the test track.

At the conclusion of the 2003 research cycle, the sections were still performing well (e.g., no cracking, minimal rutting, low roughness) and were left in place for the 2006 research cycle. Another 10 million ESALs were applied to the sections with still no cracking, minimal rutting, and low roughness at the conclusion of the 2006 research cycle. The sections were again left in place for the 2009 research cycle to further evaluate long-term performance and structural characteristics as the pavements were pushed to 6 years of trafficking service (30 million ESALs). The main areas of this investigation related to backcalculated asphalt concrete moduli and performance characteristics, as discussed below. Though the sections did have embedded instrumentation installed in 2003, very few gauges were working by 2009, which prevented a detailed analysis of measured pavement responses.
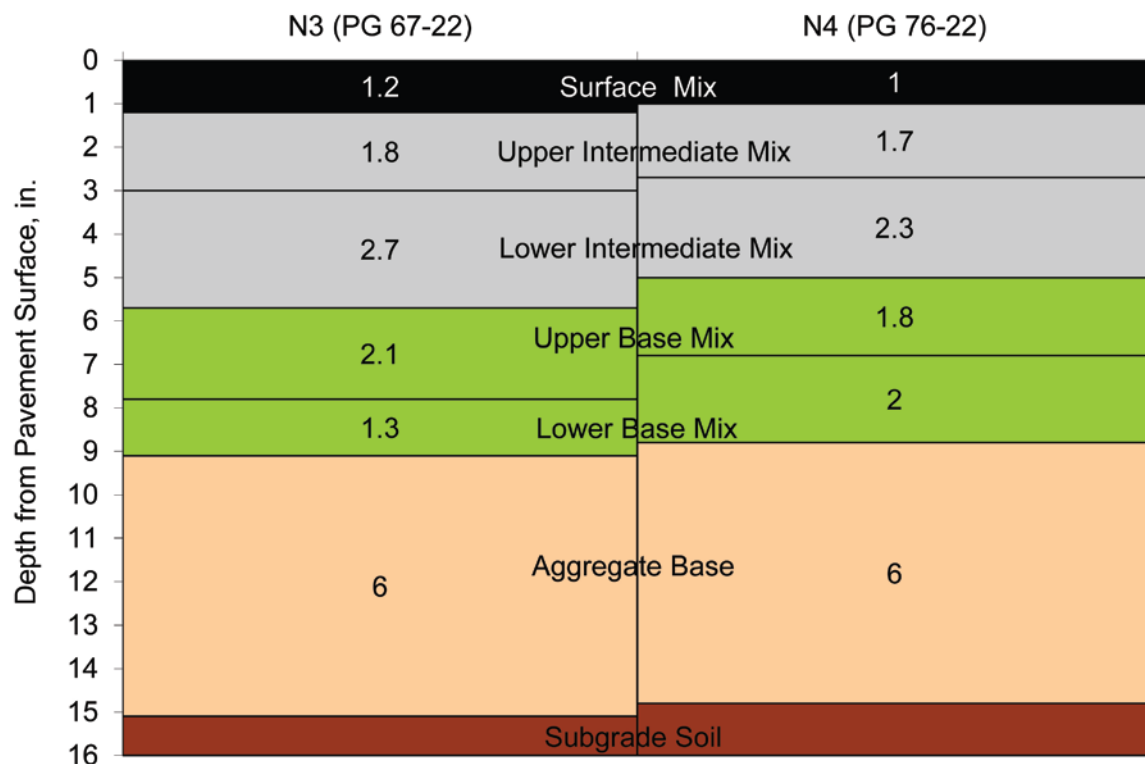
Figure 3.45 Sections N3 and N4

Objective

The main objective of this investigation was to evaluate the long-term structural characteristics and performance of two sections placed in the 2003 NCAT Pavement Test Track research cycle.

Backcalculated AC Modulus

During the 2009 research cycle, falling weight deflectometer (FWD) testing was conducted several times per month. Within each section, 12 locations were tested with three replicates at four drop heights. The data presented below only represent the results at the 9,000 lb load level using EVERCALC 5.0 to backcalculate layer properties with RMSE errors less than 3%.

Figure 3.46 shows the strong relationship, as characterized by exponential regression equations, between mid-depth pavement temperature and backcalculated modulus for both N3 and N4. Figure 3.36 also contains data collected during the 2003 research cycle for comparison. There appears to be a noticeable increase in modulus, caused by aging, during this six-year interval.

To statistically evaluate the aging effect, the moduli for each section were normalized to a 68°F reference temperature using the section-specific regression equations in Figure 3.46. Figure 3.47 summarizes the average and standard deviations of each section at 68°F. Tukey-Kramer statistical testing of the mean values (α=0.05) indicated significant differences between all sections at 68˚F. In other words, there was a statistically discernible aging effect in these sections. Section N3 increased by about 12% during the six-year period, while N4 increase by 20%. Furthermore, as expected, the PG 76-22 section (N4) had higher moduli than the 67-22 section (N3). The difference between the sections during 2003 was about 7%, which increased to a 15% difference in average moduli during the 2009 study.
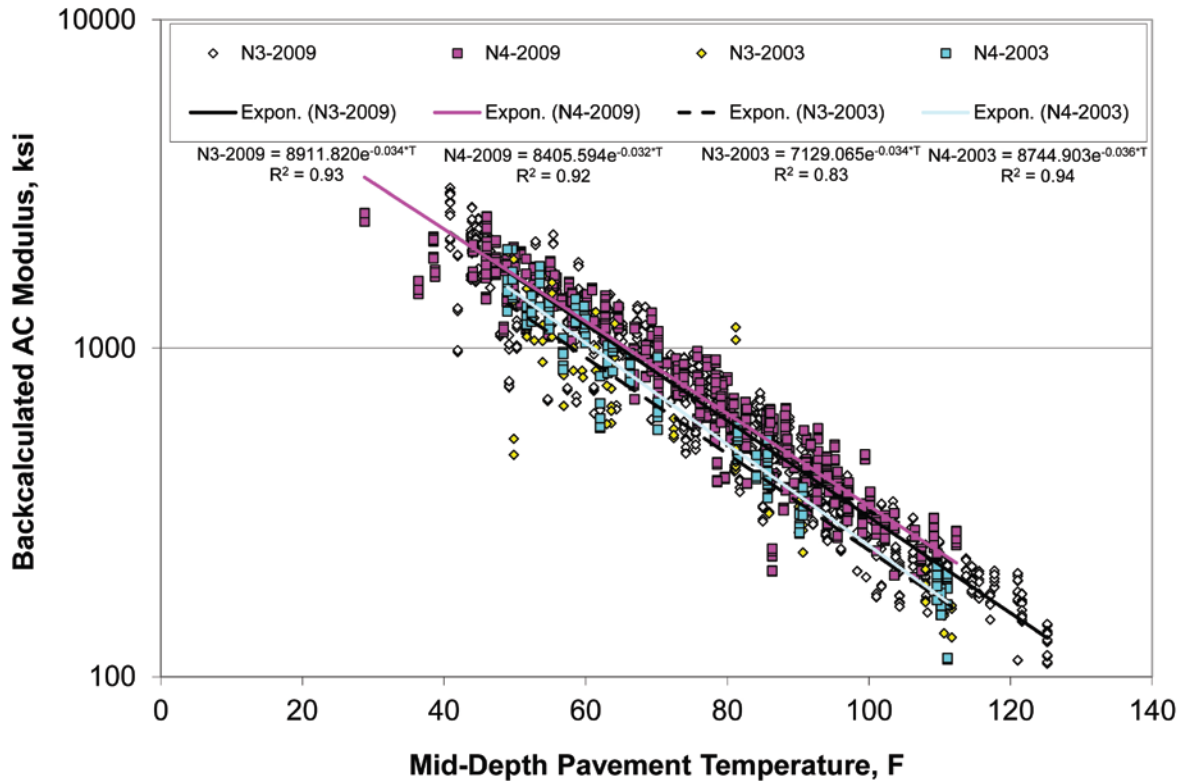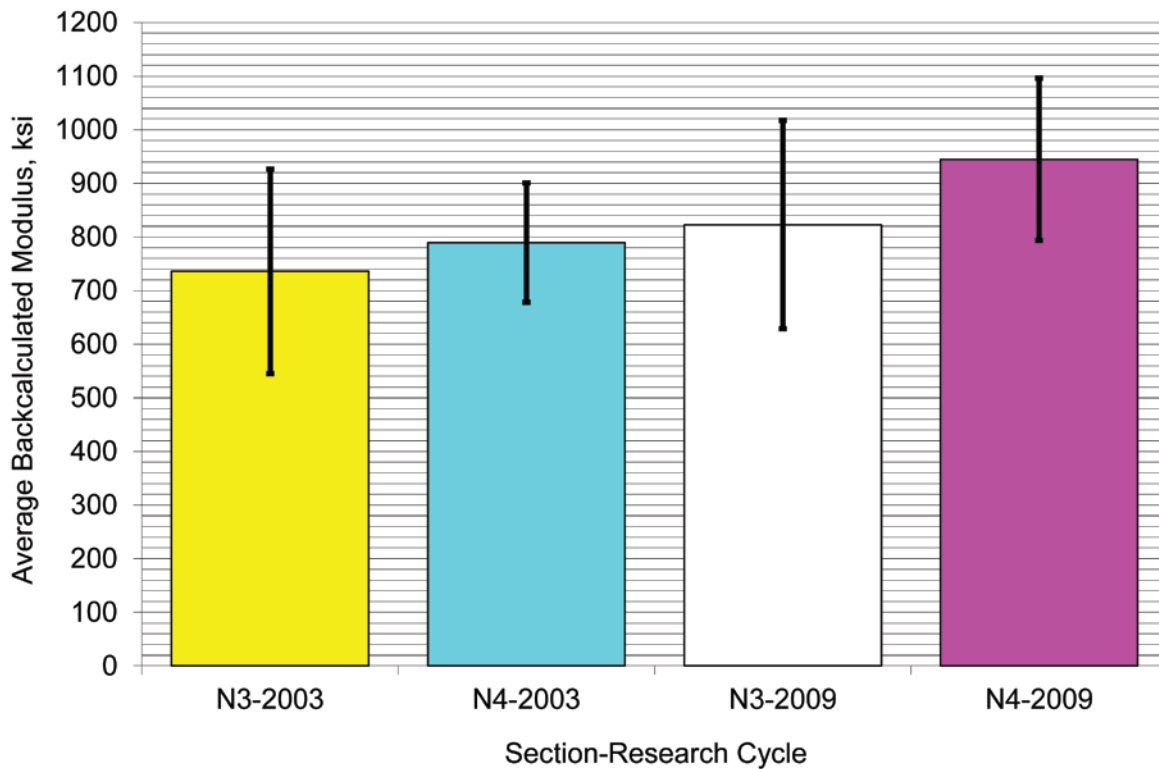
Figure 3.46 Backcalculated Modulus vs Temperature

Figure 3.47 Temperature-Normalized Backcalculated Moduli

Section Performance

Both sections performed extremely well during the 2009 research cycle with little to no additional rutting, as shown in Figure 3.48. Section N3, after 30 million ESALs, has just over 5 mm of rutting while N4 has just below 5 mm. In terms of rutting, these sections have excelled and could be considered perpetual.

Some minor top-down cracks, presumably related to the age of the sections, have developed and are plotted in Figure 3.49. No bottom-up fatigue cracks have been observed, which indicates that the sections will not likely develop classical fatigue cracking if they have not after 30 million ESALs. Again, this is an indication that the pavement may be perpetual. It is recommended that one of the two sections be milled and inlaid for the 2012 research cycle. This will allow an evaluation of perpetual pavement rehabilitation relative to leaving the other section in place for further potential top-down cracking. Since N3 has slightly more rutting and some interconnected cracks, it is recommended for mill and inlay.

Roughness, as measured weekly in terms of the International Roughness Index (IRI), and pavement texture (mean texture depth [MTD]) were remarkably stable during the 2009 cycle. Both N3 and N4 began and finished the research cycle at 50 in/mile (IRI), which is considered very smooth by any standard. For example, the default *initial* IRI in the Mechanistic-Empirical Pavement Design Guide is 63 in/mile. Furthermore, many states that use inertial profilers for smoothness acceptance testing have 50 in/mile either in full or bonus pay range (*46*).
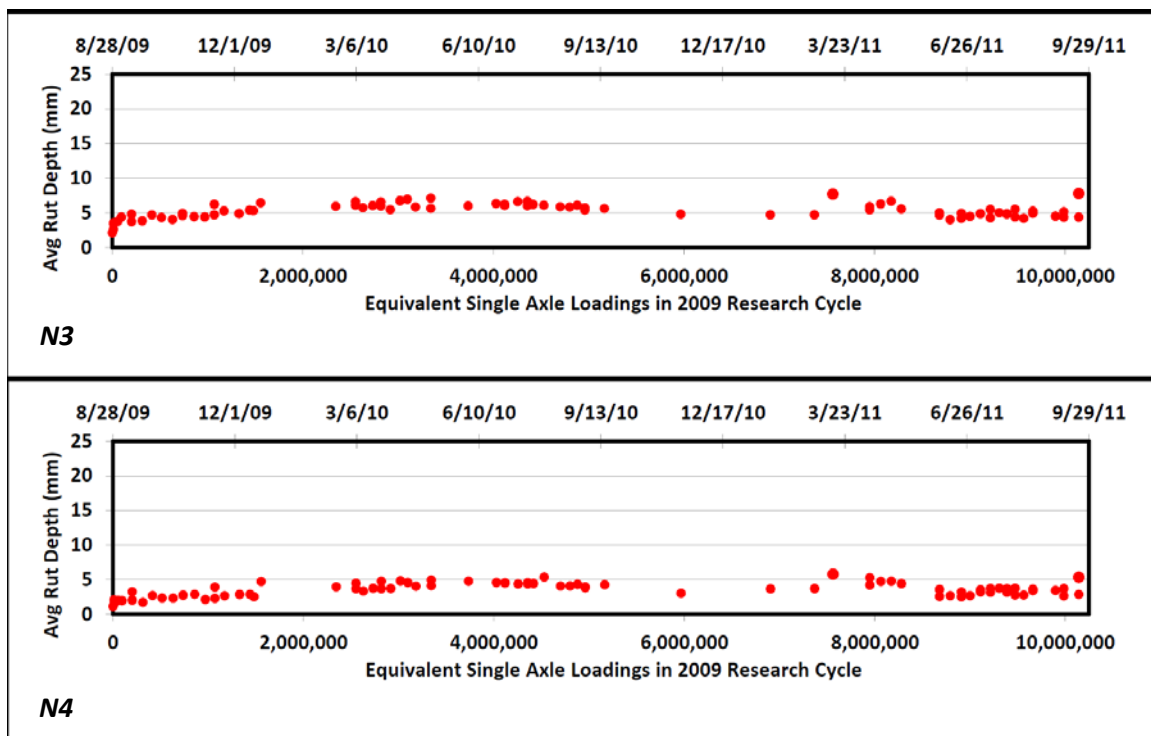

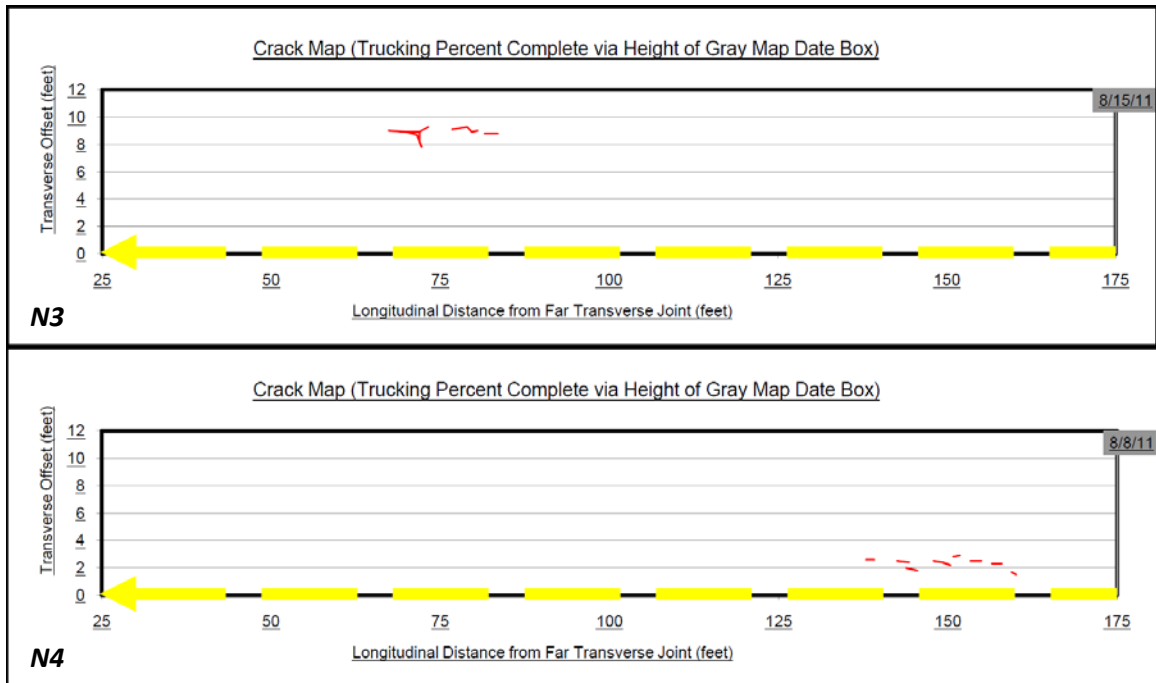**Figure 3.48 Rutting Performance During the 2009 Cycle**

Figure 3.49 Crack Maps at the End of Three Cycles
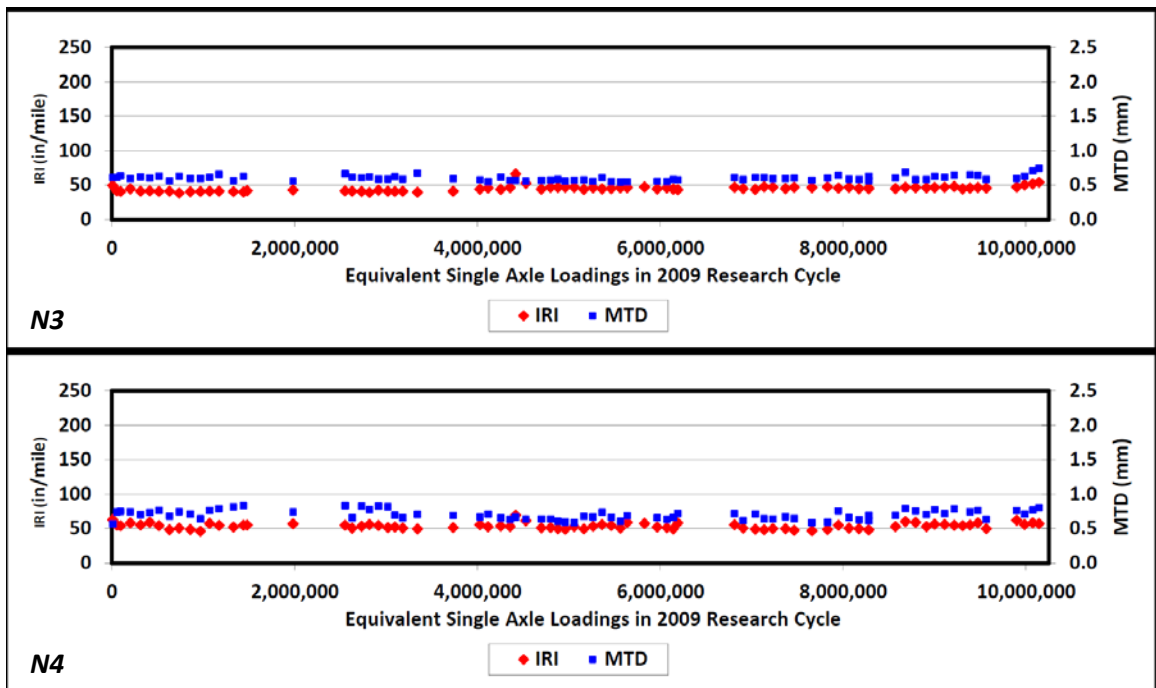
Figure 3.50 Roughness and Texture During the 2009 Cycle

Conclusions and Recommendations

Sections N3 and N4, originally built in 2003 and expected to withstand only 10 million ESALs, have performed extremely well for 30 million ESALs. Thus far, the only signs of distress are minor amounts of top-down cracking, while rutting performance and smoothness have been excellent in both sections. The data from this experiment suggest that these sections are perpetual. An aging effect is evident from backcalculated moduli of the asphalt pavements whereby N3 has increased by about 12% and N4 has increased 20%. It is recommended that N3 have a mill-and-inlay treatment for the 2012 research cycle, while N4 is left in place to evaluate the effectiveness of the mill-and-inlay treatment.

3.8 Florida DOT Study: Effectiveness of a Heavier Tack Coat on Performance of Open-Graded Friction Course

Background

Open-graded friction course (OGFC) is a hot-mix asphalt (HMA) mixture with porosity as a built-in feature for special application purposes. It is placed as a thin surface layer to provide several safety and environment benefits, including improved friction, minimized hydroplaning, reduced splash and spray, and reduced noise level (*47*).

The Florida Department of Transportation (FDOT) has customarily used OGFC as the final riding surface on interstate and high traffic-volume roadways because of its safety benefits. Over the past few decades, OGFC performance has significantly improved due to improvements in design and construction practices and use of better materials, especially polymer-modified asphalt binders (*48*). However, compared to a conventional HMA mixture, OGFC in Florida is still more prone to pavement distresses such as cracking and raveling, shortening its service life (*49*).

The performance of OGFC as a surface layer depends on the durability of the OGFC mixture and the integrity of the underlying layer and the interface bond. Hence, one way to potentially improve the performance of OGFC is to enhance the interface bond between the OGFC and underlying layers by applying a heavier tack coat. To evaluate this concept, FDOT sponsored a study in the 2009 NCAT Pavement Test Track research cycle to evaluate the effectiveness of a heavier tack coat on the field performance of OGFC.
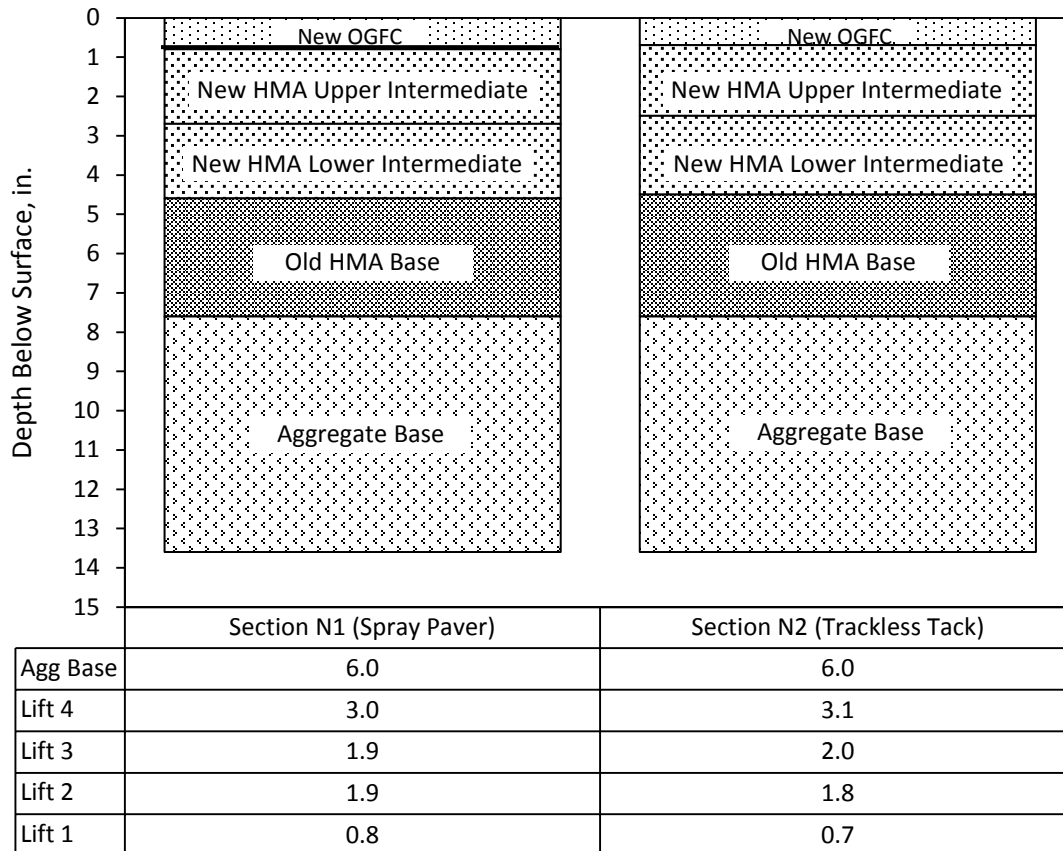
Objective

The main objective of this study was to evaluate the influence of a heavier tack coat on the field performance of OGFC by comparing the performance of the same OGFC mixture placed in Sections N1 and N2. In Section N1, a heavier polymer-modified tack coat was applied using a spray paver right before the OGFC layer was placed. In Section N2, a trackless tack was applied at a regular application rate using a distributor truck. A secondary objective of this study was to evaluate the use of RAP in an OGFC mixture.

Test Sections

Sections N1 and N2 were first built in 2006 for a study sponsored by FDOT in the 2006 test track research cycle to evaluate the Energy Ratio concept for evaluating the top-down cracking resistance of HMA. To prepare for the study on the effectiveness of a heavier tack coat on the field performance of OGFC in the 2009 research cycle, approximately 5 inches of HMA were milled from the two sections. Then, three asphalt layers were inlaid in these sections in 2009. The buildup, which consisted of four asphalt layers as shown in Figure 3.51, was the same for the two sections. The only difference in the two sections was the tack coat applied at the interface between the OGFC surface and the underlying layer. A polymer-modified tack coat (CRS-2P modified with SBS) was applied at a spray rate of 0.21 gal/yd^2 in Section N1 using a spray paver, and a trackless tack was applied at a regular spray rate of 0.05 gal/yd^2 in Section N2. The spray rate for the trackless tack is between the specified application rates of 0.04 and 0.08 gal/yd^2. The CRS-2P and trackless tack materials were supplied as per requirements for emulsified asphalts specified in Section 337-2.3 and Section 916-4, respectively, of the FDOT Standard Specifications.

The OGFC mix design was conducted in accordance with Florida DOT Construction Specifications Section 337 for designing an FC-5 mixture. The asphalt binder used in the mix was a PG 76-22 modified with SBS. The aggregate mixture was a blend of virgin granite aggregate, hydrated lime, and 15% reclaimed asphalt pavement (RAP). The RAP consisted of two fractionations from East Alabama Paving in Opelika, Alabama. The first RAP stockpile was crushed and screened on a 1-inch screen. The second stockpile was fractionated on the #4 (4.75mm) sieve. Table 3.25 summarizes the as-built properties of the asphalt layers in the two sections.

	Section N1 (Spray Paver)	Section N2 (Trackless Tack)
Agg Base	6.0	6.0
Lift 4	3.0	3.1
Lift 3	1.9	2.0
Lift 2	1.9	1.8
Lift 1	0.8	0.7

Figure 3.51 Cross Sections for N1 (Spray Paver) and N2 (Regular Tack) – As-built Thicknesses

Table 3.25 As-built Asphalt Concrete Layer Properties

Lift	1-Surface	2-Upper Intermediate	3-Lower Intermediate	4-Base
Year Built	2009	2009	2009	2006
NMAS, mm	12.5	12.5	12.5	19
Modifier	SBS	NA	NA	NA
PG Grade	76-22	67-22	67-22	67-22
Asphalt, %	5.1	4.6	4.6	4.6
Air Voids, %	20.7	6.4	6.0	7.9
Plant Temp, °F[c]	335	325	315	315
Paver Temp, °F[d]	325	310	300	290
Comp. Temp, °F[e]	290	280	270	280

[c]Asphalt plant mixing temperature
[d]Surface temperature directly behind paver
[e]Surface temperature at which compaction began

Laboratory Testing of OGFC Mixture

Before the production of the OGFC mixture, the OGFC mix design was evaluated for drain-down susceptibility, moisture susceptibility, and abrasion resistance. Additional laboratory testing on the cores extracted from Sections N1 and N2 is underway at the University of Florida to characterize the influence of the heavier tack coat on the OGFC resistance to top-down cracking.

Testing of drain-down susceptibility was carried out in accordance with AASHTO T 305-09, and the results are shown in Table 3.26. The mix did not have significant drain-down of binder at production temperatures or elevated production temperatures.

Table 3.26 Drain-down Susceptibility Test Results

Mix Design	Test Temperature (°F / °C)	Draindown (%)
Control – PG 76-22 w/ SBS	335 / 168 (Production)	0.01
Control – PG 76-22 w/ SBS	362 / 183 (Production Plus 27°F)	0.01
PG 76-22 w/ GTR	320 / 160 (Production)	0.00
PG 76-22 w/ GTR	347 / 175 (Production Plus 27°F)	0.00

The OGFC mix was also evaluated for moisture susceptibility in accordance with AASHTO T 283 using six specimens compacted to 50 gyrations. The results of this testing are given in Table 3.27. Since the tensile strength ratio (TSR) is greater than 0.8, a commonly used TSR criterion, the mix shows sufficient resistance to moisture-induced damage.

Table 3.27 Moisture Susceptibility Results

Parameters	Results
Conditioned Strength, psi	65.9
Unconditioned Strength, psi	75.0
Tensile Strength Ratio	0.88

Finally, the abrasion resistance of the OGFC mixture was evaluated using the Cantabro abrasion test in accordance with ASTM D7064/D7064M-08. As for the specimens used for the moisture susceptibility test, the specimens used for the Cantabro test were also compacted to 50 gyrations. Four samples of the OGFC mix were tested, and the results of this testing are given in Table 3.28. Generally, a percent loss due to abrasion of 20.0% or less is desirable. The mix passed this criterion.

Table 3.28 Cantabro Abrasion Results

Parameters	Results
Test Temperature, °C	25
Average Air Voids, %	17.0
Percent Loss	17.9

Deflection Testing and Backcalculation

During the two-year research cycle, Sections N1 and N2 were subjected to falling-weight deflectometer testing several times per month. This schedule was necessary because of time constraints and the need to test a total of 16 sections within the structural experiment. Within each section, 12 locations were tested with three replicates at four drop heights. The data presented below only represent the results at the 9,000-lb. loading level using EVERCALC 5.0 to backcalculate layer properties. Furthermore, only backcalculated data from within the embedded gauge array (outside wheelpath at random location 4) are presented, as they provided the best correlation to measured pavement responses.

When performing backcalculation, the root mean square error (RMSE) is a general indicator of the accuracy of the backcalculation. A typical cutoff of 3% represents very little difference between measured and computed deflection basins. Figure 3.52 illustrates the backcalculated moduli, normalized to 68°F, and RMSE from N1 and N2 over the two-year research cycle. The modulus data are divided into results from backcalculation with RMSE below 3% and all backcalculated moduli.
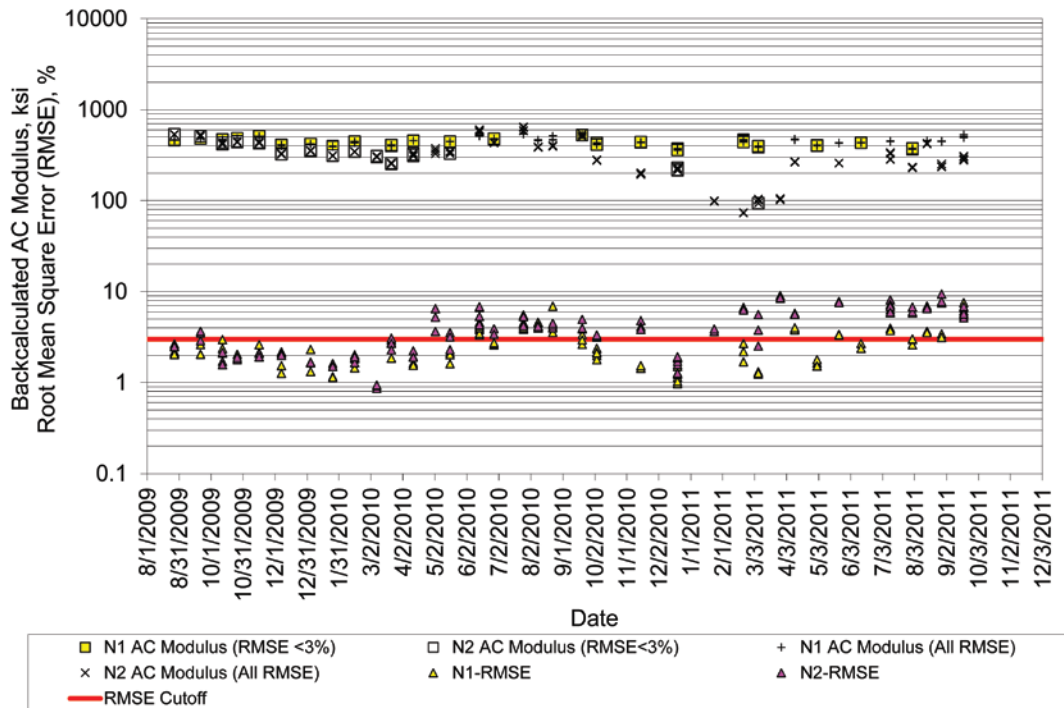
Figure 3.52 Backcalculated AC Modulus at 68°F and RMSE

At the start of the experiment through April 2010, N1 and N2 moduli were very similar, with most RMSEs below 3%. During summer 2010, as pavement temperatures increased, errors also increased above the 3% threshold. This was expected since EVERCALC assumes a linear elastic system and asphalt materials exhibit viscous effects at warmer temperatures, which can lead to poor modeling and higher RMSE. However, the backcalculated moduli with an RMSE greater than 3% were generally consistent with earlier moduli (400 – 500 ksi) with generally similar moduli between the two sections.

In early October 2010, RMSE generally fell below 3% for N1 but remained above 3% for N2. This corresponded to an overall decline in AC modulus for N2, reaching a minimum of 75 ksi in February 2011. Some recovery was noted after this point, but moduli still trended lower than N1, and RMSE remained above 3% through the end of the experiment.

Until a detailed forensic investigation can be conducted, it is not possible to pinpoint the exact cause of the decline in modulus for N2. Potential causes could be layer slippage and/or cracking extending deeper into the pavement structure. Regardless of cause, an important consideration is the impact on measured pavement response as further discussed below.

Pavement Response Measurement and Analysis

On a weekly basis over the two-year research cycle, asphalt strain, vertical pressure in the aggregate base, and subgrade pressure measurements from 15 truck passes were obtained in each section. Figure 3.53 summarizes these data normalized to a 68°F reference temperature for each section. Included in the figure are the measurements and 4 point (monthly) moving averages.

The N1 data in Figure 3.53 are remarkably stable over time for AC strain, base pressure, and subgrade pressure, respectively. This observation is supported by the relatively stable moduli for N1 shown in

Figure 3.52. These observations (i.e., AC modulus and measured response) taken together indicate a structure in reasonably good health.

Conversely, the N2 data in Figure 3.53 all show a marked increase between mid-November 2010 and early February 2011. This time period corresponds with the general decline in AC modulus experienced in N2 from October 2010 through February 2011. Clearly, the drop in AC modulus had an impact on measured pavement response. Again, without detailed forensic investigation, it is difficult to pinpoint the cause, but it could be related to layer slippage and/or cracking extending deeper into the structure.
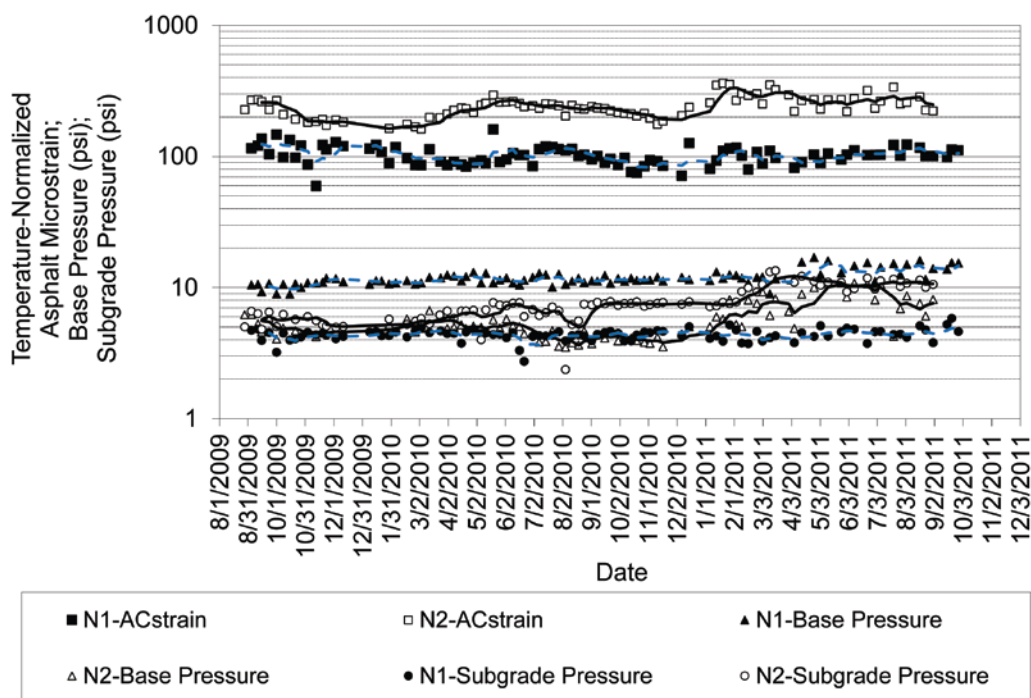
Figure 3.53 Measured Pavement Response at 68°F

Field Performance

Weekly monitoring of each section was conducted on Mondays. Sections were inspected for signs of cracking, and multiple measurements of rutting and surface texture were made. Figures 3.54 and 3.55 illustrate the field performance measurements of each test section. Section N1 had approximately half the total rutting compared to Section N2. The IRI for Section N2 started lower than that for N1 but increased quicker starting in October 2010, corresponding to the time period when the AC strain increased and the AC modulus declined, as mentioned above. Cracks can be seen throughout Section N2, and the level of severity and the area of severe cracks are greater in Section N2 than in Section N1.

Permeability test results for these test sections are reported in Chapter 4 of this report. Those results show that permeability was not significantly affected by the tack coat application rate or method.

However, during heavy rains, Section N2 with the lower tack coat rate, appeared to provide better drainage than Section N1.
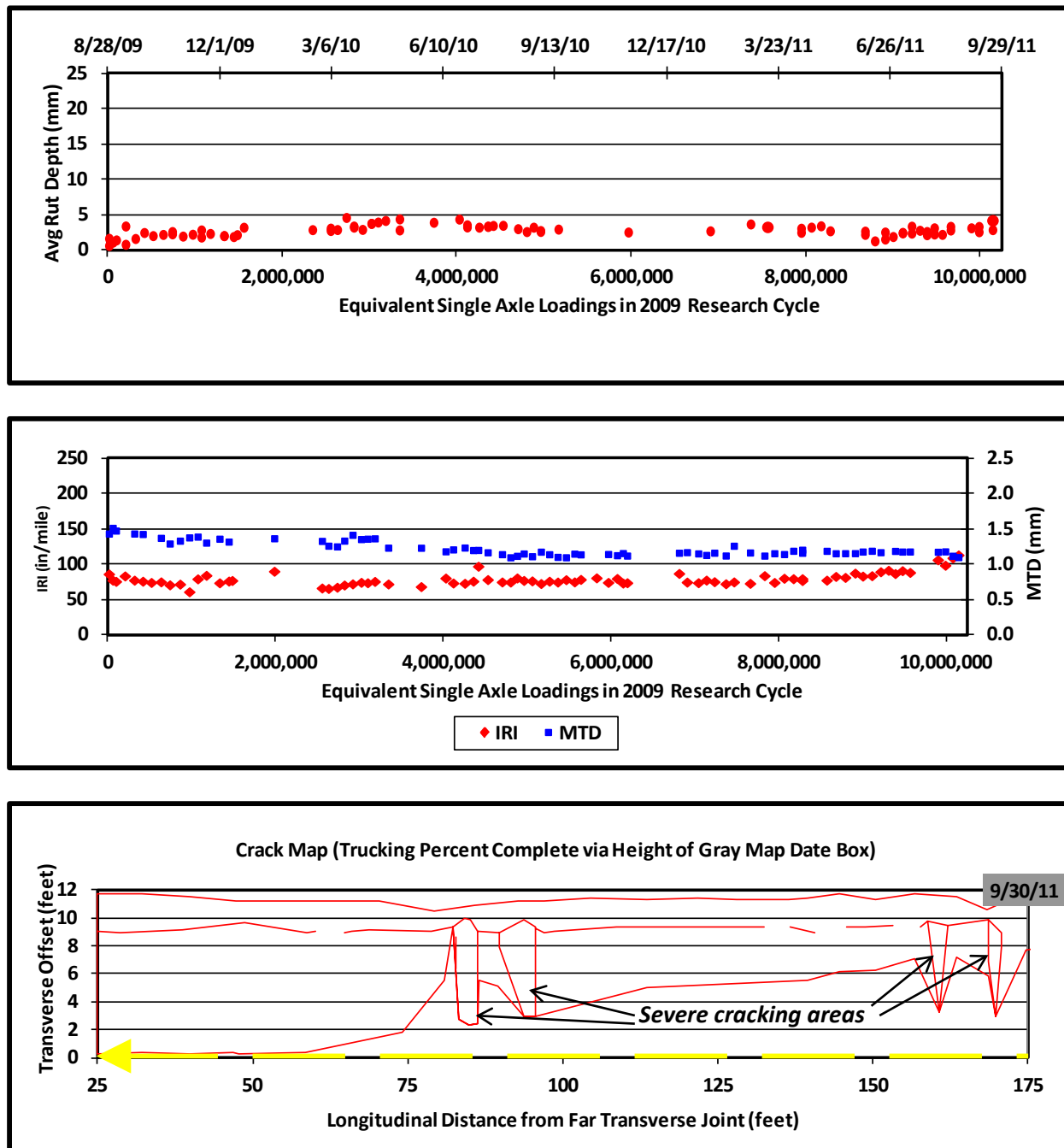
Figure 3.54 Rutting, Surface Texture, and Cracking Measurements for Section N1
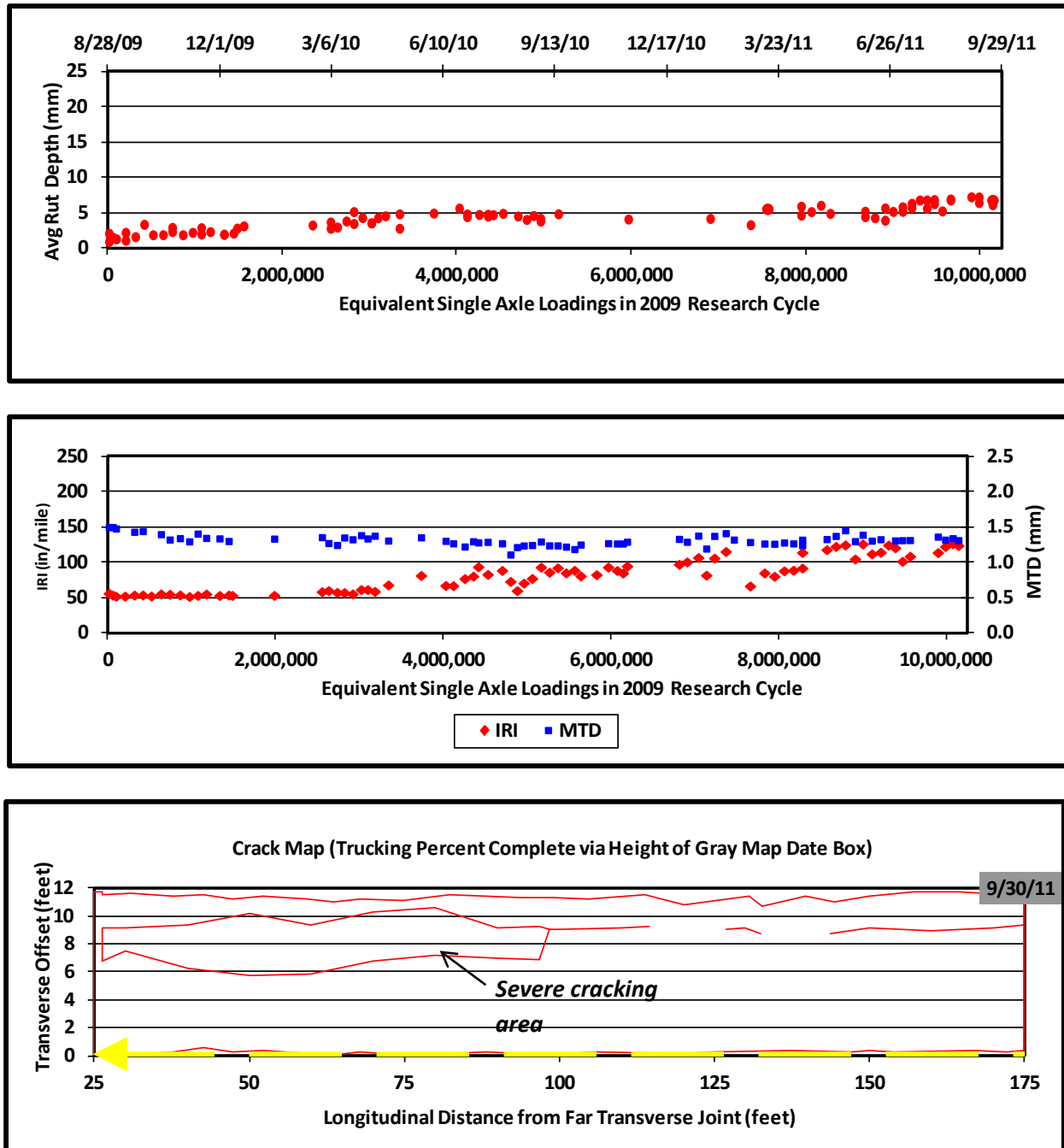
Figure 3.55 Rutting, Surface Texture, and Cracking Measurements for Section N2

Conclusions and Recommendations

1. The OGFC layer of Section N1 in which a heavier tack coat was applied has performed better than that of Section N2 in which a conventional tack coat was used.
2. Based on laboratory testing, the OGFC mixture paved in the two sections met the FDOT requirements for an FC-5 mixture. The use of 15% RAP in the OGFC did not have any negative effects on the mix characteristics or field performance.

3. The backcalculated AC modulus and measured strain data were stable over time for Section N1; however, the N2 data started increasing from October 2010.
4. While both sections had cracking, the level of severity and the area of severe cracks were greater in Section N2 than in Section N1.
5. It is recommended that a heavier tack coat be used to improve the performance of OGFC surfaces.

3.9 Structural Characterization and Performance of TLA Test Section

Background

Trinidad Lake Asphalt (TLA), a unique natural asphalt binder, has been used in heavy duty hot-mix asphalt (HMA) pavements in many countries. TLA is often blended with neat or polymer-modified asphalt binders to improve high-temperature stability and skid resistance of HMA mixtures (*50*).

TLA was first used in 1595 by Sir Walter Raleigh to caulk his ships; however, the first use of TLA in roadways was not documented until 1815 in Port-of-Spain. TLA has been used as a paving binder since the earliest days of asphalt pavements in prominent locations throughout the U.S. such as Pennsylvania Avenue in Washington, D.C. (*51*). In the past several decades, TLA-blended HMA mixtures have been used in roads, airports, tunnels, and bridges in the United States. The Port Authority of New York and New Jersey used TLA-blended mixtures in projects such as the George Washington Bridge, JFK Airport, and Lincoln Tunnel (*52*). The Massachusetts Port Authority installed a test section using a TLA-blended AC-20 mixture at Logan International Airport in 1997 (*53*). Several other state agencies, including the Nevada Department of Transportation (DOT), Utah DOT, Colorado DOT, and Washington State DOT, have also constructed trial sections using TLA-blended mixtures (*50, 52, 53, 54, 55*).

Recently, Lake Asphalt of Trinidad and Tobago (1978) Limited has produced a new TLA product called the TLA pellet (Figure 3.56). This product was designed to ease transporting, blending, and processing TLA in HMA. The pellets can also include a compaction aid used for warm-mix asphalts or a polymer used for polymer-modified asphalt binders.


Figure 3.56 TLA Pellets

Objective

The main objective of this investigation was to evaluate the structural behavior and performance of an NCAT Pavement Test Track test section containing TLA pellets relative to a control section.

Test Section

In this study, there were two mix designs using two design gradations (Figure 3.57). The surface layer utilized a 9.5 mm nominal maximum aggregate size (NMAS) while the intermediate and base mixtures used a 19 mm NMAS gradation. The aggregate gradations were a blend of granite, limestone, and sand using locally available materials. The TLA gradations were very similar to those of the control mixes.

Table 3.29 contains pertinent as-built information for each lift in each section. The primary difference between S9 (control) and S12 (TLA) was the 25% TLA pellets used in S12 compared to conventional polymer modification used in the upper lifts of the control section. The virgin binder PG grade of the TLA mixtures was 67-28, which after blending with 25% TLA pellets and performing an extraction to recover binder, resulted in a PG 76-16.

Also noteworthy in Table 3.29 are the significantly lower air void contents in the TLA section lifts compared to the control lifts. Clearly, adequate compaction of the TLA-modified mixtures was not an issue at compaction temperatures comparable to (lift 3) or below (lifts 1 and 2) those of the control section.

	TLA	Control
Agg Base	5.3	5.8
Lift3	2.7	3.0
Lift2	2.8	2.8
Lift1	1.5	1.2
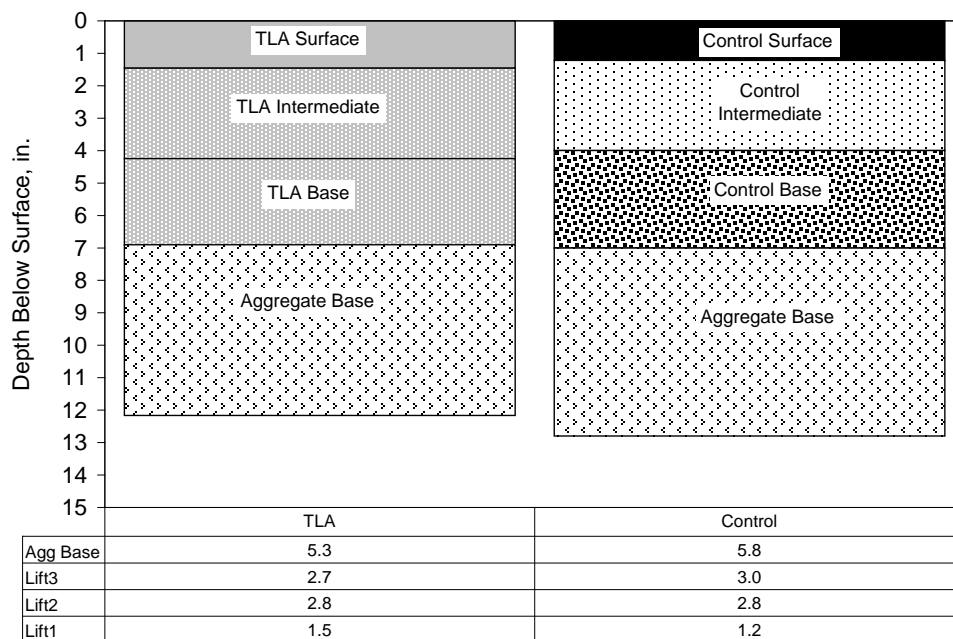
Figure 3.57 TLA and Control Cross Sections – As-built Thicknesses

Table 3.29 Asphalt Concrete Layer Properties – As Built

| Lift	1-Surface		2-Intermediate		3-Base	
Section	*S12-TLA*	*S9-Control*	*S12-TLA*	*S9-Control*	*S12-TLA*	*S9-Control*
Thickness, in.	1.5	1.2	2.8	2.8	2.7	3.0
NMAS, mm	9.5	9.5	19.0	19.0	19.0	19.0
% TLA (S12) % SBS (S9)	25	2.8	25	2.8	25	0.0
PG Grade	76-16	76-22	76-16	76-22	76-16	67-22
Asphalt, %	6.1	6.1	4.7	4.4	4.9	4.7
Air Voids, %	5.5	6.9	4.8	7.2	6.1	7.4
Plant Temp, $^{\circ}F^{c}$	335	335	335	335	335	325
Paver Temp, $^{\circ}F^{d}$	285	275	293	316	293	254
Comp. Temp, $^{\circ}F^{e}$	247	264	243	273	248	243

[c]Asphalt plant mixing temperature
[d]Surface temperature directly behind paver
[e]Surface temperature at which compaction began

Laboratory Performance Testing

During production of the mixtures at the plant, samples of mix were obtained for laboratory testing and characterization.

Figure 3.58 compares the unconfined E* testing results performed in accordance with AASHTO TP79-09 for the surface (9.5mm NMAS) mixtures used in the control and TLA test sections. These results show the control and TLA-modified surface mixes have similar stiffness values across the full range of temperatures and frequencies, represented by the dynamic modulus mastercurve. The results show the control mixture to be slightly stiffer than the TLA mixture at the high-temperature, slow-loading frequency (left-hand side) end of the curve while the TLA mixture is stiffer at the cold-temperature, fast-loading frequency (right-hand side) end of the curve. Figure 3.59 compares the unconfined E* testing results for the intermediate and base layer (19 mm NMAS) mixtures used in the control and TLA test sections. These results show all three mixes (control-intermediate, control-base, and TLA-intermediate/base) have similar stiffness values at the cold-temperature, fast-loading frequency end of the curve. At the high-temperature, slow-loading frequency end of the curve, the mastercurves for each of the three mixes begin to diverge. The control intermediate mixture is the stiffest (PG 76-22), and the control base mixture is the softest (PG 67-22), with the TLA 19mm NMAS mixture falling between those two mixtures in terms of stiffness.
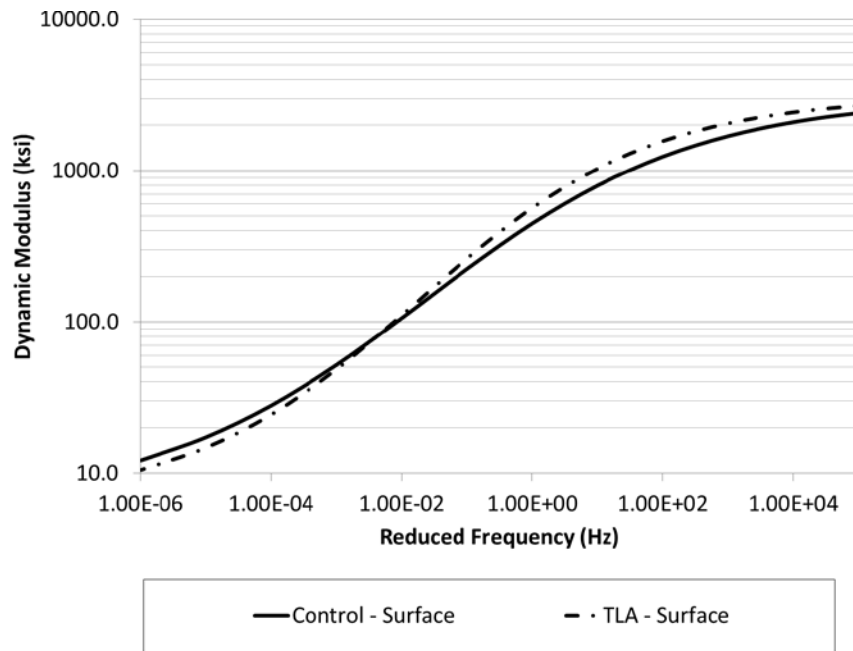
Figure 3.58 Comparison of Unconfined E* Testing Results – 9.5 mm Mixes
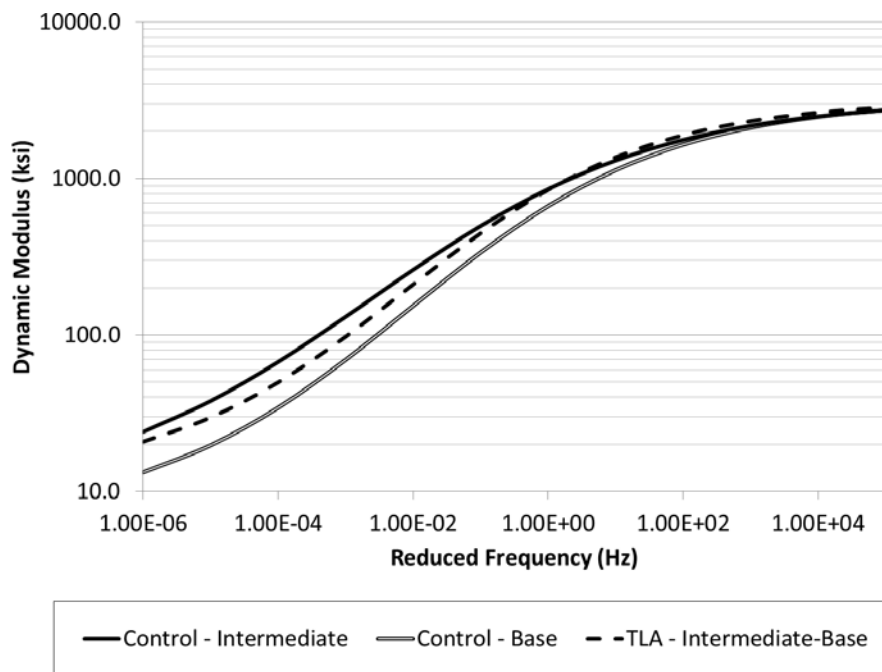
Figure 3.59 Comparison of Unconfined E* Testing Results – 19 mm Mixes

Bending beam fatigue testing was performed in accordance with AASHTO T 321-07 to determine the fatigue limits of the 19 mm NMAS control and TLA-modified base mixtures. Nine beam specimens were tested for each mix. Within each set of nine, three beams each were tested at 200, 400, and 800 microstrain. It should be noted that the number of cycles to failure of some of the 200 microstrain beams had to be determined by an extrapolation method using a three-stage Weibull function. Past research has shown this to be the most efficient method for estimating the number of cycles to failure

without running the beam past 12 million cycles (*32*). Figure 3.60 compares the bending beam fatigue test results of the two mixtures. It shows the control mixture to have greater cycles to failure than the TLA mixture at the high strain level of 800 microstrain by 70%. However, as the strain level decreased, the TLA mixture became more strain tolerant than the control mixture. At 400 and 200 microstrain, respectively, the TLA mixture had 205 and 794% greater cycles to failure than the control mixture. However, at 200 microstrain, the percent increase should be viewed cautiously since the two beams for the TLA-modified mixture had not yet failed when the tests were terminated at 12 million loading cycles.
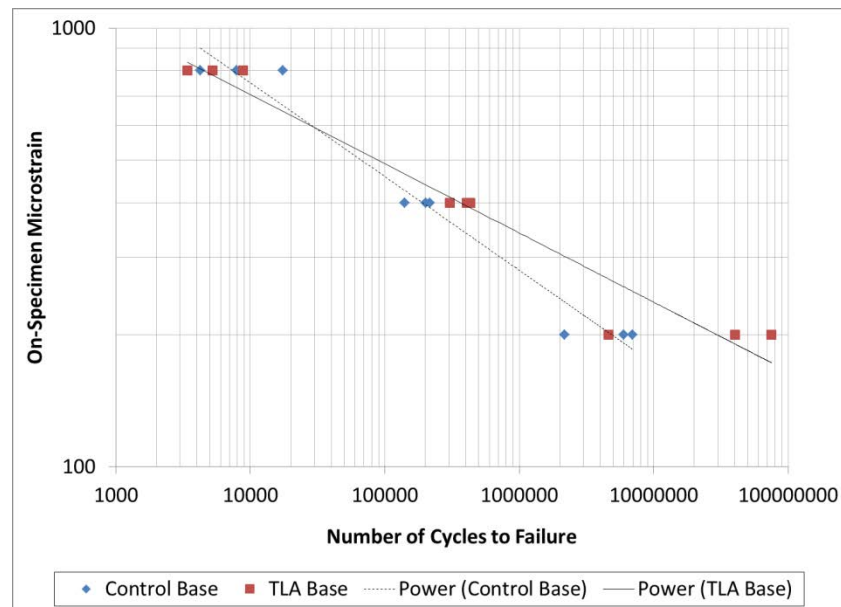
Figure 3.60 Comparison of Fatigue Resistance

Table 3.30 shows the 95% one-sided lower prediction of endurance limit for each of the two base mixes based on the number of cycles to failure (Figure 3.60) determined in accordance with AASHTO T 321-07. The procedure for estimating the endurance limit was developed under NCHRP 9-38 (*32*). This evaluation shows the TLA-modified mixture had an endurance limit 49% higher than the control mixture.

Table 3.30 Predicted Endurance Limits

Mixture	% Asphalt Binder	% TLA	% Total Binder	Endurance Limit (Microstrain)
Control Base	4.7	0.0	4.7	92
TLA Base	4.9	0.7	4.2	137

Note that percentages are of total mixture.

The rutting susceptibility of four mixtures—TLA base, TLA surface, control base, and control surface—was evaluated using the APA test procedure in accordance with AASHTO TP 63-09. The samples were tested at a temperature of 64°C (the 98% reliability temperature for the high PG grade of the binder for the test track). Manual depth readings were taken at two locations on each sample after 25 loading cycles and at the conclusion of testing (8,000 cycles) to determine the sample rut depth.

The rate of secondary rutting was also determined for each mixture by fitting a power function to the rut depths measured automatically in the APA during testing. Rutting typically occurs in three stages: primary, secondary, and tertiary. The confined state provided by the molds prevents the mixture from

truly ever achieving tertiary flow. Therefore, once the mixture has overcome the stresses induced during primary consolidation, it is possible to determine the rate at which secondary rutting occurs.

Table 3.31 summarizes the APA test results. Past research at the test track has shown that if a mixture has an average APA rut depth less than 5.5 mm, it should be able to withstand 10 million ESALs of traffic at the test track without accumulating more than 12.5 mm of field rutting. According to the data in Table 3.31 all four mixtures tested met this criterion. These results agree with the field results since neither the control nor the TLA section failed due to rutting during the 2009 research cycle.

Table 3.31 Summary of APA Test Results

| Mixture	Average Rut Depth, mm	StDev, mm	COV,%	Rate of Secondary Rutting, mm/cycle
Control-Surface	3.07	0.58	19	0.000140
Control-Base	4.15	1.33	32	0.000116
TLA-Surface	2.82	0.46	16	0.000145
TLA-Base	3.32	0.72	22	0.000119

Table 3.31 indicates that both surface mixtures had the lowest total rutting with the highest rates of rutting. The results also show both base mixtures had the highest total rutting with lower rates of rutting. These results suggest the base mixtures had more initial (primary) consolidation than the surface mixtures due to their lower rutting rates and higher overall rutting values. TLA modification appeared to slightly reduce rutting susceptibility in the APA for both the base and surface layer mixes. However, the results for all four mixes met the required criteria.

FWD Testing and Analysis

During the two-year research cycle, the control section was subjected to FWD testing three Mondays per month. The TLA section was tested on corresponding alternating Mondays. This schedule was necessary because of time constraints and the need to test a total of 16 sections within the structural experiment. Within each section, 12 locations were tested with three replicates at four drop heights. The data presented below only represent the results at the 9,000-lb. load level using EVERCALC 5.0 to backcalculate layer properties with RMSE errors less than 3%.

Figure 3.61 illustrates the strong relationship between mid-depth AC temperature and backcalculated AC modulus. As expected, due to the PG binder grade in the TLA section and higher compacted densities throughout the depth of the AC, the TLA section had higher modulus across the entire temperature spectrum.

To statistically examine the differences between sections in backcalculated AC moduli over a range of temperatures, the moduli were normalized to three reference temperatures (50, 68 and 110˚F) that represented the range of FWD test temperatures. The results are summarized in Figure 3.62. Two-tailed t-tests (α=0.05) at each temperature found statistically significant differences at all three temperatures, which indicates the differences seen in Figure 3.61, despite the scatter in data, are significant. Across the entire spectrum, the TLA moduli were 19 to 24% higher than the control moduli.
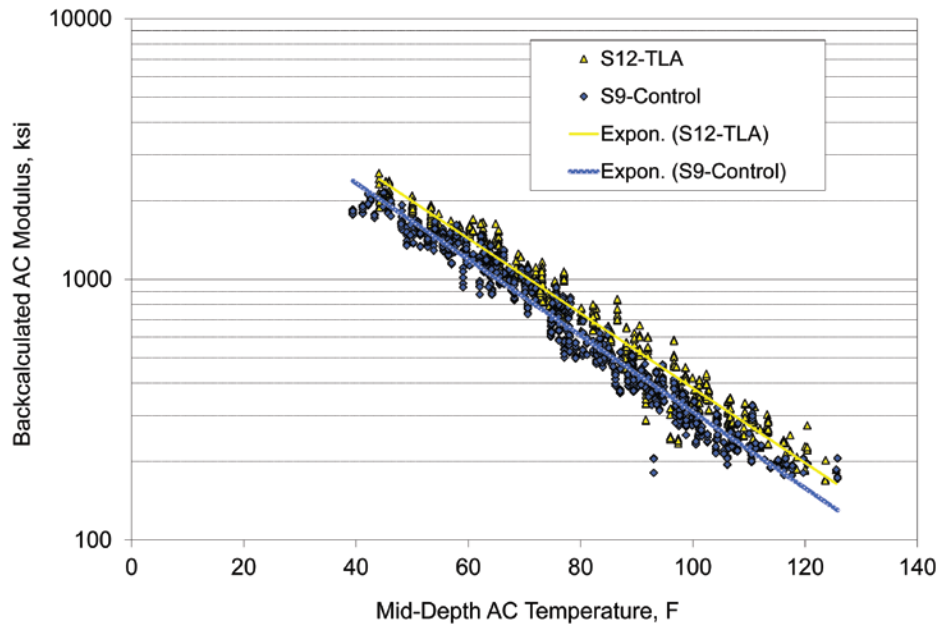
Figure 3.61 Backcalculated AC Modulus vs Temperature
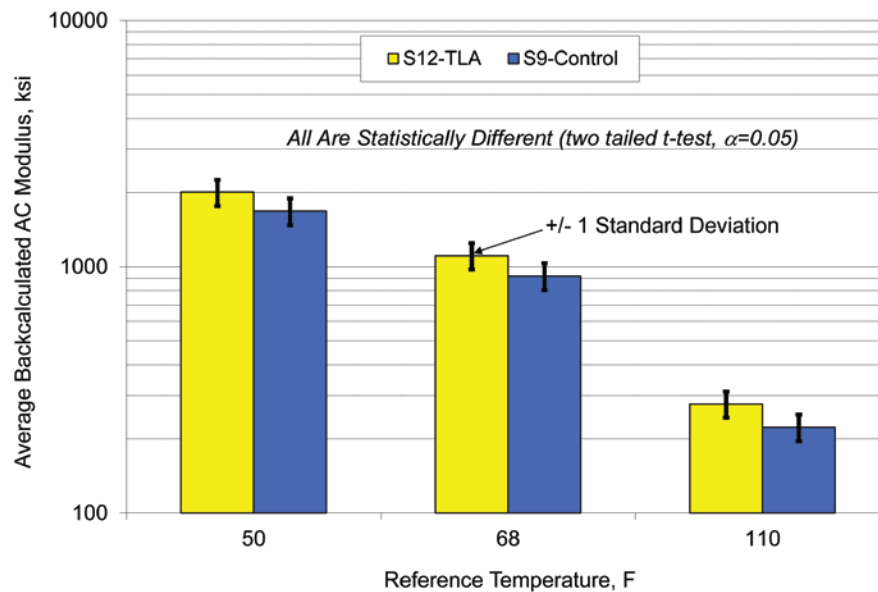
Figure 3.62 Temperature-normalized Backcalculated AC Modulus

Pavement Response Measurement and Analysis

On a weekly basis over the two-year research cycle, asphalt strain measurements from 15 truck passes were obtained in each section. Considerable scatter in the longitudinal strain data for S12 (TLA) began at the end of April 2010 but was not evident in other measurements (i.e., transverse strain, vertical pressure in base and subgrade). Therefore, the problem was likely faulty longitudinal asphalt strain gauges rather than pavement distress. Analyses were conducted with and without data after the increased scatter was noted and similar trends were found between the two sets. Figure 3.63 shows

best-fit exponential regression lines relating mid-depth AC temperature to measured asphalt strain. Very little difference was seen when using all the data for S12 and limiting the analysis to data prior to the increased scatter. Consequently, all the data were used in the analyses.

Figure 3.63 shows that, over the range of temperatures tested, the TLA section had generally lower strain compared to the control. The effect was more pronounced at higher temperatures. The exponential regression curves in Figure 3.63 were used to normalize strain measurements to three reference temperatures (50, 68, 110˚F) to enable statistical testing between the sections. Figure 3.64 illustrates average, standard deviation and the results of two-tailed *t*-testing between the sections. At 50 and 68˚F, there was no statistical difference between the sections, while at 110˚F there was a 10% reduction in asphalt strain.

One may expect that the TLA strains should have been lower at all temperatures since the backcalculated moduli were higher at all temperatures. Theoretically, however, there is a negative power function relationship between strain and modulus. This means that a 20% difference in modulus at the highest temperature (lowest moduli) has a bigger impact on strain than a 20% difference in modulus at the lowest temperature (highest moduli). Therefore, it makes sense that it would be more difficult to discern statistical differences at the lower temperatures.

Since no cracking had been observed in either section at the conclusion of traffic, estimates of fatigue cracking performance were made based on field-measured strain at 68˚F. Laboratory-derived fatigue transfer functions using AASHTO T321 were found for the base mixtures in each section. Using these transfer functions to predict fatigue performance from measured strain, Table 3.32 shows the fatigue function coefficients, average measured strain at 68˚F, expected repetitions until fatigue cracking failure, and corresponding life as a percentage of the control section. The better fatigue characteristics of the TLA material contribute to an estimated fatigue life approximately 3.2 times that of the control.

Table 3.32 Expected Fatigue Life at 68˚F

Section	AASHTO T321 Coefficients		Average Strain at 68F	Expected Repetitions	% of Control
	$\alpha 1$	$\alpha 2$			
S12-TLA	3018.5	-0.158	331	1,183,558	322%
S9 - Control	5374.2	-0.214	346	367,368	100%
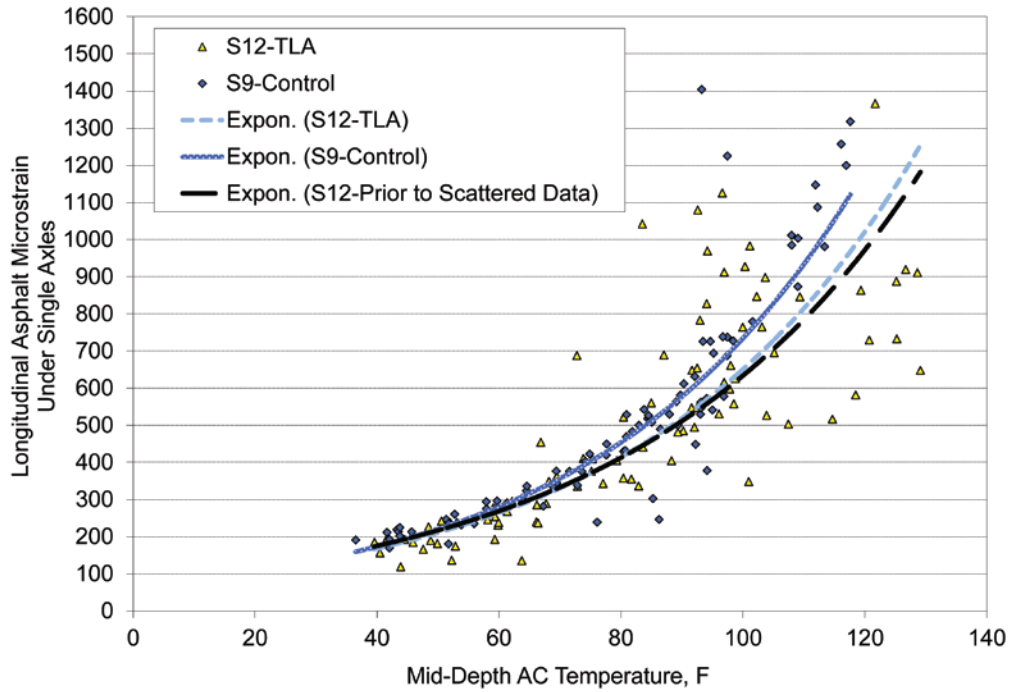
Figure 3.63 Measured Asphalt Strain versus Temperature
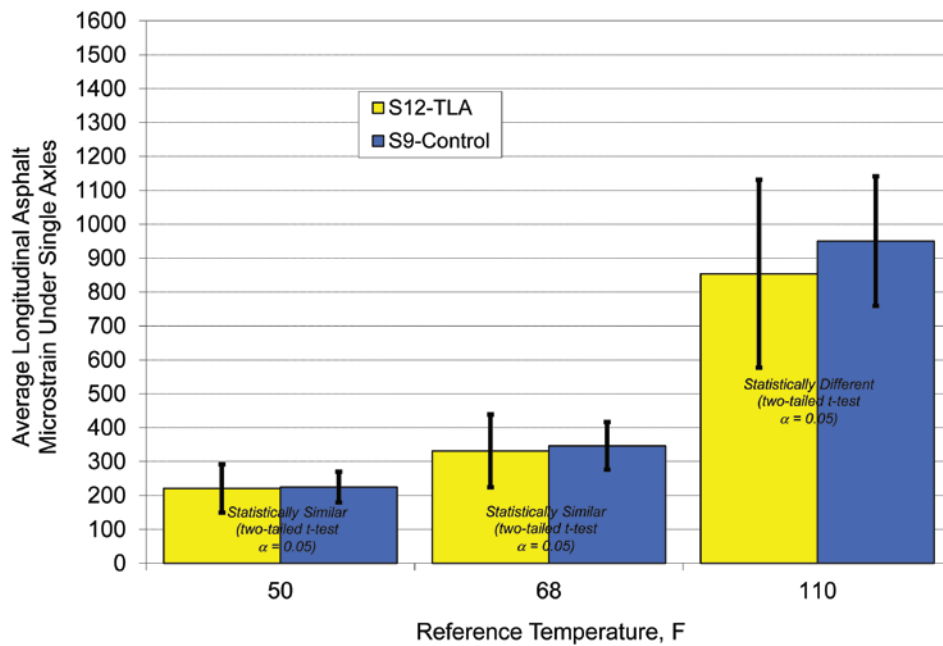
Figure 3.64 Temperature-normalized Asphalt Strain

Performance

Weekly monitoring of each section was conducted on Mondays. Sections were inspected for signs of cracking, and multiple measurements of rutting were made. Throughout the experiment, there was no observed cracking in either section. The rutting performance of each section is shown in Figure 3.65. The TLA section had slightly less rutting overall, but both sections performed very well with total rut depths less than 7 mm.
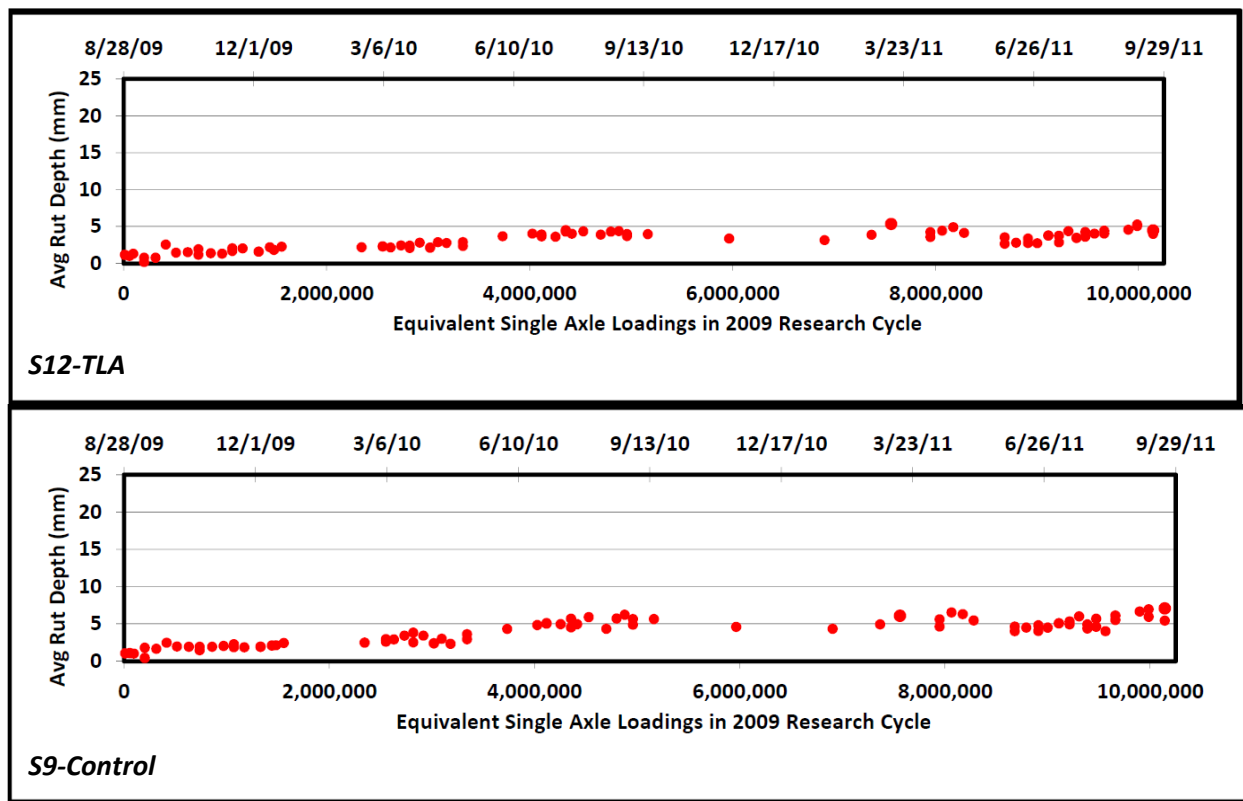
Figure 3.65 Rutting Performance of TLA (S12) and Control (S9) Sections

Conclusions and Recommendations

1. The TLA section has performed as well as the control section over the two-year traffic cycle.
2. The APA test results showed that the resistance of TLA-modified mixtures to rutting was greater than that of the corresponding control mixtures.
3. The bending beam fatigue testing results showed that the TLA-modified base mixture had an endurance limit 49% higher than the control base mixture.
4. Backcalculated AC moduli indicated approximately 20% higher moduli in the TLA section relative to the control.
5. Significant scatter in the measured longitudinal strain data was noted in the TLA section. This was not noted in the other measurements, and analysis with and without the highly scattered data resulted in similar trends. Statistical testing indicated no differences in measured strains at the lower two reference temperatures. At the warmest temperature (110˚F), the TLA section exhibited statistically lower strain levels (10% lower). These observations were attributed to differences in moduli having a larger impact at lower overall modulus levels. At cooler temperatures, the differences in moduli combined with scattered data were not enough to detect a decrease in average strain levels in the TLA section.
6. It is expected that the TLA section will exhibit increased fatigue resistance upon further trafficking. Preliminary estimates based on measured strain at 68˚F and laboratory-determined fatigue transfer functions indicate the TLA section has over three times the fatigue life of the control section.

7. It is recommended that the TLA and control sections be left in place for the 2012 research cycle to further validate these findings.

CHAPTER 4   ADDITIONAL ANALYSES

4.1 MEPDG Predictions versus Actual Performance

Background

The successful implementation of the Mechanistic-Empirical Pavement Design Guide (MEPDG), now known as DARWin-ME, requires local validation and calibration of the performance prediction equations to account for climatic and regional-specific materials and traffic conditions. Furthermore, the original calibration factors included with the MEPDG were based on Long Term Pavement Performance (LTPP) experimental sections that did not include any polymer-modified materials, warm-mix asphalt or other modern advancements in asphalt technology. Therefore, there exists a need to conduct validation and calibration of the MEPDG for state agency use in the Southeast U.S.

Objectives

The first objective of this study was to evaluate the capability of the mechanistic-empirical pavement design guide (MEPDG) to predict pavement performance. The second objective was to calibrate the performance equations to measured performance at the NCAT Pavement Test Track.

Methodology

This investigation relied on performance data from the 2003 and 2006 Pavement Test Track structural studies (*15, 45*) and established a framework for future validation/calibration using data from the 2009 research cycle. The investigation focused on predictions and measurements of bottom-up fatigue cracking and rutting.

MEPDG Inputs. To simulate each test section in the MEPDG, categories of inputs were developed that included pavement cross section, material properties, traffic, and climate. The inputs were considered "Level 1" by MEPDG standards since each input was measured directly as part of the experimental plan.

Each pavement cross-section was input according to average as-built layer thicknesses determined during construction. Laboratory-determined dynamic moduli (E*) were entered for each asphalt concrete (AC) material in addition to as-built volumetric properties determined through quality-control activities during construction. Properties of the underlying, non-AC layers were determined from construction records and results of falling-weight-deflectometer testing to establish representative moduli.

Detailed trafficking records were kept during each research cycle. Test track-specific load spectra were input to the MEPDG that represented the known axle weights, axle types, relative frequency, seasonal volume, and hourly distributions on a daily basis.

An on-site weather station stored climatic conditions on an hourly basis during each research cycle. These records were used to create test track-specific MEPDG hourly climatic data files for the specific environmental conditions of each section.

Performance Monitoring and Prediction. Each test section was inspected on a weekly basis for cracking. When cracking was observed, forensic coring was conducted to confirm whether it was bottom-up or top-down. Though both types of cracking were observed in this study, only bottom-up cracking was considered within the MEPDG analysis since the top-down models in the MEPDG are currently considered placeholders pending implementation of findings from NCHRP 1-42A (*56*). Maps of observed cracking were created from which percent areas of cracking were computed for comparison against MEPDG predictions.

Weekly rut-depth measurements were made on each section. These measurements were compared directly against MEPDG predictions. It is important to recognize that the test track measurements were only made at the pavement surface, while the MEPDG predicts total rutting in addition to sublayer rutting. This investigation only utilized total measured and predicted rutting.

Validation and Calibration. The MEPDG was evaluated in two ways: validation and calibration. During the validation analysis, the default nationally calibrated transfer function coefficients in MEPDG version 1.1 were used to make performance predictions. Direct comparisons were then made between measured and predicted performance to evaluate the accuracy of the MEPDG predictions. The calibration analysis adjusted the so-called "β" local calibration terms available within each set of performance equations. Comparisons between these predictions and measured performance allowed an assessment of the available improvement when using locally calibrated coefficients. The calibration procedure involved running the MEPDG repeatedly while adjusting the β terms to minimize the error between predicted and measured performance.

Results and Discussion

Rutting. Using the national calibration coefficients to predict rutting within each section, Figure 4.1 compares measured and predicted rutting. In the figure, each series is denoted by its section identifier and research cycle. For example, "N1-03" refers to section N1 from the 2003 research cycle. As demonstrated in Figure 4.1, the MEPDG clearly overpredicted rutting for every section using the national calibration coefficients. The resulting R^2, considering all the data from this exercise, was -8.43, which means there is really no accuracy in the MEPDG predictions when using the national calibration coefficients.

In conducting the calibration analyses, it was found that the reason for overprediction was primarily due to predicted rutting of unbound layers. Through iteration, the best set of calibration coefficients did not adjust the asphalt rutting terms ($\beta r1$, $\beta r2$, $\beta r3$ = 1) at all, but significantly reduced the unbound terms ($\beta s1$, $\beta s2$ = 0.05). Figure 4.2 shows the comparison between measured and predicted rutting using these terms. The corresponding R^2 for this plot was -.18, a significant improvement over the national calibration but still a negative R^2.

In Figure 4.2, there were two clear outlier sections; N1-2006 and N2-2006. Both sections were built on a limerock base that were likely not modeled well by the MEPDG. Additionally, there were several sections left in place for more traffic in 2006, but the MEPDG did not allow the

entry of an initial rutting condition. Figure 4.3 excludes these sections from analysis, resulting in an R2 of 0.67, which is considered acceptable for design purposes.
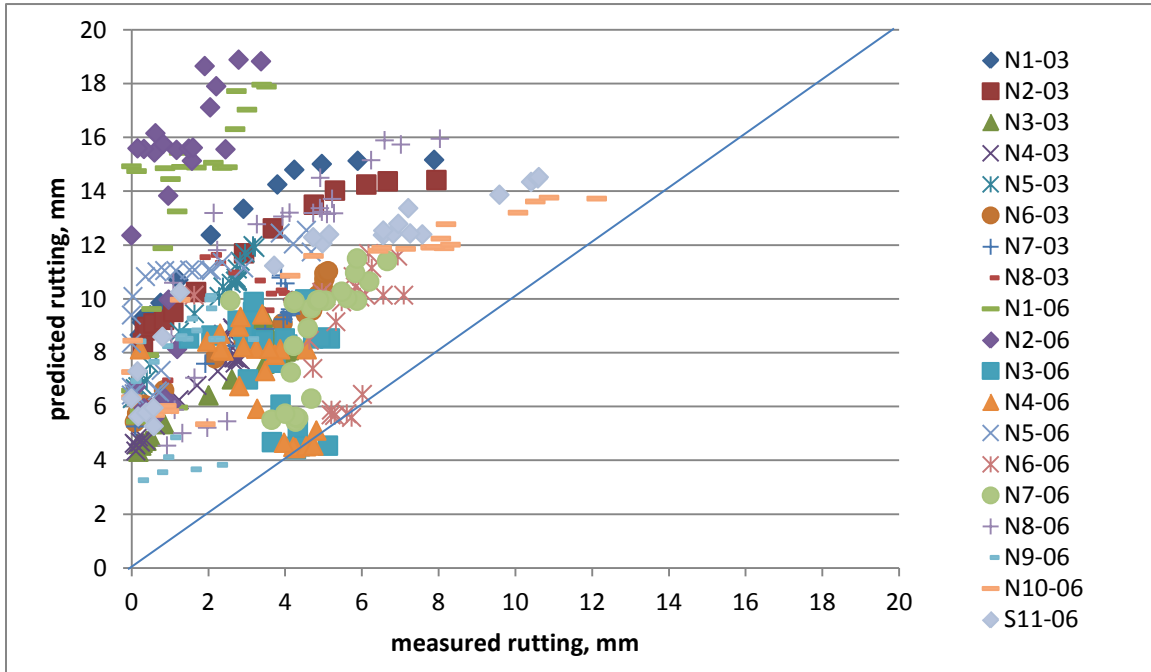
Figure 4.1 Measured vs. Predicted Rutting with National Calibration
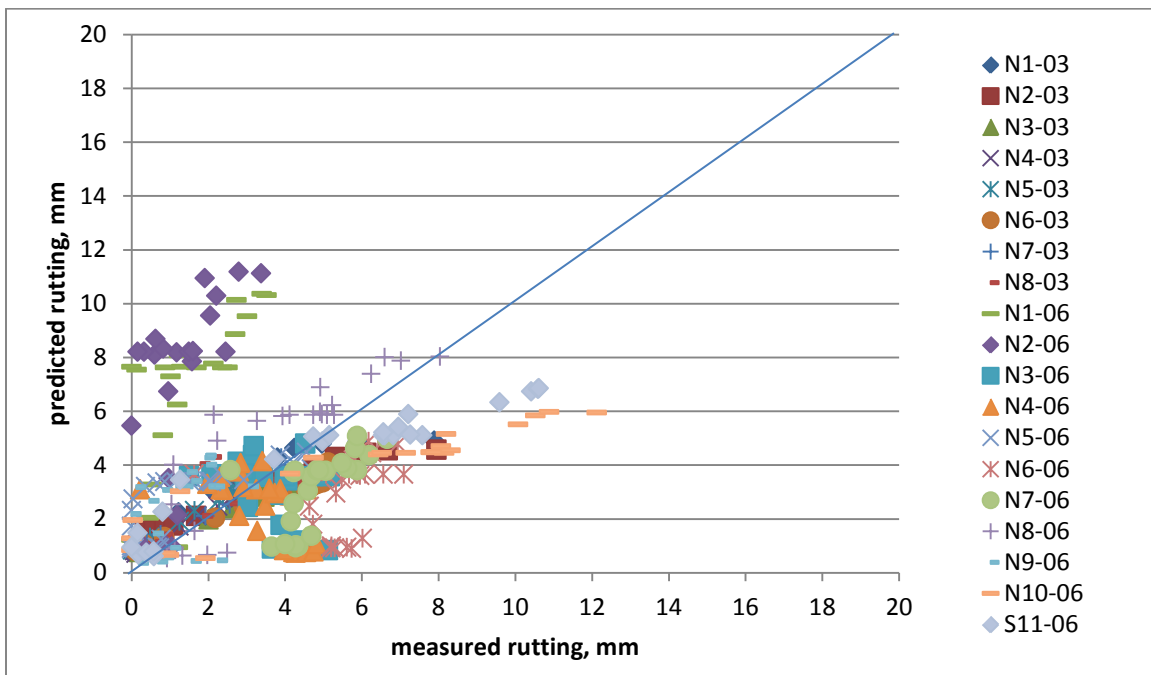
Figure 4.2 Measured vs. Predicted Rutting with Test Track Calibration
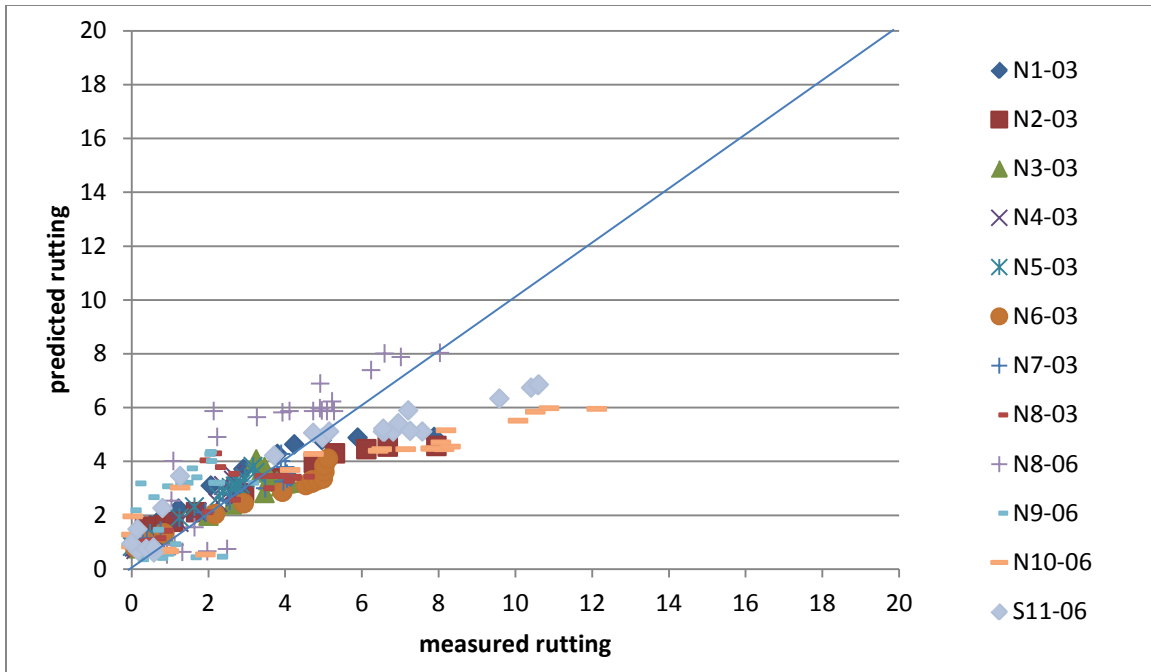
Figure 4.3 Measured vs. Predicted Rutting with Test Track Calibration – Some Sections Excluded

Fatigue Cracking. Figure 4.4 illustrates measured versus predicted bottom-up fatigue cracking using the national calibration coefficients. Clearly, there was a large degree of scatter within the data, and the only reasonably accurate predictions were for N1-2003 and N2-2003. The remainder was grossly over- or under-predicted. The resulting R^2 from this exercise was again negative: -0.08.

Calibration simulations were attempted, and after 28 combinations of new coefficients, no better sets that reduced the error between measured and predicted fatigue cracking were found. It is suggested that further calibration exercises focus on groups of sub-sections rather than all sections together.
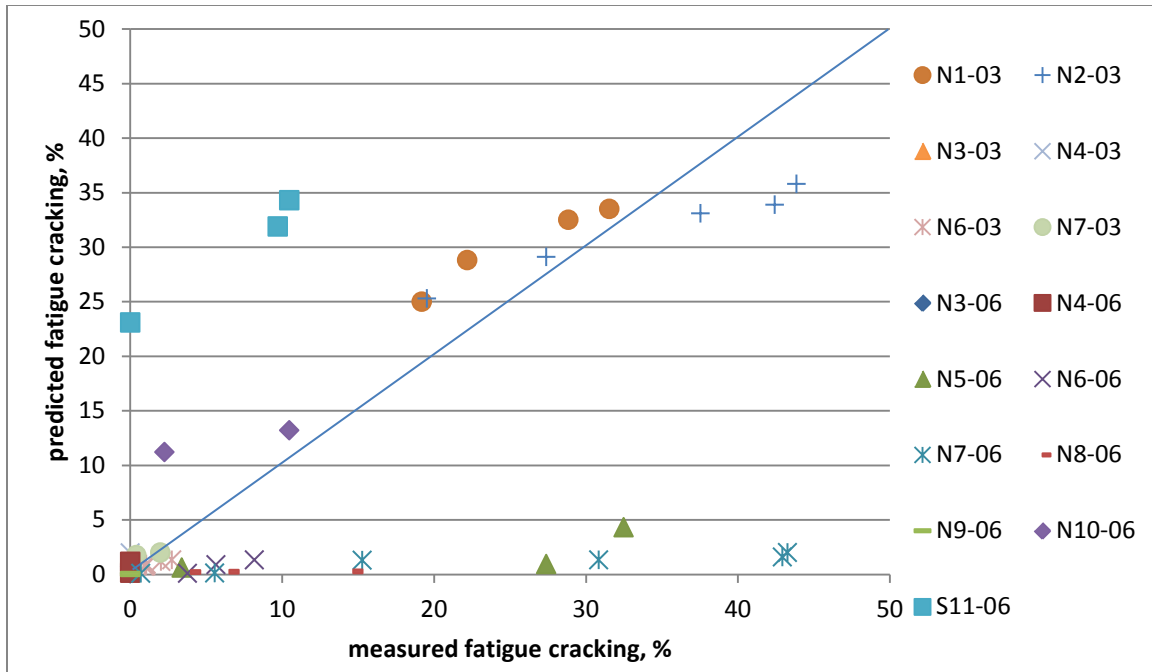
Figure 4.4 Measured vs. Predicted Fatigue Cracking – National Calibration

Conclusions and Recommendations

This investigation evaluated structural sections within the MEPDG from the 2003 and 2006 test track research cycles. Generally speaking, the MEDPG made inaccurate predictions of Test Track performance using the national default calibration coefficients. This clearly demonstrates the need for local calibration prior to using the MEPDG for design purposes. The rutting analysis indicated overpredictions primarily in the base and subgrade layers. New calibration coefficients (βs1, βs2 = 0.05) were recommended that improved the predictive capability, and when excluding some outliers, resulted in reasonably accurate rutting predictions. Predictions of fatigue cracking were not as successful; no better coefficients than the national coefficients were found, resulting in generally very poor agreement between measured and predicted cracking. The sections may require subgrouping into sections with similar characteristics to achieve better calibration results. The 2009 sections should also be analyzed in this framework to further refine the calibration coefficients.

4.2 Speed and Temperature Effects on Pavement Response

Background

It is well known that temperature plays a significant role in flexible pavement response to loading. In general, pavement stiffness decreases as temperature increases. The reduction in modulus due to temperature increase leads to higher pavement strains under loading. Willis et al. (*15*) showed that an increase in mid-depth pavement temperature resulted in a very large increase in tensile strain. It is important to consider pavement temperature when designing flexible pavements. Understanding the temperature effect on pavement response can lead to better designs and longer-lasting pavement structures.

It is also well known that load duration (i.e., vehicle speed) has a significant effect on flexible pavement response. Many pavement design models ignore the dynamic loading effects that are inherent to any pavement structure. Several studies have shown that speed, or load duration, can have a significant effect on the strain response of flexible pavements *(57, 58, 59, 60, 61)*. The strain response dependency on speed can be explained by the viscoelastic nature of the hot-mix asphalt (HMA). Because of the viscoelastic nature of the asphalt concrete (AC) material, the material will show stiffer behavior under shorter loading times (*61*).

Theoretical pavement models are used to determine pavement response to wheel loads and ultimately predict pavement life. These models often fail to accurately characterize field conditions and result in erroneous pavement life prediction. There is added uncertainty in the case of modeling non-conventional materials. Some of these non-conventional materials include sulfur-modified mixes, polymer-modified mixes, and new warm-mix technologies. These and other non-conventional materials are growing in popularity within the paving industry. Research is needed to characterize these new materials for use in both pavement modeling and pavement life prediction.

The increase in use of non-conventional materials poses many questions about their response to vehicle loading and temperature changes. Although traditional HMA pavements respond in a predictable way to both variables, it cannot be assumed that the same relationships apply to these new materials. Therefore, a need for proper response characterization for these materials was needed and addressed through direct measurement in this investigation.

Objective

The objective of this investigation was to compare the effects of temperature and speed on pavement response in non-conventional materials to the effects on conventional asphalt concrete (AC).

Methodology

Nine sections on the NCAT Pavement Test Track were used for this investigation, as shown in Figure 4.5, which included sulfur-modified material, high polymer content, WMA, high RAP

content, and Trinidad Lake Asphalt pellets. The sections were constructed on the same foundation materials (i.e., granular base and subgrade) and featured embedded instrumentation to measure dynamic pavement responses under moving loads as well as temperature probes to measure mid-depth temperature at the time of testing.

Testing was conducted on four test dates between December 2009 and May 2010 to capture a relatively wide temperature range (45-125°F). Four testing speeds (15, 25, 35, and 45 mph) were utilized, and at least three passes of five trucks at each speed were measured. The primary measure in this investigation was longitudinal strain at the bottom of the asphalt concrete (AC), which can be used as a predictor of bottom-up fatigue cracking. Figure 4.6 illustrates the "strain magnitude" definition used for this investigation. After data were collected, regression analyses were conducted to evaluate the influence of truck speed (v) and mid-depth temperature (T) on measured strain response.

Figure 4.5 Test Section Composition – AC Layers Only *(62)*

123
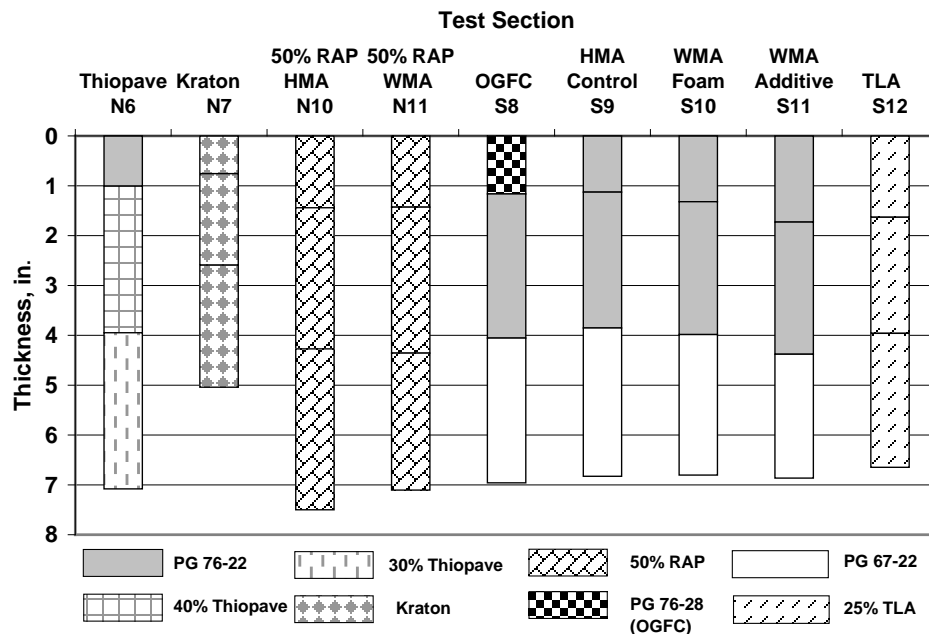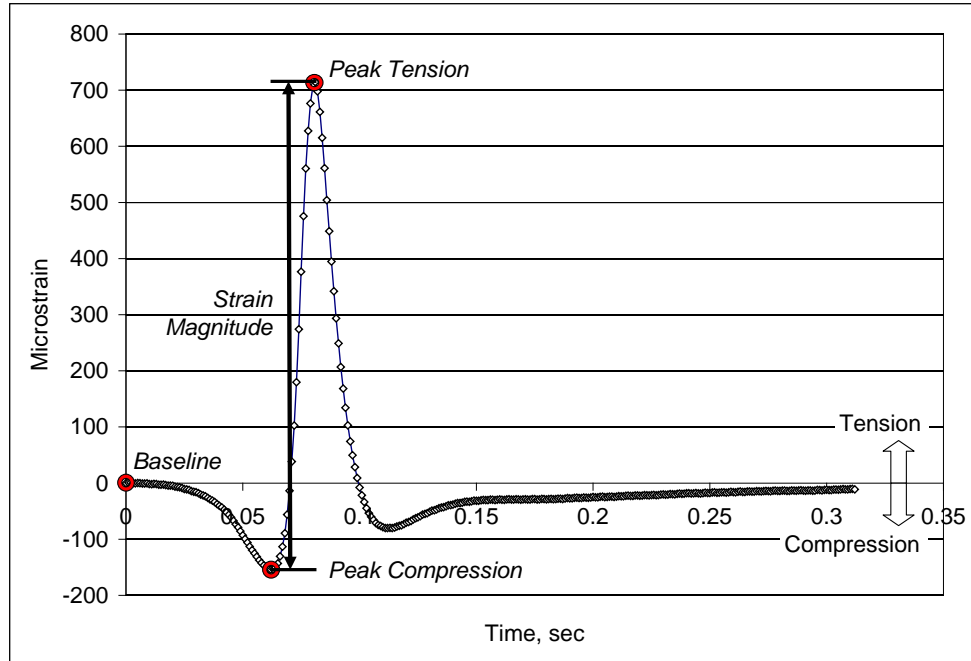
Figure 4.6 Strain Magnitude Definition (*62*)

Results and Discussion

The regression analysis utilized a non-linear equation best fit to the data from each test section (*61*):

$$\varepsilon = a * v^{b} * c^{T} \tag{1}$$

Where:

ε = longitudinal microstrain at bottom of asphalt concrete

v = vehicle speed, mph

T = mid-depth pavement temperature, ^{o}F

a,b,c = section-specific regression coefficients

Equation 1 provided very good correlation for longitudinal strain under single-axle load in each of the test sections. Table 4.1 shows the regression coefficients for Equation 1, coefficients of determination (R^2), and significance values (*p*-values) for each test section. It should be noted that all coefficients were significant (*p*-value <0.05) with the exception of N10-a, S12-a, and S12-b.

Table 4.1 Correlation Coefficients and R^2 Values (61)

Section	a	p-value(a)	b	p-value(b)	c	p-value(c)	R^2
N6	128.772	0.00	-0.209	0.00	1.027	0.00	0.997
N7	173.651	0.00	-0.167	0.00	1.022	0.00	0.983
N10	1373.058	**0.20**	-0.843	0.00	1.019	0.00	0.737
N11	135.253	0.00	-0.168	0.00	1.020	0.00	0.989
S8	154.340	0.00	-0.168	0.00	1.023	0.00	0.995
S9	167.563	0.00	-0.243	0.00	1.025	0.00	0.988
S10	332.815	0.00	-0.353	0.00	1.019	0.00	0.949
S11	277.173	0.03	-0.250	0.04	1.018	0.00	0.872
S12	58.318	**0.14**	0.242	**0.18**	1.017	0.00	0.827

As shown in Table 4.1, six of the nine sections had R^2 values greater than 0.94. The lowest R^2 value was found to be 0.737 for Section N10. Due to the high correlation values given here, Equation 1 was determined adequate for prediction of strain response of the flexible pavements. Sections N10 and S12 did not correlate well to the model and, therefore, required further investigation.

Sections N10 and S12 sections were investigated to determine the cause for their deviation from the model. A closer look revealed that both N10 and S12 data were erratic for the last data-collection date, which corresponded to the highest test temperatures. Examination of additional test track data, gathered on a weekly basis since August 2009 at variable temperatures but speeds approximately equal to 45 mph, indicated highly variable readings for these two sections with data collected after April 2010. Due to the variability of the data for sections N10 and S12, as well as their corresponding insignificant *p*-values of regression constants, these sections were excluded from further analyses.

The negative sign of the *b*-coefficients indicated that an increase in speed resulted in a decrease in strain. This relationship was expected and was supported by the literature review (*57, 58, 59, 60, 61*). It can be noted from the *c*-values in Table 4.1 that temperature had a nearly identical effect on each section. The conclusion that these non-conventional materials show similar responses to temperature was a promising finding since it would imply that they can be modeled like conventional materials. The *a*-values for each equation are primarily related to the overall thickness and modulus properties of the materials in each section.

Referring to the *b*-regression constants in Table 4.1, it appears that the warm-mix sections (S10, S11) are slightly more sensitive to speed relative to the control section (S9). The other sections were slightly less sensitive to speed relative to the control. However, overall, it could again be stated that they have similar responses to speed and could be modeled using standard pavement models. This is an important finding as pavement engineers consider using these kinds of materials in conventional models.

Conclusions and Recommendations

Though several sections exhibited erratic data, it can generally be stated that the non-conventional materials behaved in a similar manner to those of the control. These materials are not expected to require more sophisticated load-response models than what is typically used to

model conventional flexible pavements (e.g., layered elastic). The effects of both speed and temperature were significant to the measured pavement response and should be taken into account when modeling. It should be emphasized that these models were developed specifically for test track conditions (i.e., climate, pavement cross-section, and loading). Though the trends may be applicable to other conditions, the coefficients themselves are specific to the test track.

4.3 Noise Analysis

Background

Tire-pavement noise has become an increasingly important consideration for the part of highway agencies that are seeking the use of quieter pavements to mitigate traffic noise. As the public consistently demands that highway traffic noise be mitigated, sound walls may provide a competitive way to reduce highway noise. However, there are no widely accepted procedures for measuring solely tire-pavement noise under in-service conditions (*63*). The interest in quieter pavements has been driven largely by the cost and, at times, the public's resistance to the traditional sound wall approach (*64*) along with increased public demand of highway traffic noise reduction. In addition, there is more public awareness that pavement selection can affect traffic noise levels (*63*).

Therefore, pavement surfaces that affect the portion of freeway noise generated from tires as they roll across pavement have been evaluated. Among different types of road surfaces, open-graded friction course (OGFC) pavements are the successful candidates used to reduce tire-pavement noise in few states (*65*). The pavement classification summarized in Table 4.2 has been considered in this study in order to evaluate different surface types in 2009 NCAT Pavement Test Track cycle.

Table 4.2 Family Groups of Noise Test Sections in 2009 NCAT Test Track

Design Methodology	Gradation Classification	No. of Sections	Test Track Sections
Superpave	Fine-graded	23	E5, E6, E7, E8, E9, N3, N4, N5, N6, N7, N8, N10, N11, W2, W3, W4, W5, W6, W7, S9, S10, S11, S12
	Coarse-graded	5	E4, W10, S2, S6, S7
Open-graded Friction Course (OGFC)		6	N1, N2, N13, S3, S4[*], S8
Stone Mastic Asphalt (SMA)		5	E1, N9, N12, W1, S1
Other asphalt pavements [**]		7	E2, E3, E10, W8, W9, S5, S13

[*] S4 was not considered in this study because of the poor data.
[**] The remaining sections were not included in this study because of the change of surface types.

Research Objective

The objective of this research was to utilize two methods for measuring tire-pavement noise to assess which pavement surface characteristics have the greatest influence on noise generation. Testing was conducted on NCAT test track sections using the close proximity (CPX) and on-board sound intensity (OBSI) methods to evaluate changes in these characteristics over time. The content of this study should be of immediate interest to pavement engineers and others concerned with pavement design and construction as well as the noise impacts on nearby communities.

Overview of Evaluation Testing

This study was based on two methods for measuring tire-pavement noise at the source. The first method used the NCAT close-proximity noise (CPX) trailer that utilizes small trailer pulled by a vehicle. The trailer contains an anechoic chamber with the test tire and two free-field microphones to isolate the tire-pavement noise and the sound pressure. The second method, known as the OBSI method uses a pair of microphones mounted on the right rear tire of a vehicle, three inches above the pavement surface, to ensure that only the tire/pavement noise is being measured. This procedure has been found to be the preferred approach for measuring tire-pavement noise at the source, both in the U.S. and internationally. The test measurements provided in this report are based on the *Standard Test Method for the Measurement of Tire/Pavement Noise Using the On-Board Sound Intensity (OBSI) Method* (*66*). Repeated sound measurements (at least 3 runs) were done on each test section. Testing was done with a Michelin standard reference test tire (SRTT) at a speed of 45 mph and tire pressure of 30 psi. Sound-intensity testing with an NCAT triple trailer truck was also completed by attaching a frame around the rear wheels on the rear trailer. Sound-intensity microphones could be mounted to record leading-edge and trailing-edge measurements. Details of the configurations are given elsewhere (*15).*

An analysis was also conducted to compare CPX data against the corresponding OBSI data for all test sections, as shown in Figure 4.7. These data show that CPX sound-pressure level and OBSI sound-intensity level are not numerically equivalent, but are strongly correlated at given frequencies. It should be noted that the two methods react differently with porous pavements. This is likely due to the CPX sound-pressure measurement being affected more by pavement sound absorption than the sound-intensity measurement. For practical consideration, the OBSI method was selected for further analysis of at-the-source tire-pavement noise in this study.
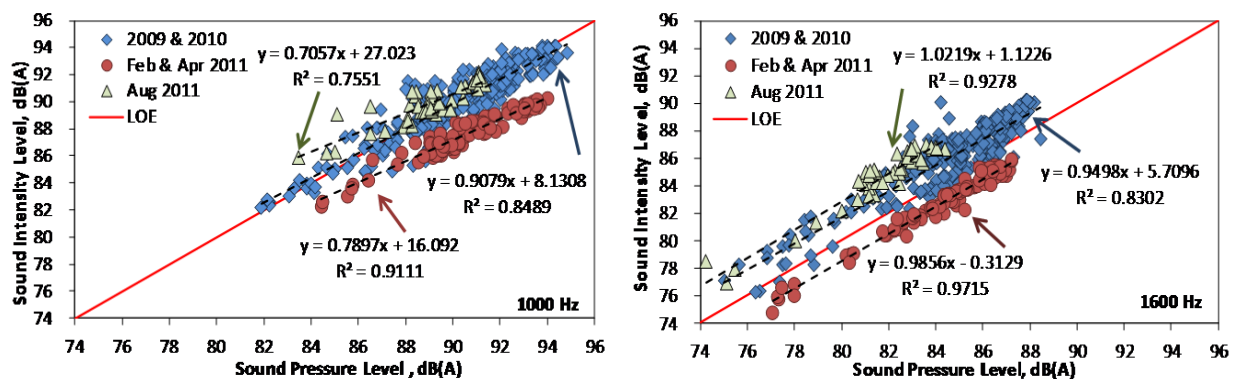
Figure 4.7 Sound-intensity Level (SIL) Versus Sound-Pressure Level (SPL) at 1/3 Octave Band for All Asphalt Pavements at Different Ages

The results of the sound-intensity measurements over a wide range of frequencies on sections with various surface mixes at different pavement ages are illustrated in Figure 4.8. The first observation is that pavement age does not appear to influence tire-pavement noise for any of the surface types at any frequency within the range of data available. The one exception may be the Superpave fine-gradation section, which shows an increase in the sound-intensity level at 500 Hz. Although this increase in noise could be due to raveling of the fine-graded layer, it is

clear that the trend is strongly influenced by the data point at about 4 years. Another observation is that the OGFC section is much quieter than all of the other surface types at the mid-range frequencies between 1,000 and 2,500 Hz. Noise experts agree that sound levels must differ by at least three decibels to be noticeable to the human ear (audibly quieter) (*63*).

OGFCs are designed to have small voids throughout the layer. These air voids are believed to absorb and dissipate the sound generated by the tires on the pavement surface. Overall, conventional asphalt mixtures have smaller and fewer voids, which gives them better durability than OGFC pavements but do not allow much absorption of noise. Although OGFC mixtures are found to be the quietest pavement over time among the investigated surface mixtures, climate is one of the big challenges when using OGFC pavements in some states (e.g., Washington) (*65*). Most states successfully using OGFC pavements are located in the southern U.S. and have relatively warm climates (e.g., Alabama, Arizona, California, Georgia, Florida, and Texas).
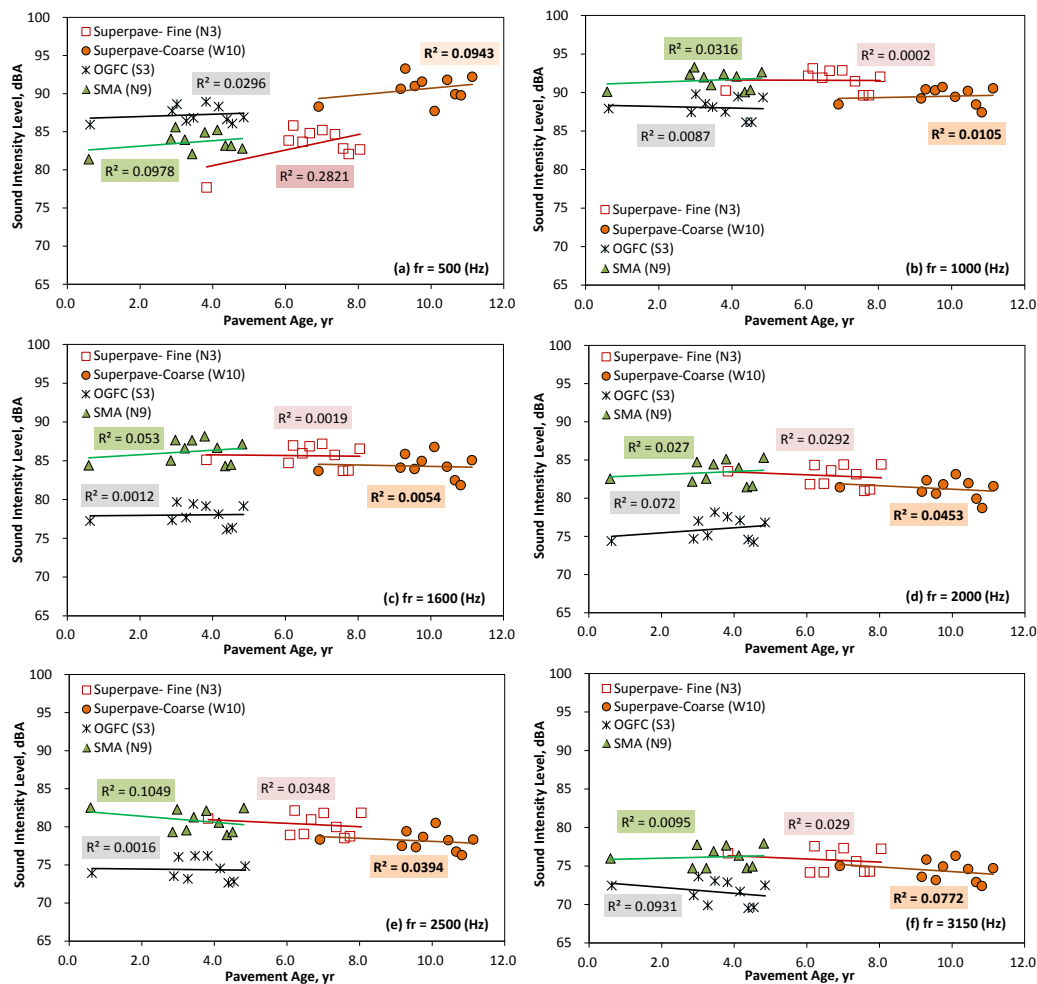
Figure 4.8 Sound-Intensity Level for Different Mixture Types Versus Pavement Age in Year at Different Frequencies of (a) 500, (b) 1000, (c) 1600, (d) 2000, (e) 2500 and (f) 3150 Hz.

Macrotexture

Macrotexture is among the dominant factors influencing the sound measured at the tire-pavement interface. But the relationship between this characteristic and noise is not well defined due to the other factors (e.g., porosity and stiffness of pavement mixture) influencing the tire-pavement interaction.

In this study, surface texture of the test track sections was quantified by mean profile depth using the high-frequency laser on the ARAN van. Pavement surface layer types were categorized by mean texture depth into three texture family groups summarized in Table 4.3.

Table 4.3 Texture Family Groups of Noise Test Sections on the 2009 NCAT Test Track

Group	Mean Profile Depth (MPD) Magnitude	Pavement Type	Noise Test Section	No. of Sections
A	< 1.0 (mm)	Superpave (Fine-Graded)	E5, E6, E7, E8, E9, N3, N4, N5, N6, N7, N8, N10, N11, W2, W3, W4, W5, W6, W7, S9, S10, S11, S12	32
		Superpave (Coarse-Graded)	E4, S2, S6, S7	
		SMA	E1, N9, S1	
		Other Pavements	E2, E3	
B	1.0 <MPD<1.5 (mm)	OGFC	N1, N2, N13, S3, S8	7
		SMA	N12, W1	
C	> 1.5 (mm)	Severely raveled Superpave (Coarse-graded)	W10	1

Based on the surface type and texture classification, the results of the OBSI measurements are summarized in Table 4.4 and Figure 4.9 (a) and (b) for different test track sections. The noise data have been measured over time and are compared for pre-traffic and post-traffic on different families of pavement surface.

Table 4.4 Average On-Board Sound Intensity (OBSI) Measurements for Different Families

| Family Group | Section | Average OBSI | | Texture Family Group |
| | | Pre-traffic | Post-Traffic | |
		8/23/2009	12/15/2011	
Fine-Graded	E5	98.5	99.35	A
	E6	98.1	99.55	A
	E7	98.45	99.85	A
	E8	99.3	97.1	A
	E9	96.7	96.75	A
	N3	98.6	98.75	A
	N4	98.4	99	A
	N5	93.25	96.35	A
	N6	92.6	96.35	A
	N7	92.5	96.75	A
	N8	95.1	95.3	A
	N10	92.1	96.4	A
	N11	92.45	97.1	A
	W2	99.8	96.8	A
	W3	97.7	99.3	A
	W4	97.7	98.8	A
	W5	98.7	99.6	A
	W6	97.5	97.95	A
	W7	99	97.25	A
	S9	93.65	96.2	A
	S10	93.3	96.2	A
	S11	93.95	96.25	A
	S12	93.05	97.4	A
Coarse-Graded	E4	99.65	100.1	A
	S2	91.7	94.55	A
	S6	92.95	96.3	A
	S7	93.15	95.85	A
OGFC	N1	98.8	99.55	B
	N2	98.1	100	B
	N13	93.65	94.9	B
	S3	99.4	99.6	B
	S4	99	100.45	N.A.
	S8	98.05	100.4	B
SMA	E1	98.35	99.05	A
	N9	98.9	99.5	A
	S1	98.5	99.5	A
	N12	96.55	98.65	B
	W1	99.5	100.1	B
Others	E2	96.5	97.65	A
	E3	98.7	98.85	A
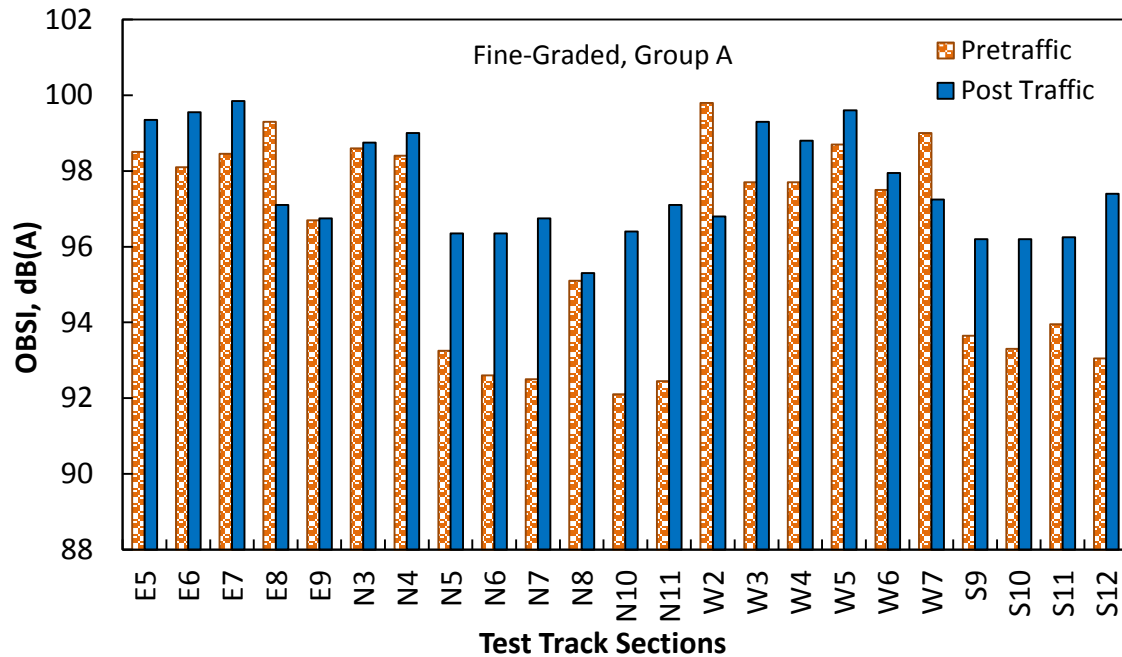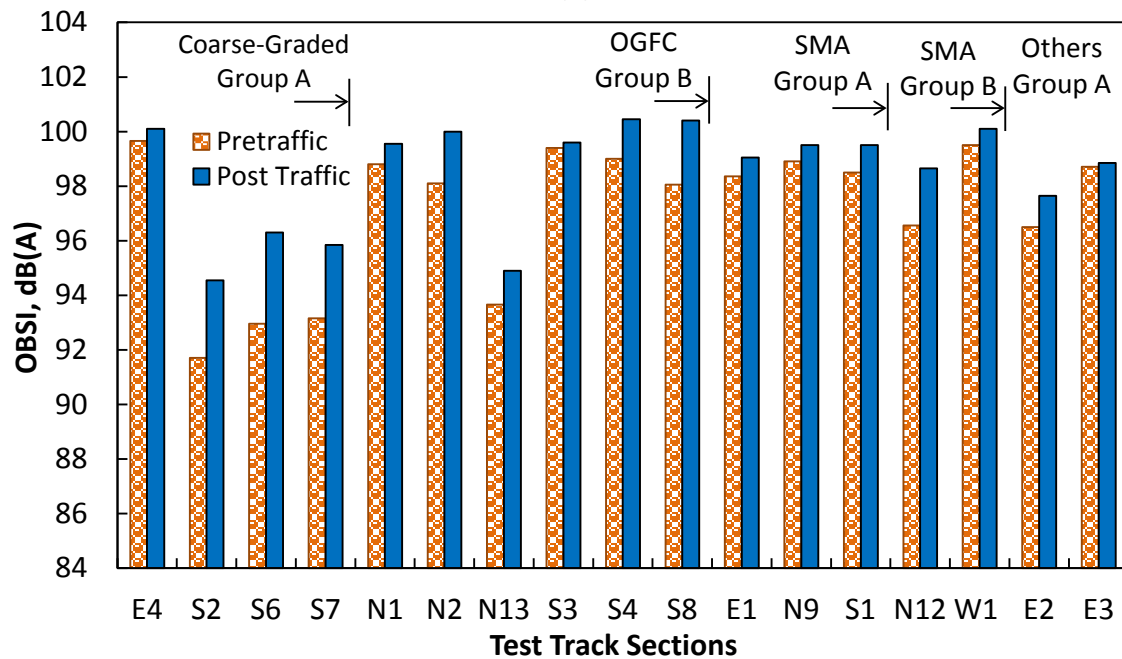
Figure 4.9 Pre-traffic and Post-traffic Noise Data on the 2009 NCAT Test Track for (a) Fine-graded and (b) Coarse-graded, OGFC, SMA, and Other Pavement Family Groups

Figure 4.10 shows the SIF at 1/3 octave bands for characteristic mixes from the three groups. For the sake of brevity, only A-weighted global sound-intensity levels calculated by logarithmic addition of the sound levels between the third octave band frequencies of 315 and 4,000 Hz are reported. At 1/3 octave band levels below 1,000 Hz, the sound-intensity level for the section from group A is 5 to 6 dBA lower than relative group B, which is 2 to 5 dBA lower than the

section with the highest macrotexture. At 1/3 octave band frequencies above 1,585, group B, which included OGFC and some SMA surfaces, are the quietest surfaces, and group A includes the loudest. The higher SILs at the higher frequency indicate a tonal noise generated on these smoother surfaces. Other researchers have related this high frequency noise to the squeaky sound of rubber-soled shoes on a smooth floor.
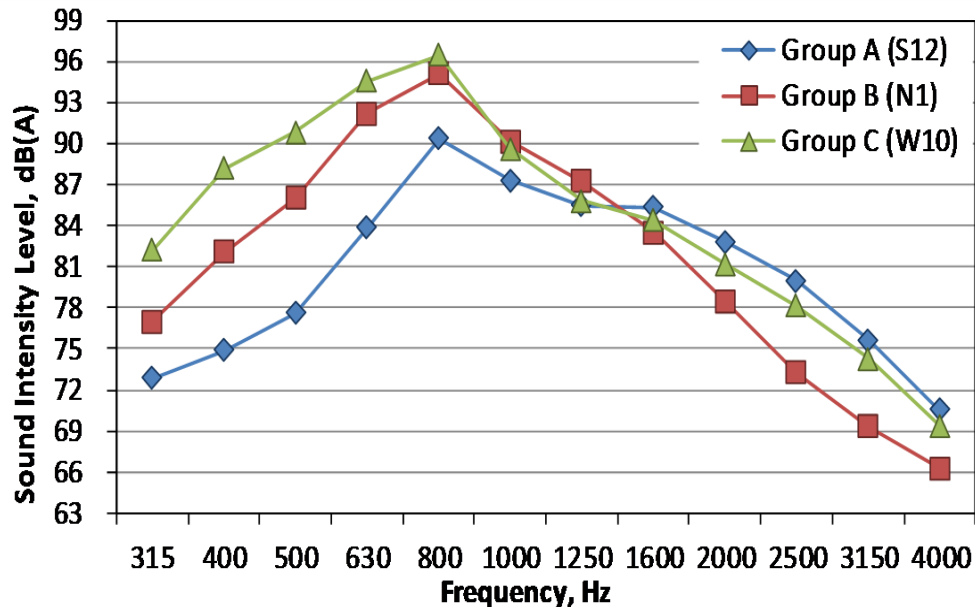
Figure 4.10 1/3 Octave Band Levels for Pavement Groups A, B, and C

Results of Parameter Investigation

The influence of other mix characteristics on tire-pavement noise was also analyzed. Sensitivity of the sound-intensity levels to variations of each mix characteristic was evaluated at two levels of frequency for the three texture groups.

Pavement Texture and Smoothness. Sound-intensity level versus mean profile depth in Figure 4.11(a) indicates that the smoother surface mixtures generate lower sound levels at the lower frequencies (<1,000 Hz), but higher noise levels at the higher frequencies (>1,600 Hz) compared to the coarser surface mixtures. This partly explains why mixtures with low texture seem noisier, as the human ear is more sensitive to higher frequency sound levels, and the A-weighting factors effectively filter out the lower-frequency sound levels.

Air Voids. By comparing the sound-intensity level sensitivity with in-place pavement air voids for different groups, shown in Figure 4.11(b), group B was within the same sound-intensity level range as group A in the low frequency band (1,000 Hz). However, in the higher frequency band (1,600 Hz), the OGFC mixtures were audibly quieter, and the SMA mixtures were grouped with the other dense-graded mixtures despite their higher macrotexture. It is important to note that one of the OGFC sections has significant raveling at the beginning of the section, which certainly influences the results for that section.

Stiffness. As illustrated in Figure 4.11 (c), pavement stiffness is not correlated with the sound-intensity level especially at a lower frequency band (1,000 Hz). While the stiffness estimates are based on theoretical calculations, the plots indicate that pavement stiffness does not influence tire-pavement noise.

Nominal Maximum Aggregate Size. As shown in Figure 4.11(d), larger nominal maximum aggregate size mixes tend to generate more noise (possibly related to the forces applied at the surface) at a low frequency (1,000 Hz). The smaller nominal aggregate size would serve to attenuate noise levels here.

(a)

(b)

(c)
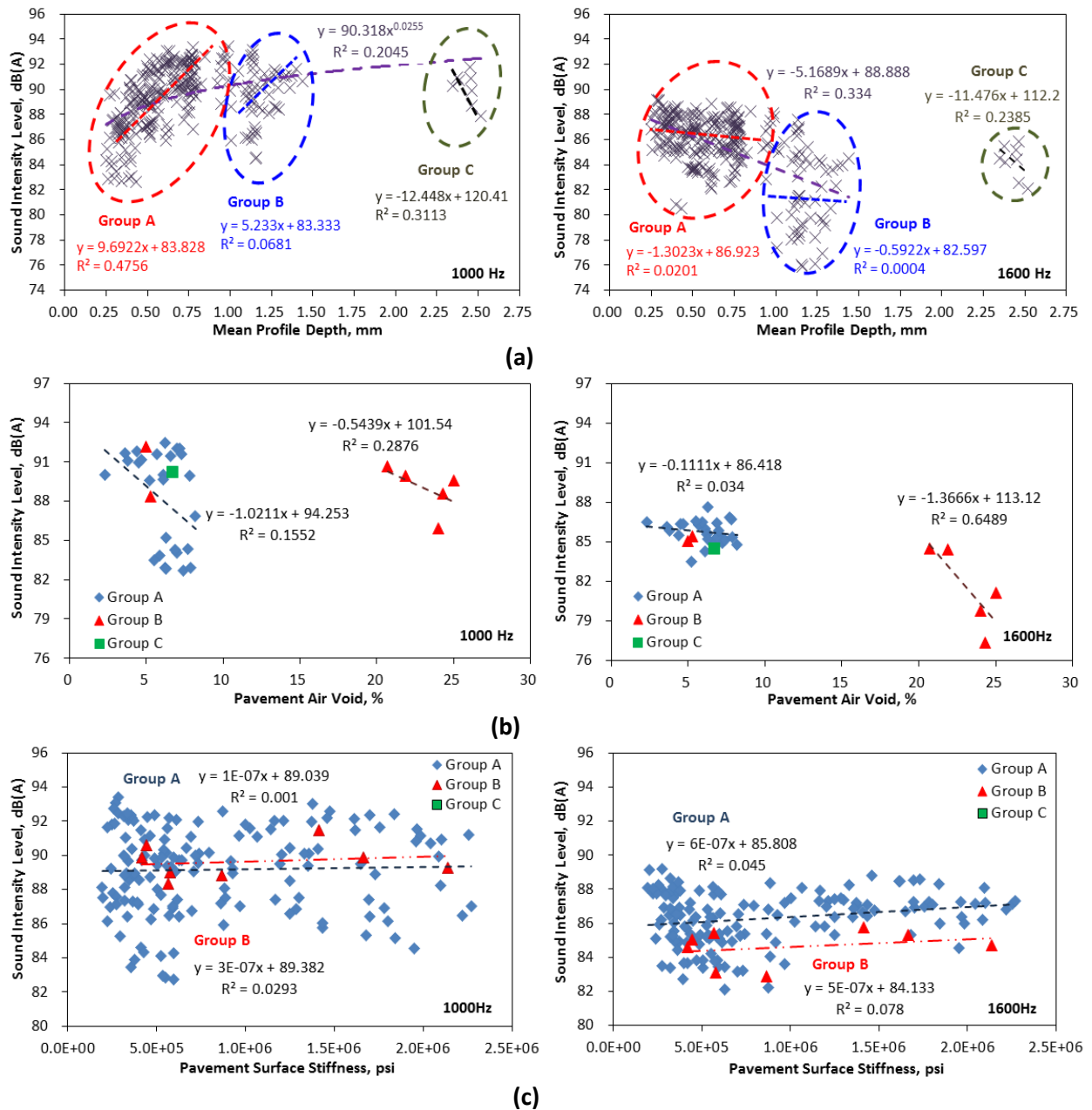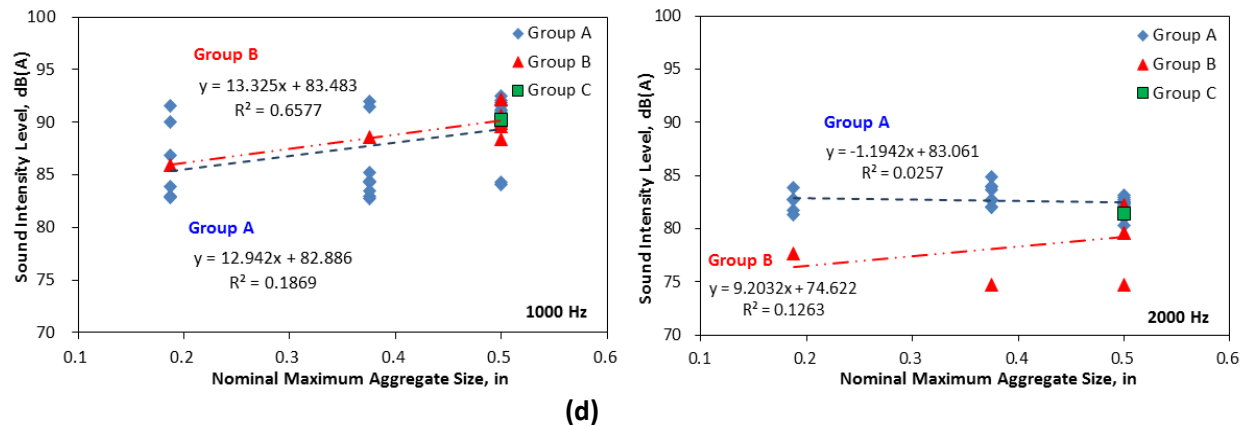
Figure 4.11 Sound-intensity Level (SIL) Versus (a) Mean Profile Depth (MPD), (b) Pavement Air Void, (c) Pavement Surface Elasticity and (d) Nominal Maximum Aggregate Size for All Pavement Types (Group A, B, and C) at Low- and High-Frequency Band.

Summary of Findings

An analysis of noise data from the test track sections provides some insight into the effects of surface layer characteristics on long-term durability of different surface mixtures. Findings of this ongoing noise analysis conducted during the 2009 NCAT Pavement Test Track cycle include the following:

1. The sound-intensity level (SIL) noise correlates well with the sound-pressure level (SPL) noise at all third-octave bands from 315Hz through 4,000Hz, with a relatively high correlation coefficient (R^2) in most of the frequency bands.
2. The coarser surface mixtures (OGFC, SMA, and coarse-graded Superpave) are found to be noisier pavements at low frequency, whereas the OGFC mixes were quietest at high frequencies.
3. The noise levels generated from tire-pavement interaction is influenced by macrotexture, in-place air void content, and at low frequencies by nominal maximum aggregate size.
4. Pavement surface texture (MPD) is the most significant variable that affects SIL at lower frequencies (below 1,600Hz). Higher MPD was found to have a positive effect on SIL below 1,600 Hz and a negative effect on SIL above 1,600 Hz.

Additional research is needed to better understand the nature of the factors that influence the tire-pavement noise and to define the interaction at the tire-pavement interface. More comprehensive and in-depth sensitivity analyses of influencing variables are needed to fully characterize the behavior.

4.4 Permeability of Test Track Mixtures

While one purpose of placing the open-graded friction course (OGFC) mixtures on the 2009 Test NCAT Pavement Test Track was to determine their structural value for pavement design, additional efforts sought to quantify the permeability of six permeable mixtures produced between 2003 and 2009. Permeable mixtures have been seen as a safety tool for preventing water accumulation on roadways and preventing the dangerous driving conditions that can lead to hydroplaning. However, research is still needed to understand how these mixtures perform over time and what factors influence the overall permeability of the mixtures.

Objective

The objective of this study was to assess the field permeability of six permeable mixtures on the test track over time. While one mix was produced in 2003 (Section S4) and two mixtures were placed in 2006 (Sections N13 and S3), three mixtures were placed in 2009 that varied in thickness and tack application methodology. The permeability of each mixture was measured approximately quarterly using a field permeameter developed at NCAT.

Methodology

Three sections containing permeable surfaces were left in place for the 2009 trafficking cycle at the track. In addition to the in-place mixtures, three open-graded mixtures were placed on the 2009 Test Track using different thicknesses and tack application methodologies. The first open-graded mixture (N1) was produced and placed three-quarter inches thick using a spray paver to achieve the bond between the open-graded wearing course and the dense-graded mixture beneath it. The second mixture (N2) was placed three-quarter inches thick and used a conventional tacking methodology to achieve bond between the open-graded mixture and the dense-graded mixture beneath. The final open-graded mixture (S8) placed in 2009 was constructed 1.25 inches thick and bonded to the underlying dense-graded mixture with a conventional tacking methodology. The quality control results and placement details of all six mixtures are provided in Table 4.5.

Table 4.5 Quality Control and Placement Details of Permeable Mixtures

Test Section	N1	N2	S8	N13	S3	S4
Sponsor	FL	FL	Group Exp.	GA	MS	TN
Construction Year	2009	2009	2009	2006	2006	2003
Gradation	*Percent Passing, %*					
19 mm	100	100	100	100	100	100
12.5 mm	97	97	97	100	100	95
9.5 mm	78	78	71	100	92	78
4.75 mm	24	25	21	41	31	19
2.36 mm	11	12	11	12	12	5
1.18 mm	9	10	9	8	9	3
0.60 mm	8	8	7	7	8	3
0.30 mm	6	6	6	6	6	2
0.15 mm	5	5	4	5	5	2
0.075 mm	3.9	3.5	3.1	4.2	3.8	1.6
Gyrations	50	50	50	50 blows	50	50
Binder Grade	76-22	76-22	76-22	76-22	76-22	76-22
Asphalt content, %	5.1	5.4	5.1	5.4	7.6	5.8
Average Mat Compaction, %	79.3	78.1	75.0	76.0	75.7	NA
Thickness, inches	0.8	0.8	1.3	0.63	1.3	1.0
Tack Material	CRS-2P	NTSS-1HM	NTSS-1HM	NA	67-22	67-22
Tack Rate, gal/sy	0.21	0.05	0.05	NA	0.05	0.03

Field permeability for each mixture was measured over the course of trafficking using an in-house permeameter designed using a standpipe of a constant diameter (Figure 4.12). The standpipe is then sealed to the pavement using a flexible rubber base and metal base plate to force the sealant into the surface voids. Head loss is then recorded from the standpipes over time. A more detailed description of this test method is given elsewhere (*67*).

Figure 4.12 Field Permeameter

Results

The results from the field permeameter testing are given in Figures 4.13-4.15. Figure 4.13 provides the permeability results over time for the three open-graded mixtures placed in 2009. Figure 4.14 provides the field permeameter test results for the 2006 mixtures, while Figure 4.15 shows the test results for the mixture placed in 2003. The bars represent the average of six measurements in the sections; the whiskers represent ± one standard deviation. Note that deicing treatments were not used at the test track. Some ice and snow treatments contain fine aggregates and sands that can fill the pores of permeable mixes and reduce the overall permeability of the layer.

Three important observations can be made from the test results. First, the mixtures placed before 2009 had less reduction in permeability over time than the two thinner OGFC layers placed in 2009. The OGFC placed in N1 and N2 showed some signs of declining permeability; however, the other four OGFC layers had fairly consistent permeability readings over the course of trafficking.

Additionally, it should be noted that though the tack coat applied in N1 was heavier than the tack coat placed in N2, there was no real difference in the field permeameter results between the two sections. While these results showed minimal difference in the performance of these two sections, visual differences in the capacity of the two test sections were noticed during heavy rains. Section N2 showed signs of a higher capacity for handling heavier rainfalls than Section N1.

Finally, Section S8 and N2 used the same mixture and tack coat application. The only difference between the two mixtures was Section S8 was placed one-half inch thicker than N2. Initially, Section S8 was more than twice as permeable as N2; however, after trafficking began on the

test sections, S8 had 6 to 10 times the capacity to handle water compared to N2. The additional half-inch of material greatly increased the permeability of the pavement structure.

While using conventional tack showed equal or better permeability for OGFC mixtures compared to heavier tack rates, it is recommended to use heavier track coats to improve the durability of OGFC surfaces. Additionally, increasing the thickness of OGFC mixtures should be considered to increase the capacity of the pavement layer to handle water infiltration.
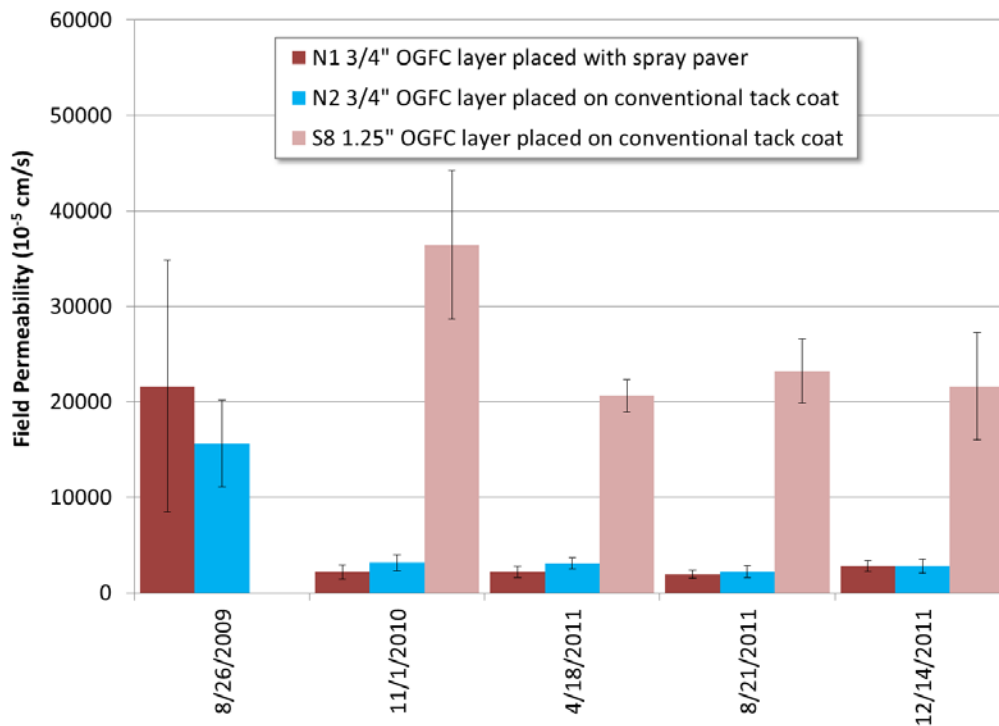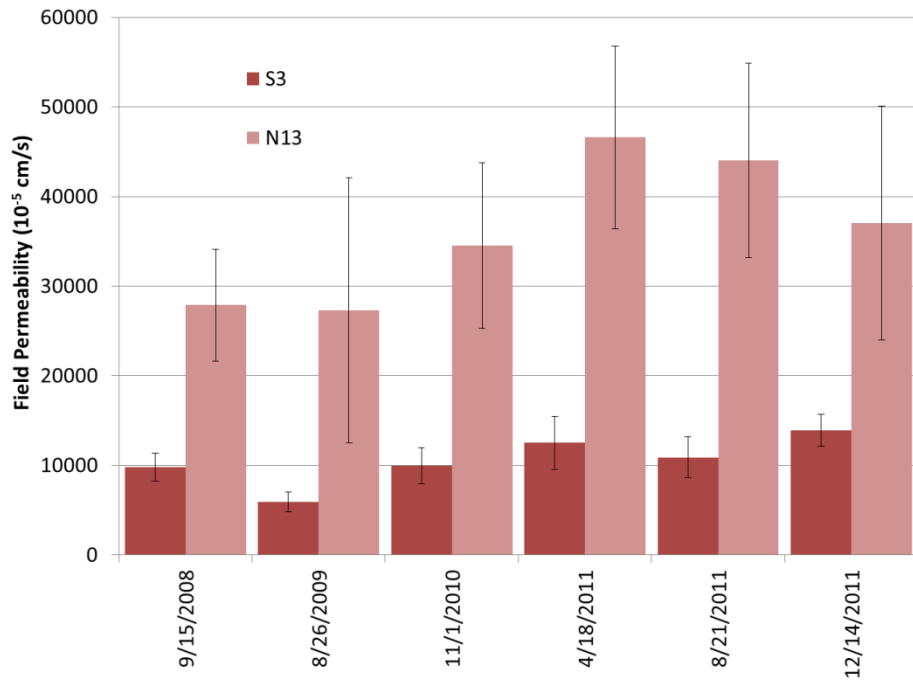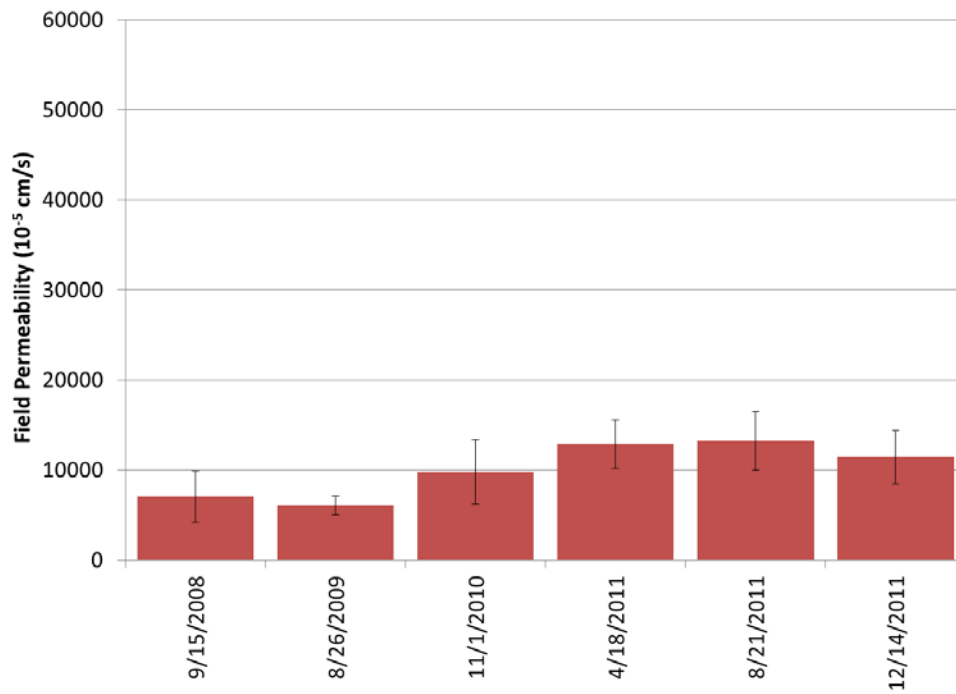

Figure 4.13 2009 Mixture Field Permeability Results

Figure 4.14 2006 Mixture Permeability Results

Figure 4.15 2003 Mixture Permeability Results

4.5 Laboratory Assessment of Mixture Durability

Cracking is one of the most common distresses in flexible pavement structures; however, the mechanisms for cracking can vary. Fatigue cracking occurs over time as repeated trafficking loads a pavement structure. This type of cracking is typically considered a structural problem that develops due to heavy loads, too many load repetitions, or poor subgrade support resulting in high pavement deflections (*68, 69).*

Low-temperature cracking develops through a completely different mechanism. Low-temperature cracking, also known as thermal cracking, is believed to result from the accumulation of high tensile stresses at the surface due to contraction of the pavement during rapid drops in temperature. As the pavement tries to contract, the resulting tensile stress can exceed the tensile strength of the mixture, producing a crack *(70, 71)*. This type of cracking is generally considered unrelated to traffic loads.

Another type of cracking distress that has been documented more recently is surface cracking. These cracks are evident only in the upper layers of the pavement and often exist in or along the edges of the wheelpath, implying a relationship to pavement loading. Some surface cracking has been related to a construction defect caused by segregation in the mat due to the paver's slat conveyor or auger gear box. Roque et al. *(11)* have proposed that surface cracking is a complex interaction of tire-pavement contact stresses and thermal and aging effects *(72)*. The following subsections detail the procedures and results from cracking performance testing conducted on NCAT Pavement Test Track mixtures.

Objective

The objective of this work was to characterize the mixtures placed at the 2009 Pavement Test Track for durability. Surface mixtures would be assessed for resistance to surface cracking using the energy ratio testing regime and low-temperature cracking via AASHTO T322-07. The base mixtures from the group experiment were assessed for fatigue performance using the AASHTO T321-07 and the simplified visco-elastic continuum damage procedure recently developed by North Carolina State University.

Methodology

The following subsections describe the methodologies used for characterizing the 2009 NCAT Pavement Test Track asphalt mixtures for resistance to cracking.

Energy Ratio. The energy ratio testing regime was developed to assess an asphalt mixture's resistance to surface cracking (*73*). Since the energy ratio is specifically associated with top-down or surface cracking, only the twelve unique surface mixtures produced for the 2009 test track were tested using this methodology.

To determine a mixture's energy ratio, three specimens 150 mm in diameter and approximately 38 mm thick, cut from gyratory-compacted samples, were prepared. The target air voids for these samples were 7 ± 0.5 percent. A Material Testing System (MTS) was then used to conduct the resilient modulus, creep compliance, and indirect tensile strength test of each mixture at

10°C. The exact methodology of the individual test components has been documented elsewhere (*11*).

The resultants from these tests were then used to evaluate each mixture's resistance to surface cracking using Equation 1. A higher energy ratio results in a mixture that is more resistant to surface cracking.

$$ER = \frac{DSCE_f[7.294\times10^{-5}\times\sigma^{-3.1}(6.36-S_t)+2.46\times10^{-8}]}{m^{2.98}D_1}$$
(1)

Where: σ = tensile stress at the bottom of the asphalt layer, 150 psi
M_r = resilient modulus
D_1, m = power function parameters
S_t = tensile strength
$DSCE_f$ = dissipated stress creep energy at failure

The current criteria for ER test results are given in Table 4.6.

TABLE 4.6 Energy Ratio Criteria (*11*)

Traffic, ESALS/year X 1000	Minimum Energy Ratio
<250	1
<500	1.3
<1,000	1.95

Indirect Tension Creep Compliance and Strength. The critical cracking temperature where the estimated thermal stress exceeds the tested indirect tensile strength of a mixture can be used to characterize the low-temperature cracking performance of asphalt mixtures. This type of analysis has been referred to as a critical temperature analysis. A mixture exhibiting a lower critical cracking temperature than that of the other mixtures would have better resistance to thermal cracking. Twelve surface mixtures were evaluated using a critical temperature analysis in this study.

To estimate the thermal stress and measure the tensile strength at failure, the indirect tensile creep compliance and strength tests were conducted on three replicates of each mix, as specified in AASHTO T 322-07.   A thermal coefficient of each mixture was estimated based on its volumetric properties and typical values for the thermal coefficient of asphalt and aggregate. This computation is explained in more detail below.

The IDT system, which has been used to predict thermal stress development and low-temperature cracking in asphalt mixtures, was used to collect the necessary data for the critical cracking temperature analysis. The testing was conducted using an MTS load frame equipped with an environmental chamber capable of maintaining the low temperatures required for this test. Creep compliance at 0°C -10°C, and -20°C and tensile strength at -10°C in accordance with AASHTO T 322-07 were measured. These temperatures were specified as a function of the low-temperature PG grade of the binder in AASHTO T322-07. The creep test applied a constant load to the asphalt specimen for 100 seconds while the horizontal and vertical strains were measured on each face of the specimen using on-specimen instrumentation.

Four samples were prepared for each mix. The first sample was used to find a suitable creep load for that particular mix at each testing temperature. The remaining three samples were tested at this load for the tested data set.   Specimens used for the creep and strength tests were 38 to 50 mm thick and 150 mm in diameter prepared to 7 ± 0.5% air voids.

Theoretical and experimental results indicate that for linear visco-elastic materials, the effect of time and temperature can be combined into a single parameter through the use of the time-temperature superposition principle. From a proper set of creep compliance tests under different temperature levels, the creep compliance mastercurve can be generated by shifting the creep compliance data to a curve based on a reference temperature. This reference temperature was typically the lowest creep compliance test temperature (-20°C for this study). The relations between real time t, reduced time ξ, and a shifting factor a_T are given as Equation 2.

$$\xi = t/a_T \tag{2}$$

An automated procedure to generate the mastercurve was developed as part of the Strategic Highway Research Program (SHRP) *(73)*. The system required the measurement of creep compliance test data at three different test temperatures. The final products of the system were a generalized Maxwell model (or Prony series), which was several Maxwell elements connected in parallel, and temperature shifting factors. The generalized Maxwell model and shifting factors were used for predicting thermal stress development of the asphalt mixture due to a change in temperature. The mathematical models used to determine the critical temperature and failure time for each mixture are documented elsewhere (*74*).

Bending Beam Fatigue. Bending beam fatigue testing was performed under the guidance of AASHTO T 321-07 to determine the fatigue endurance limits of the base mixtures placed in the structural study. Only the base mixtures of the test sections were evaluated for fatigue performance since the critical fatigue location in a pavement cross-section is the bottom of the asphalt layer. Nine beam specimens were tested for each mixture. Within each set of nine, three beams each were tested at 200, 400, and 800 microstrain at 10Hz and 20°C. The lone exception to this testing protocol was the polymer-modified mixture placed in Section N7 by Kraton Polymers. The beams for this mixture were tested at 400, 600, and 800 microstrain due to the performance of the beams at 400 microstrain. Failure was defined as a 50% reduction in beam stiffness in terms of the number of cycles until failure. Further documentation of the testing is given by Willis et al. elsewhere (*75*).

Using a proposed procedure developed under NCHRP 9-38 (*32)*, the endurance limit for each of the eight mixes was estimated using Equation 3 based on a 95% lower prediction limit of a linear relationship between the *log-log* transformation of the strain levels and cycles to failure. All the calculations were conducted using a spreadsheet developed under NCHRP 9-38.

$$\text{Endurance Limit} = \hat{y}_0 - t_\alpha s \sqrt{1 + \frac{1}{n} + \frac{(x_0 - \bar{x})^2}{S_{xx}}} \tag{3}$$

Where:

$\hat{y}_0$ = log of the predicted strain level (microstrain)

t_α = value of *t* distribution for n-2 degrees of freedom = 2.131847 for n = 9 with α = 0.05

s = standard error from the regression analysis

n = number of samples = 9

S_{xx} = $\displaystyle\sum_{i=1}^{n}\left(x_i - \bar{x}\right)^2$ (Note: log of fatigue lives)

x_o = log (50,000,000) = 7.69897

$\bar{x}$ = log of average of the fatigue life results

Simplified Visco-elastic Continuum Damage (S-VECD). Uni-axial fatigue testing based on the continuum damage mechanics has been studied and conducted in universal servo-hydraulic load frames to characterize the fatigue characteristics of asphalt mixtures. The theoretical background of this method has been presented in several publications (*76, 77, 78, 79).*

The recent development of a draft test procedure, titled *Determining the Damage Characteristic Curve of Asphalt Concrete from Direct Tension Fatigue Tests* (*80),* by the asphalt pavement research group led by Dr. Richard Kim at North Carolina State University allows the uniaxial fatigue test (known as the S-VECD test) to be conducted in the AMPT.

To characterize the fatigue characteristics of a mixture using the S-VECD model, two tests are performed in AMPT. First, the dynamic modulus of the mixture is determined according to the AASHTO TP 79-10 test protocol to quantify the linear viscoelastic (LVE) characteristics of the mix. Second, a controlled crosshead (CX) cyclic fatigue test is performed using the fatigue testing software in AMPT to acquire the necessary fatigue data. The test protocol this software utilizes was discussed by Hou et al. (*78).* To conduct this test, an AMPT sample was glued with a steel epoxy to two end platens. The sample and end platens were then attached with screws to the actuator and reaction frame of the AMPT prior to installing on-specimen LVDTs.

The controlled crosshead fatigue test was performed at 19°C with a frequency of 10 Hz and consisted of two phases. First, a small strain (50 to 75 on-specimen microstrain) test was performed to determine the fingerprint dynamic modulus of the sample. This was done to determine the ratio of the fingerprint dynamic modulus ($|E*|_{Fingerprint}$) of the testing sample to the dynamic modulus determined from AMPT dynamic modulus testing ($|E*|_{LVE}$). This value was known as the dynamic modulus ratio (DMR) and was expected to be between 0.9 and 1.1 (Equation 4) (*78).* This ratio was used for controlling the quality of the fatigue testing and was incorporated into the S-VECD fatigue model *(78).*

Second, the sample was subjected to a fatigue test in which the AMPT actuator was programmed to reach a constant peak displacement with each loading cycle. During this test, the dynamic modulus and phase angle of the sample are recorded. Failure of the sample was defined as the point at which the phase angle peaks and then drops rapidly (*78).* This concept is demonstrated graphically in Figure 4.16

$$DMR = \frac{|E*|_{Fingerprint}}{|E*|_{LVE}} \tag{4}$$
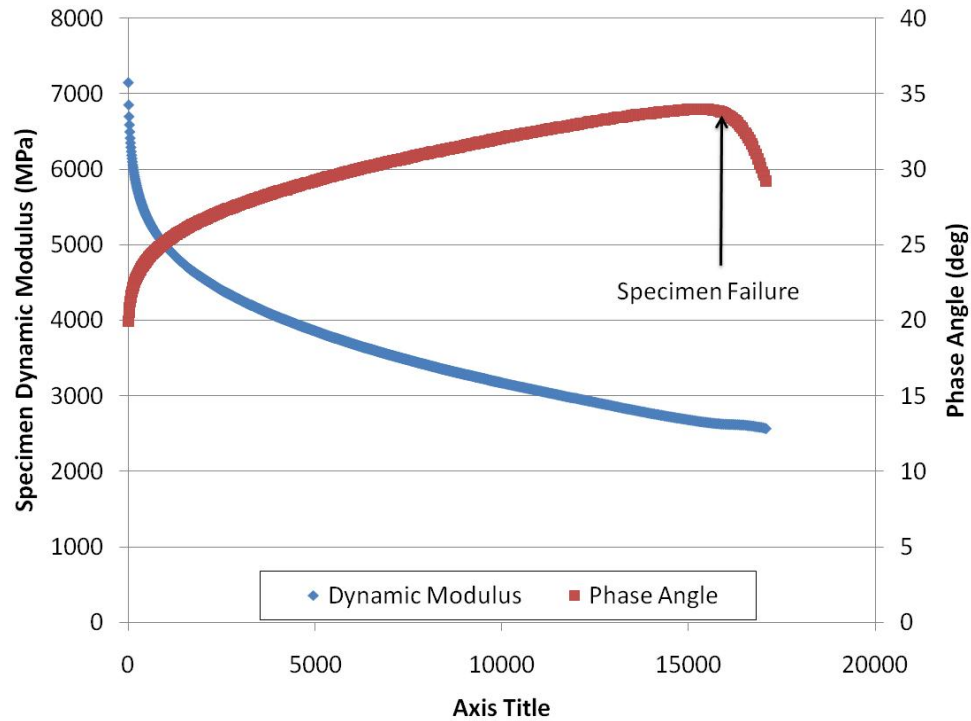
Figure 4.16 Determination of Cycles to Failure for S-VECD Fatigue Test

The initial target peak-to-peak on-specimen strain was specified in the software prior to the start of the test. It was desired that four fatigue samples be tested with two replicates at two different strain levels. These strain levels were selected empirically so that the cycles to failure of the mix at the two strain levels were approximately an order of magnitude apart (i.e., 1,000 cycles to failure for one strain level versus 10,000 cycles to failure for another strain level). However, past research has shown that sufficient S-VECD fatigue predictions can be made with only two samples (*78*). Both the dynamic modulus test and controlled crosshead cyclic test were performed using samples prepared in accordance with AASHTO PP60-09. All samples were prepared to 7 ± 0.5% air voids. Typically, three samples of mix were required for dynamic modulus testing, and four to six samples were needed to get sufficient fatigue data.

The S-VECD fatigue data analysis was performed using an analysis package developed at North Carolina State University. This software has been used for S-VECD fatigue testing on servo-hydraulic load frames in the past, but was updated to process the data generated by the fatigue testing software in the AMPT. Five primary steps were needed for the data processing:
1. The number of testing cycles to failure was determined for each specimen based on the phase angle curve (see Figure 4.16).
2. The AMPT dynamic modulus data were entered into the fatigue analysis software. The software utilized this data to compute the Prony series coefficients for creep compliance and relaxation modulus of the mixture (*79*). The dynamic modulus data were also used to determine the dynamic modulus mastercurve and the DMR value as discussed earlier.
3. The individual fatigue data files were individually analyzed to determine the C (pseudo-stiffness) versus S (damage parameter) curve. During this step, the individual files must be examined to determine the value of C that corresponds to the "failure" cycle for each mix.

4. The combined C versus S curve for the mix was then determined based on the individual C versus S curves. The composite C versus S curve is fit using a power law, shown as Equation 2 (where C_{11} and C_{12} are the regression coefficients) (*78*). These curves are fit to the point of failure (defined by C at failure) for each mix.

$$C = 1 - C_{11}S^{C_{12}} \tag{5}$$

5. Finally, a fatigue prediction is made using the S-VECD model. Fatigue predictions for this study were made using the controlled-strain assumption based on the formula in Equation 6 (*78*). These fatigue simulations can be performed in the fatigue analysis software package. However, for this project, these simulations were performed in an EXCEL® spreadsheet using the parameters developed by the fatigue analysis software for each mix.

$$N_f = \frac{(f_R)(2^{3\alpha})S_f^{\alpha - \alpha * C_{12} + 1}}{(\alpha - \alpha * C_{12} + 1)(C_{11}C_{12})^\alpha \left[(\beta + 1)(\epsilon_{0,pp})(|E^*|_{LVE})\right]^{2\alpha} K_1} \tag{6}$$

Where: C = pseudo-stiffness
S = damage parameter
f_R = reduced frequency for dynamic modulus shift factor at fatigue simulation temperature and loading frequency
α = damage evolution rate for S-VECD model
$\epsilon_{0,pp}$ = peak-to-peak strain for fatigue simulation
$|E^*_{LVE}|$ = dynamic modulus of mix from dynamic modulus mastercurve at the fatigue simulation temperature and loading frequency
C_{11}, C_{12} = power law coefficients from C vs S regression
β = mean strain condition (assumed to be zero for this project)
K_1 = adjustment factor based on time history of loading – function of α and β

Results

The test results for the previously described testing methodologies are presented below. Energy ratio and indirect tension creep compliance and strength testing were typically conducted on the surface mixtures placed at the track, while bending beam fatigue and S-VECD tests were conducted on base mixture testing.

Energy Ratio. Twelve surface mixtures placed on the 2009 Pavement Test Track were evaluated for their susceptibility to top-down or surface cracking using the energy ratio methodology. Since the data from the tests on specimens for each section were aggregated into a singular value, statistical comparisons between the mixtures could not be conducted. Table 4.7 provides the energy ratio test results for the twelve mixtures tested. A complete list of all the parameters determined during the energy ratio test is found in Appendix A.

The mixture that showed the most resistance to surface cracking was the 9.5 mm control mixture placed in Section S9; however, when considering the previously listed critical energy ratios (*11*), only two mixtures (S2-1 and N8-1) had energy ratios below the criterion for trafficking of 1,000,000 equivalent single axle loads (ESALs) per year. Mix N8-1 had an energy ratio acceptable for trafficking of 500,000 ESALs per year, while mix S2-1 did not meet any of the three minimum energy ratio requirements. One reason these two mixtures performed poorly in the energy ratio testing methodology was fracture energy. Both mixtures had fracture energies below 2 kJ/m^3, while most mixtures had fracture energies greater than 3 kJ/m^3. These fracture

energies reduced the overall energy ratio of the mixture enough to classify them in different trafficking classifications.

Table 4.7 Energy Ratio Test Results

Mixture	Description	Energy Ratio	Fracture Energy (kJ/m^3)
S9-1	Control	11.10	8.1
N7-1	Kraton	10.97	4.2
N8-1	OK SMA	1.56	1.9
N10-1	50% RAP	5.53	1.6
N11-1	50% RAP- WMA	3.77	3.4
N12-1	GA SMA	4.84	3.1
S2-1	MS 45% RAP	0.64	0.2
S6-1	SBS Modified	4.96	5.1
S7-1	GTR Modified	4.43	4.1
S10-1	WMA – Foam	5.77	12.5
S11-1	WMA – Additive	5.06	9.56
S12-1	TLA	3.92	3.04

While direct correlations to field performance were not possible due to the lack of cracking observed during the 2009 trafficking cycle, the only section that truly exhibited signs of surface cracking was the mixture with the lowest energy ratio (S2-1). In February 2011, at 6.9 million ESALs, cracks were first mapped in Section S2. By the end of trafficking, numerous transverse and longitudinal cracks were observed in the wearing course, as discussed in Chapter 2.

While N8-1 also had a low energy ratio, the mixture was eventually removed due to slippage, which occurred shortly after construction. It was impossible to directly correlate the energy ratio to field performance due to the confounding variable of debonding.

Indirect Tension Creep Compliance and Strength. While low-temperature cracking is not a concern in many southern states, it was still important to characterize the mixtures for low - temperature properties. AASHTO T322-07 was used to characterize the mixtures in terms of both indirect tensile strength and creep compliance. These results were then used to predict the thermal cracking   temperature for twelve mixtures. These results are shown in Table 4.8.

Table 4.8 Indirect Tension Testing Results

Mixture ID	Average IDT Strength (MPa)	Failure Time (hours)	Critical Mixture Low Temperature (°C)	True Critical Low Binder Temperature (°C)
N7-1	4,546,297	4.472	-24.7	-26.4
N8-1	3,559,809	4.639	-26.4	-30.8
N10-1	4,100,718	4.250	-22.5	-15.5*
N11-1	4,060,877	4.306	-23.1	-17.7*
N12-1	3,531,736	4.306	-23.1	-29.3
S2-1	4,426,482	4.000	-20.0	-18.5*
S6-1	4,394,770	4.444	-24.4	-26.3*
S7-1	4,667,902	4.500	-25.0	-25.0
S9-1	4,711,264	4.639	-26.4	-24.7*
S10-1	4,478,804	5.000	-30.0	-23.9*
S11-1	4,460,519	4.722	-27.2	-25.7*
S12-1	5,058,616	5.083	-30.8	-21.4*

*Tests run on extracted binder.

While there are no consensus-required tensile strengths or failure times for asphalt mixtures, and low-temperature cracking has not occurred for any section on the Test Track, one trend was noticed when comparing the critical mixture low temperature to the critical binder low temperature (Figure 4.17). When extracted binder was used to determine the performance grade of the asphalt binder, the mixture critical temperature was typically lower than the critical binder temperature. The lone exception was the Missouri SBS-modified mixture. All the mixtures where binder from the tank was compared to the critical mixture temperature had critical binder temperatures that were lower than the critical mixture temperature. This suggests that using the extracted binder critical temperatures for low temperature is a more conservative estimate of the true mixture performance.
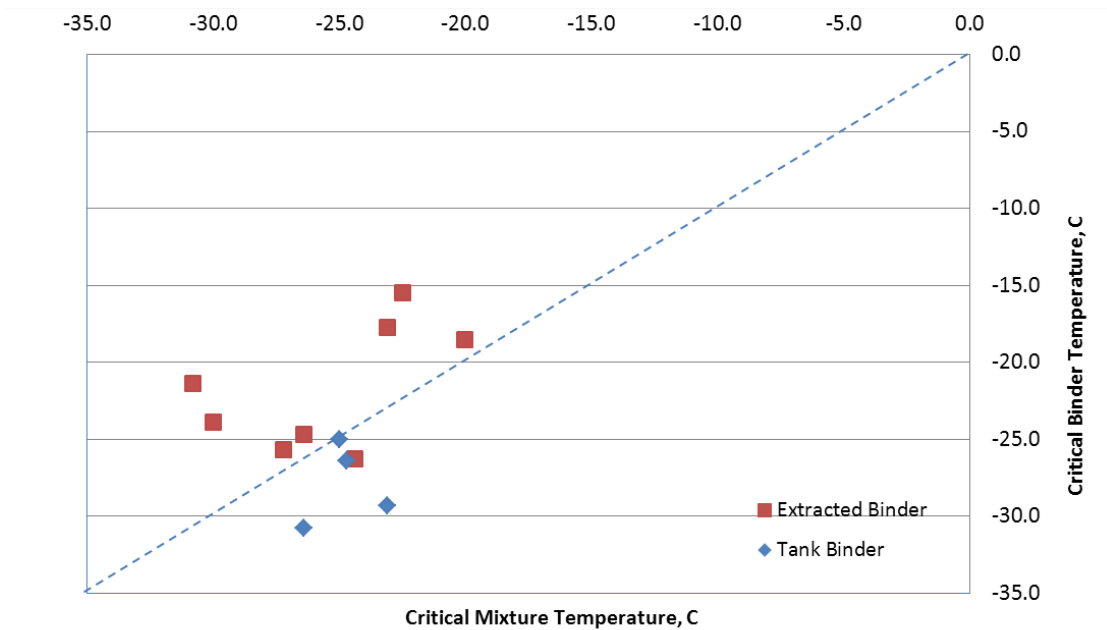
Figure 4.17 Indirect Tension Critical Temperature Comparison

Bending Beam Fatigue. The bending beam fatigue test was conducted in accordance with AASHTO T321-07 on the base mixtures produced for the structural study. The primary purpose of conducting this experiment was to characterize the fatigue endurance limits of the asphalt mixtures using the methodology previously described. The average beam fatigue results and fatigue endurance limits for each mixture are given in Table 4.9. Individual beam fatigue results are provided in Appendix A.

Table 4.9 Average Beam Fatigue Results for Group Experiment Mixtures

Mixture	Description	Cycles Until Failure				Fatigue Endurance
		200 με	*400 με*	*600 με*	*800 με*	**Limit (FEL), microstrain**
S9-3	Control	5,083,040	186,193	NA	9,887	92
N10-3	50% RAP - HMA	9,441,897	52,523	NA	2,317	100
N11-3	50% RAP - WMA	37,367,083	124,093	NA	2,587	134
S10-3	WMA – Foam	5,333,953	184,737	NA	9,147	99
S11-3	WMA – Additive	3,719,113	199,847	NA	10,493	84
N5-4	Thiopave	26,992,143	257,690	NA	7,337	109
N7-3	Kraton	NA	6,043,907	223,313	39,450	241
S12-3	TLA	39,986,988	381,070	NA	5,807	137

When comparing the beam fatigue test results of the different mixtures to the beam fatigue results of the control section, two sample *t*-tests (α = 0.05) were initially conducted comparing each mixture's test results to the control mix. However, due to the variability of the test results, limited statistical differences were found. Therefore, Table 4.10 compares the average beam

fatigue cycles until failure in terms of percent increase or decrease from the control mixture performance. The table also compares the fatigue endurance limit (FEL) of each mixture to that of the control mixture using a similar methodology.

The fatigue endurance limit of each mixture characterizes how the mixture will perform over numerous strain magnitudes. The only mixture that had a fatigue endurance limit less than the control mixture was the WMA additive mixture. The FEL in this case was approximately 91% of the FEL of the control mixture. All the other base mixtures exhibited performance either equal to or better than the FEL of the control mixture.

Table 4.10 Beam Fatigue Comparisons to Control Mixture

Mixture	% Increase Cycles Until Failure of Control Mixture			% Increase Fatigue Endurance Limit of Control Mixture
	200 με	*400 με*	*800 με*	
N10-3	87.4	-71.8	-76.3	8.7
N11-3	641.7	-33.4	-73.8	45.7
S10-3	5.9	0.8	-7.5	7.6
S11-3	-26.4	7.3	6.1	-8.7
N5-4	435.8	38.4	-25.8	18.5
N7-3	NA	314.6	299.0	162
S12-3	693.7	104.7	-41.3	48.9

Simplified Visco-elastic Continuum Damage. S-VECD testing was also completed on the base mixtures in the structural study. At least four fatigue tests (two at a relatively high strain input level, and the other two at a relatively low strain input level) were performed at a single temperature (19^oC). Hou et al. reported that 19^oC is a suitable temperature for the material's viscoelastic damage characterization because the material is not as brittle as at a low temperature, and the effect of viscoplasticity is negligible (*78*). Using these test results, the fatigue behavior at all other conditions is predicted with the S-VECD model. Table A.6 in Appendix A summarizes the cyclic test results for all mixtures used in this study. All tests were performed at a constant frequency of 10 Hz and at a constant temperature of 19^oC.

After each cyclic test, the pseudo stiffness and damage are computed according to the S-VECD model to be used for fatigue performance prediction. The damage characteristic curves generated from the S-VECD model are now combined with the material's modulus in order to fully evaluate the fatigue resistance of the mixtures. Figure 4.18 shows the predicted number of cycles to failure for 200, 400, 600, and 800 microstrain, considering a 20^oC test temperature, 10Hz testing frequency, and logarithmic scale of base 10.
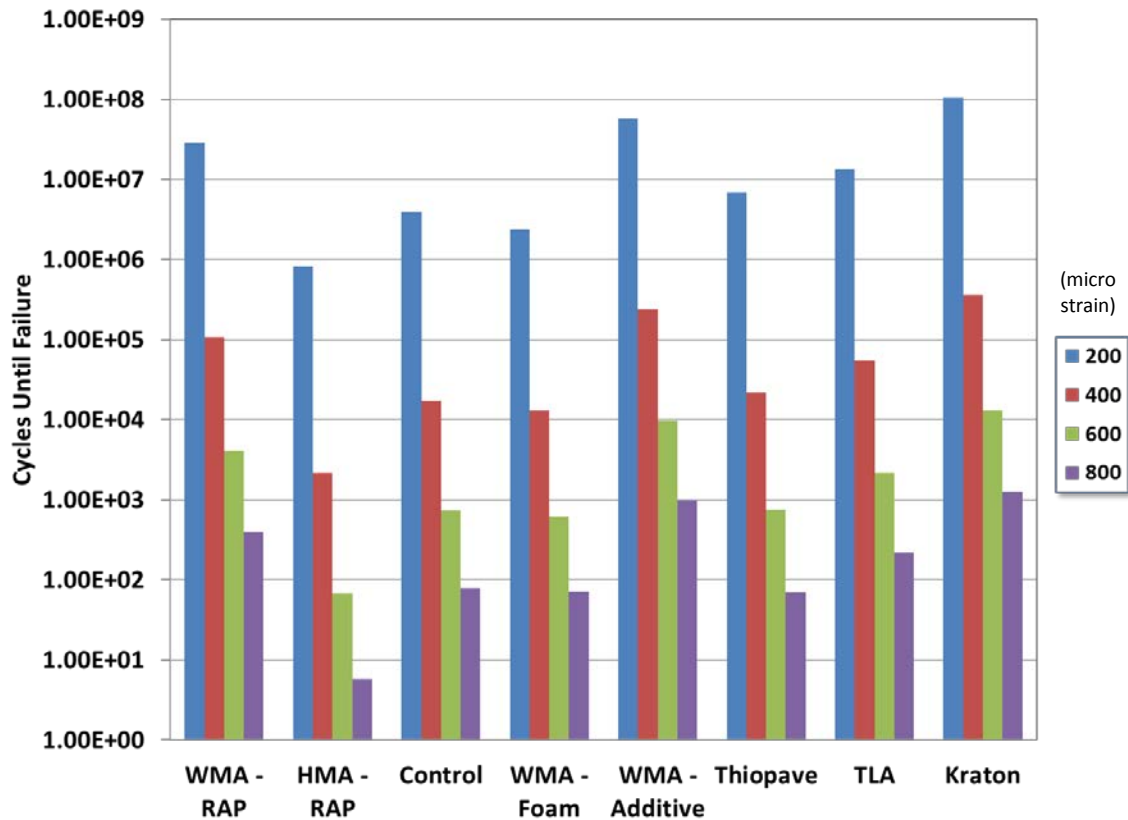
Figure 4.18 Predicted Number of Cycles to Failure from S-VECD Testing

As can be seen in Figure 4.18, only the 50% RAP mixture had predicted number of cycles until failure substantially less than the control mixture. The WMA-Foam mix had slightly lower S-VECD fatigue results compared to the control mix, but results were within the same order of magnitude at each strain level. While this is only a preliminary finding, notice that the rankings of the mixtures do not change based on the strain magnitude, as seen with the beam fatigue results. The lone exception to this was the Thiopave mixture in Section N5. At the lower strain levels, this mixture performed better than the control mixture, while at the higher strain levels, the performance was almost equivalent to the control mixture.

Table 4.11 compares the predicted cycles until failure for each mix in terms of percent increase or decrease number of cycles to failure compared to the control mixture. The 50% RAP mixture compacted hot and foamed WMA mixture always lasted fewer cycles in the prediction, while the 50% RAP mixture compacted warm, additive WMA, Kraton polymer-modified mixture, and TLA mixture always performed better than the control mixture. As mentioned previously, the Thiopave mixture tested in this analysis performed better than the control mixture at lower strains but had an 11.3% fewer predicted number of cycles until failure than the control mixture at the highest strain magnitude.

Table 4.11 S-VECD Comparisons to Control Mixture

Mixture	Description	% Increase Cycles Until Failure of the Control Mixture			
		200 µε	*400 µε*	*600 µε*	*800 µε*
N10-3	50% RAP-HMA	-78.9	-87.5	-90.8	-92.6
N11-3	50% RAP-HMA	627	507	446	407
S10-3	WMA-Foam	-38.6	-25.3	-16.5	-9.48
S11-3	WMA-Additive	1359	1261	1207	1170
N5-4	Thiopave	77.5	25.5	2.54	-11.3
N7-3	Kraton	2617	1988	1689	1507
S12-3	TLA	250	213.3	194	180

Summary

Two testing methodologies (energy ratio and indirect tension creep compliance and strength) were used to assess the resistance to cracking of the 2009 test track surface mixtures. The energy ratio was used to assess each mixture's resistance to surface cracking, whereas the IDT testing was used to assess resistance to low-temperature cracking. The mixtures with the two lowest energy ratios had the poorest field performance in terms of cracking. The IDT critical temperature results were compared to the critical binder temperatures of each mixture. Using extracted binder test results proved to be more conservative when estimating the true low-temperature performance of the mixture. Binder tests taken from tank samples were typically lower in terms of critical low temperature than the mixture results.

Fatigue performance of the 2009 test track base mixtures was characterized using the bending beam fatigue test and S-VECD analysis procedure. Using the BBFT results, only the WMA additive mixture had a fatigue endurance limit less than that of the control mixture. The ranking of each mixture's cracking resistance was dependent on the magnitude of the applied strain.

S-VECD predictions showed the 50% RAP mixture compacted hot always failed in cracking well before the control mixture. However, the 50% RAP mixture compacted warm, the additive WMA mix, the Kraton polymer-modified mixture, and TLA mixture always performed better than the control mixture. The Thiopave mixture tested in this analysis performed better than the control mixture at lower strains but worse than the control mixture at higher strains. The ranking of the mixtures did not typically change at the different strain magnitudes.

4.6 Laboratory Assessment of Mixture Rutting Susceptibility

Rutting, also known as permanent deformation, in asphalt layers can occur by one of two mechanisms. First, rutting can be the result of a volumetric consolidation, or densification, of the pavement layer under trafficking. Second, rutting can also result from shear strain developing near the surface of the pavement. If the surface layers experience high shear strains, dilation occurs and the layer deforms. Structural rutting can occur when pressures on the base or subgrade exceed the capacity of the material to carry load *(69, 81).*

To characterize the rutting susceptibility of the surface mixtures produced for the 2009 NCAT Pavement Test Track, mixtures were sampled in the field for extensive laboratory testing. Additional base and binder layer mixtures were tested at the request of the sponsors.

Objective

The objective of this work was to evaluate the mixtures placed at the 2009 NCAT Pavement Test Track for susceptibility to rutting using popular laboratory tests and to determine how well those lab results correlate with actual rutting measured on the test track. Three tests were used to assess each mixture's resistance to permanent deformation: the Asphalt Pavement Analyzer (APA), Hamburg wheel-tracking test (HWTT), and flow number (Fn) test.

Methodology

The following subsections describe the methodologies used for characterizing the 2009 test track asphalt mixtures for resistance to rutting.

Asphalt Pavement Analyzer. The rutting susceptibility of 19 mixtures was evaluated using the APA. Often, only surface mixtures are evaluated using the APA. For this experiment, however, six mixtures from either a binder or base course were tested at the direction of the sponsor.

Testing was performed in accordance with AASHTO TP 63-09. The samples were prepared using a Superpave Gyratory Compactor to a height of 75 mm and an air void level of 7 ± 0.5 percent. Six replicates were tested for each mix. The samples were tested at 64°C (the 98% reliability temperature for the high PG grade for the Test Track). The samples were loaded by a steel wheel (loaded to 100 lbs) resting atop a pneumatic hose pressurized to 100 psi for 8,000 cycles. Manual depth readings were taken at two locations on each sample after 25 seating cycles and at the conclusion of testing to determine the sample rut depth.

The APA is typically used as a "go/no go" test to ensure that mixtures susceptible to rutting are not placed on heavily trafficked highways. Past research at the test track has shown that if a mixture has an average APA rut depth less than 5.5 mm, it should be able to withstand 10 million equivalent single axle loads (ESALs) of traffic at the test track without accumulating more than 9.5 mm of field rutting (*82*).

Hamburg Wheel-Tracking Test. The Hamburg wheel-tracking test was conducted to assess the rutting susceptibility of surface mixtures placed on the 2009 test track. Additional testing was conducted on intermediate or base mixtures as requested by sponsors. Testing was performed in accordance with AASHTO T 324. For each mix, a minimum of two replicates were tested. The

specimens were originally compacted to a diameter of 150 mm and a height of 115 mm. These specimens were then trimmed so that two specimens, with a height between 38 mm and 50 mm, were cut from the top and bottom of each gyratory-compacted specimen. The air voids of these cut specimens were 7 ± 2%, as specified in AASHTO T 324.

The samples were tested under a 158 ± 1 lbs wheel load for 10,000 cycles (20,000 passes) while submerged in a water bath that was maintained at a temperature of 50°C (Figure 4.18). While being tested, rut depths were measured by an LVDT, which recorded the relative vertical position of the load wheel after each load cycle. After testing, these data were used to determine the point at which stripping occurred in the mixture under loading and the relative rutting susceptibility of those mixtures. Figure 4.20 illustrates typical data output from the Hamburg device. These data show the progression of rut depth with number of cycles. From this curve two tangents are evident: the steady-state rutting portion of the curve and the portion of the curve after stripping. The intersection of these two curve tangents defines the stripping inflection point of the mixture. The slope of the steady-state portion of the curve is also quantified and multiplied by the number of cycles per hour (2520) to determine the rutting rate per hour.
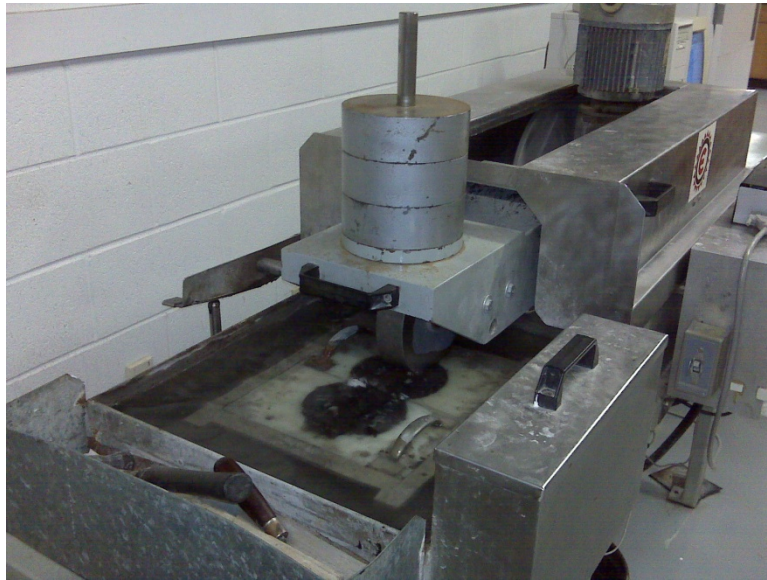
Figure 4.19 Hamburg Wheel-Tracking Device
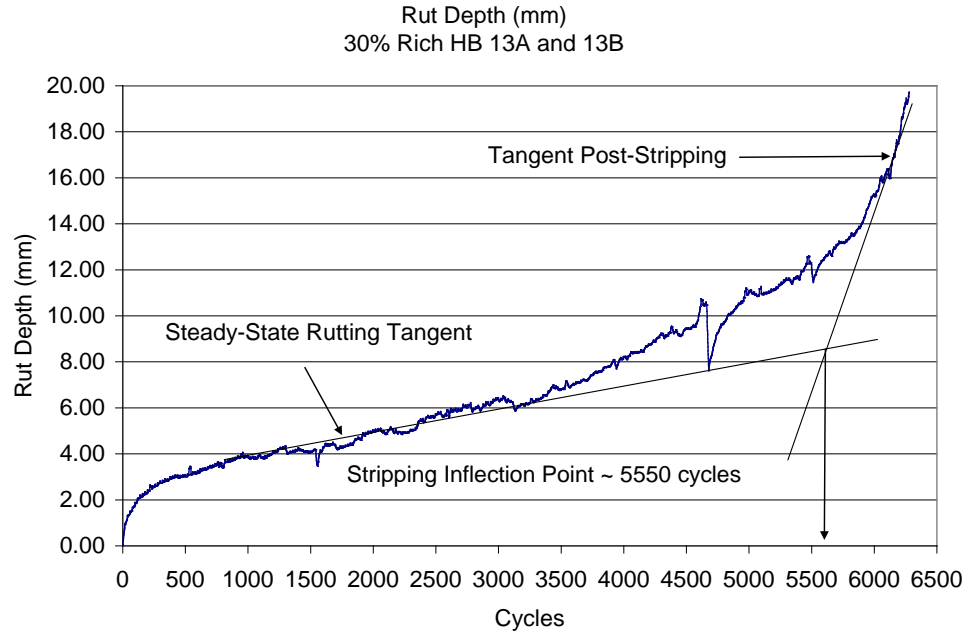
Figure 4.20 Example of Hamburg Raw Data Output

Flow Number. Flow number testing for the mixtures was performed using the AMPT. This testing was performed using the new specimens that had not been tested for E* for each of the surface courses as well as base and binder courses requested by section sponsors. Flow number tests were conducted at a temperature of 59.5°C, which is the LTPPBind 3.1 50% reliability temperature for the test track location at 20 mm from the surface of the pavement. The specimens were tested at a deviator stress of 87 psi without confinement. The tests were terminated when the samples reached 10% axial strain. For the determination of tertiary flow, the Francken model *(83)* was used (Equation 1). Non-linear regression analysis was used to fit the model to the test data.

$$\varepsilon_p(N) = aN^b + c(e^{dN} - 1) \tag{1}$$

Where:

    $\varepsilon_p(N)$ = permanent strain at 'N' cycles
    N = number of cycles
    a,b,c,d = regression coefficients

Recommended minimum Fn cycles have been specified for the previously described testing methodology for both HMA and WMA mixtures in National Cooperative Highway Research Program Projects 9-33 and 9-43, respectively. The minimum acceptable Fn values based on trafficking levels are shown in Table 4.12.

Table 4.12 Minimum Flow Number Requirements (*84, 85*)

Traffic Level, Million ESALs	Minimum Flow Number	
	HMA	*WMA*
< 3	--	--
3 to < 10	53	30
10 to < 30	190	105
≥ 30	740	415

Results

The test results for the APA, HWTT, and Fn testing methodologies are presented in the following sections. Additionally, an attempt was made to correlate each permanent deformation test to the actual measured field rut depths to determine which test best correlates to field rutting.

Asphalt Pavement Analyzer. Nineteen mixtures placed at the 2009 test track were tested for rutting susceptibility using the APA methodology previously described. The results are given in Table 4.13.

As stated earlier, past research at the test track has shown that mixtures with less than 5.5 mm of rutting in the APA should be able to withstand 5 million ESALs of trafficking while rutting less than 9.5 mm or 10 million ESALS with less than 12.8 mm of rutting at the track. Of the 19 mixtures tested in the APA, only one mixture (50% RAP with WMA) barely exceeded this criterion; however, it rutted only 3.7 mm in the field.

Table 4.13 APA Test Results

Mixture	Description	Manual Rut Depth, mm	COV, %
S9-1	Control - Surface	3.1	19.0
S9-3	Control – Base	4.2	32.0
N2-3	Florida - Binder	2.5	14.1
N5-4	40% Thiopave	4.1	33.5
N5-2	30% Thiopave	2.0	33.9
N7-1	Kraton - Surface	0.6	51.9
N7-3	Kraton – Base	0.9	23.0
N8-1	OK SMA	1.2	28.2
N10-1	50% RAP	4.6	19.1
N11-1	50% RAP- WMA	5.7	24.6
N12-1	GA SMA	1.4	35.3
S2-1	MS 45% RAP	1.0	52.2
S6-1	SBS Modified	1.4	24.4
S7-1	GTR Modified	1.4	17.5
S8-1	OGFC	1.2	41.2
S10-1	WMA – Foam	4.3	20.4
S11-1	WMA – Additive	3.7	19.6
S12-1	TLA – Surface	2.8	16.4
S12-3	TLA – Base	3.3	21.7

The reliability of any laboratory test must be determined by comparing results with actual field measurements. The test track is ideal for this type of assessment because the loading and environmental conditions are consistent among all test sections. In this case, the average APA rut depths for surface mixtures were compared to the average measured field rut depth using a wire line reference at the end of the cycle. This relationship is graphically portrayed in Figure 4.21.

As seen, there was a poor correlation between the APA rut depths and the rut depths measured in the field. However, results with the two high RAP mixtures (N10-1 and N11-1) appeared as outliers. Both of the 50% RAP surface mixtures exhibited more susceptibility to rutting in the laboratory than they did in the field. Therefore, the APA might not be the most appropriate permanent deformation test for high RAP mixtures.

When these two mixtures were removed from the data set (Figure 4.22), a linear relationship was formed between the rut depths seen in the laboratory test and those in the field. Using this linear relationship, and a maximum-allowable field rut depth of 12.5 mm, the corresponding maximum-allowable APA rut depth is 5.8 mm. The proximity of this criterion to the previously established criterion of 5.5 mm validates the original criterion for very heavy traffic conditions such as the test track.
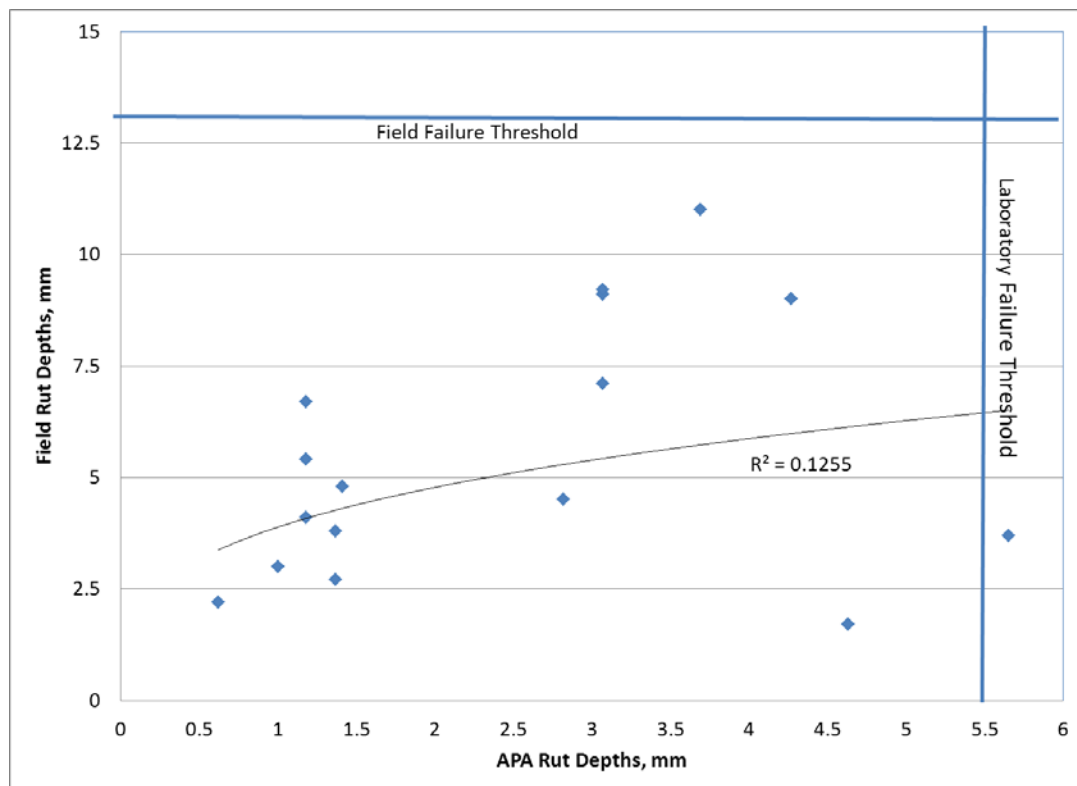
Figure 4.21 APA Laboratory and Field Comparisons
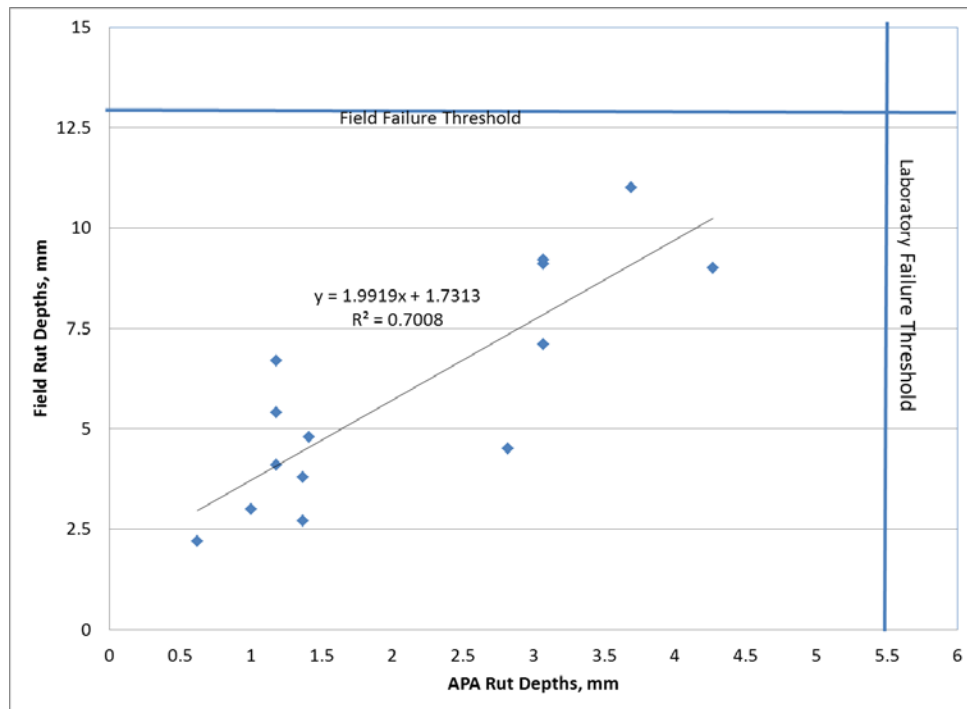
Figure 4.22 APA Laboratory and Field Comparisons with Outlier Removal

Hamburg Wheel-Tracking Test. The results of HWTT testing are shown in Table 4.14. There is no current consensus on a rut depth criterion for this test. Current recommendations for maximum-allowable rutting range from 4 mm to 10 mm depending on the governing body (*69*). Every mixture tested for the track cycle passed the 10 mm criterion for rut depth, while only three mixtures (S9-3, N5-4, and S11-1) failed to meet the more stringent 4 mm criteria. Two of the three mixtures in question were base mixtures and would typically not be assessed for rutting susceptibility. S11-1, a 9.5 mm NMAS mixtures using a WMA additive, was the only surface mixture that did not pass the 4 mm criterion.

To assess the current recommendations and see if refinements were needed, the field rut depths from wireline rut depth measurements were compared to HWTT rut depths. Failure in the field was set as 12.5 mm of rutting. Graphical comparisons between the HWTT rut depths, HWTT rutting rates, and the field wireline rut depths are shown in Figures 4.23 and 4.24.

Both the HWTT rut depths and rutting rates showed good correlations to the wireline rut depths, as seen by R-squared values of 0.75 and 0.74, respectively. Based on the relationships developed between the HWTT results and field rut depths, mixtures with HWTT rut depths less than 8.2 mm and rutting rates less than 2.18 mm/hr would prevent rutting greater than 12.5 mm on the test track. Since the test track represents a very heavy traffic condition, these results indicate that the 4 mm criterion is probably too conservative, while the 10 mm criterion might be more appropriate for lower traffic pavements.

Table 4.14 HWTT Results

Mixture	Description	Rut Depth, mm	Rate of Rutting, mm/hr
S9-1	Control - Surface	3.7	0.943
S9-3	Control – Base	5.4	1.362
N2-3	Florida – Binder	3.6	0.906
N5-4	40% Thiopave	5.5	1.396
N5-2	30% Thiopave	3.5	0.888
N7-1	Kraton - Surface	1.2	0.297
N7-3	Kraton – Base	1.7	0.424
N8-1	OK SMA	2.9	0.728
N10-1	50% RAP	1.3	0.321
N11-1	50% RAP- WMA	3.3	0.832
N12-1	GA SMA	2.2	0.566
S2-1	MS 45% RAP	1.2	0.311
S6-1	SBS Modified	4.1	1.034
S7-1	GTR Modified	1.9	0.483
S10-1	WMA – Foam	4.2	1.059
S11-1	WMA – Additive	8.6	2.155
S12-1	TLA – Surface	2.1	0.521
S12-3	TLA – Base	3.2	0.802
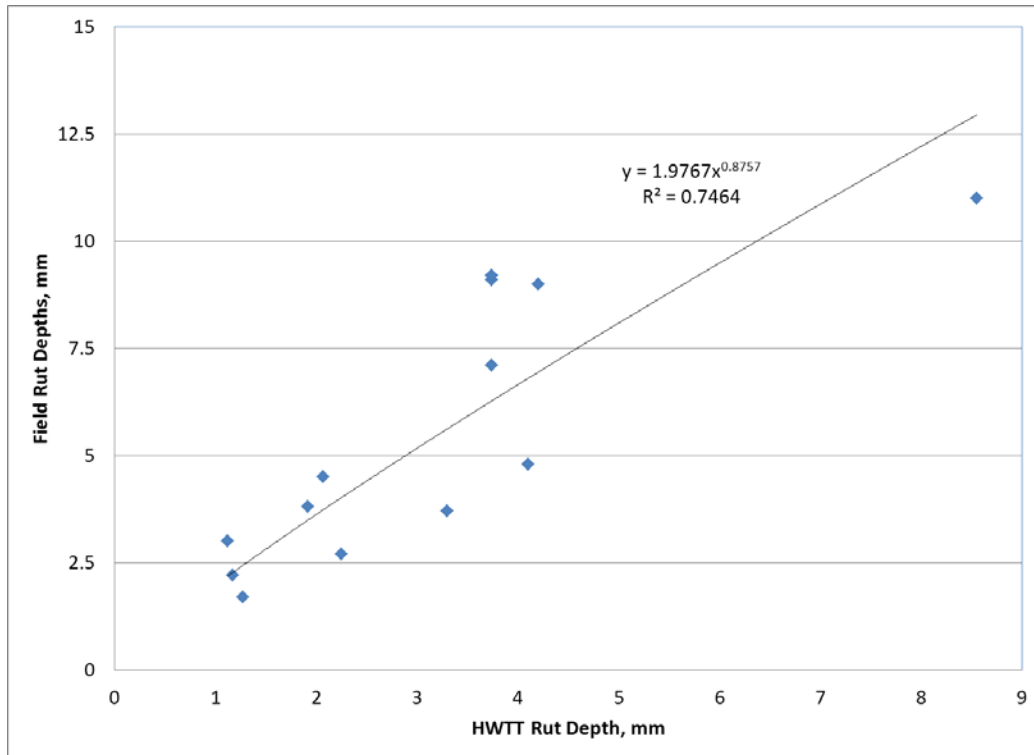
Figure 4.23 HWTT Rut Depths Versus Field Rut Depth
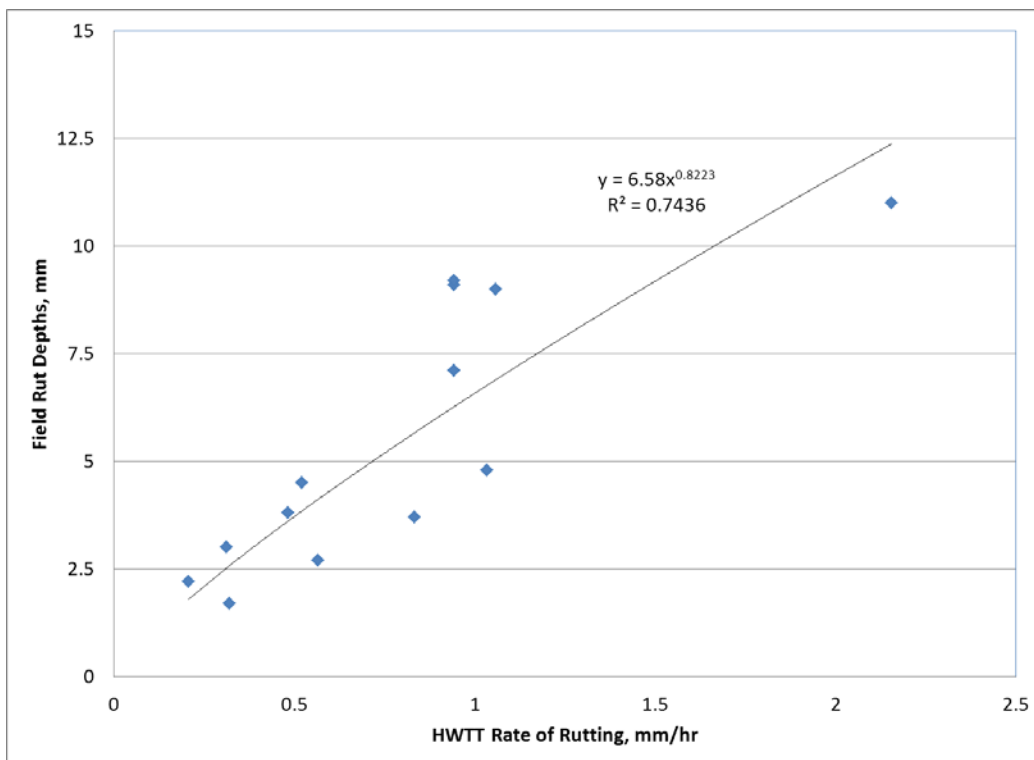
Figure 4.24 HWTT Rut Depths Versus Field Rut Depth

Flow Number. Flow number testing was conducted using the methodology previously described. The average Fn results are given in Table 4.15 with a complete set of test results in

Appendix B. In addition to the average flow number, the allowable traffic level based on the previously discussed minimum flow number criteria is provided. It should be noted again that HMA and WMA have different criteria for each trafficking level.

Table 4.15 Flow Number Test Results

Mixture	Description	Flow Number, Cycles	Allowable Traffic Level, Million ESALs
S9-1	Control - Surface	164	3 to < 10
S9-3	Control – Base	129	3 to < 10
N2-3	Florida – Binder	85	3 to < 10
N5-4	40% Thiopave	47	3 to < 10
N5-2	30% Thiopave	286	10 to < 30
N7-1	Kraton – Surface	9883	≥ 30
N7-3	Kraton – Base	944	≥ 30
N8-1	OK SMA	169	3 to < 10
N10-1	50% RAP	73	3 to < 10
N11-1	50% RAP- WMA	47	3 to < 10
N12-1	GA SMA	315	10 to < 30
S2-1	MS 45% RAP	9065	≥ 30
S6-1	SBS Modified	321	10 to < 30
S7-1	GTR Modified	659	10 to < 30
S10-1	WMA – Foam	51	3 to < 10
S11-1	WMA – Additive	36	3 to < 10
S12-1	TLA – Surface	123	3 to < 10
S12-3	TLA – Base	243	10 to < 30

The majority of the mixtures used in this test track cycle had flow number results that put them in the category as appropriate for 3 to 10 million ESALs of trafficking. However, after 10 million ESALs of trafficking, all of the mixtures had proven to be rut-resistant. Five mixtures had flow numbers that would allow between 10 and 30 million ESALs of trafficking, while only 3 mixtures had flow numbers high enough to handle 30 million ESALs of traffic.

To compare the test results to field measurements, the average flow numbers for both HMA and WMA were graphically compared to the wireline rut depths for each field section. As can be seen, poor correlations exist between the flow number and measured rut depth for both HMA and WMA mixtures. Only three WMA mixtures were available for correlation; therefore, there was not enough data to develop a true correlation.

As with the APA correlations, the two high RAP mixtures in the Group Experiment seemed to be outliers. When these two outliers were removed from the dataset, a slightly stronger non-linear correlation was found between flow number and field rutting. Using this relationship, a minimum flow number of 6 would prevent rutting of less than 12.5 mm in the field for up to 10 million ESALs of trafficking. This value is significantly less than the current flow number recommendations for HMA mixtures. Further research is needed to establish a better relationship between flow number and field rutting.
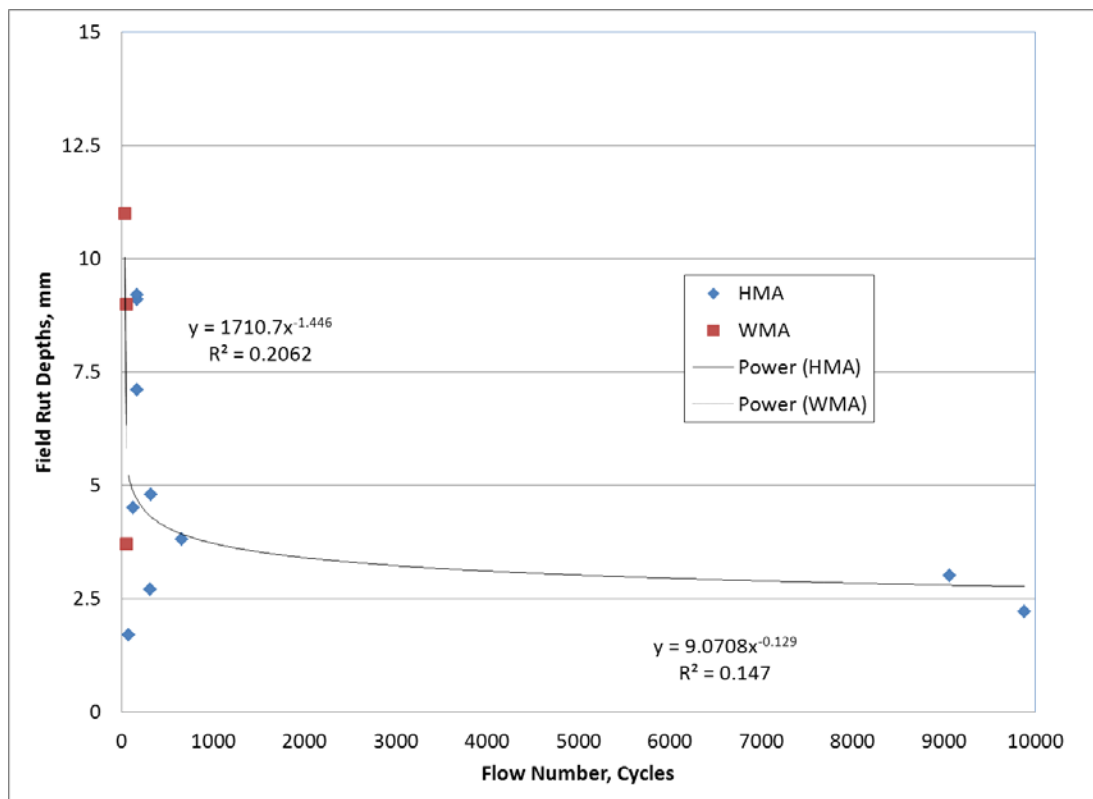
Figure 4.25 Flow Number Versus Field Rut Depths
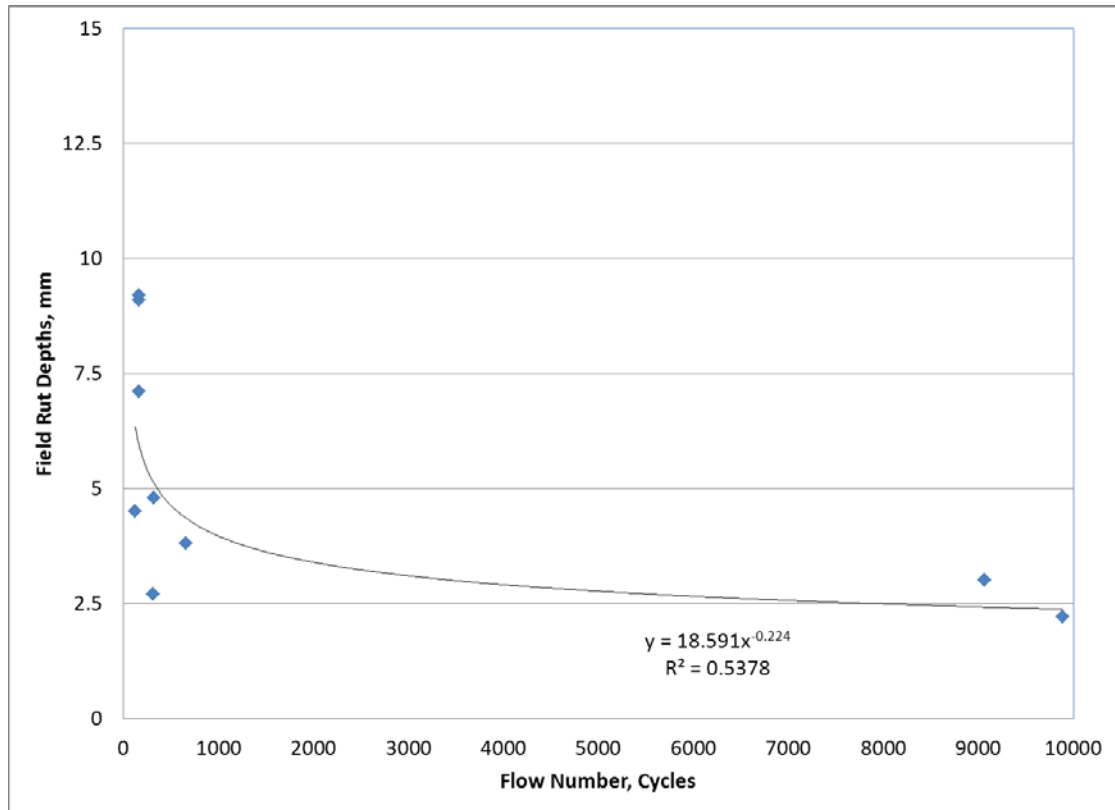
Figure 4.26 Flow Number Versus Field Rut Depths for HMA Mixtures without High RAP Group Experiment Mixtures

Summary

Three tests were used to assess the rutting susceptibility of the mixtures placed at the 2009 NCAT Pavement Test Track: Asphalt Pavement Analyzer, Hamburg wheel-tracking test, and flow number. Additionally, these test results were also correlated to field rut depths to determine which test had the best relationship with field rut depths and refine rutting criteria for these tests. When outliers were removed from the datasets, both the APA and HWTT had strong correlations between the lab and the field. To prevent 12.5 mm of rutting in the field at 10 million ESALS, maximum-allowable rut depths of 5.8 and 8.2 mm should be used as criterion for the APA and HWTT, respectively.

The relationship developed between the laboratory flow number results and the field rut depths was not as strong. This could partially be due to two mixtures that had low flow numbers but were resistant to rutting the field. Additionally, two mixtures had flow numbers greater than 9000 that could have skewed the relationship. Using the testing methodology presented earlier, the relationship between field and lab results suggests that mixtures only need a flow number of 6 to prevent 12.5 mm of rutting in the field at 10 million ESALs.

CHAPTER 5   BENEFIT/COST OF TEST TRACK STUDIES

The NCAT Pavement Test Track offers an opportunity for sponsors to quickly and safely answer major questions about pavement performance that would take many years to answer without using accelerated loading. Full-scale test tracks are the best and quickest way to obtain real-world answers concerning performance under actual traffic conditions. Other methods of accelerated loading, where the loads applied are not representative of actual trucks, require that data be extrapolated to estimate the expected performance under actual traffic. This extrapolation is difficult to do in a way that will provide reliable answers.

One question that often arises with regard to research investments is "what is the benefit of the research compared to the cost of the research?" While it is challenging to quantify the monetary benefits of some research, this section examines the impact of many of the studies conducted at the test track and, where possible, estimates the payoffs associated with implementation of the research findings.

Four test track cycles have now been completed at a total cost of approximately $36 million, or about $3.0 million per year. These studies and the implementation of findings by state transportation agencies have resulted in a significant amount of savings by the sponsors.

There have been a number of findings during the track's 12 years of operation that clearly have had tangible as well as non-tangible benefits to the sponsors. Many of these findings have been implemented by the sponsoring department of transportation (DOT), DOTs involved in the track pooled-fund projects, and DOTs that have not participated in the test track studies but have used the results of the track to implement cost saving benefits. Some of the most important benefits and a summary of the benefit/cost of the track operations are discussed below.

Benefits of Using Fine-Graded Mixes Compared to Coarse-Graded Mixes

When SHRP research was completed and the implementation of Superpave began, there were several changes to the practices of designing HMA. One of the items that were recommended in Superpave guidance and by those helping to implement Superpave was aggregate gradation requirements that included a restricted zone. Gradations that plotted below the restricted zone were referred to as coarse-graded mixtures, and gradations that plotted above the restricted zone were referred to as fine-graded mixtures.

Most initial guidance concerning Superpave also recommended the use of coarse-graded mixtures because they were believed to provide better resistance to rutting. Rutting was a serious problem for the asphalt paving industry in the 1970s and 1980s prior to SHRP, and many experts believed that using fine-graded mixtures were a big part of the problem. However, with the implementation of the coarse-graded Superpave mixes in the mid 1990's, DOTs quickly learned that coarse-graded mixtures often resulted in pavements that were permeable to water. Yet they were afraid to return to the use of fine-graded mixtures because of the rutting history.

The test track provided state DOTs with an opportunity to quickly compare the performance of these coarse- and fine-graded mixtures. The test track results indicated that fine-graded mixtures, designed using Superpave, performed just as well as coarse-graded mixtures in preventing rutting. While durability was not specifically evaluated at the track, most sponsors believed that the fine-graded mixtures with better in-place densities would be more durable than the coarse-graded mixes.

As a result of good performance of fine-graded mixes at the test track, many states began to modify their specifications to allow more fine-graded mixtures to be used. North Carolina DOT revised its specifications to allow fine graded mixtures, modified $N_{initial}$ criteria, deleted the N_{max} criteria, and adopted the Asphalt Pavement Analyzer to serve as an end-result performance test to help evaluate the quality of the mixture. NCDOT gives the contractor the option of using fine-graded or coarse-graded mixes except for the surface course, which is required to be a fine-graded mixture. This typically results in the contractor selecting the gradation type that provides the lowest mixture cost. While they have not been able to determine savings associated with these changes, allowing the contractor to select between fine-graded and coarse-graded mixtures certainly results in lower cost.

The state of Florida estimates having increased the use of fine-graded mixes by 1.6 million tons per year as a result of the test track findings. They estimate that the cost of coarse-graded aggregate is $2-5 more per ton than for fine-graded aggregates. This has resulted in an annual savings of $3.2 million per year based on a $2 savings in aggregate per ton. This does not include the possible improvements in constructability and durability for fine-graded mixtures. Several other state DOTs have increased their amounts of fine-graded mixtures as a result of the test track study. This results in an annual savings of $3.2 million per year in the state of Florida alone.

Benefits of Using Polymers

State DOTs began using polymers to modify asphalt cements long before Superpave, but there was very little guidance about which modifiers to use, how much to use, and how to grade the asphalt binder. The performance-grading (PG) system that was developed in the SHRP program provided a better method for ensuring that the modified asphalt binder has the desired properties. AASHTO Superpave standards provided some guidance concerning when modified asphalts should be used. However, there was limited field performance data to verify if this guidance was satisfactory. The test track provided an excellent opportunity to evaluate the guidelines.

Several side-by-side comparisons of mixes with modified and unmodified asphalts have been conducted at the test track. Most comparisons were made between mixes containing a PG 64-xx or 67-xx to a polymer modified PG-76-xx. Results from the test track have shown a significant decrease in rutting when using asphalt mixtures containing modified asphalt binder in comparison to asphalt mixtures containing unmodified asphalt binder.

Several states revised their specifications based on these findings. Florida DOT changed its policies to require a PG grade for pavements designed for high-traffic roadways and projects with a history of rutting problems. That policy change has resulted in polymer-modified asphalt binders being used in about 1/3 of the mixes placed. Although this results in a cost increase, Florida DOT estimates that polymer-modified binders typically increase the life of a pavement for these higher-volume roads by more than 2 years. Based on these estimates, the cost savings to Florida DOT for using modified asphalt binders is approximately $27 million per year.

The improvement in performance with mixes containing polymers observed at the test track was sufficient evidence for Georgia DOT to specify Superpave mixes with modified asphalt binder instead of the more expensive stone-matrix asphalt (SMA) mixtures on lower-volume interstate highways, resulting in significant savings to Georgia DOT. However, these savings have not been quantified.

Missouri DOT compared the use of ground tire rubber (GTR) against the more common styrene-butadiene-styrene (SBS) polymer modifier. This comparison was needed because, in the past, contractors in the state were sometimes unable to obtain SBS when it was in short supply. Allowing the

use of GTR as an optional modifier had the potential to provide an asphalt binder with performance characteristics similar to those of the SBS modified binder. So, in 2008, Missouri began allowing the use of ground tire rubber in place of SBS. Sections constructed at the test track confirmed that mixes containing GTR-modified asphalt binder performed as good as mixtures containing SBS modifier. This allowed Missouri DOT to use approximately 1,500 tons of ground tire rubber modifier, which alone is a major environmental benefit in eliminating a large number of old tires. Since a typical car tire weighs about 20 pounds, this resulted in approximately 35,000 tires per year being used to improve asphalt mixtures. Missouri specifications require that all blends of GTR-modified asphalt binder contain 4.5% transpolyoctenamer (TOR) by weight of the rubber.

Oklahoma found that high-polymer mixtures appear to provide quick and effective repair options for rutting versus a full-depth replacement. These high polymer mixes may also show that more structural strength is obtained.

Comparison of Nominal Maximum Aggregate Size Mixtures

As a result of research at the track, South Carolina now allows the use of 9.5 mm nominal maximum aggregate size (NMAS) mixtures on high-volume roads. They also allow the use of 4.75 mm NMAS mixtures as leveling course on high-volume roads and as a thin surfacing to compete with microsurfacing and chip seals on low-volume roads. These smaller NMAS mixes allow thinner sections to be used and can thus significantly reduce the cost of construction. North Carolina is also beginning to use more 9.5 mm mixtures based on performance of these mixtures on the test track.

Reducing the NMAS by one size will result in a reduction in the minimum layer thickness of approximately 25%. This allows the state DOT to potentially reduce the layer thickness of HMA for overlays and save approximately 10-25% on the cost of the overlay. Since it is not clear how much work has actually been performed at these decreased thicknesses, cost savings cannot be estimated.

Effect of LA Abrasion on Performance of Asphalt Mixtures

LA abrasion requirements for aggregates used in asphalt mixtures have evolved over the years to the values currently recommended. There has been little data to support these requirements. While making a small change in the LA abrasion requirements may not seem significant, it can have a significant effect on the aggregate costs, depending on the locations of the quarries.

South Carolina investigated the performance of a higher LA abrasion aggregate at the test track to see how it affected performance. Prior to this work, the LA abrasion requirements had been established for dense-graded mixtures and open-graded friction courses (OGFC). As a result of test track findings, South Carolina was able to relax the LA abrasion requirements for dense mixes and for OGFC. For friction courses, the Micro-Deval test was adopted in place of the LA abrasion. Relaxing the LA abrasion requirements resulted in more breakdown of aggregate during construction, but this could be managed as part of the quality control process. The results indicated that there was no loss in performance for the mixtures containing the higher LA abrasion requirements. As a result of raising the maximum LA abrasion requirements, aggregate prices were reduced significantly at some locations. This has resulted in significant savings to the state DOT, but the savings have not been quantified.

Evaluation of Friction Characteristics of Local Aggregates

South Carolina had an aggregate source that had not previously been used in wearing course layers and needed to be evaluated prior to acceptance for use. The aggregate was used in a surface mix placed on

the test track. In less than 2 years of trafficking, the aggregate polished and made the test section unsafe, which provided clear evidence that the aggregate was unacceptable for use in surface layers.   If these tests had been conducted on a South Carolina highway, it would have created a safety problem and public relations issue. While a monetary value cannot be placed on the benefit of this work, it is clear that the track allowed the DOT to evaluate this aggregate without having any adverse effect on the driving public of South Carolina.

Evaluation of WMA Technologies

Based on the good performance of Evotherm and the foaming technology at the test track, South Carolina has approved these materials to be used on DOT projects. As a result of performance of warm-mix asphalt (WMA) at the track, Tennessee has adopted a permissive specification for WMA. The Alabama DOT has adopted WMA technologies that have proven successful at the test track. All these states could have evaluated the WMA technologies on their roadways, but it is cheaper and safer to have these products evaluated on the test track. States also indicated that using WMA technologies have increased the amount of reclaimed asphalt pavement (RAP) that can be used, resulting in significant savings to the DOTs.

Performance of High RAP Mixtures at the Test Track

With shrinking budgets and higher raw materials prices, DOTs are looking for ways to decrease the cost of pavement maintenance and construction. One method that has been identified for significantly lowering the cost of asphalt mixtures is increasing the amount of RAP. However, performance data is needed to support this change. The national goal established by FHWA and NAPA is to increase RAP used in asphalt mixtures to an average of 25%.

The test track has been a proving ground for evaluation of RAP in asphalt mixtures. In the first cycle (2000) of the test track, no sponsor elected to use RAP in any of the test sections. However, beginning in the second cycle (2003), highway agencies started using moderate RAP contents in their test sections and had excellent performance. In 2006, the experiment with 45% RAP contents proved that very high RAP contents would hold up to heavy traffic. Continued evaluation of those sections through a second cycle showed that a softer virgin binder and the standard binder grade helped the 45% RAP mixes to resist cracking whereas using polymer-modified binders with high RAP contents tended to increase cracking. The 2009 Group Experiment further evaluated how high RAP content mixes affected the structural response of the pavement. This experiment showed that higher-stiffness 50% RAP mixes can provide a structural benefit to pavements and that the combination of WMA technologies and high RAP contents was very beneficial for cracking resistance based on laboratory tests.

As a result of the good performance of these high RAP content mixtures at the track, South Carolina has increased the allowable RAP in asphalt mixtures. Mississippi DOT designed and used a mixture containing 45% RAP with gravel aggregate from Mississippi. The mixture used a PG 67-22 and was designed to 3% air voids to help resist cracking. Results indicate that the mixture is performing similar to a virgin mixture, using a PG 76-22 asphalt binder. Based on this performance, Mississippi plans to use some high RAP mixtures on selected projects. There are significant savings from the amount of RAP used and in the utilization of a PG 67-22 instead of a PG 76-22 binder.

North Carolina and Alabama have also increased the amount of allowable RAP in asphalt mixtures as a result of the performance of the high RAP test track sections. Alabama now allows 35% RAP in asphalt mixtures, and they are building a test section using 40% RAP. This is being done while using the normal PG grade. Some state DOTs are allowing higher RAP contents when warm-mix asphalt is used.

It is estimated that as a result of the test track, the amount of RAP in asphalt mixtures will increase an average of 3% (a very conservative number) within the sponsoring DOTs. It is estimated that the amount of asphalt produced by the eight state sponsors of the track is 40 million tons. A 3% increase in RAP content is likely to save approximately $1 per ton or $40 million per year. It is also estimated that 4 million of these tons with high RAP would be used in a location that would normally require modified asphalt, but due to the high RAP modification would not be needed. This will result in a savings of approximately $6.00 per ton, or $24 million, for the sponsoring states. Hence, increasing RAP and reducing the amount of modified asphalt where high RAP is used can result in a total savings of $64 million per year.

Effect of Design Asphalt Content on Performance of Asphalt Mixtures

The initial gyration table provided in the Superpave mix design standards was based on very limited data. As DOTs were adopting Superpave, many learned that the design asphalt content of most Superpave-designed mixtures had decreased from pre-Superpave mixtures. Field performance of many early Superpave projects across the country led to the belief that Superpave mixes were rut resistant but lacked long-term durability. Many state DOTs wanted to study the effect of asphalt content on performance and how to best determine the optimum asphalt content. A few highway agencies reduced the number of gyrations for all traffic categories as a way to increase the optimum asphalt content. South Carolina did not adjust the number of gyrations based on performance of mixes at the track but instead adjusted the design air void level based on amount of traffic.

Early test sections at the track, designed using the recommended Superpave gyrations, failed early due to cracking. As a result, Tennessee adjusted their laboratory compactive effort to allow higher asphalt content. Tennessee has estimated that the increased life due to the increased asphalt content results in a savings of approximately 20% of the construction budget, or $22 million per year. While the DOT would have eventually determined that an increase in asphalt content would have been necessary based on performance of highways, this would likely have taken at least 5 to 10 years, resulting in significant additional expenditures during this time. This test track study did not require any learning curve on the DOT pavements.

Performance of gravel mixes from Mississippi also showed some early cracking, and the DOT adjusted the number of gyrations to provide for higher asphalt content. The gravel mixes performed satisfactorily for rutting. This adjustment of gyration level has improved the cracking resistance of asphalt mixtures in Mississippi and continues to produce rut-resistant mixtures.

DOTs believe that reducing the number of gyrations has improved the life of their mixtures. While most DOTs have not been able to put a cost savings on this conclusion, Tennessee has estimated a yearly savings of $22 million.

Increased use of SMA and Open-Graded Friction Courses

As a result of track studies, more states are using SMA and OGFC mixtures. Tennessee has begun to use more OGFC primarily on interstate highways. They know that these mixes can significantly reduce wet-weather accidents. Mississippi DOT built sections with SMA and OGFC at the track with its local aggregate materials. Performance was good, and in 2007, the DOT constructed a test section on an interstate highway. The design included an SMA layer covered with an open-graded friction course. The performance has been good, and the DOT has implemented a policy to use SMA and OGFC on high-volume interstate highways. They anticipate the OGFC surface will last about 8-10 years before needing

to be replaced. At that time, they plan to micro-mill the OGFC from the roadway and leave the underlying SMA in place. They will then apply another OGFC.

Georgia DOT evaluated the performance of SMA mixtures at the test track, confirming its practice of using SMA on interstates and high-volume roadways. Georgia DOT also evaluated the flat and elongated count in aggregates used in SMA mixtures. As a result of these tests, Georgia DOT is considering adoption of new flat and elongated aggregate requirements for SMA that will be more like the Superpave requirements. The sections using the new aggregate requirements have shown good performance at the test track, and implementing the new requirements would result in a savings of $6.3 million per year in aggregate costs. The performance appears to be the same with these more Superpave-like aggregate requirements than with the existing cubical SMA aggregate requirements.

North Carolina DOT continues to use open-graded friction courses as a result of the benefits demonstrated on the test track. Missouri has modified their aggregate requirements based on performance of SMA mixtures at the track. This change in aggregate requirements has been shown to reduce the cost per ton of mix by $6 to $7 in Missouri. This has resulted in a savings of approximately $2.3 million—about $500,000 per year.

Although some states have been able to estimate the financial pay-offs for track research on SMA and OGFC, some of the benefits are not easily quantified. SMA and OGFC are higher-cost mixes than conventional Superpave mixtures. SMA is believed to extend the life of the pavement surface, resulting in a lower life-cycle cost. However, no data has been gathered to date to quantify the improved life of SMA compared to Superpave. Most agencies use OGFC for its enhancements to safety. Few studies have documented the reduction in wet-weather accidents when OGFC was used. More traffic safety studies are needed, and the costs of accidents will have to be considered to better justify the economic benefit of OGFC to highway users.

Pavement Design

As a result of data from the test track, Alabama DOT has increased the structural coefficient of HMA from 0.44 to 0.54. This adjustment has resulted in an 18.5% thickness reduction for new construction and overlays for asphalt pavements in Alabama. Alabama DOT estimates that this conservatively saves the agency $40 million per year.

One of the topics that Oklahoma DOT has investigated is perpetual pavements. Sections at the 2006 track proved that perpetual pavements can be built and ultimately result in significant savings in time and money when compared to traditional 20-year designs. The findings from the 2006 track were further validated in the 2009 track with additional validation expected in the 2012 track. While this clearly results in savings, no estimate of the savings is available.

Conclusion

There are significant financial payoffs for sponsors of the NCAT Pavement Test Track. The yearly savings based on input from state DOTs easily exceeds $160 million per year for all sponsors compared to a track operational cost of approximately $3.0 million per year. This is a benefits/cost factor of over 50 to 1. There are also other benefits, including improved safety for the driving public. Most of the tangible benefits occur due to increased use of RAP, adjustment of layer structural coefficients, improved selection of optimum asphalt content, and improved guidance for use of modified asphalts.

CHAPTER 6   SUMMARY OF TEST TRACK FINDINGS

This report has described the studies and reported the findings for the 2009 NCAT Pavement Test Track. Seventeen of the track's 46 200-ft. test sections were either reconstructed or rehabilitated for the 2009 cycle, while the remaining 29 were left in place for additional traffic loading. Highway agency and industry sponsors had individual objectives for their own sections as well as shared objectives for the track as a whole.

Several test track findings, including those that have been further validated from previous cycles, can be used by DOT sponsors to improve their materials specifications and pavement design polices. The majority of the research findings from this cycle can be categorized into one of the following areas: (1) mix design, (2) alternative binders and binder modifiers, (3) structural design, (4) prediction testing, or (5) tire-pavement interaction. The following is a summary of the most significant findings from the 2009 NCAT Pavement Test Track.

Mix Design

High Reclaimed Asphalt (RAP) Mixes. High RAP content mixes have shown excellent rutting performance and durability on the test track. Two full-depth sections containing 50% RAP that were constructed in 2009 have performed as well as the control section after 10 million ESALs, exhibiting minimal rutting and no visible cracking. One of the 50% RAP sections used a warm-mix asphalt (WMA) technology to lower the production temperature. Although no difference was evident between the field performance of the hot 50% RAP test section and the WMA-50% RAP test section, lab tests indicate that using WMA improved the fatigue resistance by fivefold. The high RAP mixes increased the stiffness of the pavement structure, which reduced critical tensile strains by up to 31% and base pressures by up to 55%.

Additionally, four sections with surface layers containing 45% RAP and different virgin binder grades (PG 52-28, PG 67-22 and PG 76-22) were left in place from the 2006 test track cycle, accumulating a total of 20 million ESALs. Mixes with the stiffer binder grades exhibited minor cracking earlier than those with softer binders, indicating that using a softer virgin binder grade improves the durability of high RAP mixes. However, all four sections had excellent rutting performance, with rut depths less than 5 mm.

The Mississippi DOT also sponsored a section containing a 45% RAP surface layer in the 2009 test track cycle. While the mix contains a PG 67-22 binder, results indicate that performance is similar to a virgin mix with polymer-modified PG 76-22. This finding could result in significant cost savings for the Mississippi DOT and other agencies who choose to implement high-RAP content mixtures with unmodified binders.

Warm-Mix Asphalt (WMA). In addition to the WMA section containing 50**%** RAP, two test sections built with different WMA technologies were constructed for the 2009 test track cycle. One of them was built using the water-injection foaming method and the other, a chemical additive. Rutting was minimal in both of these sections, but slightly increased from the control section. Neither WMA section exhibited cracking, and laboratory testing indicated greater fatigue life expectations for the WMA sections compared to the control. Structural analyses proved that the WMA sections have equivalent back-calculated moduli and the same response to loads and temperature as typical HMA.

Stone-Matrix Asphalt (SMA). A study sponsored by the Georgia Department of Transportation for the 2009 test track indicated that specifications for SMA aggregate properties based on early guidelines are unnecessarily restrictive, eliminating materials that may have good performance under heavy loading conditions. Aggregate with up to 29% flat and elongated particles, as measured by the GDOT procedure GDT 129 at the 3:1 ratio, performed well on the test track. The SMA containing the higher flat and elongated aggregate had excellent resistance to rutting, raveling, and cracking.

Numerous agency-sponsored SMA test sections through the first four cycles of the test track have not only demonstrated excellent performance for this premium, heavy-traffic mix, many of the experiments have provided clear evidence that many different aggregate sources can be used, which has helped reduce mix costs.

Alterative Binders and Binder Modifiers

A number of alterative binders and modifiers were evaluated on the 2009 test track to help reduce the quantity of virgin asphalt binder needed for construction. Two alternative binders—Shell Thiopave, a warm-mix sulfur technology, and Trinidad Lake Asphalt, a natural asphalt from Trinidad and Tobago— both successfully replaced refined liquid asphalt in three sections.

Kraton Polymers sponsored a section on the 2009 track that utilized highly polymer-modified (HPM) mixes that were very stiff yet strain-tolerant. The pavement was designed with an 18% thinner cross-section and exhibited excellent fatigue and rutting resistance.

Other sections on the 2009 track compared binder modification with ground-tire rubber (GTR) and styrene-butadiene-styrene (SBS) polymer using laboratory testing and field measurements. GTR, a more sustainable option, performed comparably to SBS mixes in every aspect.

Structural Design

Perpetual Pavements. Test track research has shown that pavements can withstand higher levels of strain than suggested by lab tests without accumulating fatigue damage, allowing perpetual pavements to be designed with thinner cross sections. Two test sections placed in 2003 that were expected to reach the end of their life at 10 million ESALs have survived 30 million ESALs with minimal rutting and no fatigue cracking. Several sponsors have used pavement designs based on the *PerRoad* software to establish pavement thicknesses using a variety of pavement materials. All of those sections have performed as expected with no damage through multiple cycles.

Asphalt Layer Coefficient. Recent test track research showed that the 0.44 asphalt concrete structural coefficient should be increased to 0.54, resulting in an 18.5% reduction in pavement thickness. This conclusion was reached after evaluating the structural performance of test sections representing a broad range of asphalt thicknesses, mix types, bases and subgrades. States that are not yet ready to implement the Darwin-ME Pavement Design Guide can save millions in construction costs by implementing the revised coefficient.

Open-Graded Friction Course. Many highway agencies are aware of the benefits of open-graded friction course mixes (OGFC), such as reduced water spray, improved skid resistance, and less tire-pavement noise, but the structural contribution of OGFC was previously unknown. During the 2009 test track cycle, structural characterization of a section containing OGFC, or porous friction course, indicated

that the OGFC does contribute to the structural integrity of the section. States that previously have not attributed any structural value to OGFC can now use a provisional OGFC structural coefficient of 0.15.

Test track research also showed that an open-graded friction course can improve a pavement structure's resistance to top-down cracking. Further improved pavement performance can be achieved by paving the OGFC with a heavy tack coat using a spray paver, as compared to conventional tack methods.

Speed and Temperature Effects on Pavement Response. It is well known that both temperature and vehicle speed have a significant effect on flexible pavement response to loading. However, theoretical pavement models, which are used to determine pavement response and ultimately predict pavement life, often fail to accurately characterize speed and temperature effects, resulting in erroneous predictions. Modeling with non-conventional materials, such as sulfur-modified mixes, polymer-modified mixes, and WMA technologies can add uncertainty.

Test track results showed that non-conventional materials behave similar to conventional materials, so existing load-response models do not have to be adjusted for special mixes. However, the effects of speed and temperature must be taken into account. It should be noted that the specific pavement response models developed based on test track conditions are unique to the climate, pavement cross-section, and loading conditions used at the track. However, the form of the models could be applied to other conditions.

MEPDG Predictions vs. Actual Performance. Evaluation of structural sections from the 2003 and 2006 test cycles using the mechanistic-empirical pavement design guide (MEPDG) showed mixed results. Rutting was over-predicted primarily due to errors in expected deformations in the base and subgrade pavement layers. New calibration coefficients ($\beta s1$, $\beta s2 = 0.05$) appear to improve the predictive capability and, when excluding some outliers, resulted in reasonably accurate rutting predictions. Predictions of fatigue cracking were less successful; no better coefficients than the national coefficients were found, resulting in poor agreement between measured and predicted cracking. Better calibration results may be achieved by grouping together sections with similar characteristics.

Prediction Testing

The Energy Ratio concept, developed in Florida, was validated at the test track, enabling mix designers to successfully screen mixtures for top-down cracking potential.

Test track results have been correlated with the Asphalt Pavement Analyzer, Hamburg wheel-tracker, and Flow Number tests to provide confidence in all three methods as rutting predictors and for establishing mix design criteria.

Tire-Pavement Interaction

Noise levels generated from tire-pavement interaction are influenced by macrotexture, in-place air void content and, at low frequencies, by nominal maximum aggregate size. The ongoing noise analysis conducted during the 2009 test track cycle indicated that coarser surface mixtures, including OGFC, SMA, and coarse-graded Superpave, are noisier pavements at low frequencies. However, OGFC mixes were found to be the quietest pavement at higher frequencies.

The sound-intensity level (SIL) of noise correlated well with the sound-pressure level (SPL) at all third-octave bands from 315 Hz to 4,000 Hz. Additionally, pavement surface texture, or mean profile depth (MPD), significantly affected SIL, with a higher MPD having a positive effect on SIL below 1,600 Hz and a negative effect on SIL above 1,600 Hz.

REFERENCES

1. Timm, D. H. Design Construction, and Instrumentation of the 2006 Test Track Structural Study. NCAT Report 09-01, National Center for Asphalt Technology, Auburn University, 2009.
2. Brown, E.R., J. Bukowski, et al. National Asphalt Pavement Association, Guidelines for Materials, Production, and Placement of Stone Matrix Asphalt (SMA). Information Series 118, Lanham, MD, 1994.
3. Ruth, B.E., R.C. West, S.C. Wang, and I. Morino. Minimum Aggregate Quality Levels for Stone Mastic Asphalt Mixtures. University of Florida, HPR Study No. 0648, Gainesville, FL, 1995.
4. Buchanan, M.S. Evaluation of the Effect of Flat and Elongated Particles on the Performance of Hot Mix Asphalt Mixtures. NCAT Report No. 2000-03, National Center for Asphalt Technology, Auburn University, 2000.
5. Barksdale, R. D., J. Hand, S. Miller, and S. Thompson. Optimum Design of Stone Matrix Asphalt Mixes. GDOT Report No. 9217, 1995.
6. Kaloush, K. E., M. W. Witczak, G. B. Way, A. Zborowski, M. Abojaradeh, and A. Sotil. Performance Evaluation Of Arizona Asphalt Rubber Mixtures Using Advanced Dynamic Material Characterization Tests. Final Report. Arizona State University, Tempe, AZ, July 2002.
7. Huang, B., L. N. Mohamed, P.S. Graves, and C. Abadie. Louisiana Experience With Crumb Rubber-Modified Hot-Mix Asphalt Pavement. *Transportation Research Record*, No. 1789, 2002, pp. 1-13.
8. Way, George B. Flagstaff I-40 Asphalt Rubber Overlay Project – Ten Years of Success, *Transportation Research Record*, No. 1723, 2000, pp. 45-52.
9. Brown, E.R., L.A. Cooley, D. Hanson, C. Lynn, B. Powell, B. Prowell, and D. Watson. NCAT Test Track Design, Construction, and Performance, NCAT Report 02-12. National Center for Asphalt Technology, Auburn University, 2002.
10. Willis, J.R., R. Powell, and M.C. Rodezno. Evaluation of a Rubber Modified Asphalt Mixture at the 2009 NCAT Test Track. 4th International Conference on Accelerated Pavement Testing, 2012 (submitted).
11. Roque, R., B. Birgisson, C. Drakos, and B. Dietrich. Development and Field Evaluation of Energy-Based Criteria for Top-down Cracking Performance of Hot Mix Asphalt. *Journal of the Association of Asphalt Paving Technologists*, Vol. 73, 2004, pp. 229-260.
12. Timm, D.H., D. Gierhart and J.R. Willis. Strain Regimes Measured in Two Full Scale Perpetual Pavements. *Proceedings, International Conference on Perpetual Pavements*, Columbus, Ohio, 2009.
13. Taylor, A.J. and D.H. Timm. Mechanistic Characterization of Resilient Moduli for Unbound Pavement Layer Materials. NCAT Report No. 09-06, National Center for Asphalt Technology, Auburn University, 2009.
14. Hansen, K.R. RAP, RAS, & WMA Survey, National Asphalt Pavement Association Annual Meeting, February 2011.
15. Willis, J.R., D.H. Timm, R.C. West, R. Powell, M.A. Robbins, A.J. Taylor, A.D.F. Smit, N.H. Tran, M.A. Heitzman, and A. Bianchini. Phase III NCAT Test Track Findings, NCAT Report No. 09-08, National Center for Asphalt Technology, Auburn University, 2009.
16. West, R.C, A.N. Kvasnak, N.H. Tran, R. Powell, and P. Turner. Testing of Moderate and High RAP Content Mixes: Laboratory and Accelerated Field Performance at the National Center for Asphalt Technology Test Track, *Transportation Research Record.* No. 2126, 2009.
17. *A Manual for Design of Hot Mix Asphalt with Commentary*. Advanced Asphalt Technologies, LLC, NCHRP Report 673, Transportation Research Board, 2011.
18. Priest, A. L. and D. H. Timm. Methodology and Calibration of Fatigue Transfer Functions for Mechanistic-Empirical Flexible Pavement Design. NCAT Report No. 06-03, National Center for Asphalt Technology, Auburn University, 2006.

19. Timm, D.H. and A.L. Priest. Flexible Pavement Fatigue Cracking and Measured Strain Response at the NCAT Test Track. Paper No. 08-0256, Presented at the 87th Transportation Research Board Annual Meeting, Washington D. C., 2008.
20. Haddock, J. E., A. J. Hand, and H. Fang. Contributions of Pavement Structural Layers to Rutting of Hot Mix Asphalt Pavements. NCHRP Report 468, National Academy Press, Washington D. C., 2002.
21. Willis, J.R. and D.H. Timm. Field-Based Strain Thresholds for Flexible Perpetual Pavement Design. NCAT Report No. 09-09, National Center for Asphalt Technology, Auburn University, 2009.
22. AASHTO. *AASHTO Guide for Design of Pavement Structures*. American Association of State Highway and Transportation Officials, Washington, D.C., 1993.
23. Timm, D.H. and A. Vargas-Nordcbeck. Structural Coefficient of Open Graded Friction Course. *Proceedings of the 91st Annual Meeting of the Transportation Research Board*, Washington, D.C., 2012.
24. Peters, K. and D. Timm. Recalibration of the Asphalt Layer Coefficient. *ASCE Journal of Transportation Engineering*, Volume 137, No. 1, 2011, pp. 22-27.
25. Van Der Zwan, J. T., T. Goeman, H.J.A.J. Gruis, J. H. Swart, and R. H. Oldenburger. Porous Asphalt Wearing Courses in the Netherlands : State of the Art Review. *Transportation Research Record No. 1265*, Transportation Research Board of the National Academies, Washington, D.C., 1990, pp. 95–110.
26. Yoder, E.J. and M.W. Witczak. *Principles of Pavement Design*. Second Edition. John Wiley and Sons, Inc., New York, N.Y., 1975.
27. Timm, D.H., M.M. Robbins, J.R. Willis, N. Tran and A.J. Taylor. Evaluation of Mixture Performance and Structural Capacity of Pavements Using Shell Thiopave®: Phase II - Construction, Laboratory Evaluation, and Full-Scale Testing of Thiopave Test Sections - One Year Report. NCAT Report No. 11-03, National Center for Asphalt Technology, Auburn University, 2011.
28. Timm, D., N. Tran, A. Taylor, M. Robbins and R. Powell. Evaluation of Mixture Performance and Structural Capacity of Pavements Using Shell Thiopave®. NCAT Report No. 09-05, National Center for Asphalt Technology, Auburn University, 2009.
29. Tran, N., A. Taylor, D. Timm, M. Robbins, B. Powell, and R. Dongre. Evaluation of Mixture Performance and Structural Capacity of Pavements Using Shell Thiopave®: Comprehensive Laboratory Performance Evaluation. NCAT Report No. 10-05, National Center for Asphalt Technology, Auburn University, 2010.
30. Powell, R. and A. Taylor. Design, Construction and Performance of Sulfur-Modified Mix in the WMA Certification Program at the NCAT Pavement Test Track. NCAT Report No. 11-08, National Center for Asphalt Technology, Auburn University, 2011.
31. Tran, N. and A. Taylor. Moisture Resistance of Sulfur-Modified Warm Mix. NCAT Report No. 11-07, National Center for Asphalt Technology, Auburn University, 2011.
32. Prowell, B.D., E.R. Brown, R.M. Anderson, J. Sias-Daniel, H. Von Quintus, S. Shen, S.H. Carpenter, S. Bhattacharjee and S. Maghsoodloo. Validating the Fatigue Endurance Limit for Hot Mix Asphalt. NCHRP Report 646, Transportation Research Board, Washington, D.C., 2010.
33. Von Quintus, H. *Quantification of the Effects of Polymer-Modified Asphalt*. Engineering Report ER 215, Asphalt Institute, 2005, pp. 1-8.
34. Anderson, R. M. *Asphalt Modification and Additives*. The Asphalt Handbook MS-4, 7th ed., Asphalt Institute, Lexington, 2007, pp. 86-89.
35. Van de Ven, M.F.C., M.R. Poot and T.O. Medani. Advanced Mechanical Testing of Polymer Modified Asphalt Mixtures. Report 7-06-135-3, Road and Rail Engineering, Delft University of Technology, the Netherlands, April 2007.

36. Molenaar, A.A.A., M.F.C. van de Ven, X. Liu, A. Scarpas, T.O. Medani and E.J. Scholten. Advanced Mechanical Testing of Polymer Modified Base Course Mixes. Proceedings, Asphalt – Road for Life, Copenhagen, May 2008, pp. 842-853.

37. Kluttz, R. Q., A. A. A. Molenaar, M. F. C.van de Ven, M.R. Poot, X. Liu, A. Scarpas and E.J. Scholten. Modified Base Courses for Reduced Pavement Thickness and Improved Longevity. *Proceedings of the International Conference on Perpetual Pavement*, October 2009, Columbus, OH..

38. Scarpas, A. and J. Blaauwendraad. Experimental Calibration of a Constitutive Model for Asphaltic Concrete. Proceedings of Euro-C Conference on the Computational Modelling of Concrete Structures, Badgastein, Austria, April 1998.

39. Erkens, S. M. J. G. *Asphalt Concrete Response (ACRe), Determination, Modelling and Prediction*. Ph.D. Dissertation, Delft University of Technology, The Netherlands, 2002.

40. Halper, W. M, and G. Holden. Styrenic Thermoplastic Elastomers in Handbook of Thermoplastic Elastomers. 2nd ed., B. M. Walker and C. P. Rader, Eds., Van Nostrand Reinhold, New York, 1988.

41. Timm, D.H., M.M. Robbins, J.R. Willis, N. Tran and A.J. Taylor. Field and Laboratory Study of High-Polymer Mixtures at the NCAT Test Track. NCAT Draft Report, 2011b.

42. Timm, D.H., M. M. Robbins and R.Q. Kluttz. Full-Scale Structural Characterization of a Highly Polymer-Modified Asphalt Pavement. Proceedings of the 90th Annual Transportation Research Board, Washington, D.C., 2011.

43. Timm, D.H., A.L. Priest, and T.V. McEwen. Design and Instrumentation of the Structural Pavement Experiment at the NCAT Test Track. NCAT Report No. 04-01, National Center for Asphalt Technology, Auburn University, 2004.

44. Timm, D.H. and A.L. Priest. Material Properties of the 2003 NCAT Test Track Structural Study. NCAT Report No. 06-01, National Center for Asphalt Technology, Auburn University, 2006.

45. Timm, D.H., R. West, A.L. Priest, S.S. Immanuel, J. Zhang, and E.R. Brown. Phase II NCAT Test Track Results. NCAT Report No. 06-05, National Center for Asphalt Technology, Auburn University, 2006.

46. Federal Highway Administration. Pavement Smoothness Index Relationships: Final Report. Publication No. FHWA-Rd-02-057, October 2002.

47. Colloley, Jr. L. A., E. R. Brown, and D. E. Watson. Evaluation of OGFC Mixtures Containing Cellulose Fibers. NCAT Report No. 00-05, National Center for Asphalt Technology, Auburn University, 2000.

48. Mallick, R. B., P.S. Kandhal, L. A. Cooley, Jr., and D. E. Watson. Design, Construction, and Performance of New Generation Open-Graded Friction Courses. NCAT Report No. 00-01, National Center for Asphalt Technology, Auburn University, 2000.

49. Birgisson, B., R. Roque, A. Varadhan, T. Thai, and L. Jaiswal. Evaluation of Thick Open Graded and Bonded Friction Courses for Florida. Final Report of Florida Department of Transportation, University of Florida, Gainesville, FL, 2006.

50. Russell, M., J. Uhlmeyer, K. Anderson, and J. Weston. Evaluation of Trinidad Lake Asphalt Overlay. Report WA-RD 710.1, Washington State Department of Transportation, 2008.

51. Widyatmoko, I., R. Elliot, and J. Reed. Development of Heavy-Duty Mastic Asphalt Bridge Surfacing, Incorporating Trinidad Lake Asphalt and Polymer Modified Binders. *Journal of Road Materials and Pavement Design*, Vol. 6, No. 4, 2005, pp. 469-483.

52. LaForce, R. I 70 Glenwood Canyon Overlay with Trinidad Lake Asphalt/Steel Slag Hot Mix Asphalt. Report CDOT-DTD-R-2005-13, Colorado Department of Transportation, September 2006.

53. Pelland, R., J. Gould, and R. Mallick. Selecting a Rut Resistant Hot Mix Asphalt for Boston-Logan International Airport. Airfield Pavements: Challenges and New Technologies, Airfield Pavements Specialty Conference, ASCE, 2003.

54. Sebaaly, P., G. Bazi, and Y. Vivekanathan. Evaluation of New Pavement Technologies in Nevada. Report No. 13AX-1, Nevada Department of Transportation, 2003.

55. Biel, T., B. Sharp, and R. Lindsey. Trinidad Lake Asphalt (TLA) Two Experimental Applications on I-80 from Echo to Canyon Rock. Final Report, Experimental Feature X(02)18, Utah Department of Transportation, 2006.

56. Roque, R., J. Zhou, Y.R. Kim, C. Baek, S. Thirunavukkarasu, B.S. Underwood and M.N. Guddati. Top Down Cracking of Hot-Mix Aphalt Layers: Models for Initiation and Propagation, Final Report, NCHRP Project 1-42A, 2010.

57. Chatti, K., H.B. Kim, K.K. Yun, J.P. Mahoney, and C.L. Monismith. Field Investigation into Effects of Vehicle Speed and Tire Pressure on Asphalt Concrete Pavement Strains. *Transportation Research Record*, No. 1539, 1996, pp. 66-71.

58. Dai, S.T., D. Van Deusen, M. Beer, D. Rettner, and G. Cochran. Investigation of Flexible Pavement Response to Truck Speed and FWD Load Through Instrumented Pavements. Eighth International Conference on Asphalt Pavements, Proceedings, Vol. 1, Seattle, Washington, 1997.

59. Mateos, A. and M. B. Snyder. Validation of Flexible Pavement Structural Response Models with Data from the Minnesota Road Research Project. *Transportation Research Record*, No. 1806, 2002, pp. 19-29.

60. Sebaaly, P. E. and N. Tabatabaee. Influence of Vehicle Speed on Dynamic Loads and Pavement Response. Transportation Research Record, 1410, 1993, pp. 107-114.

61. Siddharthan, R., J. Yao, and P.E. Sebaaly. Field Verification of Moving Load Model for Pavement Response. Transportation Research Record, 1540, 1996, pp. 125-131 .

62. Ellison, A. and D. Timm. Speed and Temperature Effects on Full-Scale Pavement Responses in Non-Conventional Flexible Pavements. Proceedings, T&DI Congress 2011: Integrated Transportation and Development for a Better Tomorrow, Proceedings of the First T&DI Congress 2011, American Society of Civil Engineers, Chicago, IL, 2011, pp. 824-833 .

63. Donavan, P. R. and D. M. Lodico. Measuring Tire-Pavement Noise at the Source. NCHRP 6-30, Washington, D. C., 2009.

64. Rymer, B. and P. Donavan. Tire-Pavement Noise Intensity Testing in Europe: The NITE Study and Its Relationship to Ongoing Caltrans Quiet Pavement Activities. Proceedings of the 80th Meeting of the Association of Asphalt Paving Technologists, Long Beach, CA, March 7-9, 2005.

65. WSDOT. Quieter Pavement Performance in Washington. WSDOT Newsletter 0638, Washington State Department of Transportation, June 2011.

66. Standard Method of Test for Measurement of Tire/Pavement Noise Using the On-Board Sound Intensity (OBSI) Method, American Association of State Highway and Transportation Officials, AASHTO Designation TP 76-11, Washington D.C., 2011.

67. Cooley, L.A. Permeability of Superpave Mixtures: Evaluation of Field Permeameters. NCAT Report 99-01, National Center for Asphalt Technology, February 1999.

68. Brown, E.R., P.S. Kandhal, and J. Zhang. Performance Testing for Hot Mix Asphalt. NCAT Report 01-05, National Center for Asphalt Technology, Auburn University, November 2001.

69. Azari, H., A. Mohseni, and N. Gibson. Verification of Rutting Predictions from Mechanistic-Empirical Pavement Design Guide by Use of Accelerated Loading Facility Data. *Transportation Research Record: Journal of the Transportation Research Board*, No. 2057, 2008, pp. 157-167.

70. Zubeck H.K. and T.S. Vinson. Prediction of Low-Temperature Cracking of Asphalt Concrete Mixtures with Thermal Stress Restrained Specimen Test Results. *Transportation Research Record: Journal of the Transportation Research Board,* No. 1545, pp. 50-58.

71. Hiltunen, D.R. and R. Roque. A Mechanics-Based Prediction Model for Thermal Cracking of Asphaltic Concrete Pavements. *Journal of the Association of Asphalt Paving Technologists*, Vol. 63, 1994, pp. 81-117.

72. Harmelink, D., S. Shuler, T. Aschenbrener. Top-Down Cracking in Asphalt Pavements: Causes, Effects, and Cures. *Journal of Transportation Engineering*, Vol. 134, No. 1, 2008, pp. 1-6.

73. Buttlar, W.G., R. Roque, and B. Reid. Automated Procedure for Generation of Creep Compliance Master Curve for Asphalt Mixtures. *Transportation Research Record*, No. 1630, 1998, pp. 28-36.

74. Hiltunen, D. R. and R. Roque. A Mechanics-Based Prediction Model for Thermal Cracking of Asphaltic Concrete Pavements. *Journal of the Association of Asphalt Paving Technologists*, Vol. 63, 1994, pp. 81-117.

75. Willis, J.R., A. Taylor, N. Tran, B. Kluttz, and D. Timm. Laboratory Evaluation of High Polymer Plant-Produced Mixtures. Accepted for publication in the *Journal of the Association of Asphalt Paving Technologists,* 2012.

76. Kim, Y. R., H. Lee, and D. N. Little. Fatigue Characterization of Asphalt Concrete Using Viscoelasticity and Continuum Damage Theory. *Journal of Association of Asphalt Paving Technologists*, 1997, pp. 520-569.

77. Daniel, J.S. and Y. Richard Kim. Development of a Simplified Fatigue Test and Analysis Procedure Using a Viscoelastic, Continuum Damage Model. *Journal of Association of Asphalt Paving Technologists*, 2002.

78. Hou, T., B.S. Underwood, and Y. Richard Kim. Fatigue Performance Prediction of North Carolina Mixtures Using the Simplified Viscoelastic Contiuum Damage Model. *Journal of Association of Asphalt Paving Technologists*, 2010.

79. Underwood, B. S., Y. Richard Kim, and Murthy Guddati. Characterization and Performance Prediciton of ALF Mixtures Using a Viscoelastoplastic Contiuum Damage Model. *Journal of Association of Asphalt Paving Technologists*, 2006.

80. Determining the Damage Characteristic Curve of Asphalt Concrete from Direct Tension Cyclic Fatigue Tests. Draft Specification*.* North Carolina State University, 2010.

81. Christensen, D. Analysis of Creep Data from Indirect Tension Test on Asphalt Concrete. *Journal of the Association of Asphalt Paving Technologists*. Vol. 67, 1998, pp. 458-492.

82. Tran, N.H., R.C. West, R.B. Powell, and A.N. Kvasnak, Evaluation of AASHTO Rut Test Procedure Using the Asphalt Pavement Analyzer. *Journal of the Association of Asphalt Paving Technologists*. Vol. 78, 2009, pp. 1-24.

83. Biligiri, K.P., K.E. Kaloush, M.W. Mamlouk, and M.W. Witczak, Rational Modeling of Tertiary Flow of Asphalt Mixtures. *Transportation Research Record: Journal of the Transportation Research Board*, No. 2001, 2007, pp. 63-72.

84. Advanced Asphalt Technologies, LLC. *A Manual for Design of Hot Mix Asphalt with Commentary*. NCHRP Report 673, National Academies of Sciences, Transportation Research Board, 2011.

85. Bonaquist, R. *Mix Design Practices for Warm Mix Asphalt*, NCHRP Report 691, National Academies of Sciences, Transportation Research Board, 2011.

86. Kim, Y. R., and H. Wen, *Fracture Energy from Indirect Tension*, Journal of Association of Asphalt Paving Technology", Volume 71, 2002, pp. 779-793.

APPENDIX A

TABLE A.1 Energy Ratio Test Results

Mix ID	m-value	D_1 (E-07)	S_t (MPa)	M_r (GPa)	FE (kJ/m^3)	$DCSE_{HMA}$ (kJ/m^3)	a (E-08)	$DSCE_{MIN}$ (kJ/m^3)	ER
S9-1	0.327	9.00	2.51	9.93	8.1	7.78	4.61	0.70	11.10
N7-1	0.282	7.08	2.51	9.23	4.2	3.86	4.61	0.35	10.97
N8-1	0.347	13.9	1.44	7.81	1.9	1.77	5.20	1.14	1.56
N10-1	0.338	2.99	2.39	14.12	1.6	1.40	4.67	0.25	5.53
N11-1	0.419	5.17	2.43	10.84	3.4	3.13	4.65	0.83	3.77
N12-1	0.325	8.73	1.75	10.63	3.1	2.96	5.03	0.61	4.884
S2-1	0.287	2.22	2.14	17.88	0.2	0.07	4.81	0.11	0.64
S6-1	0.410	6.51	2.37	10.34	5.1	4.83	4.68	0.97	4.96
S7-1	0.408	5.50	2.71	10.69	4.1	3.76	4.50	0.85	4.43
S10-1	0.427	12.8	2.16	8.00	12.5	12.21	4.80	2.11	5.77
S11-1	0.408	13.0	2.26	7.53	9.9	9.56	4.75	1.89	5.06
S12-1	0.387	6.15	2.36	10.70	3.3	3.04	4.69	0.77	3.92

TABLE A.2 Beam Fatigue Test Results at 800 Microstrain

Mix	Cycles Until Failure				
	Beam 1	Beam 2	Beam 3	Average	COV, %
N5-4	8,840	6,760	6,410	7,337	18%
N7-3	83,600	20,520	14,230	39,450	97%
N10-3	3,320	2,950	680	2,317	62%
N11-3	2,560	3,100	2,100	2,587	19%
S8-3	7,890	4,260	17,510	9,887	69%
S10-3	3,610	6,980	16,850	9,147	75%
S11-3	9,090	14,670	7,720	10,493	35%
S12-3	5,240	8,780	3,400	5,807	47%

TABLE A.3 Beam Fatigue Test Results at 600 Microstrain

Mixture	600 Microstrain				
	Beam 1	Beam 2	Beam 3	Average	COV, %
N5-4					
N7-3	287,290	195,730	186,920	223,313	25%
N10-3					
N11-3					
S8-3					
S10-3					
S11-3					
S12-3					

TABLE A.4 Beam Fatigue Test Results at 400 Microstrain

Mix	400 Microstrain				
	Beam 1	Beam 2	Beam 3	Average	COV, %
N5-4	398,100	292,860	82,110	257,690	62%
N7-3	11,510,940	1,685,250	4,935,530	6,043,907	83%
N10-3	13,480	31,460	112,630	52,523	101%
N11-3	101,150	146,210	124,920	124,093	18%
S8-3	201,060	216,270	141,250	186,193	21%
S10-3	157,270	261,010	135,930	184,737	36%
S11-3	114,370	185,490	299,680	199,847	47%
S12-3	304,320	431,510	407,380	381,070	18%

TABLE A.5 Beam Fatigue Test Results at 200 Microstrain

Mixture	200 Microstrain				
	Beam 1	Beam 2	Beam 3	Average	COV, %
N5-4	24,700,000	54,400,000	1,876,430	26,992,143	98%
N7-3					
N10-3	15,200,000	9,797,400	3,328,290	9,441,897	63%
N11-3	53,100,000	54,500,000	4,501,250	37,367,083	76%
S8-3	6,953,800	5,994,840	2,165,480	5,038,040	50%
S10-3	4,233,170	7,244,350	4,524,340	5,333,953	31%
S11-3	1,746,710	4,789,300	4,594,330	3,710,113	46%
S12-3	4,617,890	40,247,181	75,095,892	39,986,988	88%

TABLE A.6 S-VECD Test Results

Sample Identification	Specimen number	Initial Strain (ms)	Cycles to failure N_f
N5-4	9	200	60000
	10	335	2100
	11	255	2700
	15	200	130000
	18	255	17500
N7-3	6	375	18500
	10	250	140000
	11	250	57000
	12	375	850
N10-3	8	200	3900
	10	200	3400
	12	150	28000
	13	150	31500
N11-3	5	200	36000
	6	200	20500
	8	300	1050
	9	300	1450
S8-3	10	250	19000
	12	250	15000
	13	350	1150
	14	350	520
S10-3	4	350	3100
	5	350	1400
	6	250	8500
	7	250	20000
	8	250	44000
	9	250	18000
	11	350	3400
S11-3	10	250	40000
	16	250	27000
	17	400	2900
	18	400	950
S12-3	8	250	12000
	12	250	32000
	13	350	1700
	14	350	8500

TABLE A.7 S-VECD Prediction of Cycles Until Failure

Microstrain	Predicted Cycles to failure			
	200	400	600	800
N11-3	28400245	106419.3	4052.516	398.7664
N7-3	1.06E+08	366005.4	13275.81	1262.008
S10-3	2399056	13070.58	619.5674	71.21135
N10-3	824939.7	2185.775	67.9617	5.791468
S8-3	3907296	17532.44	741.8747	78.66987
N5-4	6933632	21999.45	760.0713	69.80119
S12-3	13677915	54931.46	2178.385	220.6086
S11-3	56990157	238595.9	9694.869	998.909

APPENDIX B

Table B.1 APA Rut Depths

Mixture	APA Rut Depth, mm						
	1	*2*	*3*	*4*	*5*	*6*	*Average*
N2-3	2.47	2.13	2.99	2.51	2.07	2.72	2.48
N5-2	2.14	2.94	1.78	1.10	1.50	2.54	2.00
N5-4	3.37	3.36	6.64	2.78	4.18	4.08	4.07
N7-1	1.08	0.11	0.82	0.63	0.57	0.53	0.62
N7-3	0.88	0.85	1.10	0.71	0.59	1.07	0.86
N8-1	1.08	1.01	1.69	0.70	1.22	1.27	1.16
N10-1	4.11	4.15	6.39	4.57	4.08	4.49	4.63
N11-1	4.58	3.99	6.92	5.20	5.62	7.63	5.65
N12-1	0.84	1.71	1.69	1.04	0.95	1.99	1.37
S2-1	1.52	1.12	0.81	0.94	0.12	1.53	1.00
S6-1	1.65	1.54	1.92	1.15	1.13	1.08	1.41
S7-1	1.24	1.37	1.67	1.10	1.21	1.66	1.37
S8-1	1.78	0.58	1.41	0.79	0.93	1.63	1.18
S9-1	2.61	3.95	2.28	3.13	3.36	3.11	3.07
S9-3	4.09	4.49	5.32	2.52	2.72	5.78	4.15
S10-1	4.71	5.24	5.10	3.08	3.83	3.66	4.27
S11-1	3.55	3.50	4.62	2.66	3.40	4.44	3.69
S12-1	2.71	2.58	3.63	3.03	2.68	2.29	2.82
S12-3	2.35	3.46	3.26	3.06	4.57	3.23	3.32

Table B.2 Flow Number Results

Mixture	Flow Number			
	1	*2*	*3*	*Average*
N2-3	57	49	150	85
N5-2	363	333	163	286
N5-4	61	54	25	47
N7-1	6,609	20,000	3,040	9,883
N7-3	740	733	1,359	944
N8-1	173	182	152	169
N10-1	74	69	77	73
N11-1	51	43	47	47
N12-1	310	344	291	315
S2-1	5,229	20,000	1,965	9,065
S6-1	301	390	271	321
S7-1	503	645	829	659
S9-1	153	182	156	164
S9-2	240	291	253	261
S9-3	117	248	22	129
S10-1	47	35	72	51
S11-1	30	37	42	36
S12-1	128	118	124	123
S12-3	83	217	430	243

Table B.3 Hamburg Wheel-Tracking Results

Mixture	Rut Depth, mm			Rate of Rutting, mm/hr		
	1	*2*	*3*	*1*	*2*	*3*
N10-1	1.41	1.14	NA	0.355	0.287	NA
N11-1	3.20	3.40	NA	0.806	0.857	NA
N12-1	0.512	0.675	0.512	2.03	2.68	2.03
N2-1	2.92	2.84	5.05	0.736	0.717	1.264
N5-2	4.826	2.41	3.34	1.216	0.608	0.847
N5-4	5.673	4.978	5.969	1.43	1.255	1.504
N7-1	0.87	1.63	1.02	0.224	0.41	0.256
N7-3	1.19	2.54	1.32	0.30	0.64	0.33
N8-1	4.191	1.63	2.84	1.056	0.41	0.717
S10-1	3.3	5.1	NA	0.832	1.285	NA
S11-1	11.20	5.9	NA	2.822	1.487	NA
S12-1	2.16	2.71	1.33	0.544	0.683	0.336
S12-3	2.03	3.88	3.64	0.512	0.978	0.917
S2-1	1.67	0.8	NA	0.421	0.201	NA
S6-1	2.29	4.88	5.14	0.579	1.229	1.296
S7-1	1.11	1.23	3.4	0.311	0.28	0.858
S8-3	4.4	6.99	4.83	1.109	1.760	1.216
S9-1	3.914	3.567	NA	0.986	0.899	NA